

AD-A046 011

COLORADO UNIV BOULDER SYSTEMS ENGINEERING LAB
SYNTHESIS OF OSCILLATING ADAPTIVE SYSTEMS.(U)
JUL 77 A SHAPIRO, I HOROWITZ

F/G 9/4

UNCLASSIFIED

1 OF 4

AD
A046011

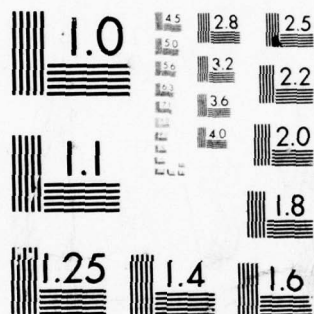


AFOSR-TR-77-1223

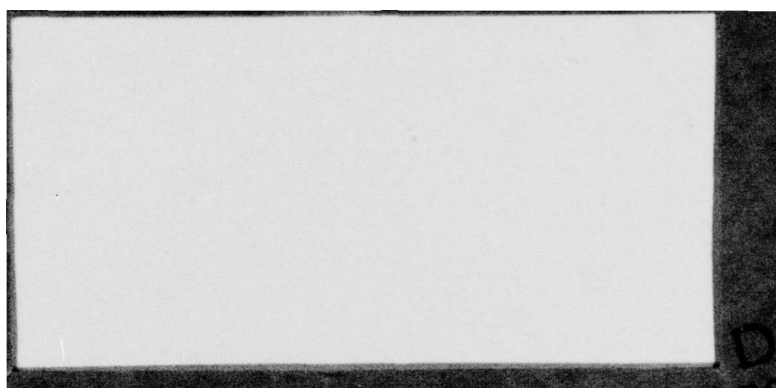
AFOSR-76-2946

NL





MICROCOPY RESOLUTION TEST CHART
NATIONAL BUREAU OF STANDARDS-1963-A



UNCLASSIFIED

1 SECURITY CLASSIFICATION OF THIS PAGE (When Data Entered)

19 REPORT DOCUMENTATION PAGE		READ INSTRUCTIONS BEFORE COMPLETING FORM
1. REPORT NUMBER 18 AFOSR-TR-77-1223	2. GOVT ACCESSION NO.	3. RECIPIENT'S CATALOG NUMBER 9
4. TITLE (and Subtitle) SYNTHESIS OF OSCILLATING ADAPTIVE SYSTEMS	5. TYPE OF REPORT & PERIOD COVERED Interim rept.	
7. AUTHOR(s) Aharon/Shapiro Isaac/Horowitz	6. PERFORMING ORG. REPORT NUMBER	
9. PERFORMING ORGANIZATION NAME AND ADDRESS University of Colorado Department of Electrical Engineering Boulder, Colorado 80309	8. CONTRACT OR GRANT NUMBER(s) 15 AFOSR-76-2946	
11. CONTROLLING OFFICE NAME AND ADDRESS Air Force Office of Scientific Research/NM Bolling AFB DC 20332	10. PROGRAM ELEMENT, PROJECT, TASK AREA & WORK UNIT NUMBERS 61102F 16 2304/A1 17 A1	
14. MONITORING AGENCY NAME & ADDRESS (if different from Controlling Office) 12 299p.	12. REPORT DATE 11 25 Jul 77	
	13. NUMBER OF PAGES 289	
	15. SECURITY CLASS. (of this report) UNCLASSIFIED	
	15a. DECLASSIFICATION/DOWNGRADING SCHEDULE	
16. DISTRIBUTION STATEMENT (of this Report) Approved for public release; distribution unlimited.		
17. DISTRIBUTION STATEMENT (of the abstract entered in Block 20, if different from Report)		
18. SUPPLEMENTARY NOTES		
19. KEY WORDS (Continue on reverse side if necessary and identify by block number)		
20. ABSTRACT (Continue on reverse side if necessary and identify by block number) Oscillating adaptive systems are non-linear feedback systems in which there circulates in the feedback loop (or loops), a signal whose frequency components are large relative to the bandwidths of the control (command and disturbance) signal components. Under certain conditions the system response to these control components is quasi-linear, permitting linear analysis accurate within stringent engineering tolerances. The system response to these control inputs can also then have zero sensitivity to the (linear time-invariant) plant high-frequency gain factor. If a linear time-invariant feedback system is designed to		

DD FORM 1 JAN 73 1473

EDITION OF 1 NOV 65 IS OBSOLETE

UNCLASSIFIED

SECURITY CLASSIFICATION OF THIS PAGE (When Data Entered)

410 446

LB

UNCLASSIFIED

SECURITY CLASSIFICATION OF THIS PAGE(When Data Entered)

20 Abstract (continued)

cope with such plants, the uncertainty in this gain factor, if very large, can lead to enormous, possibly impractical, loop bandwidths. Hence, the zero sensitivity property of the oscillating system makes them very attractive as adaptive systems.

The quasi-linearity conditions permit the development of quantitative frequency-response synthesis techniques, whereby one may proceed from a statement of quantitative performance specifications and plant uncertainty bounds, step by step towards an optimum design. One significant result is that the gain factor uncertainty, inherently banished as a direct adaptive problem by the oscillating condition, reappears in different forms as a significant design constraint.

UNCLASSIFIED

2

SYNTHESIS OF OSCILLATING ADAPTIVE SYSTEMS

by
Aharon Shapiro
Isaac Horowitz

- ③ Systems Engineering Laboratory
Department of Electrical Engineering
① UNIVERSITY OF COLORADO
② Boulder, Colorado 80309



410446 New

AIR FORCE OFFICE OF SCIENTIFIC RESEARCH (AFSC)
NOTICE OF TRANSMITTAL TO DDC
This technical report has been reviewed and is
approved for public release under AFR 190-12 (7b).
Distribution is unlimited.
A. D. BLOSE
Technical Information Officer

This research was supported by the
AIR FORCE OFFICE OF SCIENTIFIC RESEARCH
under Research Grant AFOSR-76-2946

July 25, 1977

SYNTHESIS OF OSCILLATING ADAPTIVE SYSTEMS

Abstract

Oscillating adaptive systems are non-linear feedback systems in which there circulates in the feedback loop (or loops), a signal whose frequency components are large relative to the bandwidths of the control (command and disturbance) signal components. Under certain conditions the system response to these control components is quasi-linear, permitting linear analysis accurate within stringent engineering tolerances. The system response to these control inputs can also then have zero sensitivity to the (linear time-invariant) plant high-frequency gain factor. If a linear time-invariant feedback system is designed to cope with such plants, the uncertainty in this gain factor, if very large, can lead to enormous, possibly impractical, loop bandwidths. Hence, the zero sensitivity property of the oscillating system makes them very attractive as adaptive systems.

The quasi-linearity conditions permit the development of quantitative frequency-response synthesis techniques, whereby one may proceed from a statement of quantitative performance specifications and plant uncertainty bounds, step by step towards an optimum design. One significant result is that the gain factor uncertainty, inherently banished as a direct adaptive problem by the oscillating condition, reappears in different forms as a significant design constraint. Six oscillating adaptive structures, four of them new, are presented each with its own quantitative design procedure. Each has its own package of feedback benefits, costs and trade-offs, with the gain factor uncertainty appearing in different forms. Numerical design examples are presented for each structure, including verification by computer simulation.

TABLE OF CONTENTS

ADDITIONAL for	
NPIS	Write Section <input checked="" type="checkbox"/>
DDC	Buff Section <input type="checkbox"/>
UNANNOUNCED	<input type="checkbox"/>
JUSTIFICATION	
BY	
DISTRIBUTION/AVAILABILITY CODES	
Dis	SPECIAL
A	

ABSTRACT

CHAPTER 1	Preliminary Background	1
1.1	Introduction	1
CHAPTER 2	THE SOAS STRUCTURE	7
2.1	General	
2.2	Model of the Non-linear Element and the Resulting Constraints	10
2.3	Mathematical Relations	18
2.4	SOAS Sensitivity to Uncertainty in Plant Dynamics $P_h(j\omega)$	21
2.5	Synthesis Procedure for the SOAS	21
2.5.1	Specifications and Data	22
2.5.2	The Constraints	24
2.5.3	Synthesis Procedure (Smooth Solution)	25
2.6	Numerical Example (Smooth Solution)	40
2.6.1	Specifications and Constraints	40
2.6.2	The Design Solution	42
2.6.3	Simulations and Results	50
2.7	Synthesis Procedure (Non-smooth Solution)	59
CHAPTER 3	THE EXTERNALLY EXCITED OSCILLATING ADAPTIVE SYSTEM (EEAS)	
3.1	General	64
3.2	Model of the Non-linear Element and the Constraints Involved	65
3.3	Mathematical Relations	67
3.4	Mathematical Relations - Interpretation	76
3.4.1	Zero Sensitivity Property of the EEAS to Pure Gain Changes of the Plant	76
3.4.2	Physical Interpretation of the Mathematical Relations	80

3.4.3	EEAS Sensitivity to Dynamic Changes of the Plant	89
3.5	Synthesis Procedure for the EEAS	91
3.5.1	Specifications and Data	91
3.5.2	The Constraints	92
3.5.3	Synthesis Procedure (Smooth Solution)	93
3.6	Numerical Example for the EEAS	107
CHAPTER 4	SOAS WITH SECONDARY LOOP (SOAL)	
4.1	General	127
4.2	The Stability and Dynamics of the Secondary Loop	130
4.3	Mathematical Relations	133
4.4	SOAL Sensitivity to Uncertainty in Plant Dynamics	135
4.5	Synthesis Procedure for the SOAL	135
4.5.1	Specifications and Data	135
4.5-2	The Constraints	137
4.5-3	SOAL - Synthesis Procedure (Smooth Solution)	137
4.6	Numerical Example - SOAL (Smooth Solution)	143
4.7	Comparison with Minneapolis-Honeywell System	156
CHAPTER 5	SOAL WITH NON-LINEAR SECONDARY LOOP (SOANL)	
5.1	General	157
5.2	Stability and Dynamics of the Secondary Loop - SOANL	158
5.3	Synthesis Procedure and Numerical Example (Smooth Solution) - SOANL	160
CHAPTER 6	EEAS WITH SECONDARY LOOP (EEAL)	
6.1	General	178
6.2	Possible EEAL Structures	179
6.3	Mathematical Relations	184
6.4	EEAL Sensitivity to Changes in the Plant Dynamics	186
6.5	Dynamics and Stability of the Secondary Loop - EEAL	187
6.6	Synthesis Procedure for the EEAL	191
6.6.1	Specifications and Data	191
6.6.2	The Constraints	192
6.6.3	The Synthesis Procedure - EEAL (Smooth Solution)	194
6.7	Numerical Example - EEAL (Smooth Solution)	202
6.8	EEAL Numerical Example - Simulation Results	213

CHAPTER 7	EEAL WITH NON-LINEAR SECONDARY LOOP (EEANL)	
7.1	General	246
7.2	The Stability and Dynamics of the Secondary Loop	247
7.3	Synthesis Procedure and Numerical Example	249
CHAPTER 8	CONCLUSIONS	269
APPENDIX I	Review of Optimum Single Loop Synthesis	271
APPENDIX II	Derivation of Frequency Response Bound from Time Domain Bound	277
APPENDIX III	Extrapolation to $\omega = \omega_o$	281
APPENDIX IV	Dynamics of Limit Cycle Build-up in SOAS System	285
BIBLIOGRAPHY		287

CHAPTER ONE

PRELIMINARY BACKGROUND

1.1 Introduction

One of the most important reasons for using feedback is to reduce system sensitivity to uncertain parameters of a constrained part (plant). In the theoretical development, the plant is assumed linear time-invariant, but with uncertain parameters. Rate of parameters variation and ability of the system to adjust to fast rates of variation, are discussed in Chapters 4-7, where pertinent. If linear time-invariant feedback compensation is used, giving a totally linear time-invariant feedback system, it has been shown [1,2,3] that the principal "cost of feedback" is in the bandwidth of the loop transmission, which may make the system very sensitive to sensor noise and high frequency parasitics. The principal factor causing the loop transmission bandwidth to be large, is the uncertainty in the high frequency gain factor K of the plant transfer function $P(s) = KP_h(s)$, where $\lim_{s \rightarrow \infty} P_h = s^{-p}$, p being the excess of plant poles over zeros. The above factors have been discussed in considerable detail in the literature [4,5,6,7] and are therefore not further elaborated here.

One of the important motivations for non-linear (so-called adaptive) systems, is to reduce this "cost of linear feedback", i.e., to obtain the same benefits with effectively less loop transmission bandwidth. However, with the exception of the Non-linear Oscillating Adaptive Systems [8,9,10], there has hardly appeared any quantitative synthesis theory for these adaptive systems, i.e., wherein one can design to achieve assigned quantitative performance bounds over a given quantitative range of plant parameter values.

The essential feature of an oscillating adaptive system is the introduction of a non-linear element and a signal whose frequency components are sufficiently large relative to those of the control components. This high frequency signal may be due to self-oscillation or it may be externally applied. There are obvious practical reasons for it to be a pure sinusoidal (so assumed in this work), although theoretically even aperiodic signals may be used [11]. One vital element in the system operation is its quasi-linearity i.e., under certain "quasi-linearity" conditions, the non-linear system behaves effectively like a linear system towards the "control" signal components of major interest, which are those due to the useful "command" inputs and to the unwanted "disturbance" inputs. Quasi-linearity permits one to characterize these low-frequency components as distinct and separate from the "high-frequency carrier" signal in the system - just as if linear superposition is applicable.

The errors involved in assuming such linear superposition are finite but can be made as small as desired [12] by designing the system that at the input to the non-linearity, the low-frequency control components are commensurately sufficiently "small and slow" relative to the high-frequency signal. This quasi-linearity phenomena has long been known [13,14,15,16] and has been studied extensively, with some interesting results recently obtained with functional analysis techniques [11].

This present research concentrates on practical engineering structures and design techniques for the adaptive problem, so that in view of the extensive literature available, the quasi-linearity aspect of the problem is not treated in detail in this work, but the results

are summarized as needed. From the point of view of this work the important point is that as previously noted, the error involved in using superposition is finite but can be made as small as desired. It will be noted in subsequent chapters that it is simply a matter of making certain design parameters sufficiently large.

The second vital element in the operation of the oscillating adaptive system is its zero sensitivity to the plant high-frequency gain factor. This is related to the quasi-linear phenomenon. The latter permits the characterization of the non-linear element N by two (or if necessary, more) "describing functions", one N_O for the high-frequency component, the second N_f , for the control components. Describing function representation is very accurate for N_O , for it is easy and otherwise also desirable, to design the feedback loop to be very highly "low-pass". Also the non-linear element needs not be particularly rich in higher harmonics, and it has been shown [17] that under these conditions the N_O characterization can be extremely accurate. The use of N_f is justified by the quasi-linear conditions previously discussed. Now, N_f turns out to be inversely proportional to the amplitude of the high-frequency component, which in turn is shown later to be directly proportional to the high-frequency plant gain factor K , so that their product KN_f is independent of K .

History

The quasi-linear feature of the system under consideration has been well known and practically exploited for some time [13,14,15,16] in order to "linearize" unavoidable non-linear elements with undesirable features, sometimes present in practical control systems. However, the zero

sensitivity property was recognized only comparatively recently, apparently first by Minneapolis-Honeywell workers [18,19]. They promoted this approach in the competition among various aerospace companies in the late 1950's and early 1960's, to apply adaptive methods to the flight control problem. In fact, the oscillating adaptive approach was probably the most successful of these, and was applied to the X-15, X-20 vehicles [20,21,22] among others. However, Minneapolis-Honeywell workers, although they reported frequently in a qualitative manner on their work, never did produce any quantitative design theory. It seems quite certain that their design was by ad-hoc, engineering cut and try, because to date, long after they have ceased promoting these systems, they have not produced any such design theory. It is interesting that the final Minneapolis-Honeywell design is a two-loop system with an objective similar to that sought in the two-loop system of Chapter 4. It is superior in that sense (as will be seen) to the single-loop systems of Chapters 2-3. However, it will be shown that there are important advantages in the two-loop system of Chapter 4, over that used by Minneapolis-Honeywell.

Gelb and Vander Velde [22,23] were apparently the first to do some analytic work on the adaptive properties of oscillating adaptive systems. However, their major attention was focused on the quasi-linear properties, and no attempt was made to develop a quantitative design procedure. Consequently, one vital design parameter (later noted) was completely ignored, without which a quantitative design theory is impossible to establish. Horowitz [8] was the first to develop a quantitative design procedure for one (of the six) oscillating adaptive structures, but only for one of the two possible design categories (discussed later) for

this one structure. This category is restricted to designs whose loop transmissions are smooth in a certain sense, a constraint which is dropped in the present work.

It will be seen that each of the six structures has its own package of trade-offs between feedback costs and benefits, which offers important flexibility to the designer, for he can choose that package which is best suited to his particular problem package. Some of the important factors which appear in these trade-off packages are:

1. The amount of high-frequency gain factor uncertainty $\frac{K_{\max}}{K_{\min}}$.
2. The ratio of largest (low-frequency) control signal input which the system is to process quasi-linearly, to the smallest signal parameter, which is the maximum tolerable amplitude at the plant, of the circulating high-frequency component.
3. The maximum rate of variation of the high-frequency gain factor K .
4. The presence of higher order modes, such as elastic bending modes in an air-frame.

The work is divided into six main parts:

- a. SOAS - Single loop Self-oscillating Adaptive Systems. Chapter 2.
- b. EEAS - Single loop Externally Excited Adaptive Systems. Chapter 3.
- c. SOAL - A two loop SOAS with adaptive saturating level. Chapter 4.
- d. SOANL - SOAL with non-linear compensation in the secondary loop.

Chapter 5.

- e. EEAL - A two loop EEAS with adaptive saturating level. Chapter 6.
- f. EEANL - EEAL with non-linear compensation in the secondary loop.

Chapter 7.

The first two systems (SOAS and EEAS) involve known single-loop structures, but with hitherto unknown or incomplete analytical synthesis theory. The last four systems (SOAL, SOANL, EEAL, EEANL) involve new two loop structures, originated in this research.

CHAPTER TWO

THE SOAS STRUCTURE

(Self Oscillating Adaptive Systems)

2.1 General

An important motivation for using nonlinear compensation (i.e. an adaptive system) is to reduce the loop transmission bandwidth, and still get the desired benefits of feedback. The SOAS [8] is one of the simplest Quasilinear Adaptive Systems and its structure is shown in Figure 2.1-1. By quasilinear, is meant here a nonlinear system which acts very closely like a linear system towards the control signals of interest, if some conditions (quasilinear conditions) are met. So, a vital prerequisite for the SOAS and for all the other structures presented here is non-violation of quasilinear conditions as expressed in Section 2.2.

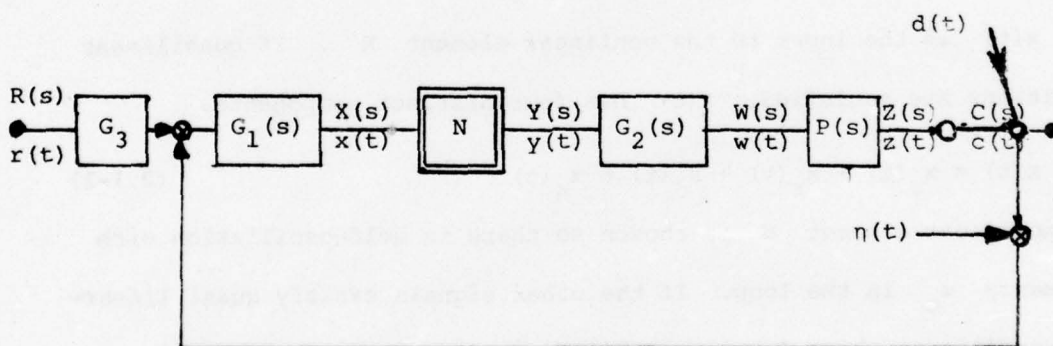


Figure 2.1-1 - SOAS Structure

$G_1(s)$, $G_2(s)$ and $G_3(s)$, are the transfer functions of the linear, time-invariant compensations that have to be found. $P(s)$ is the constrained uncertain plant transfer function. N is the introduced non linearity. The quasi-linearity conditions apply to its input.

$r(t)$ is the applied command input to the system with Laplace transform $R(s) = \mathcal{L}[r(t)]$. It is important to define the "extreme" expected command input $r_e(t)$.

$d(t)$ represents the disturbance referred to the plant output. In case the real disturbance is applied at a different point in the plant, the equivalent disturbance at the plant output should be calculated, with its Laplace transform $D(s) = \mathcal{L}[d(t)]$. As with the command input, it is important to define its "extreme" value $d_e(t)$.

$\eta(t)$ is the effective noise due to sensor or other elements. It is assumed its characteristics are stationary, gaussian with known power spectrum.

$x(t)$ is the input to the nonlinear element N . If quasilinear conditions are satisfied, $x(t)$ has four distinct components.

$$x(t) = x_o(t) + x_r(t) + x_d(t) + x_\eta(t) \quad (2.1-1)$$

The nonlinear element N is chosen so there is self-oscillation with frequency ω_o in the loop. If the other signals satisfy quasi linearity conditions, there is no possibility for "quenching" this self-oscillation. The sub o refers to the oscillatory component of $x(t)$ with frequency ω_o . The sub r refers to the component of $x(t)$ due to the applied command input $r(t)$. The sub d refers to the component of $x(t)$ due to $d(t)$ and the sub η to that due to the noise $\eta(t)$. In this work the objective is to find a design procedure

for satisfying system specifications while minimizing the effect of the noise at the plant input as defined in Appendix I.

$y(t)$ is the non-linearity output signal. Under quasi-linearity conditions $y(t)$ is also composed of four distinct components.

$$y(t) = y_o(t) + y_r(t) + y_d(t) + y_n(t) \quad (2.1-2)$$

where the subs have the same meaning as in (2.1-1).

$w(t)$ is the plant input signal. Again under quasi-linearity conditions, superposition is valid, giving

$$w(t) = w_o(t) + w_r(t) + w_d(t) + w_n(t) \quad (2.1-3)$$

The synthesis technique will minimize $w_n(t)$ in the sense described in Appendix I.

$z(t)$ is the plant output. If 2.1-3 holds, then

$$z(t) = z_o(t) + z_r(t) + z_d(t) + z_n(t) \quad (2.1-4)$$

Similarly the system output $c(t)$ is then

$$c(t) = c_o(t) + c_r(t) + c_d(t) + c_n(t) \quad (2.1-5)$$

Note that $z_o(t) = c_o(t)$, $z_r(t) = c_r(t)$, $z_n(t) = c_n(t)$, while $c_d(t) = d(t) + z_d(t)$.

The validity of the approximations used for the non-linear element N , depends on "how sinusoidal" is $x_o(t)$ around its zero value. $x_o(t)$, as explained, is the oscillating component at the non-linearity input. It will be seen that there is no problem in having $|G_1 G_2 P(j\omega)|$ decrease very rapidly vs. ω , for $\omega > \omega_o$. Hence the higher harmonics of y_o (the oscillating component of y) are greatly attenuated and $x_o(t)$ is very well approximated by a sinusoid, in a

proper design.

$$x_o(t) = A \sin(\omega_o t) \quad (2.1-6)$$

For the above reason, describing function representation of N is highly valid.

2.2 Model of the Non-linear Element and the Resulting Constraints. [12]

The results obtained in Reference [12] will be used and are repeated here.

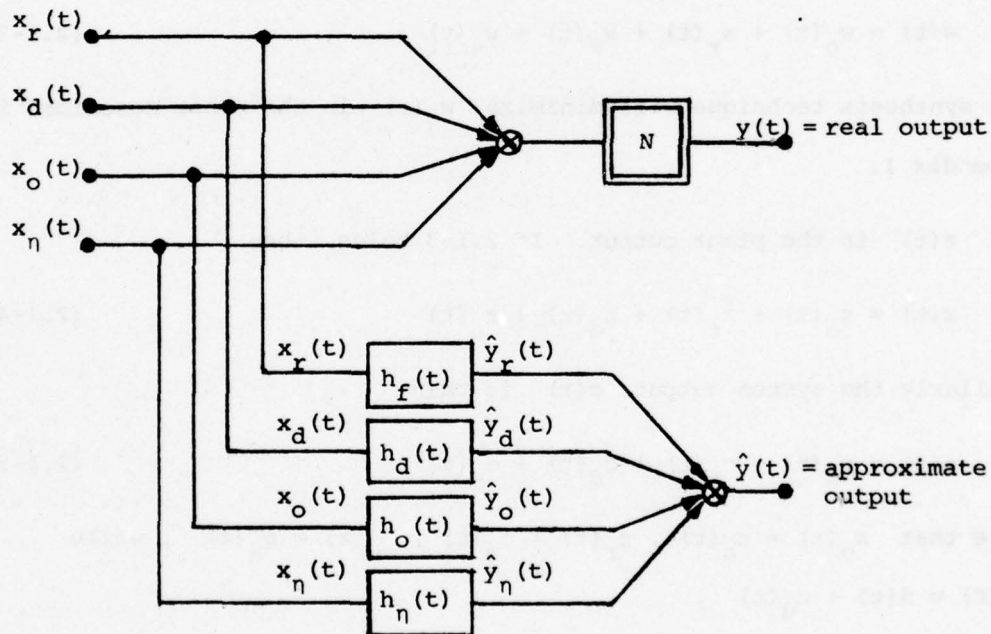


Figure 2.2-1 - General time-invariant approximator
for a non-linear operator

The model for the non-linearity is obtained by approximating the non-linearity operation for each specific signal by a corresponding linear operation. The input to the non-linearity is composed of four

different signals as per 2.1-1. For each of these inputs, and in place of the common non-linearity N , a linear operator is placed as shown in Figure 2.2-1. The criterion used to define each of the linear operators, is to minimize the mean-square difference between the real non-linearity output $y(t)$ and its approximation $\hat{y}(t)$.

$$\overline{(y(t) - \hat{y}(t))^2} \longrightarrow \text{minimum} \quad (2.2-1)$$

The signals considered are stationary ($x_i(t)$ is stationary) and the non-linearities considered are of the time invariant type.

By proper handling of the equations due to 2.2-1, the result is a set of equations on the weighting functions h_i , representing the linear approximations in Figure 2.2-1, which are also time invariant.

$$\int_0^{\infty} h_i(t) R_{x_i x_i}(t-\tau) dt = R_{y x_i}(\tau) \quad ; \quad \tau \geq 0 \quad (2.2-2)$$

$R_{x_i x_i}$ is the autocorrelation function for each input x_i , and $R_{y x_i}$ is the cross correlation function between the non-linearity output $y(t)$ and each input $x_i(t)$. The left side of Equation 2.2-2 is the cross correlation between the input $x_i(t)$ and its equivalent approximation $\hat{y}_i(t)$. Since the several inputs $x_i(t)$ are uncorrelated, the left side of 2.2-2 represents the cross correlation between the input $x_i(t)$ and the total approximate output $\hat{y}(t)$. So, Equation 2.2-2 tells us that if the cross-correlation function between each input and the non-linearity output equals the cross-correlation function between the same input and the approximate output, then the mean square error between the approximate ($\hat{y}(t)$) and real ($y(t)$) output is minimized.

The linear operators shown in Figure 2.2-1 can be derived for three types of signals. The first is a sinusoidal signal and suits the definition of $x_o(t)$. The second type is of a slow signal if compared to $x_o(t)$, and by a proper design of the system, includes $x_r(t)$ and $x_d(t)$. The third is a random signal and suits the definition of $x_n(t)$, by a proper system design. Equation 2.2-2 can be repeatedly used [12] to define the several describing functions for these linear operators:

Non-linearity model for the sinusoidal component (representing $x_o(t)$)

In the case the non-linearity is static and single valued, the approximator for the non-linearity N_o , becomes a real value

$$N_o = \frac{2}{A} \overline{y(t) \sin \psi} \quad (2.2-3)$$

Where $x_o(t) = A \sin \psi$, and $y(t)$ is the non-linearity output due to $x_o(t)$.

Non-linearity model for the "Slow component" (representing $x_r(t)$ and $x_d(t)$)

In the case $x_r(t)$ and $x_d(t)$ are "slow" compared to $x_o(t)$, the approximator for the slow components is:

$$N_r = \frac{\overline{y(t)}}{x_r(t)} \quad N_d = \frac{\overline{y(t)}}{x_d(t)} \quad N_f = N_r = N_d = \frac{\overline{y(t)}}{x_f(t)} \quad (2.2-4)$$

Where N_r and N_d represent the approximator for the signals due to the command ($x_r(t)$) and disturbance ($x_d(t)$) inputs, and N_f is the approximator for the "forcing" signals due to either the command or disturbance signals ($x_f(t)$).

Equation 2.2-4 has a very direct physical interpretation. $\overline{y(t)}$ is the d.c. value of the non-linearity output. $x_f(t)$ is the value of the "slow" input to the non-linearity. The non-linearity approximator for this signal is like a d.c. gain, being the relation between the d.c. value of the output and the value of the input. To avoid infinite values for N_f , when $x_f(t)$ tends to zero, only non-linearities that have no constant outputs when the input is zero, are considered. When $x_f(t) \rightarrow 0$, then $\overline{y(0)} \rightarrow 0$.

Non-linearity model for the random signal.

The random signal at the non-linearity input is due to noise in the system output sensor $\eta(t)$. In the case $x_n(t)$ is a random noise with gaussian distribution and zero mean, then the approximator N_η for the random input $x_n(t)$ is:

$$N_\eta = \frac{1}{\sigma^2} \overline{y(t)x_n(t)} \quad (2.2-5)$$

Where σ is the standard deviation of $x_n(t)$. Thus, for the random input, the non-linearity approximator is described as a pure gain, when the conditions stated above are satisfied.

Non-linearity model for combined inputs.

If the input to the non-linearity is composed of a sinusoidal and a slow signal, $x(t) = x_o(t) + x_f(t)$, particular approximators are used yielding the Dual-input describing function (D.I.D.F.). The D.I.D.F. "quasi-linearization" of the non-linear element will allow analysis and synthesis of systems where limit cycling exists and the command input and disturbance responses are the final issue. We can assume the "slow-signal" $x_f(t) = x_d(t) + x_r(t)$, so $x(t) = x_o(t) + x_d(t) + x_r(t)$. By

"slow signal" we assume $x_d(t)$ and $x_r(t)$ vary "little" during a cycle of oscillation of $x_o(t)$. The non-linear approximation is called "quasi-linearization" and not "linearization" for two reasons: first, each of the $h_i(t)$ in Figure 2.2-1 performs as "a linear system" to the particular set of inputs $x_i(t)$ for which it is derived, and some of the $h_i(t)$ may depend on some parameters of its own or other inputs (like the magnitude of the oscillation $x_o(t)$). Second, as a consequence of the approximator dependence on these parameters, there will be some constraints on the parameter uncertainty region which allow the same linear model.

The non-linearity used in this work is an ideal relay. The same results can be generalized for any saturating, static, single valued, odd non-linearity, if it is driven "hard" enough into saturation, twice in each cycle of the oscillating signal $x_o(t) = A \sin(\omega_o t)$. Figure 2.2-2 represents the ideal relay representation, where $x(t)$ is its input and $y(t)$ its output.

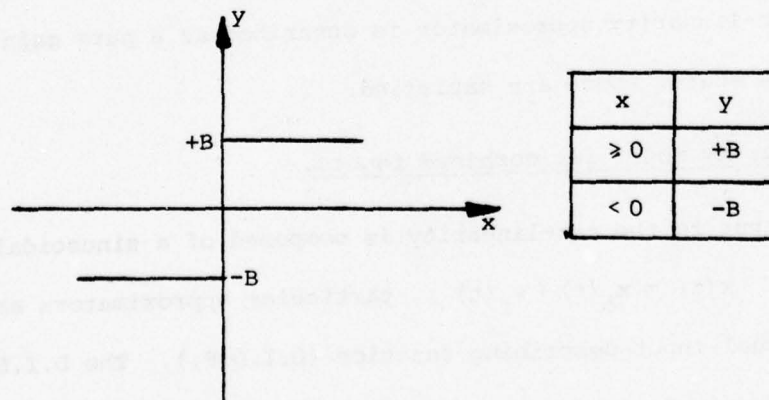
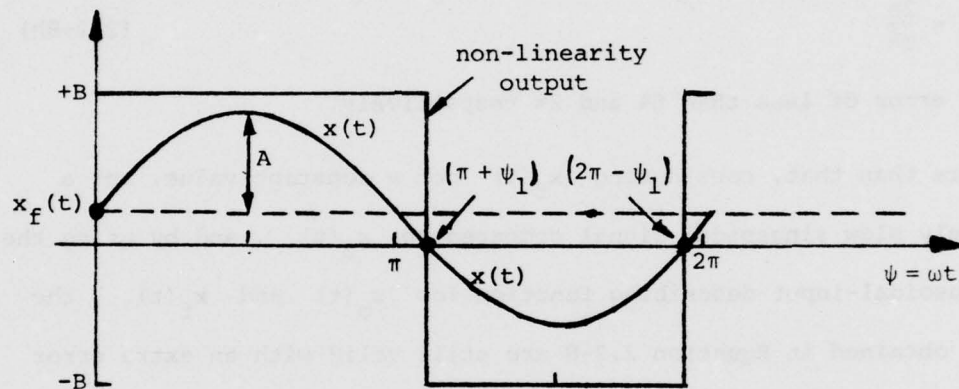


Figure 2.2-2 - Ideal relay representation

Figure 2.2-3 illustrates the ideal relay operation (input-output), when the input $x(t) = x_o(t) + x_f(t)$, and $x_f(t)$ is taken as a constant for one cycle of $x_o(t)$.

Figure 2.2-3 - Ideal relay operation

Input - $x(t) = \text{sinus} + \text{slow signal}$



Due to the constant value of $x_f(t)$, the switching point is not symmetrically related to the oscillation, so a bias component exists in y . To calculate the non-linearity approximator N_o for the sinusoidal component, Equation 2.2-3 is used, and the result is: [12]

$$N_o = \frac{4B}{\pi A} \cos \psi_1 \quad (2.2-6a)$$

$$\text{But } \cos \psi_1 = \sqrt{1 - \left(\frac{x_f}{A}\right)^2} \quad (2.2-6b)$$

$$N_o = \frac{4B}{\pi A} \sqrt{1 - \left(\frac{x_f}{A}\right)^2} \quad (2.2-6c)$$

To calculate the non-linearity approximator N_f for the slow component,

Equation 2.2-4 is used and the result is

$$N_f = \frac{2B}{\pi x_f} \sin^{-1} \left(\frac{x_f}{A} \right) \quad (2.2-7)$$

If $\left| \frac{x_f}{A} \right| \leq \frac{1}{3}$, Equations 2.2-6 and 2.2-7 can be approximated by

$$N_o = \frac{4B}{\pi A} \quad (2.2-8a)$$

$$N_f = \frac{2B}{\pi A} \quad (2.2-8b)$$

With an error of less than 6% and 2% respectively.

More than that, considering $x_f(t)$ not a constant value, but a relatively slow sinusoidal signal compared to $x_o(t)$, and by using the two sinusoidal-input describing function for $x_o(t)$ and $x_f(t)$, the results obtained in Equation 2.2-8 are still valid with an extra error of less than 5%, if the frequencies of the slow signal ω_{x_f} satisfy the relation [12]

$$\omega_{x_f} \leq \frac{\omega_o}{3} \quad (2.2-9)$$

Hence, the idea of quasi-linear approximation as stated above is quite clear. The quasi-linear approximations for both the sinusoidal component (N_o) and the bias component (N_f), are functions of parameters defining the inputs themselves (Equations 2.2-6, 2.2-7). If some constraints are included in these signals (quasi-linear conditions), the quasi-linear approximator becomes simpler, but is valid only in the region defined by the constraints. Summarizing, the quasi-linear conditions are (for reasonable engineering values of α , β):

$$\begin{aligned} \left| \frac{x_r(t)}{A} \right| &\leq \frac{1}{\alpha} & \alpha = 3 & , & \left| \frac{x_d(t)}{A} \right| &\leq \frac{1}{\alpha} & \alpha = 3 \\ \left| \frac{\omega_{br}}{\omega_o} \right| &\leq \frac{1}{\beta} & \beta = 3 & , & \left| \frac{\omega_{bd}}{\omega_o} \right| &\leq \frac{1}{\beta} & \beta = 3 \end{aligned} \quad (2.2-10)$$

If the conditions are satisfied, the non-linear approximators (for an ideal relay) for the several signals are:

$$\begin{aligned} N_o &= \frac{4B}{\pi A} = \frac{M_o}{A} & (\text{for } x_o(t)) \\ N_f = N_d = N_r &= \frac{2B}{\pi A} = \frac{M_f}{A} & (\text{for } x_r(t) \text{ and } x_d(t)) \end{aligned} \quad (2.2-11)$$

An important property to point out: If the system includes a saturating non-linearity (specifically an ideal relay), and there exists an oscillation at its input, the transmission for the relatively slow signals due to the command or disturbance inputs is defined by the oscillation amplitude. This property is going to be used and is responsible for the adaptive properties of the non-linear adaptive systems. In Equation 2.2-10 ω_{br} and ω_{bd} represent the bandwidths of the signals $x_r(t)$ and $x_d(t)$ respectively. The physical meaning of 2.2-10 is that $x_r(t)$ and $x_d(t)$ must be "small" and "slow" when compared respectively to the amplitude A and to the frequency ω_o of the oscillation $x_o(t)$.

Suppose now the input to the non-linearity is composed of a "fast" sinusoidal component $x_o(t) = A \sin(\omega_o t)$, of a "slow" sinusoidal component $x_f = b \sin(\omega_f t)$ and gaussian noise $x_\eta(t)$, with standard deviation σ and mean zero. It is shown^[12] that if

$$\begin{aligned} \frac{\omega_f}{\omega_o} &\leq \frac{1}{\beta} & \frac{b}{A} &\leq \frac{1}{\alpha} & \frac{\sigma}{A} &\leq \frac{1}{\alpha} & \alpha \approx \beta \approx 3 \end{aligned} \quad (2.2-12)$$

(a) (b) (c) (d)

Then, the approximators for the non-linearity regarding the random noise $x_n(t)$, the forced signal $x_f(t)$ and the oscillating component $x_o(t)$ are (for an ideal relay)

$$N_n = N_f = \frac{M_f}{A} = \frac{2B}{\pi A}, \quad N_o = 2N_f = \frac{M_o}{A} = \frac{4B}{\pi A} \quad (2.2-13)$$

While precise accuracies for combinations of these inputs are not available, good engineering results are expected. In any case if there is such a combination, the appropriate values of α and β can be determined.

Two points should be mentioned. First - even if $\eta(t)$ has a normal amplitude distribution, the output of the saturating non-linearity does not have the same properties, and as per Figure 2.1-1, the saturating non-linearity output is feedback, so the actual input to the non-linearity $x_n(t)$ is expected to be non-gaussian. But $G_1 G_2 P(j\omega)$ as mentioned before, has low pass characteristics, which tends to "normalize" [24] the amplitude distribution of the noise component $x_n(t)$ at the non-linearity input. Second, Equation 2.2-12c will not affect the design, because the approach is to satisfy the $r(t)$ and $d(t)$ specifications, with effectively minimum loop bandwidth.

2.3 Mathematical relations

Some relations involving the functions and the signals in the loop are developed in this section. In Figure 2.1-1, let:

$$L(j\omega) \triangleq G_1 G_2 P(j\omega) \quad (2.3-1a)$$

$$L_f(j\omega) \triangleq N_f L(j\omega) \quad (2.3-1b)$$

$$L_o(j\omega) \triangleq N_o L(j\omega) \quad (2.3-1c)$$

The well-known limit-cycling condition at frequency ω_o , is:

$$L_o(j\omega_o) = N_o L(j\omega_o) = -1 \quad (2.3-2)$$

Where $N_o = \frac{M_o}{A} = \frac{4B}{\pi A}$, in case of an ideal relay (Equation 2.2-8). So

$$\frac{4B}{\pi A} G_1 G_2 P(j\omega_o) = -1 \quad (2.3-3)$$

Which leads us to the two equations:

$$\left| \frac{4B}{\pi A} G_1 G_2 P(j\omega_o) \right| = 1 \quad (2.3-4a)$$

$$\angle \frac{4B}{\pi A} G_1 G_2 P(j\omega_o) = -180^\circ \quad (2.3-4b)$$

In any practical system there is always a frequency ω_o , for which Equation 2.3-4b is satisfied, due to the excess of poles over zeros existing in the linear part $L(j\omega)$ and/or to equivalent delays existent in the loop.

Once ω_o is determined by Equation 2.3-4b, the amplitude of the oscillating component at the non-linearity input $x_o = A \sin(\omega_o t)$ is determined by Equation 2.3-4a.

$$A = \frac{4B}{\pi} |G_1 G_2 P(j\omega_o)| \quad (2.3-5)$$

If we define the plant

$$P(j\omega) = K P_h(j\omega) \quad (2.3-6a)$$

with

$$\lim_{\omega \rightarrow \infty} P = \frac{K}{s^p} \quad (2.3-6b)$$

Where the gain K is explicitly displayed, then

$$\frac{A}{K} = \frac{4B}{\pi} |G_1 G_2 P_h(j\omega_o)| = \text{constant} \quad (2.3-7)$$

From Equation 2.3-1b the forced loop transmission, which is the one that defines the system response for both the command and disturbance input, is

$$L_f(j\omega) = N_f L(j\omega) = N_f \cdot G_1 G_2 P(j\omega) = \frac{2B}{\pi A} G_1 G_2 K P_h(j\omega)$$

So

$$L_f(j\omega) = \frac{K}{A} \cdot \frac{2B}{\pi} \cdot G_1 G_2 P_h(j\omega) \quad (2.3-8)$$

Substituting 2.3-7 in 2.3-8,

$$L_f(j\omega) = \frac{G_1 G_2 P_h(j\omega)}{2 |G_1 G_2 P_h(j\omega_o)|} \quad (2.3-9)$$

which reveals the outstanding adaptive property of the SOAS - Inherent zero sensitivity to the plant parameter K - the plant gain factor.

If there is no uncertainty in P_h (and obviously negligible uncertainty in the inserted "soft" compensation function $G_1(j\omega)$), then $L_f(j\omega)$, which is the effective loop transmission for the command and disturbance signals, has no uncertainty. The reason is that when the plant gain factor K changes its value, the limit cycle amplitude A changes proportionally, so $\frac{K}{A}$ is constant in Equation 2.3-8, i.e. the variation in K is cancelled out by the proportional variation in A . Note the strange combination of the two loop transmissions.

$L_o(j\omega) = \frac{4B}{\pi A} G_1 G_2 K P_h(j\omega)$, is valid only for the signal due to the self-oscillation, and determines the amplitude A of the oscillating component $x_o(t)$. $L_f(j\omega) = \frac{2B}{\pi A} G_1 G_2 K P_h(j\omega)$, is valid only for $\omega \leq \frac{\omega_o}{B}$, and its gain is determined by A . In the frequency regions $\frac{\omega_o}{B} \leq \omega < \omega_o$, and $\omega > \omega_o$, the loop is not well defined, so some "strange" results can be expected if we try to extrapolate results from the allowed bounds.

For example, if a command or disturbance input has strong components in the frequency range near ω_0 , it will affect $x_0 = A \sin(\omega_0 t)$, by changing its amplitude (depending on the phase of the signals relative to that of x_0), so the real gain identification and compensation accomplished by having $\frac{A}{K}$ constant (2.3-7) is spoiled. Similarly, in Figure 2.1-1, the plant output $Z(j\omega_0)$ is determined by $|Z(j\omega_0)| = \frac{4M}{\pi} |G_2 P(j\omega_0)|$, and is independent of both the command and disturbance input components at ω_0 .

2.4 SOAS sensitivity to uncertainty in plant dynamics $P_h(j\omega)$

If some of the dynamics characteristics of the plant (zeros and poles) are unknown, it will affect the loop transmission and the oscillation frequency, since the amplitude and the frequency of the oscillation must satisfy

$$\frac{4B}{\pi A} G_1 G_2 P(j\omega_0) = -1 \quad (2.4-1)$$

In this research we consider only uncertainty in the plant gain factor K of $P(j\omega) = K P_h(j\omega)$. A generalization of the methods developed here is possible by using the technique of References 9,10.

2.5 Synthesis procedure for the SOAS

In this section a synthesis procedure is derived for the SOAS to satisfy a certain specifications set. The synthesis procedure enables the designer to proceed systematically step by step, and obtain a design which satisfies the specifications and closely minimizes the effect of sensor noise at the plant input, in the sense defined in Appendix I.

The non-linearity used is an ideal relay, but the results are valid for any saturating, static, single valued, odd non-linearity, if it is driven "hard" enough into saturation.

2.5.1 Specifications and data

It is assumed that the set of specifications and data listed below are known.

Desired Command input response

The desired response to the command input is supposed to be known, in a frequency response form, either analytically or graphically. Since only the plant gain factor uncertainty is considered here, there is no need for providing bounds on the permissible variation in the system transfer function. The transmission for the command input is (Figure 2.1-1)

$$T_r(j\omega) \triangleq \frac{C_r}{R}(j\omega) = G_3 \frac{L_f(j\omega)}{1+L_f(j\omega)} \quad (2.5-1)$$

This expression is valid with good accuracy for $\omega \leq \frac{\omega_o}{\beta}$, because $L_f(j\omega)$ is valid for this range, where $\omega_o \geq \beta\omega_f$, and ω_f is the bandwidth of the desired transmission.

Disturbance Attenuation

The maximum permitted effect at the system output due to the disturbance signal is assumed given as a function of frequency, analytically or graphically. The disturbance transfer function is (Figure 2.1-1)

$$T_d(j\omega) \triangleq \frac{C_d}{D}(j\omega) = \frac{1}{1+L_f(j\omega)} \quad \forall \omega \leq \frac{\omega_o}{\beta} \quad (2.5-2)$$

Since $L_f(j\omega)$ is independent of K in $P = KP_h$, so is $T_d(j\omega)$.

Equation 2.5-2 is well valid for $\omega \leq \frac{\omega_o}{\beta}$, so if there is a special interest in defining the disturbance attenuation up to a certain frequency ω_d , then the oscillating frequency should be $\omega_o \geq \beta\omega_d$.

The plant definition

The representation of the plant by its differential equations or Laplace transform is assumed known, as well as the range of its gain uncertainty.

$$P(j\omega) = KP_h(j\omega) \quad (2.5-3)$$

$$K_1 \leq K \leq K_2 \quad (2.5-4)$$

Extreme command input

In a typical "purely linear system" this is not defined unless there are some expected non-linear problems like velocity or acceleration saturation, etc. For the SOAS, and for all the other oscillating systems, where quasi-linearity is a constraint not to be violated, the extreme signal the system is to process must be specified. The extreme command input is denoted $r_e(t)$, with Laplace transform $R_e(s)$ and has the largest magnitude and/or fastest dynamics input to be applied to the system. In general, a maximum step input will be considered.

Extreme disturbance input

The desired disturbance attenuation has already been defined. For the SOAS and for the other adaptive oscillating systems developed in later sections, it is also necessary to define the expected maximum equivalent disturbance at the plant output. The problem due to the

extreme disturbance is more complex than the one due to the extreme command, and in some cases there is no possible solution for certain extreme disturbances (Section 2.5-3). The extreme disturbance input is denoted $d_e(t)$, with its Laplace transform $D_e(s)$.

2.5-2 The Constraints

The constraints are the quasi-linear ones (Section 2.2) and another important one first used decisively by Horowitz [8], concerning the maximum oscillation component output, tolerable in any practical system. The conditions developed in detail in Section 2.2, Equations 2-10 - 2-12, are listed here for easier reference.

$$\max_t |x_i(t)| \leq \frac{A}{\alpha} \quad ; \quad i = r, d \quad (2.5-5a)$$

$$\omega_{bi} \leq \frac{\omega_o}{\beta} \quad ; \quad i = r, d \quad (2.5-5b)$$

$$\alpha = 3 \quad (2.5-5c)$$

$$\beta = 3 \quad (2.5-5c)$$

If these conditions are satisfied, the representation for the non-linearity is

$$N_r = N_d = \frac{M_f}{A} (= \frac{2B}{A} \text{ for ideal relay}) \quad (2.5-6a)$$

$$N_o = \frac{M_o}{A} = \frac{2M_f}{A} (= \frac{4B}{\pi A} \text{ for ideal relay}) \quad (2.5-6b)$$

B is the saturating level of the ideal relay (see Figure 2.2-2).

Maximum plant output oscillation

In the SOAS, with its deliberate oscillation signal, there must obviously be a maximum tolerable oscillation amplitude level at the

plant output, denoted by m , i.e.

$$|c_o(t)|_{\max} \leq m \quad (2.5-5a)$$

or (Figure 2.2-1)

$$\frac{4M}{\pi} |G_2 K P_h(j\omega_o)| \leq m \quad (2.5-5b)$$

2.5-3 Synthesis Procedure (Smooth solution)

The basic SOAS structure is drawn again in Figure 2.5-1, with N an ideal relay with saturating level B .

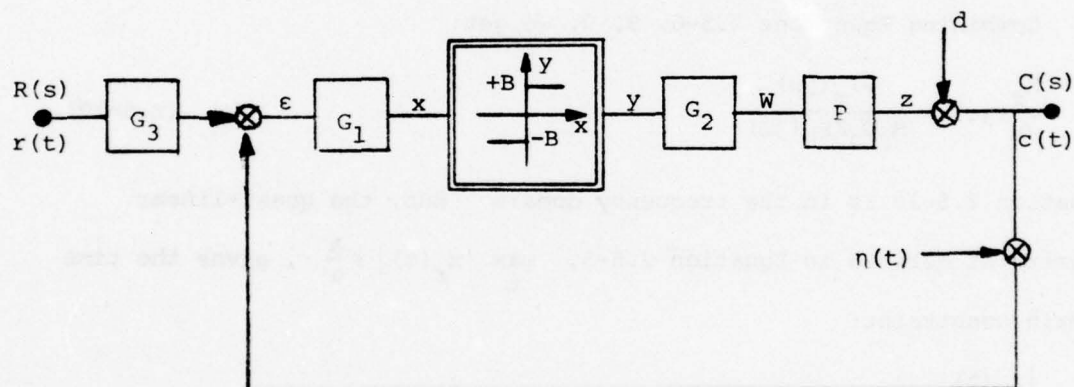


Figure 2.5-1 - Basic SOAS structure
Non-linearity - Ideal relay

The loop transmissions are:

$$L_f(j\omega) = N_f G_1 G_2 K P_h(j\omega) \quad , \quad \text{for } \omega \leq \frac{\omega_o}{B} \quad (2.5-6a)$$

$$N_f = \frac{M_f}{A} = \frac{2B}{A} \quad (2.5-6b)$$

$$L_o(j\omega_o) = N_o G_1 G_2 K P_h(j\omega_o) \quad , \quad \text{for } \omega = \omega_o \quad (2.5-7a)$$

$$N_o = \frac{M_o}{A} = \frac{4B}{A} \quad (2.5-7b)$$

Some relations will be derived based on the desired transmission $T_r(j\omega)$ for the command input and its extreme value $R_e(j\omega)$. From Equation 2.5-1 we have:

$$T_r(j\omega) \triangleq \frac{C_r}{R}(j\omega) = G_3 \frac{L_f(j\omega)}{1+L_f(j\omega)} \quad (2.5-8)$$

Also:

$$X_r(j\omega) \triangleq \frac{C_r(j\omega)}{N_f G_2 K P_h(j\omega)} \quad (2.5-9)$$

Combining Equations 2.5-6, 8, 9, we get:

$$\frac{X_r}{A}(j\omega) = \frac{RT_r(j\omega)}{M_f G_2 K P_h(j\omega)} \quad (2.5-10)$$

Equation 2.5-10 is in the frequency domain. But, the quasi-linear constraint defined in Equation 2.5-5, $\max_t |x_r(t)| \leq \frac{A}{\alpha}$, gives the time domain constraint:

$$\left| \frac{x_r(t)}{A} \right| \leq \frac{1}{\alpha} = \frac{1}{3} \quad (2.5-11)$$

There is no "direct" correspondence between constraints on $\left| \frac{x_r(t)}{A} \right|$ and on $\frac{X_r(j\omega)}{A}$. But some good engineering results can be obtained.

In Appendix II some approximate properties have been developed, which

give conditions for $\frac{X_r}{A}(j\omega)$ to satisfy Equation 2.5-11.

We assume in this section $\left| \frac{X_r}{A}(j\omega) \right|$ is "fairly smooth". Definition:

A transfer function is "fairly smooth" if all its poles and zeros are negative real. Actually, we would like to consider any transfer function $F(s)$ "fairly smooth" if $|F(j\omega)|$ can be well-approximated by another $|F_a(j\omega)|$ such that $F_a(s)$ has only negative real poles and zeros.

Hence, the definition should be that $F(s)$ is " ϵ -smooth" if $|F(j\omega)|$ can be approximated by $F_a(j\omega)$, with $\max_{\omega} |F(j\omega) - F_a(j\omega)| < \epsilon$, with all poles and zeros of $F_a(s)$, negative real. If $F(s)$ cannot be approximated by $F_a(s)$, it is considered to be "non-smooth". Figure 2.5-2 gives an example of a "smooth" and a "non-smooth" $\left| \frac{x_r}{A}(j\omega) \right|$.

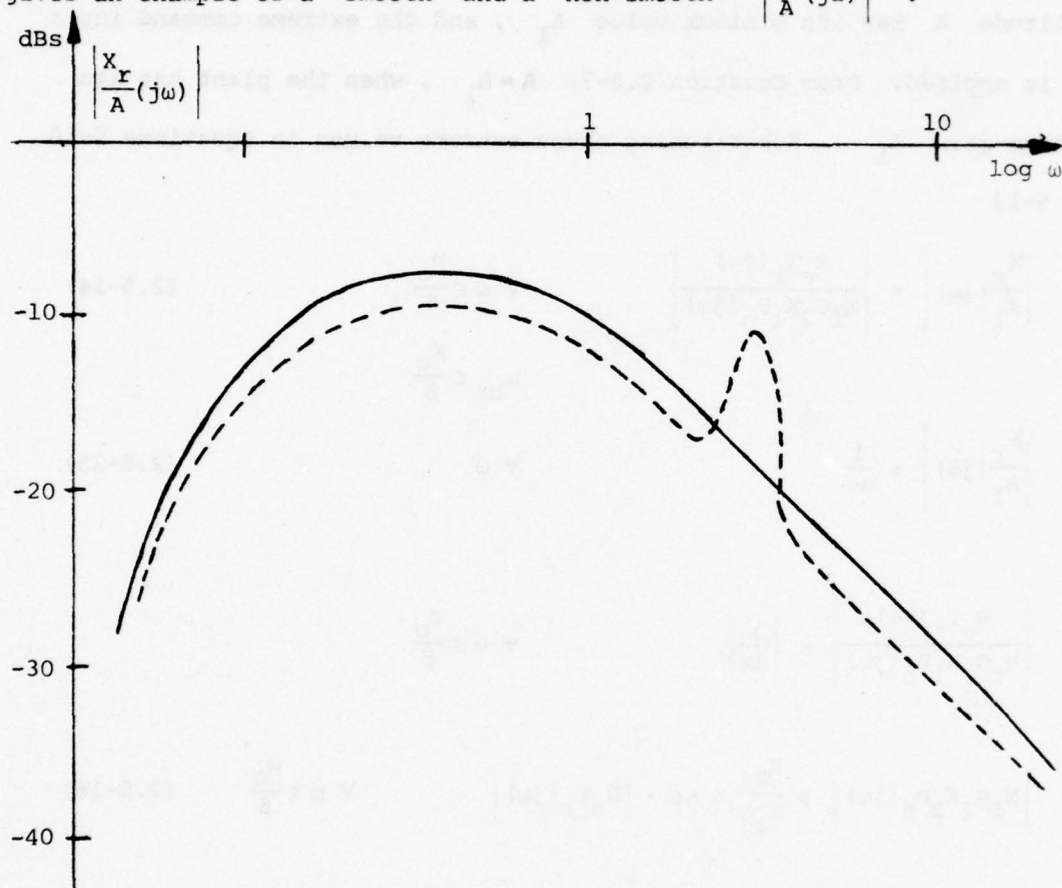


Figure 2.5-2 - Example of a "smooth" (—) and a "non-smooth" (---) $\left| \frac{x_r}{A}(j\omega) \right|$

Section 2.5-5 deals with "non-smooth" solutions for $\frac{x_r}{A}(j\omega)$, and points out some existing advantages and limitations.

In Appendix II it is shown that for a "smooth" $\frac{x_r}{A}(j\omega)$, if Equation 2.5-11 is satisfied, then

$$\left| \frac{x_r}{A}(j\omega) \right| \leq \frac{1}{\alpha\omega} \quad \forall \omega \quad (2.5-13)$$

It is most difficult to satisfy Equations 11 and 13, when the oscillation amplitude A has its minimum value A_1 , and the extreme command input r_e is applied. From Equation 2.3-7, $A = A_1$, when the plant has its minimum gain K_1 . Substituting these extreme values in Equations 5-10 and 5-13

$$\left| \frac{x_r}{A_1}(j\omega) \right| = \left| \frac{R_e T_r(j\omega)}{M_f G_2 K_1 P_h(j\omega)} \right| \quad \forall \omega \leq \frac{\omega_o}{\beta} \quad (2.5-14)$$

$$\omega_{br} \leq \frac{\omega_o}{\beta}$$

$$\left| \frac{x_r}{A_1}(j\omega) \right| \leq \frac{1}{\alpha\omega} \quad \forall \omega \quad (2.5-15)$$

so

$$\left| \frac{R_e T_r(j\omega)}{M_f G_2 K_1 P_h(j\omega)} \right| \leq \left| \frac{1}{\alpha\omega} \right| \quad \forall \omega \leq \frac{\omega_o}{\beta}$$

or

$$\left| M_f G_2 K_2 P_h(j\omega) \right| \geq \frac{K_2}{K_1} \cdot \alpha \cdot \omega \cdot \left| R_e T_r(j\omega) \right| \quad \forall \omega \leq \frac{\omega_o}{\beta} \quad (2.5-16)$$

Inequality (16) assures non-violation of quasi-linearity constraints, due to command input signals for $K_1 \leq K \leq K_2$.

An expression similar to Equation 16 may be obtained for the disturbance inputs. In Figure 2.1-1, due to disturbance inputs:

$$Z_d(j\omega) = -D(j\omega) \cdot \frac{L_f(j\omega)}{1+L_f(j\omega)} \quad \forall \omega \leq \frac{\omega_o}{\beta} \quad (2.5-17)$$

The corresponding input to N is:

$$x_d(j\omega) = \frac{Z_d(j\omega)}{N_f G_2 K P_h(j\omega)} = \frac{-D(j\omega)}{N_f G_2 K P_h(j\omega)} \cdot \frac{L_f(j\omega)}{1+L_f(j\omega)} \quad \forall \omega \leq \frac{\omega_o}{\beta} \quad (2.5-18)$$

From this point on, up to Equation 22, the same reasoning is used as in the last development (Equations 9 to 16). Substituting $N_f = \frac{M_f}{A}$ in Equation 18

$$\frac{x_d(j\omega)}{A} = \frac{-D(j\omega)}{M_f G_2 K P_h(j\omega)} \cdot \frac{L_f(j\omega)}{1+L_f(j\omega)} \quad \forall \omega \leq \frac{\omega_o}{\beta} \quad (2.5-19)$$

Again, if $\frac{x_d}{A}(j\omega)$ is "smooth", from Appendix II,

$$\left| \frac{x_d(t)}{A} \right| \leq \frac{1}{\alpha}, \text{ gives } \left| \frac{x_d}{A}(j\omega) \right| \leq \frac{1}{\alpha\omega} \quad \forall \omega \quad (2.5-20)$$

Substituting in Equations 19 and 20 the most difficult combination of parameters to satisfy, ($K=K_1$, $A=A_1$, $D(j\omega)=D_e(j\omega)$), we get:

$$\left| \frac{x_d}{A_1}(j\omega) \right| = \left| \frac{D_e(j\omega)}{M_f G_2 K_1 P_h(j\omega)} \right| \cdot \left| \frac{L_f(j\omega)}{1+L_f(j\omega)} \right| \leq \frac{1}{\alpha\omega} \quad \forall \omega \leq \frac{\omega_o}{\beta} \quad (2.5-21)$$

or:

$$\left| M_f G_2 K_2 P_h(j\omega) \right| \geq \frac{K_2}{K_1} \cdot \alpha \cdot \omega \cdot \left| D_e(j\omega) \cdot \frac{L_f(j\omega)}{1+L_f(j\omega)} \right| \quad \forall \omega \leq \frac{\omega_o}{\beta} \quad (2.5-22)$$

A difference may be noticed between Equations 16 and 22. In Equation 16 the inequality is completely defined apart from "far-off" poles and zeros that may perhaps be added to the nominal $T_r(j\omega)$. In Equation 22 $L_f(j\omega)$ is unknown, being the most important result of the system synthesis. In the meantime, let us derive additional relations involving the disturbance response. The specified maximum disturbance response provides bounds on $L_f(j\omega)$ for each frequency. Based on Equation 2.5-2, and on the defined specifications:

$$\begin{aligned} |T_d(j\omega)| &\triangleq \left| \frac{C_d}{D}(j\omega) \right| = \left| \frac{1}{1+L_f(j\omega)} \right| & \forall \omega \leq \frac{\omega_0}{\beta} & (2.5-23) \\ |T_d(j\omega)| &\leq |T_{d \min}(j\omega)| \end{aligned}$$

A very useful technique for design [1] is to use the Nichol's chart (Appendix I) and to plot on it the boundaries for a discrete number of frequencies of L_f , such that Equation 23 is satisfied. In the most general case there are bounds on L_f due to plant parameters uncertainty and to disturbance attenuation, but here the limit cycle and quasi-linearity wipe out the parameter uncertainty so the bounds are due entirely to Equation 23. It has been shown [5] that the optimum loop transmission in the sense defined in [5], is the one that "stays" on its respective bounds, for each frequency.

For plotting the bounds on $L_f(j\omega)$ at several frequencies in the Nichol's chart, once $|T_{d \min}(j\omega)|$ has been defined, the usual technique is to make a change of variables $\ell_f(j\omega) = \frac{1}{L_f(j\omega)}$, and use an "inverted" Nichol's chart, so the closed loop contours with constant gains can be used for plotting the bounds due to the disturbance attenuation (Appendix I), i.e. let

$$\begin{aligned} |T_d(j\omega)| &= \left| \frac{1}{1+L_f(j\omega)} \right| = \left| \frac{1}{1+\frac{1}{\ell_f(j\omega)}} \right| = \left| \frac{\ell_f(j\omega)}{1+\ell_f(j\omega)} \right| \leq |T_{d \min}(j\omega)| \\ & \forall \omega \leq \frac{\omega_0}{\beta} & (2.5-24) \end{aligned}$$

A typical specification for $T_{d \min}(j\omega)$, in graphical form is shown in Figure 2.5-3.

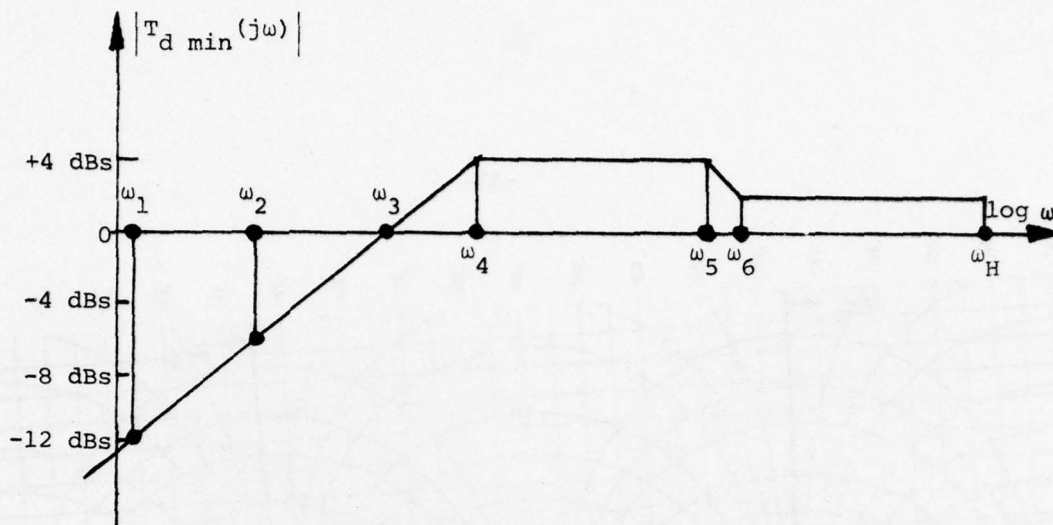


Figure 2.5-3 - Typical sketch for disturbance attenuation specifications

In Figure 2.5-3 ω_H is the highest frequency for which it is important to define the disturbance attenuation. As per Equation 2.4 we can plot the bounds for $\ell_f(j\omega)$ for several frequencies in $0 < \omega \leq \omega_H$. For example, for $\omega = \omega_1$, the bounds on the Nichol's chart for $\left| \frac{\ell_f(j\omega)}{1 + \ell_f(j\omega)} \right| = -12 \text{ dBs}$ is plotted in Figure 2.5-4 with the arrows indicating the allowed regions in the "inverted" Nichol's chart, where the minimum disturbance attenuation is satisfied. The same technique is used for $\omega = \omega_2$, $\omega = \omega_3$, $\omega_4 \leq \omega \leq \omega_5$, $\omega_6 \leq \omega \leq \omega_H$, and plotted in Figure 2.5-4. Obviously, L_f is easily obtainable from ℓ_f and vice versa.

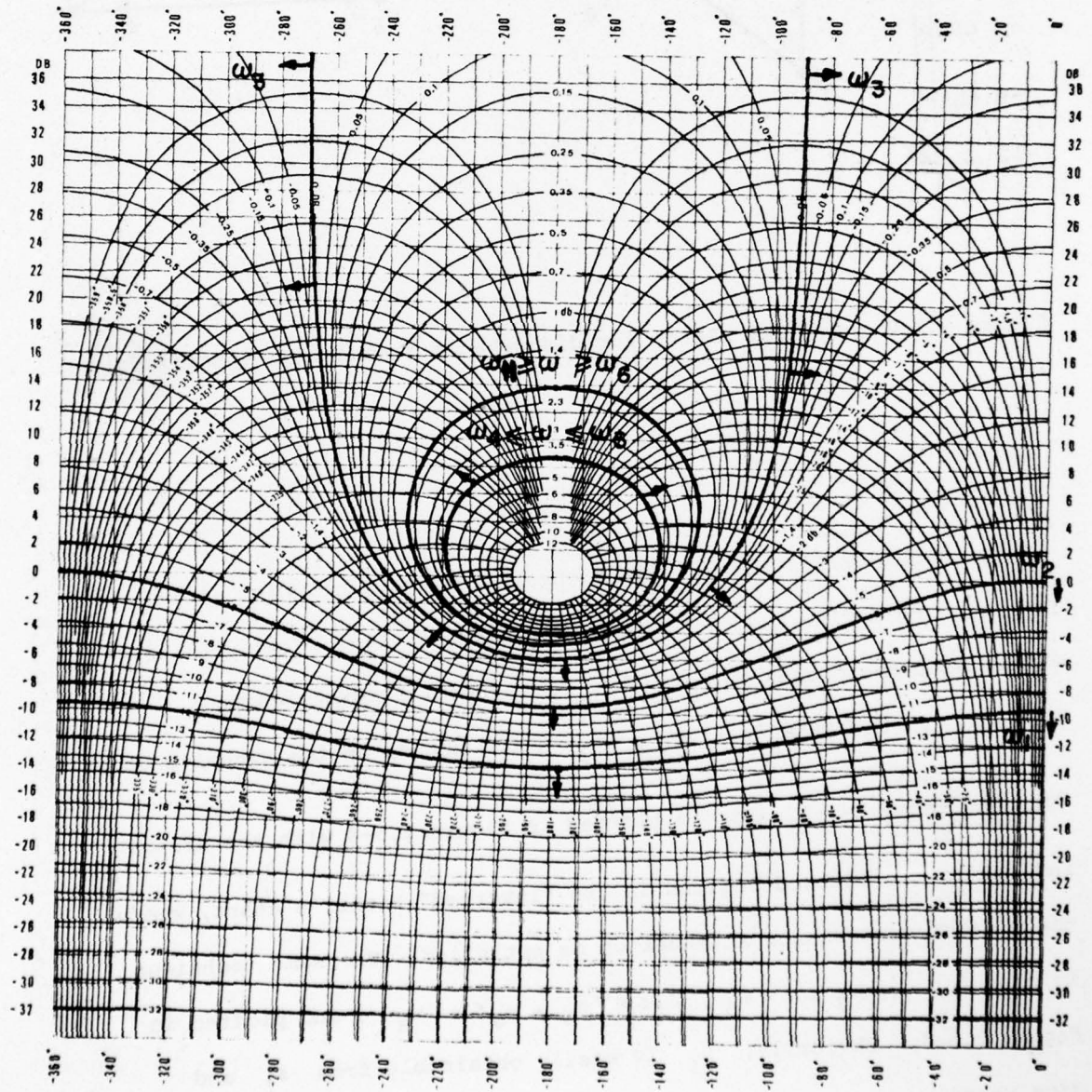


Figure 2.5-4 - Bounds on $\ell_f(j\omega) = \frac{1}{L_f(j\omega)}$,
for disturbance attenuation shown in Figure 2.5-3

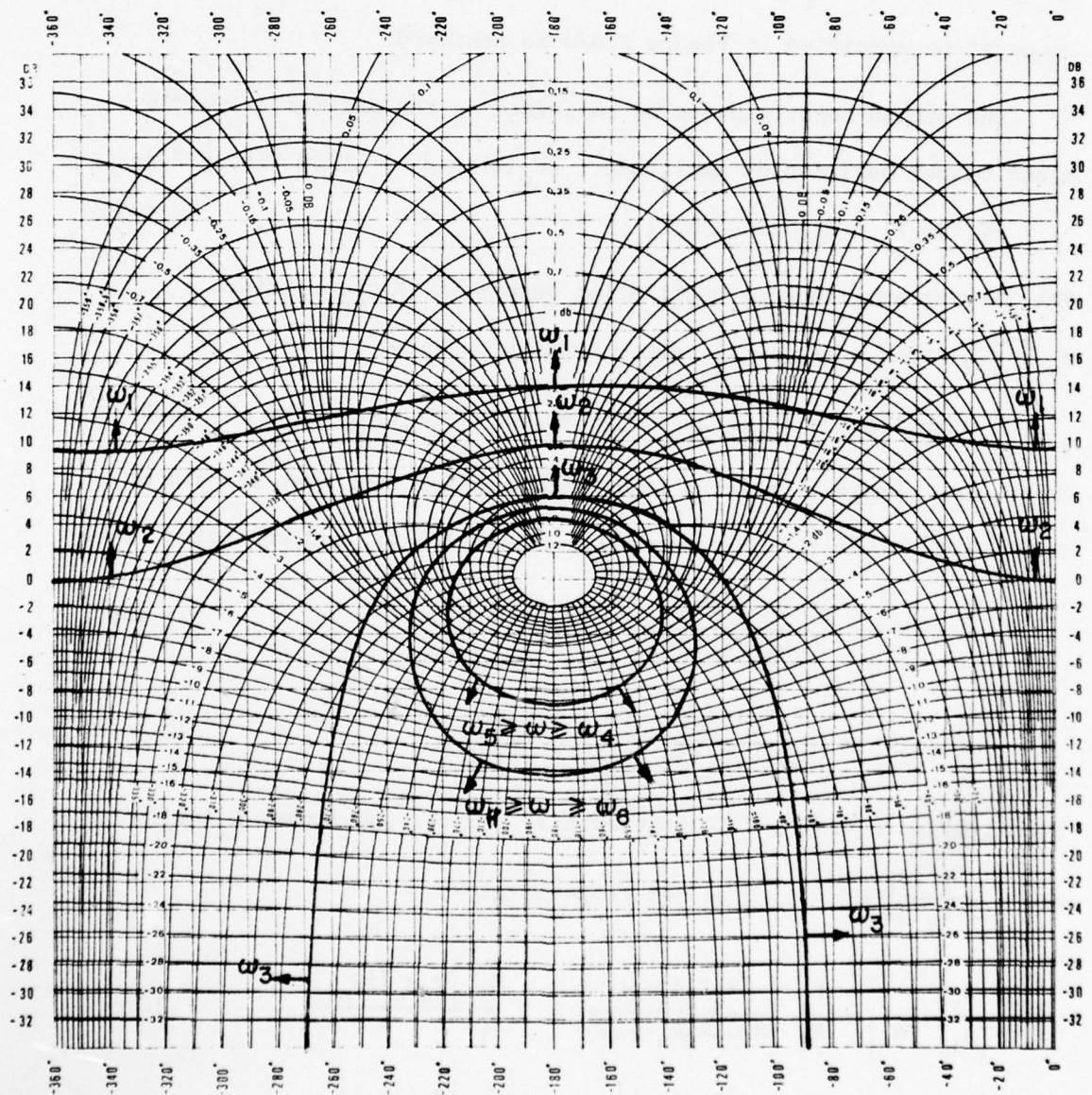


Figure 2.5-5 - Bounds on $L_f(j\omega)$,
for disturbance attenuation shown in Figure 2.5-3

By plotting the bounds of $L_f(j\omega)$ symmetrically to the origin of the Nyquist's chart ($\text{Log } |A| = 0$, $\angle\varphi = -180^\circ$, in the open loop coordinates), the bounds of $L_f(j\omega)$ are obtained. This is shown in Figure 2.5-5, where the bounds on the several frequencies for $L_f(j\omega)$ are plotted. If $L_f(j\omega)$ satisfies these bounds, then the disturbance attenuation specified in Figure 2.5-3 is achieved.

The second constraint to be satisfied is the maximum allowable plant output oscillation amplitude, $|C_o(t)| \leq m$. From Figure 2.5-1

$$|C_o(j\omega_o)| = M_o |G_2 K P_h(j\omega_o)| \quad (2.5-25)$$

The largest amplitude of oscillation occurs at $K = K_2$, since

M_o , $|G_2(j\omega_o)|$, $|P_h(j\omega_o)|$ are constants. Hence

$$|C_o(j\omega_o)|_{\max} = |M_o G_2 K_2 P_h(j\omega_o)| = |2M_f G_2 K_2 P_h(j\omega_o)| \leq m \quad (2.5-26)$$

We can now obtain a relation expressing a price that must be paid by using SOAS. Recalling Equations 2.5-14 and 2.5-21, and replacing $\omega = \omega_o$

$$\left| \frac{X_r}{A_1}(j\omega_o) \right| \approx \left| \frac{R_e T_r(j\omega_o)}{M_f G_2 K_1 P_h(j\omega_o)} \right| \quad (2.5-27)$$

$$\left| \frac{X_d}{A_1}(j\omega_o) \right| \approx \left| \frac{D_e(j\omega_o)}{M_f G_2 K_1 P_h(j\omega_o)} \right| \times \left| \frac{L_f(j\omega_o)}{1+L_f(j\omega_o)} \right| \quad (2.5-28)$$

Substituting Equation 2.5-26 in both 27 and 28, and since $L_f(j\omega_o) = -\frac{1}{2}$

and $\left| \frac{L_f(j\omega_o)}{1+L_f(j\omega_o)} \right| = 1$, we get respectively

$$\left| \frac{X_r}{A_1}(j\omega_o) \right| \approx \frac{K_2}{K_1} \left| \frac{R_e T_f(j\omega_o)}{M_f G_2 K_2 P_h(j\omega_o)} \right| \geq 2 \frac{K_2}{K_1} \frac{|T_f R_e(j\omega_o)|}{m} \quad (2.5-29)$$

$$\left| \frac{X_d}{A_1}(j\omega_o) \right| \approx \frac{K_2}{K_1} \frac{|D_e(j\omega_o)|}{|M_f G_2 K_2 P_h(j\omega_o)|} \geq 2 \frac{K_2}{K_1} \frac{|D_e(j\omega_o)|}{m} \quad (2.5-30)$$

In Equations 27 to 30, instead of the sign = (equal), there appears the sign \approx (similar). The reason is that the region of validity for Equations 2.5-14 and 2.5-21 is $\omega \leq \frac{\omega_o}{\beta}$, and we are extrapolating these equations for $\omega = \omega_o$. This extrapolation is valid as per Appendix III.

Equations 29 and 30 provide non-linear functions, which define the minimum value of the oscillation frequency when a "smooth" $\frac{x_r}{A_1}$ and $\frac{x_d}{A_1}$ are being considered.

It is very interesting to see how the factor $\frac{K_{\max}}{K_{\min}}$, which was the main reason for using an adaptive solution (in place of a linear time invariant design), reappears in the definition of ω_o , which defines the bandwidth of the loop transmission, since $|L_f(j\omega_o)| = \frac{1}{2}$. The reason for this "reappearance" is due to the fact that the quasi-linear constraint is the most difficult to satisfy when the plant has its minimum gain $K = K_{\min} = K_1$. On the other hand, the maximum oscillation level at the plant output occurs when the plant has its maximum gain, $K = K_{\max} = K_2$. These two constraints are such that the SOAS is over-designed in these aspects at the non-extreme plant gains and command and disturbance inputs.

The second NB factor is the ratio of a large signal ($Z_{ei} = T_r R_e$ or D_e) in the system to a small signal level - m . The product of these two factors gives, so to speak, the order of magnitude of the SOAS design problem. Also,

$$Z_{er}(j\omega_o) = R_e(j\omega_o) \cdot T_r(j\omega_o) \quad (2.5-31)$$

Where Z_{er} represents the extreme plant output due to the extreme command input $r_e(t)$.

Equation 29 becomes

$$\left| \frac{x_r}{A_1}(j\omega_o) \right| \geq \frac{2K_2}{K_1} \frac{|z_{er}(j\omega_o)|}{m} \quad (2.5-32)$$

Similarly

$$z_{ed}(j\omega_o) = D_e(j\omega_o) \times \frac{L_f(j\omega_o)}{1+L_f(j\omega_o)} = D_e(j\omega_o) \quad (2.5-33)$$

Where z_{ed} represents the extreme plant output due to the extreme disturbance $d_e(t)$.

Equation 30 becomes

$$\left| \frac{x_d}{A_1}(j\omega_o) \right| \geq 2 \frac{K_2}{K_1} \frac{|z_{ed}(j\omega_o)|}{m} \quad (2.5-34)$$

Let z_{ei} represent the extreme forced plant output components ($i=r,d$).

Equations 31 and 33 may be combined into

$$\left| \frac{x_e}{A_1}(j\omega_o) \right| \geq 2 \frac{K_2}{K_1} \frac{|z_e(j\omega_o)|}{m} \quad (2.5-35)$$

Where x_e is the extreme forced signal at the non-linearity input.

Still under the assumption of a smooth $\frac{x_e}{A_1}(j\omega)$, we can write

$$\left| \frac{x_e}{A_1}(j\omega) \right| \leq \frac{1}{\alpha\omega} = \frac{1}{3\omega} \quad (2.5-36)$$

So

$$2 \frac{K_2}{K_1} \frac{|z_e(j\omega_o)|}{m} \leq \left| \frac{x_e}{A_1}(j\omega_o) \right| \leq \frac{1}{3\omega_o} \quad (2.5-37)$$

A typical sketch for ω_o determination is plotted in Figure 2.5-6.

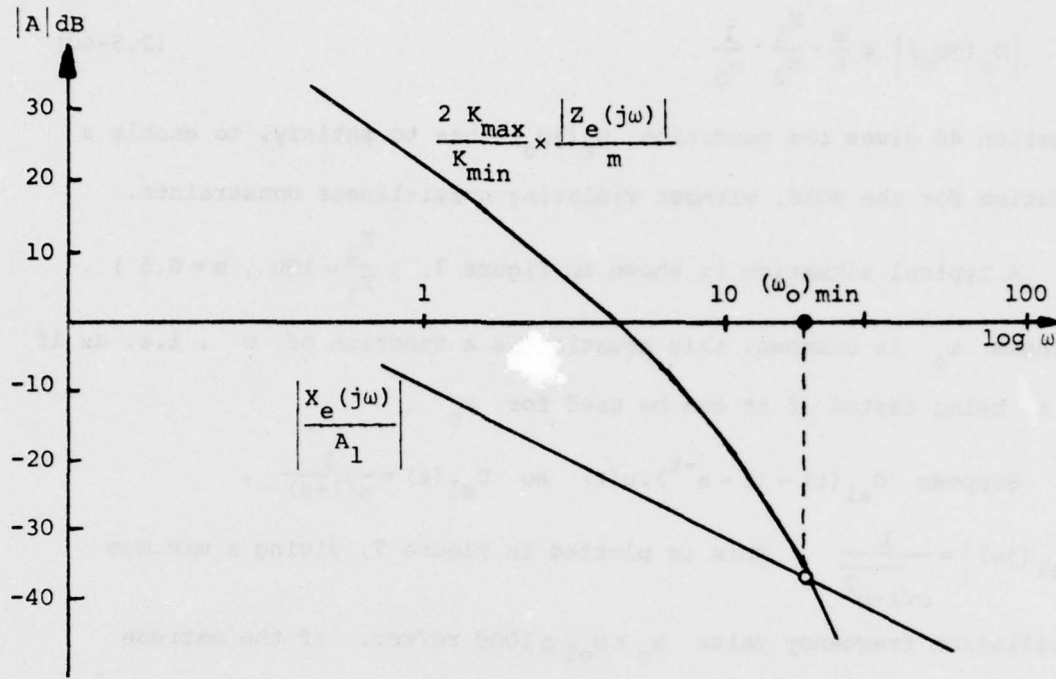


Figure 2.5-6 - Typical sketch of inequation 2.5-37
for a smooth solution

In some problems there is no possible solution, for some disturbance signals, without violating quasi-linear constraints. This can be seen by rewriting Equation 30

$$\left| \frac{X_d(j\omega_o)}{A_1} \right| \geq 2 \frac{K_2}{K_1} \frac{|D_e(j\omega_o)|}{m} \quad (2.5-38)$$

From Equation 2.5-21 at $\omega = \omega_o$

$$\left| \frac{X_d(j\omega_o)}{A_1} \right| \leq \left| \frac{1}{\alpha\omega_o} \right| = \left| \frac{1}{3\omega_o} \right|$$

So

$$2 \frac{K_2}{K_1} \frac{|D_e(j\omega_o)|}{m} \leq \frac{1}{3\omega_o} \quad (2.5-39)$$

$$|D_e(j\omega_o)| \leq \frac{m}{6} \cdot \frac{K_1}{K_2} \cdot \frac{1}{\omega_o} \quad (2.5-40)$$

Equation 40 gives the condition $D_e(j\omega_o)$ has to satisfy, to enable a solution for the SOAS, without violating quasi-linear constraints.

A typical situation is shown in Figure 7, ($\frac{K_2}{K_1} = 100$, $m = 0.6$).

Because ω_o is unknown, this equation is a function of ω , i.e. as if ω is being tested if it can be used for ω_o .

Suppose $d_{e1}(t) = (1 - e^{-t}) \cdot u(t)$ so $D_{e1}(s) = \frac{1}{s(1+s)}$,

$$|D_{e1}(j\omega)| = \frac{1}{\omega\sqrt{1+\omega^2}}. \text{ This is plotted in Figure 7, giving a minimum}$$

oscillation frequency value $\omega_o \geq \omega_{o1} \approx 1000$ rd/sec. If the extreme

disturbance is a step function $d_{e2}(t) = .1 \cdot u(t)$, so $|D_{e2}(j\omega)| = \frac{.1}{\omega}$,

$D_{e2}(j\omega)$ is parallel to $\frac{mK_1}{6\omega_o K_2}$, and there is no ω_o which satisfies

Equation 40. So, if there is a possibility of having a step disturbance at the plant output (this is usually not the case), the SOAS cannot be a recommended system, since the maximum allowed step would be

$$d_{estep} = \frac{mK_1}{6K_2} = \frac{1}{1000},$$

in our case, a ridiculously small value, compared to the oscillation component m , at the plant output. This problem does not exist for command inputs, since by rewriting Equations 29 and 21 at $\omega = \omega_o$, we get:

$$\frac{2K_2}{mK_1} |T_r R_e(j\omega_o)| \leq \frac{1}{3\omega_o} \quad (2.5-41)$$

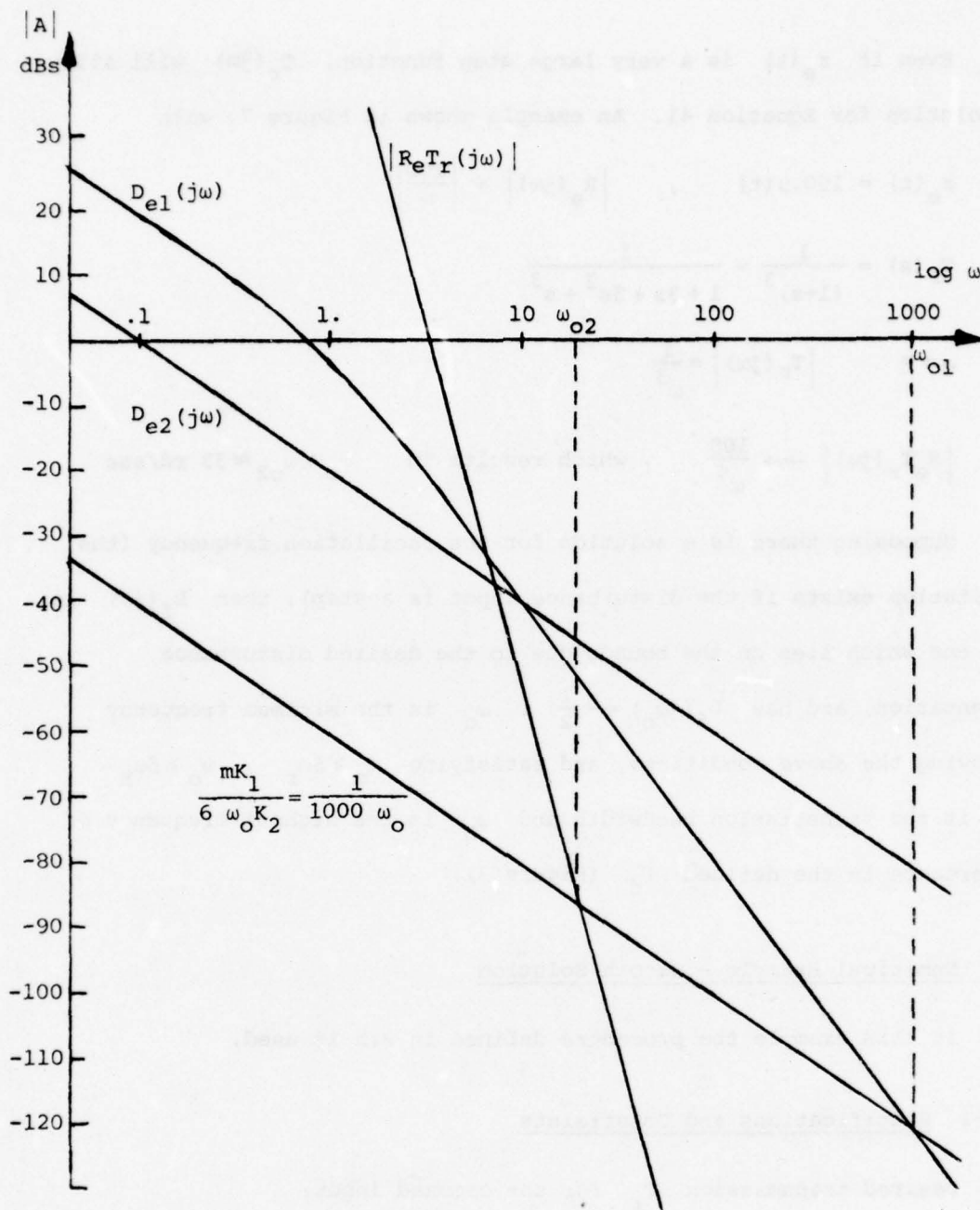


Figure 2.5-7 - Determination of ω_o
Extreme disturbance and command input signals

Even if $r_e(t)$ is a very large step function, $T_r(j\omega)$ will allow a solution for Equation 41. An example shown in Figure 7, with

$$r_e(t) = 100 \cdot u(t) \quad , \quad |R_e(j\omega)| = \left| \frac{100}{\omega} \right|$$

$$T_r(s) = \frac{1}{(1+s)^3} = \frac{1}{1+3s+3s^2+s^3}$$

$$\text{As } \omega \rightarrow \infty \quad |T_r(j\omega)| = \frac{1}{\omega^3}$$

$$\text{So } |R_e T_r(j\omega)| \rightarrow \frac{100}{\omega^4} \quad , \quad \text{which results in } \omega_o \geq \omega_{o2} \approx 33 \text{ rd/sec}$$

Supposing there is a solution for the oscillation frequency (the limitation exists if the disturbance input is a step), then $L_f(j\omega)$ is the one which lies on the bounds due to the desired disturbance attenuation, and has $L_f(j\omega_o) = -\frac{1}{2}$. ω_o is the minimum frequency allowing the above conditions, and satisfying $\omega_o \geq \beta\omega_r$, $\omega_o \geq \beta\omega_H$. ω_r is the transmission bandwidth and ω_H is the highest frequency of importance in the defined T_d (Figure 3).

2.6 Numerical Example - Smooth Solution

In this example the procedure defined in 2.5 is used.

2.6-1 Specifications and Constraints

Desired transmission T_r for the command input:

$$T_r(s) = \frac{1}{1 + \frac{2 \times .5}{.1}s + \frac{s^2}{.1^2}} \times \phi(s) \quad (2.6-1)$$

Where $\phi(s)$ includes far-off poles and zeros that can be added to the "nominal" desired transmission without significantly affecting the time response.

Disturbance Attenuation

The minimum disturbance attenuation required is plotted in Figure 2.6-1.

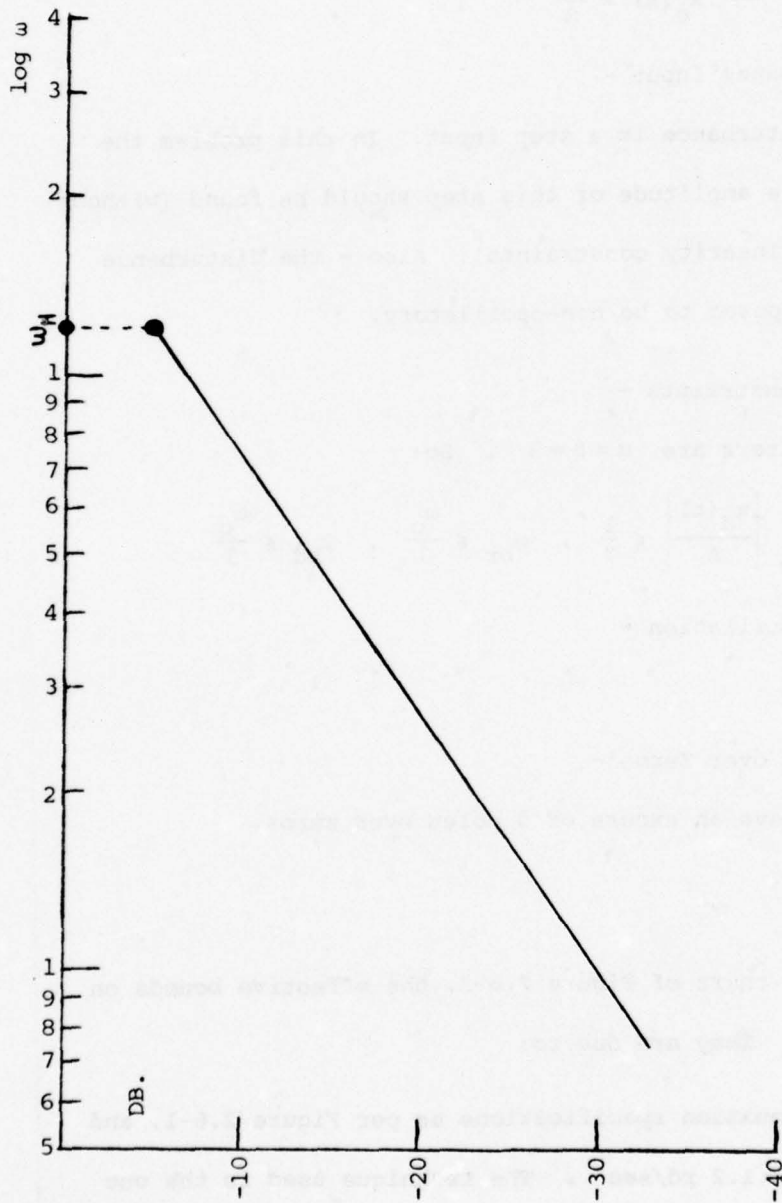


Figure 2.6-1 - SOAS - Numerical example - Minimum Disturbance Attenuation

Note there are no specifications for $\omega > \omega_H = 1.2 \text{ rd/sec.}$

- The Plant -

$$P(s) = \frac{K}{s} \quad 1 = K_1 \leq K \leq K_2 = 100$$

- Extreme Command Input -

$$r_e(t) = 75 \mu(t) \quad R_e(s) = \frac{75}{s}$$

- Extreme Disturbance Input -

The extreme disturbance is a step input. In this problem the maximum possible amplitude of this step should be found (without violating non-linearity constraints). Also - the disturbance response is supposed to be non-oscillatory.

- Quasi-linear Constraints -

The used parameters are $\alpha = \beta = 3$. So:

$$\left| \frac{x_r(t)}{A} \right| \leq \frac{1}{3} , \quad \left| \frac{x_d(t)}{A} \right| \leq \frac{1}{3} , \quad \omega_{br} \leq \frac{\omega_0}{3} , \quad \omega_{bd} \leq \frac{\omega_0}{3}$$

- Plant Output Oscillation -

$$|C_o(t)| \leq m = 1$$

- Excess of Poles over Zeros -

$L_f(j\omega)$ is to have an excess of 5 poles over zeros.

2.6-2 The solution

In the Nichol's chart of Figure 2.6-2, the effective bounds on $L_f(j\omega)$ are plotted. They are due to:

1. Disturbance attenuation specifications as per Figure 2.6-1, and valid for $\omega \leq \omega_H = 1.2 \text{ rd/sec}$. The technique used is the one explained in Section 2.5-3, Figures 2.5-3, 2.5-4, 2.5-5.

The bounds on $L_f(j\omega)$ are plotted for a certain number of frequencies.

ω (rd/sec)	$ T_d(j\omega) _{\min}$ (dB)
.08	-32
.15	-26
.29	-20
.57	-14
1.15	- 6

2. $L_f(j\omega_o)$ is the point represented by A in the Nichol's chart, with amplitude -6 dB and phase -180° .

3. A non-oscillatory step disturbance response can be handled by a very good and practical engineering solution by not allowing

$$\left| \frac{L_f(j\omega)}{1+L_f(j\omega)} \right| \text{ to be larger than } 1.3, \text{ or } \left| \frac{L_f(j\omega)}{1+L_f(j\omega)} \right| \leq 2.3 \text{ dB},$$

which is also plotted in the same Nichol's chart.

Next, using Equation 2.5-16

$$\left| M_f G_2 K_2 P_h(j\omega) \right| > \frac{K_2}{K_1} \cdot \alpha \cdot \omega \cdot \left| R_e T_r(j\omega) \right|$$

Substituting the functions as defined in this numerical example

$$\left| M_f G_2 K_2 P_h(j\omega) \right| \geq \left| \frac{22.500}{1 + 10s + 100s^2} \right|_{s=j\omega} \times \phi(j\omega)$$

(Note 22,500 \rightarrow 87 dB)

For a first reference assume $\phi(j\omega) = 1$, and this limit is plotted in Figure 2.6-3. Using Equations 2.5-22 and 2.5-26 at $\omega = \omega_o$

$$\frac{K_2}{K_1} \cdot \alpha \left| \omega_o D_e(j\omega_o) \right| \left| \frac{L_f(j\omega_o)}{1+L_f(j\omega_o)} \right| \leq \left| M_f G_2 K_2 P_h(j\omega_o) \right| \leq \frac{m}{2}$$

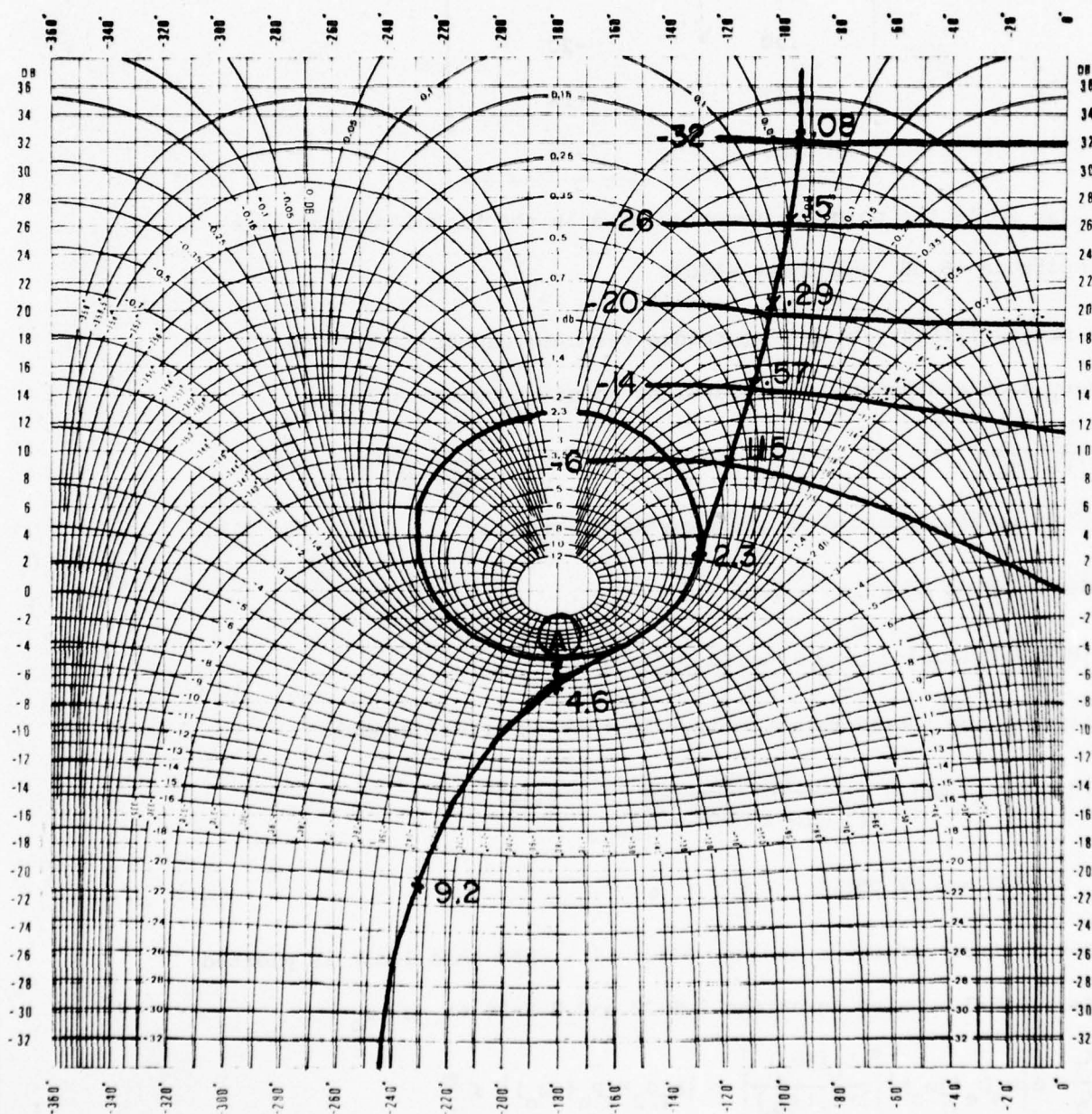
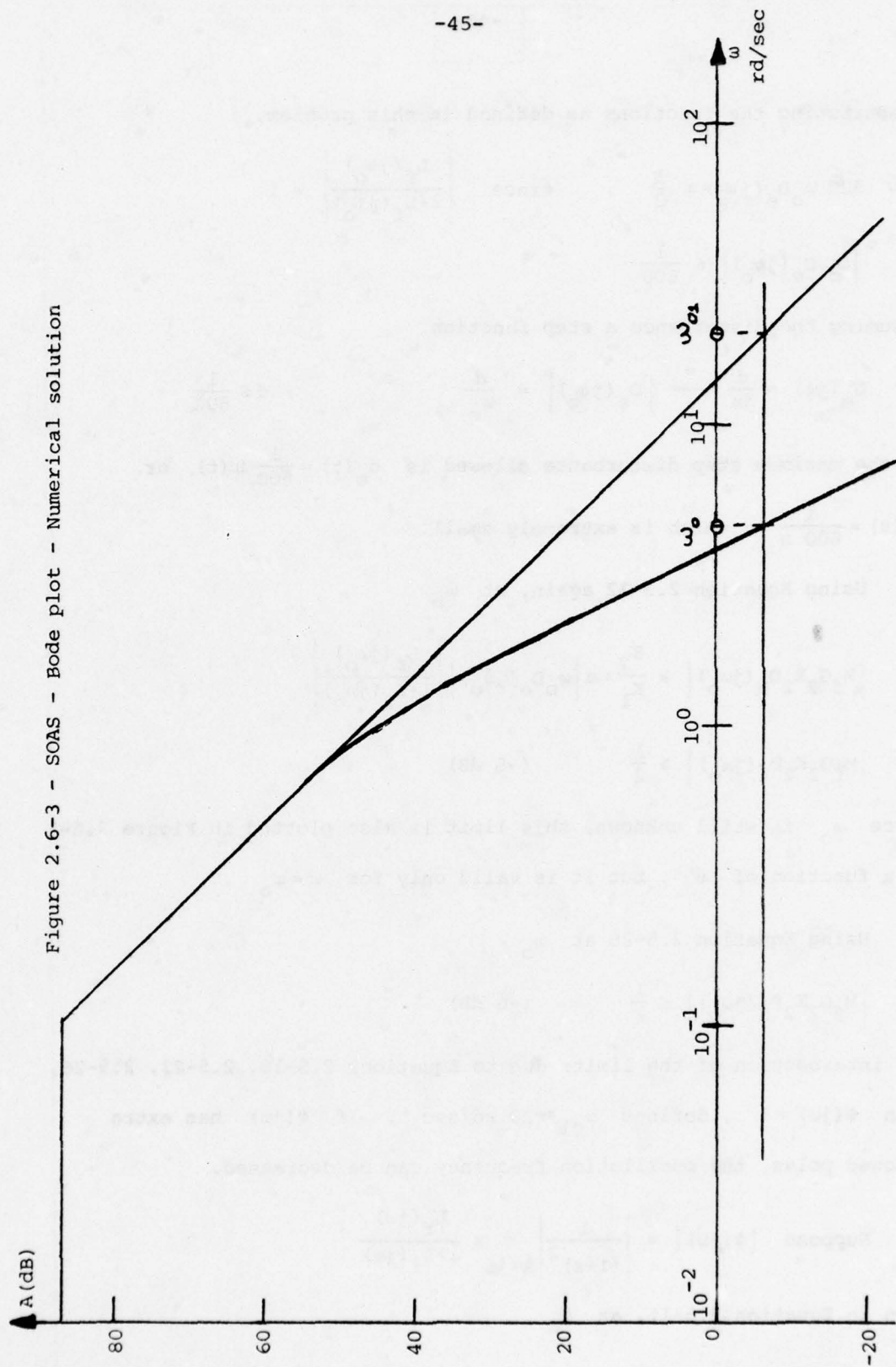


Figure 2.6-2 - SOAS - The solution for the numerical problem

Figure 2.6-3 - SOAS - Bode plot - Numerical solution



Substituting the functions as defined in this problem,

$$300 \omega_o D_e(j\omega_o) \leq \frac{1}{2} \quad , \quad \text{since} \quad \left| \frac{L_f(j\omega_o)}{1+L_f(j\omega_o)} \right| = 1$$

$$\text{or} \quad \left| \omega_o D_e(j\omega_o) \right| \leq \frac{1}{600}$$

Assuming the disturbance a step function

$$D_e(j\omega) = \frac{d}{j\omega} \rightarrow \left| D_e(j\omega_o) \right| = \frac{d}{\omega_o} \quad d \leq \frac{1}{600}$$

So the maximum step disturbance allowed is $d_e(t) = \frac{1}{600} u(t)$ or

$$D_e(s) = \frac{1}{600 s} \quad , \quad \text{which is extremely small.}$$

Using Equation 2.5-22 again, at ω_o

$$\left| M_f G_2 K_2 D_h(j\omega_o) \right| \geq \frac{K_2}{K_1} \cdot \alpha \left| \omega_o D_e(j\omega_o) \right| \left| \frac{L_f(j\omega_o)}{1+L_f(j\omega_o)} \right|$$

$$\left| M_f G_2 K_2 D_h(j\omega_o) \right| \geq \frac{1}{2} \quad (-6 \text{ dB})$$

Since ω_o is still unknown, this limit is also plotted in Figure 2.6-3 as a function of ω , but it is valid only for $\omega = \omega_o$.

Using Equation 2.5-26 at ω_o

$$\left| M_f G_2 K_2 P_h(j\omega_o) \right| \leq \frac{1}{2} \quad (-6 \text{ dB})$$

The intersection of the limits due to Equations 2.5-16, 2.5-22, 2.5-26, when $\phi(j\omega) = 1$, defines $\omega_{o1} \approx 20 \text{ rd/sec}$. If $\phi(j\omega)$ has extra allowed poles, the oscillation frequency can be decreased.

$$\text{Suppose} \quad \left| \phi(j\omega) \right| = \left| \frac{1}{(1+s)^2} \right|_{s=j\omega} \times \frac{L_f(j\omega)}{1+L_f(j\omega)}$$

Then in Equation 2.6-16, at ω_o

$$\left| M_f G_2 K_2 P_h(j\omega_o) \right| \geq \left| \frac{22.500}{1 + 10 s + 100 s^2} \right|_{s=j\omega} \times \left| \frac{1}{(1+s)^2} \right|_{s=j\omega}$$

The intersection of all the limits defines $\omega_o = 4.6$ rd/sec .

If extra poles can be allowed in the transmission, ω_o could eventually be decreased. It is assumed that no more delays can be added to the response time. Note that $\omega_o > 3 \omega_H = 3.6$ rd/sec , where ω_H is represented in Figure 2.6-1. This new constraint $\omega_o = 4.6$ rd/sec at the point A (-6 dB, -180°) is plotted back in Figure 2.6-2.

$L_f(j\omega)$ has to satisfy all the constraints in Figure 2.6-2. It has been shown [5] that the optimum loop transmission in a certain sense, is the one that "stays" on its respective bounds for each frequency. In this case

$$L_f(s) = \frac{2.7 \left(1 + \frac{s}{7.5} + \frac{s^2}{225} \right)}{s \left(1 + \frac{1.4}{4.6} s + \frac{s^2}{4.6^2} \right) \left(1 + \frac{1}{15} s + \frac{s^2}{225} \right)^2}$$

Which "stays" on the bounds for the specific frequencies (including $\omega_o = 4.6$ rd/sec at -6 dB, 180°) and it has an excess of 5 poles over zeros. $L_f(s)$ being defined, Equation 2.5-16 is used again

$$\left| M_f G_2 K_2 P_h(j\omega) \right| > \frac{K_2}{K_1} \cdot \alpha \cdot \omega \left| R_e \cdot G_3 \frac{L_f(j\omega)}{1+L_f(j\omega)} \right|$$

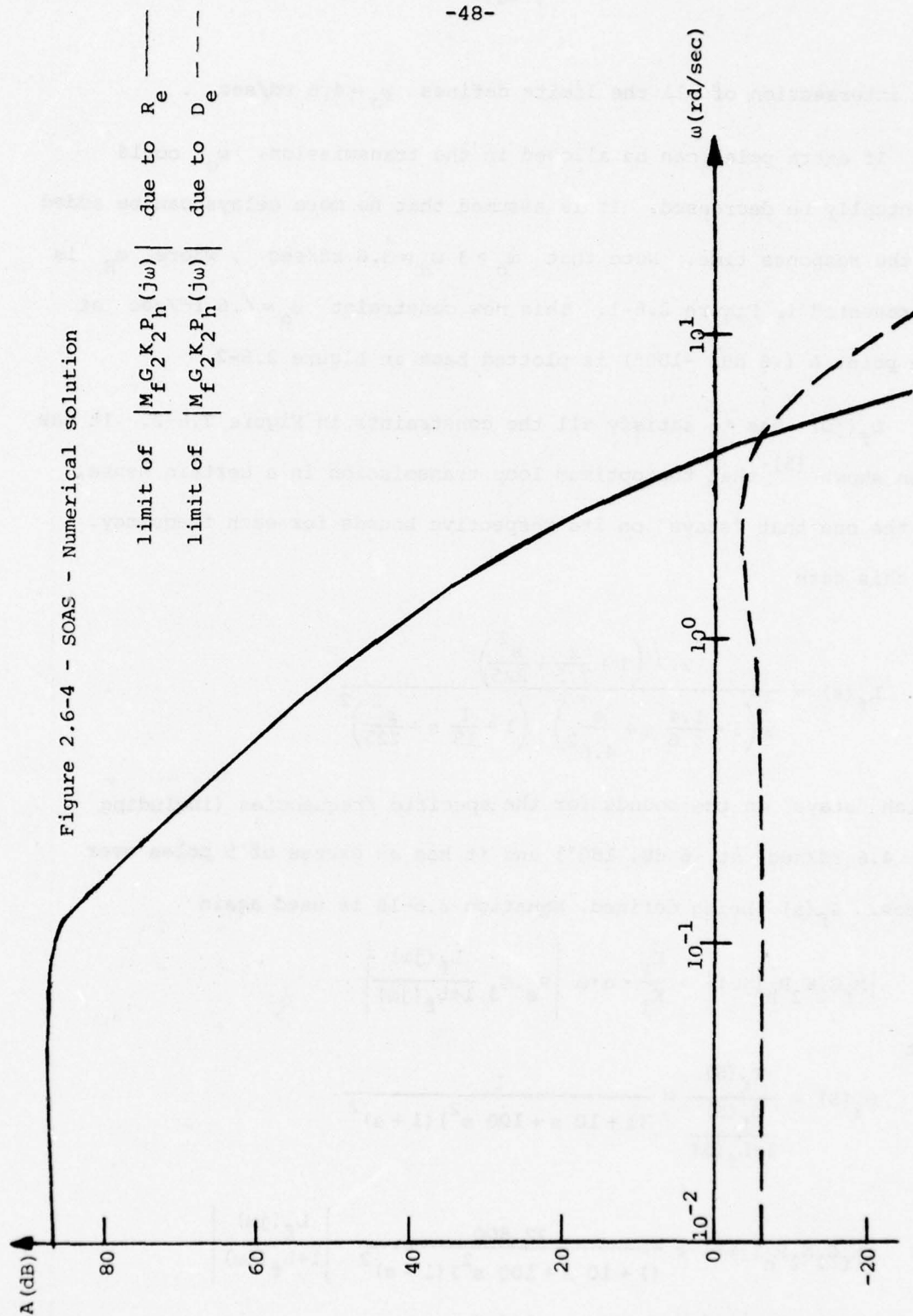
But

$$G_3(s) = \frac{T_f(s)}{\frac{L_f(s)}{1+L_f(s)}} = \frac{1}{(1+10s+100s^2)(1+s)^2}$$

So

$$\left| M_f G_2 K_2 P_h(j\omega) \right| \geq \frac{22.500}{(1+10s+100s^2)(1+s)^2} \cdot \left| \frac{L_f(j\omega)}{1+L_f(j\omega)} \right|$$

This limit is plotted in Figure 2.6-4.



Next Equation 2.5-22 is used

$$M_f G_2 K_2 P_h(j\omega) \geq \frac{K_2}{K_1} \cdot \alpha \cdot \omega \left| D_e(j\omega) \frac{L_f(j\omega)}{1+L_f(j\omega)} \right|$$

$$M_f G_2 K_2 P_h(j\omega) \geq \frac{1}{2} \frac{L_f(j\omega)}{1+L_f(j\omega)}$$

Which is also plotted in Figure 2.6-4.

As mentioned before (due to Equation 2.5-26), at ω_o ,

$$M_f G_2 K_2 P_h(j\omega_o) = \frac{1}{2}$$

We choose

$$M_f G_2 K_2 P_h(s) = \frac{3.200 (1+10s) \left(1 + \frac{.7}{4.6}s + \frac{s^2}{4.6^2}\right)}{s (1+10s+100s^2) (1+s)^2}$$

$$\text{Since } L_f(s) = G_1 G_2 \frac{M_f}{A_2} K_2 P_h(s)$$

$$\frac{G_1}{A_2}(s) = \frac{L_f(s)}{G_2 M_f K_2 P_h(s)} =$$

So

$$\frac{G_1}{A_2}(s) = \frac{1}{1200} \frac{(1+10s+100s^2)(1+s)^2 \left(1 + \frac{2s}{15} + \frac{s^2}{225}\right)}{(1+10s) \left(1 + \frac{.7}{4.6}s + \frac{s^2}{4.6^2}\right) \left(1 + \frac{1.4}{4.6}s + \frac{s^2}{4.6^2}\right) \left(1 + \frac{s}{15} + \frac{s^2}{15^2}\right)^2}$$

By defining $B = 16\pi$, $A_2 = 50$ (so $A_1 = .5$)

$$M_f = \frac{2B}{\pi} = 32, \text{ and } K_2 P_h(s) = \frac{100}{s}$$

$$G_2(s) = \frac{(1+10s) \left(1 + \frac{.7}{4.6}s + \frac{s^2}{4.6^2}\right)}{(1+10s+100s^2) (1+s)^2}$$

$$G_1(s) = \frac{1}{24} \frac{(1 + 10s + 100s^2)(1+s)^2 \left(1 + \frac{2s}{15} + \frac{s^2}{225}\right)}{(1+10s) \left(1 + \frac{.7}{4.6}s + \frac{s^2}{4.6^2}\right) \left(1 + \frac{1.4}{4.6}s + \frac{s^2}{4.6^2}\right) \left(1 + \frac{s}{15} + \frac{s^2}{15^2}\right)^2}$$

$G_3(s)$ has already been defined:

$$G_3(s) = \frac{1}{(1 + 10s + 100s^2)(1+s)^2}$$

The complete system is now fully defined.

2.6-3 Simulations and Results

Computer simulations were performed on the CDC 6400 system at the University of Colorado, using "Mimic" program. Command and disturbance step responses are calculated for three different plant gains $K=K_1=1$, $K=K_{med}=10$, $K=K_2=100$. The command input has always its extreme value $r_e(t) = 75 \mu(t-10)$, being applied at time $t=10$ seconds, after the limit cycle has achieved its steady state. The experiments last 50 seconds each.

In Figures 2.6-5 ($K=100$), 2.6-6 ($K=10$) and 2.6-7 ($K=1$), RN is the applied command input, X18 represents the input to the non-linearity and XC the system output. For a better presentation of the results, there are only two variables in each figure, corresponding to the same experiment (subtitled by a and b).

The applied step disturbance at the plant output is .012, which is larger than the expected (conservative) calculated $d_e(t)$, considering

$\left| \frac{x_d}{A_1}(j\omega) \right|$ has a smooth shape. $\left| \frac{x_d}{A_1}(j\omega) \right|$ is plotted in Figure 2.6-8 and shows how $\left| \frac{x_d}{A_1}(j\omega) \right|$ is larger than $\left| \frac{1}{3\omega} \right|$ in a certain region of

frequencies, and still its equivalent time response $\left| \frac{x_d}{A_1}(t) \right|$ is smaller than $\frac{1}{3}$. This property will be also used for a "non-smooth" $\frac{x_f}{A_1}(j\omega)$, in Section 2-7.

In Figures 2,6-9 ($K=100$) , 2.6-10($K=10$) , 2.6-11 ($K=1$) , D is the applied disturbance, X_{18} the input to the non-linearity, and X_C the system output. D is applied at $t=10$ seconds , and each experiment lasts 50 seconds. For better presentation only 2 variables are presented (for the same experiment, subtitles a, b).

Notice when $K=K_1=1$, quasi-linearity conditions at X_{18} are the most closely violated. When $K=K_2=100$, the oscillation plant output equals m .

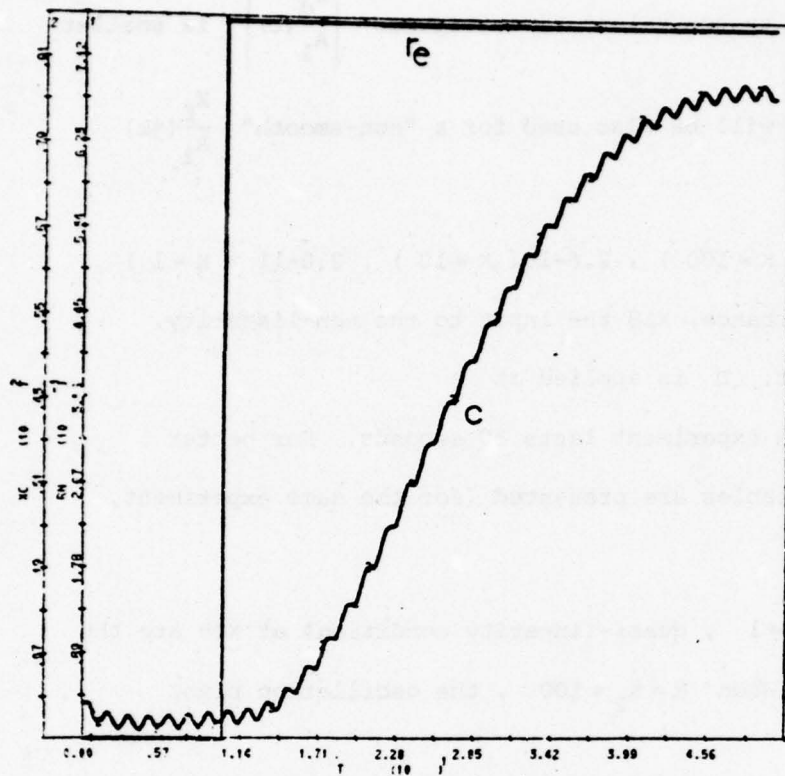


Figure 2.6-5b - SOAS - System Response

Extreme Command Input

K = 100

XC - System Output = \bar{C}

RN - Applied Command = \bar{e}

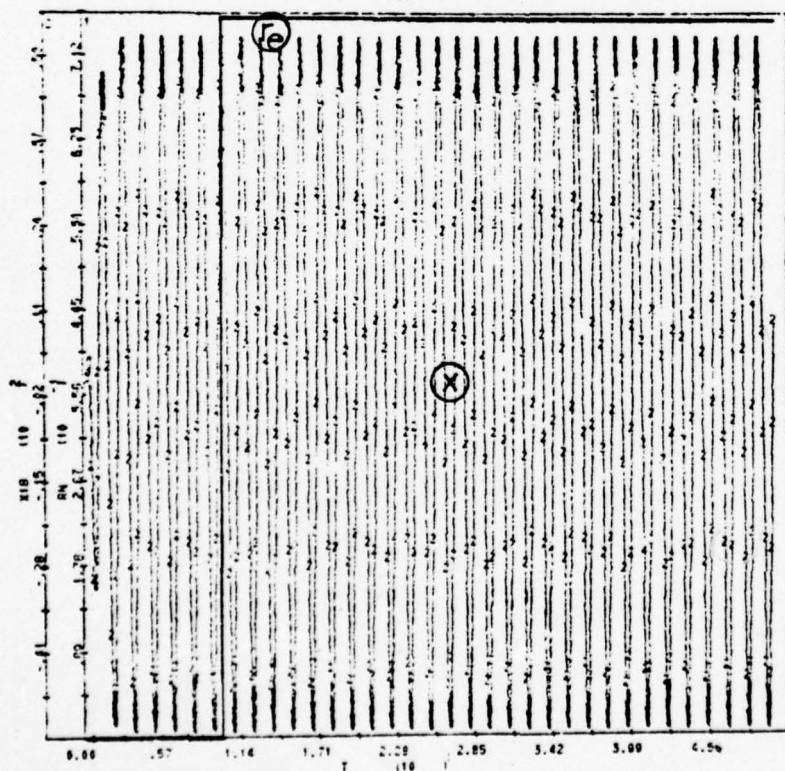


Figure 2.6-5a - SOAS - System Response

Extreme Command Input

K = 100

X 18 - Non-linearity Input = X

RN - Applied Command = \bar{e}

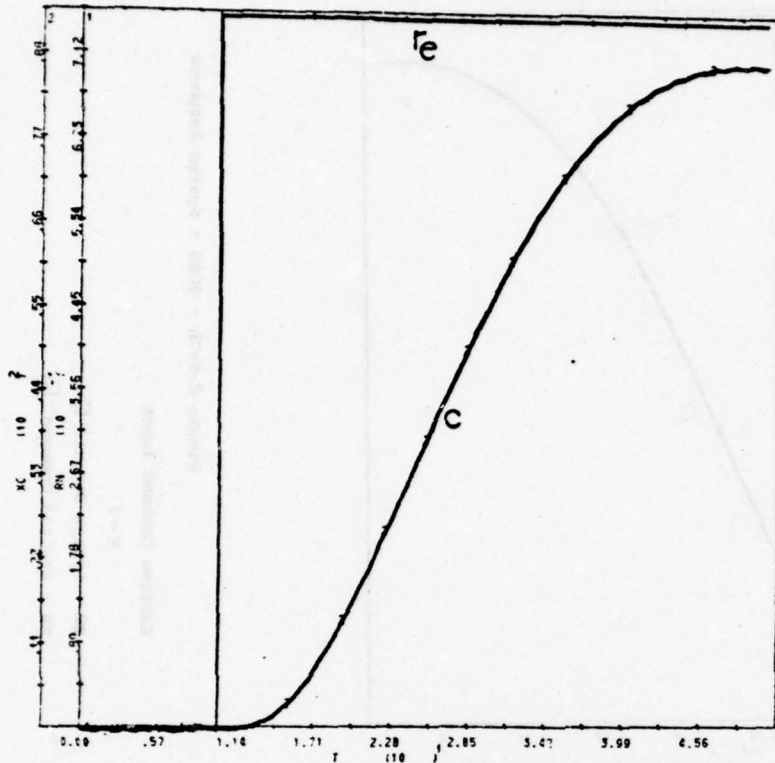


Figure 2.6-6a - SOAS - System Response

Extreme Command Input

K = 10

X 18 - Non-linearity Input = X

RN - Applied Command = e

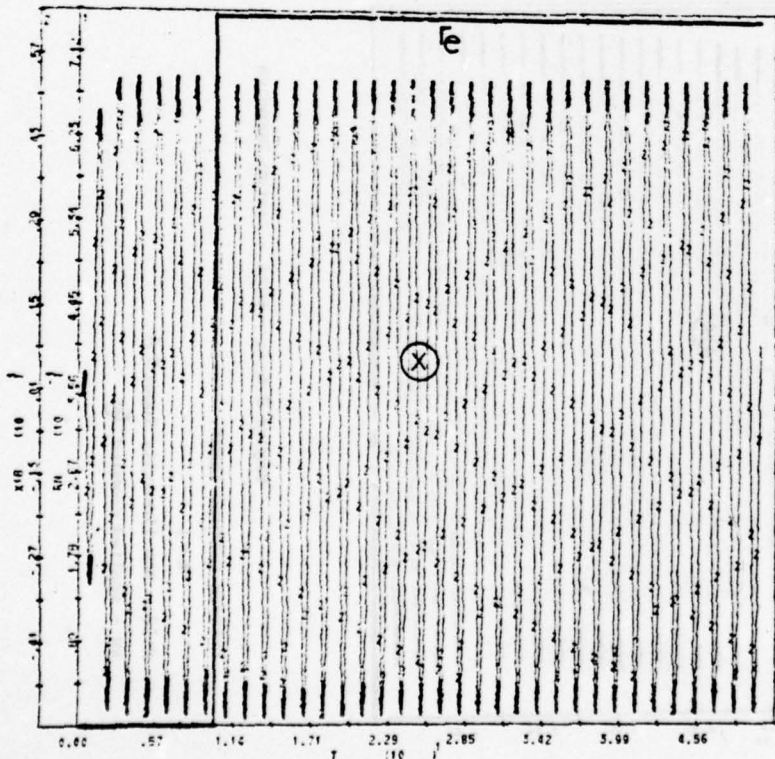


Figure 2.6-6b - SOAS - System Response

Extreme Command Input

K = 10

XC - System Output = C

RN - Applied Command = e

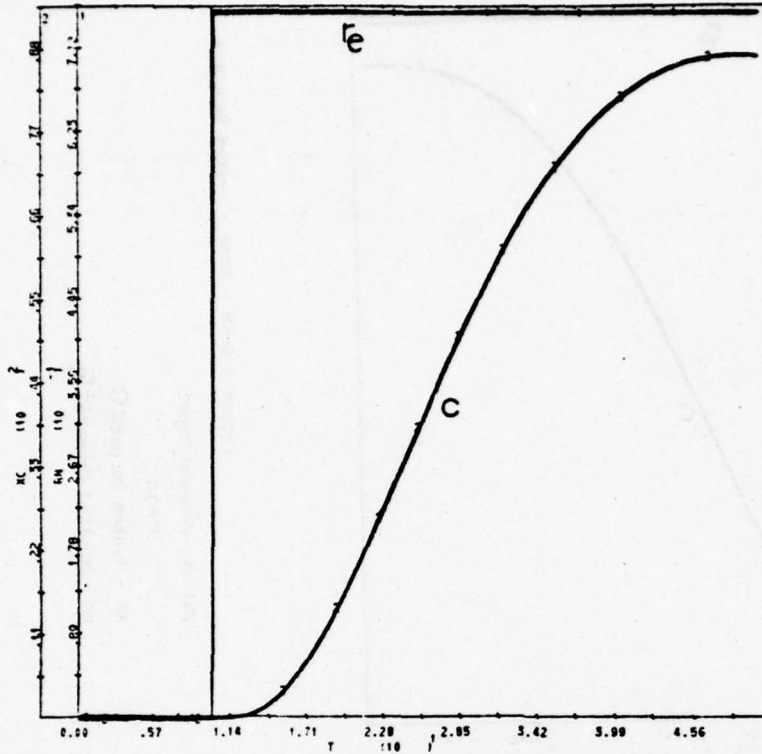


Figure 2.6-7b - SOAS - System Response

Extreme Command Input

$K = 1$

X_C - System Output = C

R_N - Applied Command = e

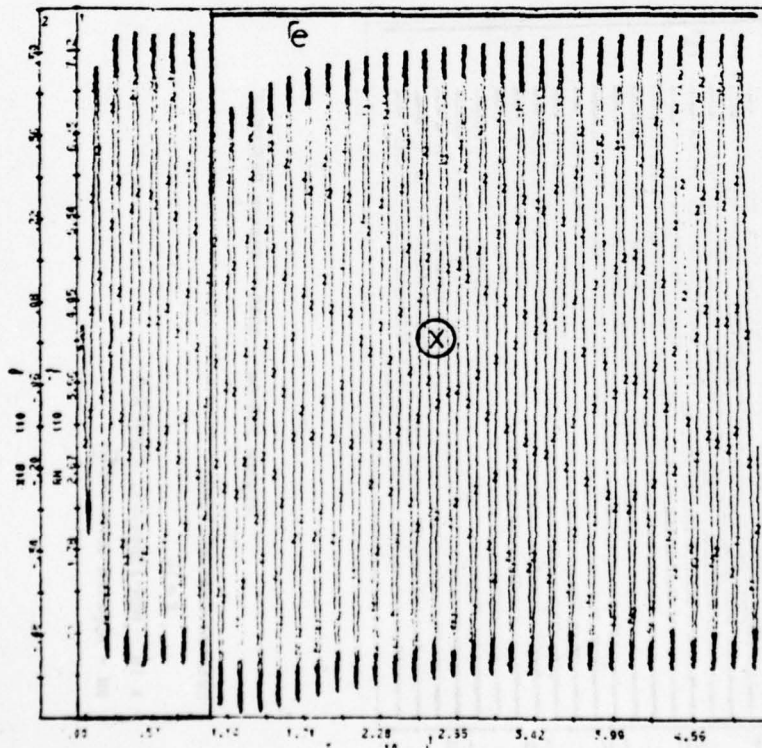


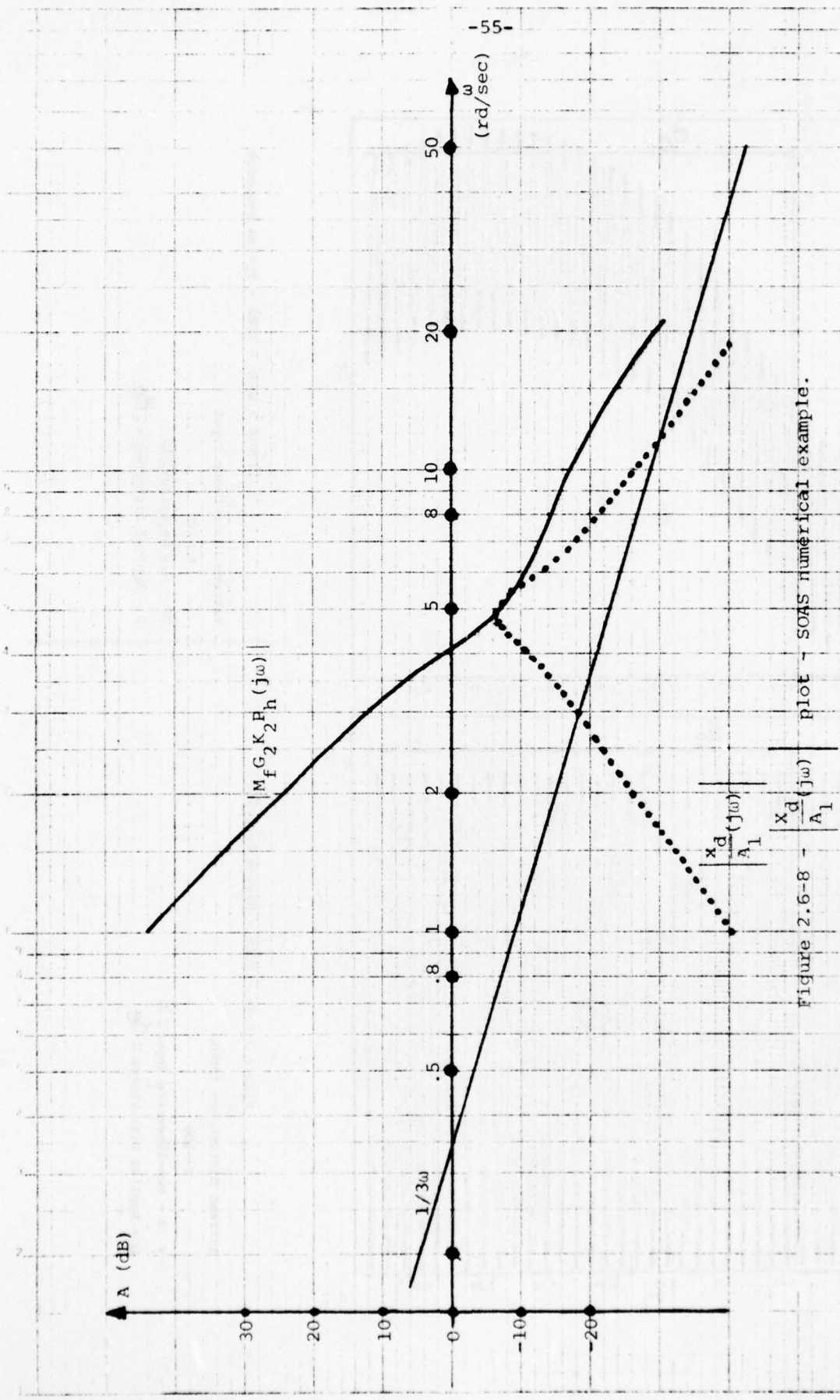
Figure 2.6-7a - SOAS - System Response

Extreme Command Input

$K = 1$

X_{18} - Non-linearity Input = X

R_N - Applied Command = e



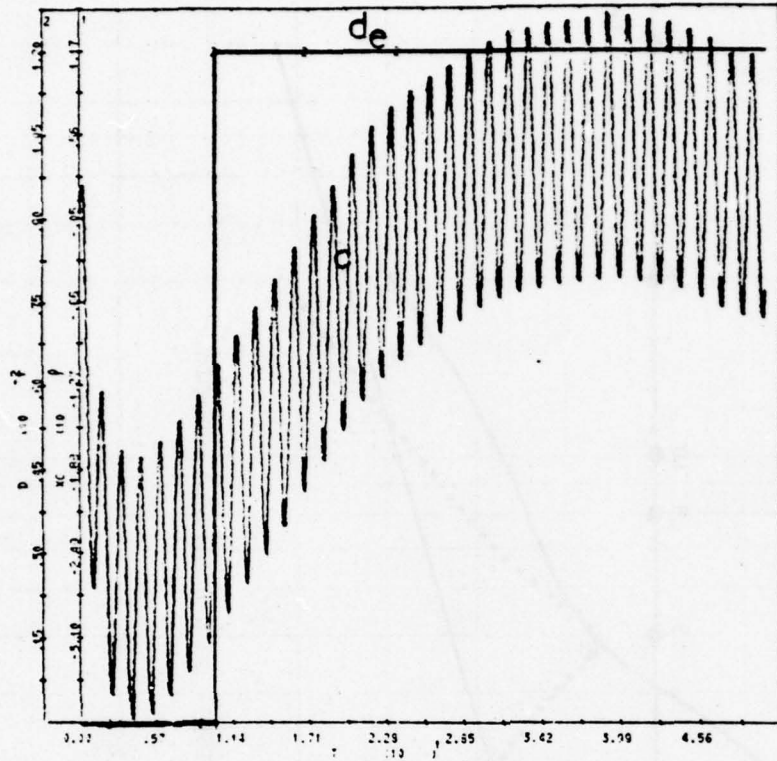


Figure 2.6-9a - SOAS - System Response

Extreme Disturbance Input

K = 100

X 18 - Non-linearity Input = X

D - Applied Disturbance = de

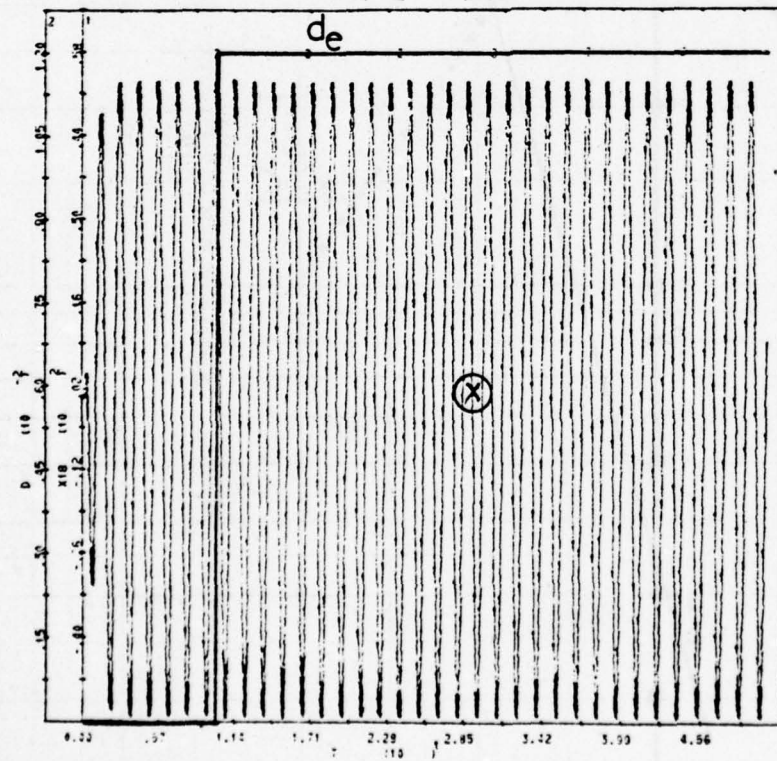


Figure 2.6-9b - SOAS - System Response

Extreme Disturbance Input

K = 100

XC - System Output = C

D - Applied Disturbance = de

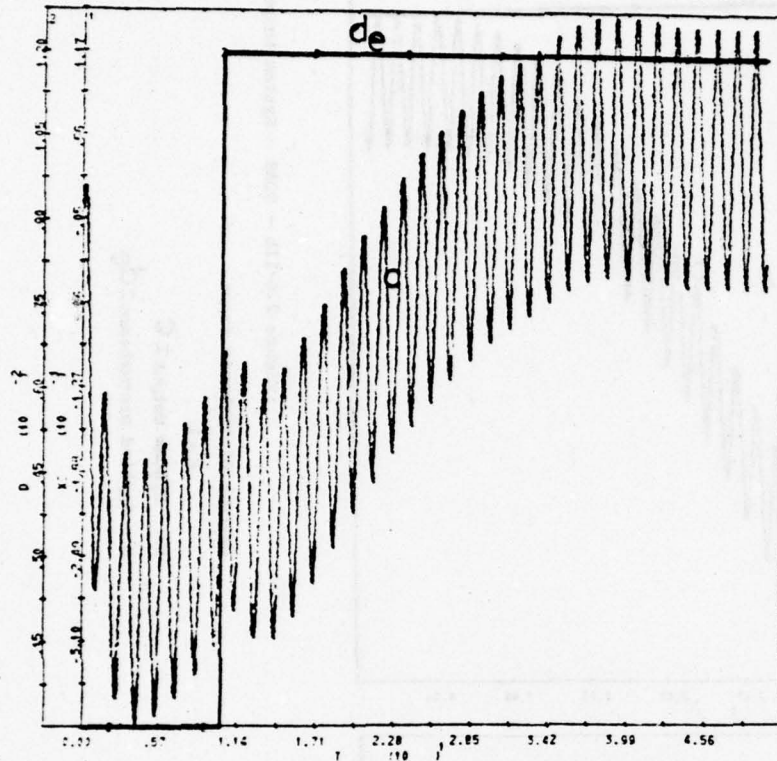


Figure 2.6-10a - SOAS - System Response

Extreme Disturbance Input

K = 10

X 18 - Non-linearity Input = X

D - Applied Disturbance = d_e

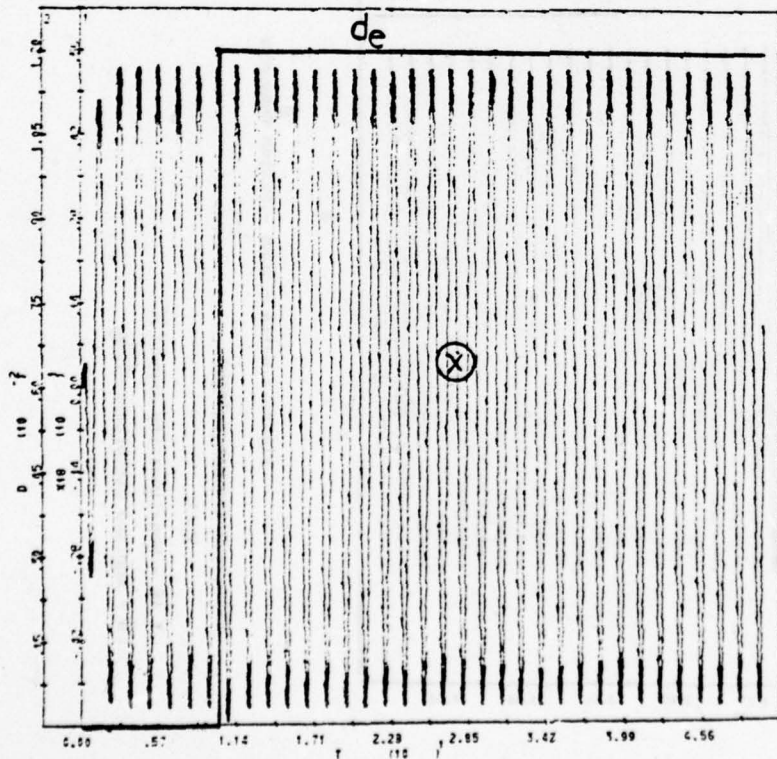


Figure 2.6-10b - SOAS - System Response

Extreme Disturbance Input

K = 10

XC - System Output = C

D - Applied Disturbance = d_e

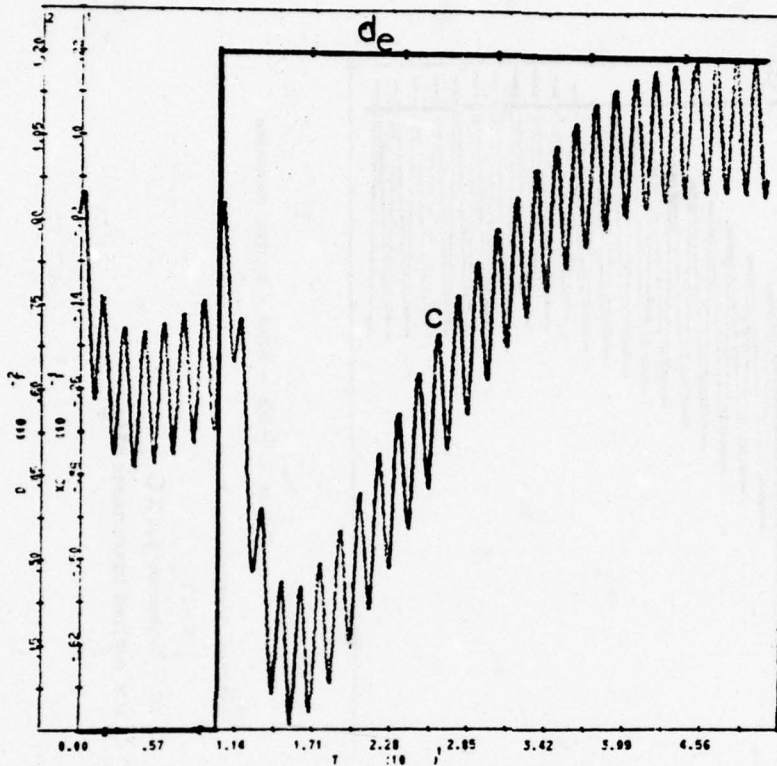


Figure 2.6-11b - SOAS - System Response

Extreme Disturbance Input

$K = 1$

XC - System Output = C

D - Applied Disturbance = d_e

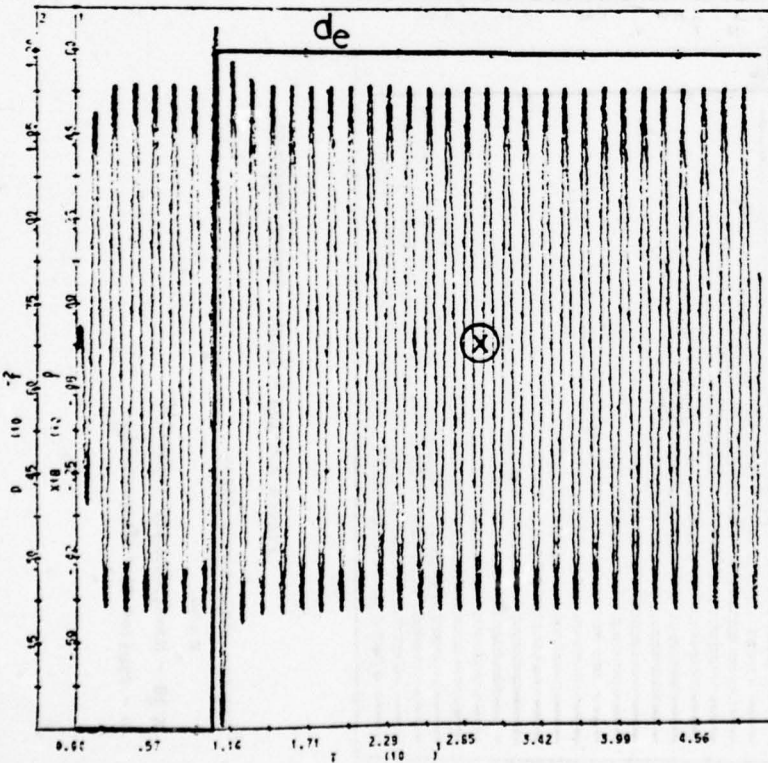


Figure 2.6-11a - SOAS - System Response

Extreme Disturbance Input

$K = 1$

X 18 - Non-linearity Input = X

D - Applied Disturbance = d_e

2.7 Synthesis Procedure (Non-smooth solution)

The previous sections gave the solution for the SOAS, considering $\frac{x_f}{A_1}(j\omega)$ is "smooth" as defined in Section 2.5-3. As a result, a superior limit was established.

$$\left| \frac{x_f}{A_1}(j\omega) \right| \leq \left| \frac{1}{3\omega} \right|$$

For example, if

$$\frac{x_f}{A_1}(j\omega) = \frac{1}{3j\omega} \longrightarrow \frac{x_f}{A_1}(t) = \frac{1}{3} u(t)$$

Suppose now a non-smooth $\frac{x_{f\eta}}{A_1}(j\omega)$

$$\frac{x_{f\eta}}{A_1}(s) = \frac{1}{\gamma s} \times \frac{\left(1 + \frac{2\zeta_z}{\omega_o} s + \frac{s^2}{\omega_o^2}\right)}{\left(1 + \frac{2\zeta_p}{\omega_o} s + \frac{s^2}{\omega_o^2}\right)}$$

where $\gamma > 3$ and $\frac{\zeta_z}{\zeta_p} \gg 1$, and $\zeta_p \ll 1$.

In this case (Appendix II)

$$\left| \frac{x_f}{A_1}(t) \right|_{\max} \cong \frac{1}{\gamma} (1 + 2\zeta_z)$$

If for example $\gamma = 4$, $\zeta_z = .16$, $\zeta_p = .016$

$$\left| \frac{x_f}{A_1}(t) \right|_{\max} \cong \frac{1}{3}$$

and at ω_o , $\left| \frac{x_{f\eta}}{A_1}(j\omega_o) \right| = \frac{2.5}{\omega_o}$

which is much larger than $\frac{1}{3\omega_o}$, which is the limit for the smooth solution at ω_o .

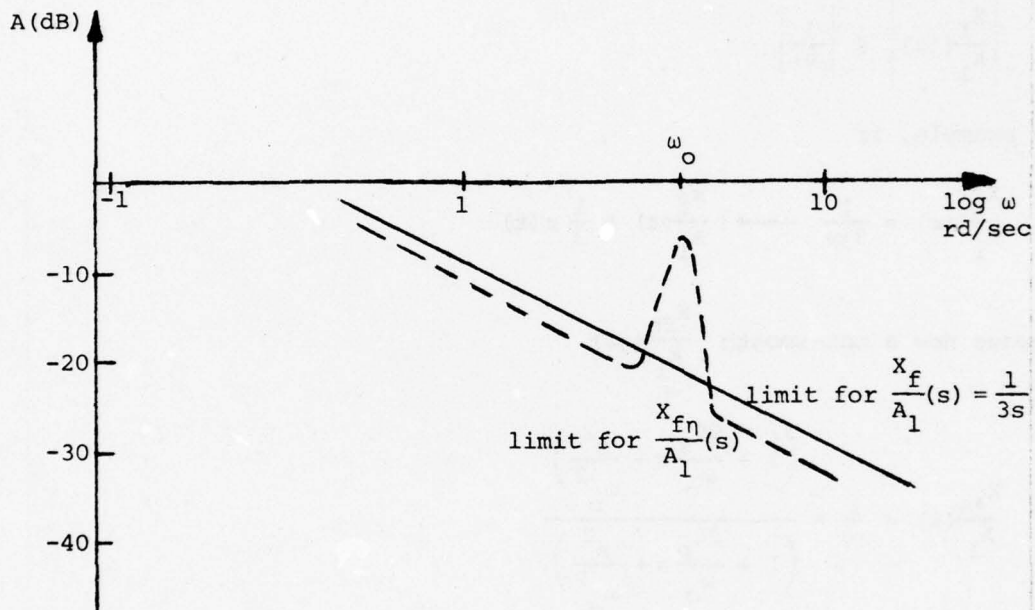


Figure 2.7-1 - Comparison of two signals with the same "peak" time response

Equation 2.5-35, which is valid also for "non-smooth" $\frac{X_e}{A_1}(j\omega)$ is repeated here:

$$\left| \frac{X_e}{A_1}(j\omega_o) \right| \geq \frac{2K_2}{K_1} \frac{|Z_e(j\omega_o)|}{m} \quad (2.7-1)$$

Figure 2.7-2 shows a possible reduction in the oscillating frequency, when using a "non-smooth" $\left| \frac{x_{en}}{A_1}(j\omega) \right|$ (oscillating frequency ω_{on}), compared with a smooth $\left| \frac{x_{es}}{A_1}(j\omega) \right|$ (oscillating frequency ω_{os}).

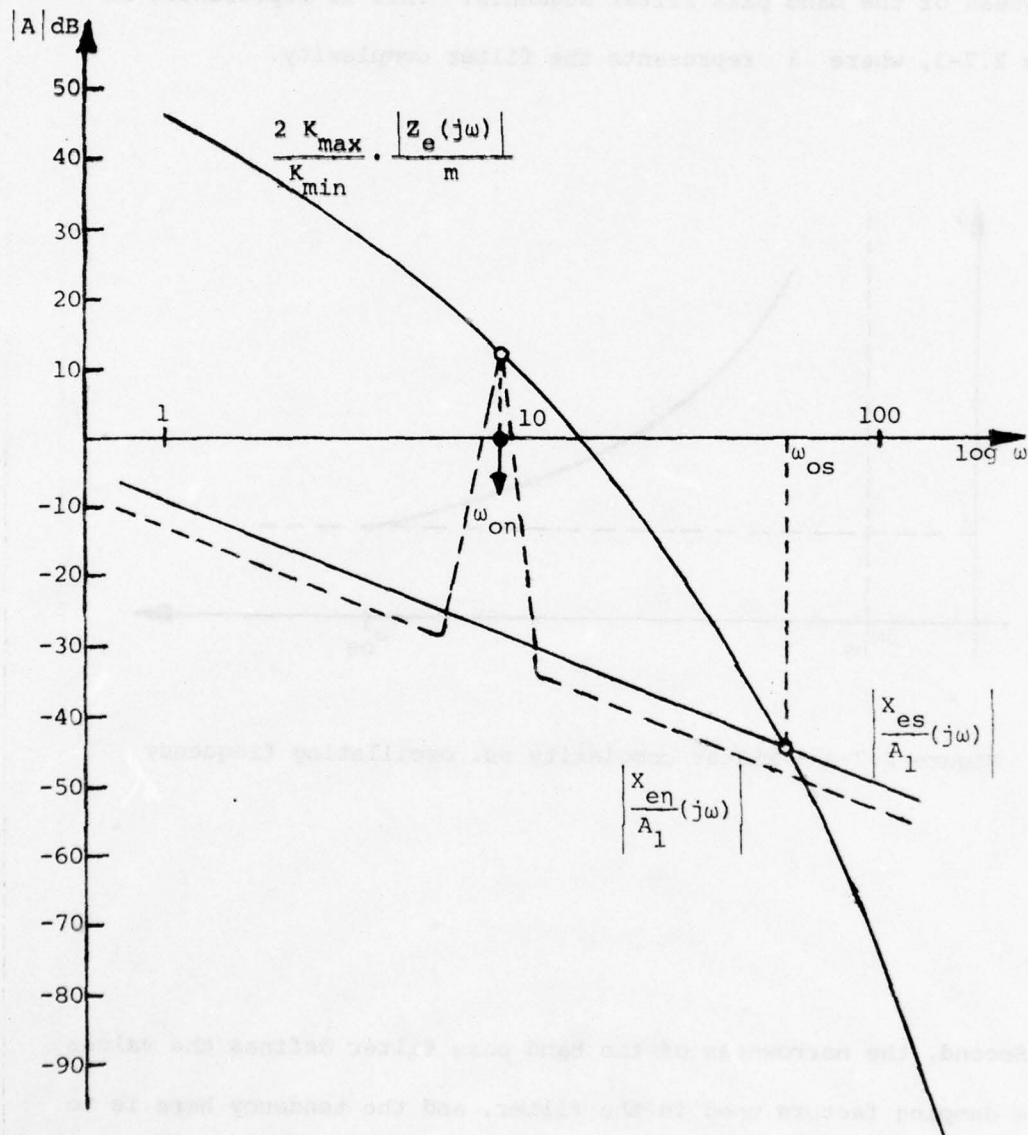


Figure 2.7-2 - Use of a non-smooth solution for $\frac{x_e}{A_1}(j\omega)$, to decrease ω_o

It seems at first that there is no limit on how small it is possible to define the oscillating frequency. But, there are two points to be considered here. First ^[9] the complexity of the band pass filter increases with the decrease in the oscillating frequency, since the narrowness of the band pass filter augments. This is represented in Figure 2.7-3, where λ represents the filter complexity.

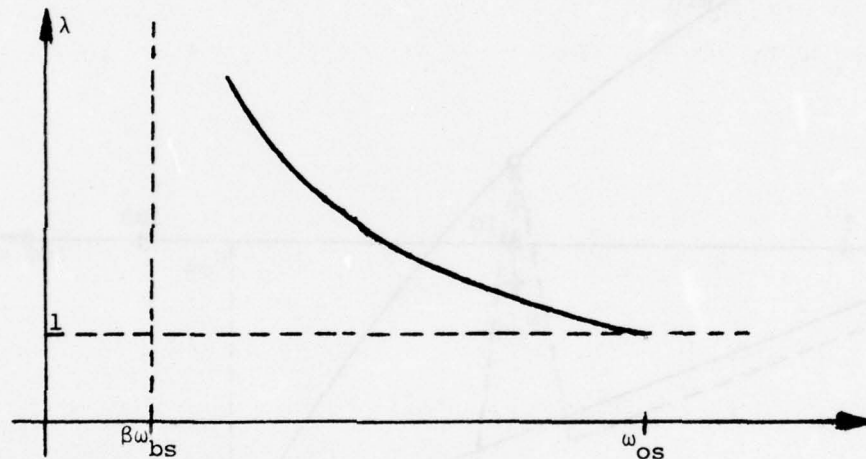


Figure 2.7-3 - Filter complexity vs. oscillating frequency

Second, the narrowness of the band pass filter defines the values of the damping factors used in the filter, and the tendency here is to decrease these values. If there are filters (poles mainly) with low damping factors, and the command or disturbance signals have "spectrum" components at ω_o , the "real information" existing in

$x_o(t)$ is masked. This masking is due to the long decay time and signal amplification (at ω_o) of band pass filters with low damping factors.

The techniques used in Chapter 2.5 can be applied to the "non-smooth" $\frac{X_e(j\omega)}{A_1}$, with minor modifications.

CHAPTER THREE

THE EXTERNALLY EXCITED OSCILLATING ADAPTIVE SYSTEM

(E.E.A.S.)

3.1 General

The limitations of the SOAS have been presented in Chapter 2. To avoid some of these limitations it is possible to "inject" an external periodic signal [10] at some points of the loop, and the system will still have its zero-sensitivity properties to the plant gain factor. This system is called - The Externally Excited Oscillating Adaptive System (EEAS) - and its structure is shown in Figure 3.1-1.

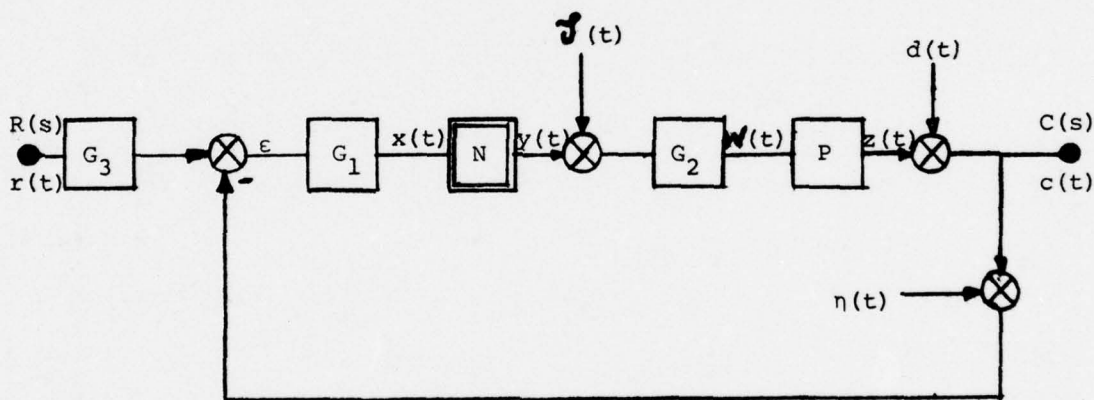


Figure 3.1-1 - EEAS Structure

In Figure 3.1, $G_1(s)$, $G_2(s)$ and $G_3(s)$ are the transfer functions of the linear, time invariant compensations available to the designer and as usual $P(s)$ is the plant transfer function. N is the introduced non-linearity. The signals $x(t) = x_o(t) + x_r(t) + x_d(t)$, where $x_o(t) = A \sin(\omega_o t + \phi)$, $y(t) = y_o(t) + y_r(t) + y_d(t)$, where

$y_o(t) = M_o \sin(\omega_o t + \varphi)$. $w(t)$, $z(t)$, $c(t)$, $d(t)$ and $n(t)$ have the same meaning as in Chapter 2 for the SOAS. $\mathcal{J}(t)$ is the injected periodic signal with period T_o , which has also to be determined, where $\omega_o = \frac{2\pi}{T_o}$ is its first harmonic equivalent frequency, and A_o its first harmonic component amplitude.

The validity of the describing function approximation depends on "how sinusoidal" the signal is at the input to the non-linearity. $G_1 G_2 P(s)$ has to have low-pass characteristics, so the high harmonics components of $y(t)$ (due to non-linear characteristics of N), and of $\mathcal{J}(t)$ (in case $\mathcal{J}(t)$ is not a sinusoid), are filtered out.

3.2 Model of the non-linear element and the constraints involved

As in the SOAS and with the notation of Chapter 2, the non-linear element can be represented by its Dual Input Describing Function (D.I.D.F.).

$$N_o = \frac{M_o}{A} \quad \text{for the oscillating signal} \quad (3.2-1)$$

$$N_r = \frac{M_r}{A} \quad \text{for the signal due to the command signal} \quad (3.2-2)$$

$$N_d = \frac{M_d}{A} \quad \text{for the signals due to the disturbances} \quad (3.2-3)$$

$$M_d = M_r = \frac{M_o}{2} \triangleq M_f \quad (3.2-4)$$

$$N_f \triangleq N_d = N_r \quad (3.2-5)$$

$$M_o = \frac{4B}{\pi} \quad \text{for an ideal relay with saturation level } = B$$

This representation is valid if two conditions are satisfied:

- Quasi-linearity constraints
- Non-existence of a self-oscillation

Quasi-linearity Constraints

These constraints are identical to those of the SOAS (Section 2.2).

Using the same notation we recall that:

$$|x_r(t)| \leq \frac{A}{\alpha} \quad (3.2-6)$$

$$|x_d(t)| \leq \frac{A}{\alpha} \quad (3.2-7)$$

$$\omega_b \leq \frac{\omega_o}{\beta} \quad (3.2-8)$$

Non-existence of Self-oscillation

Suppose there is no injected signal in the structure represented in Figure 3.1, i.e., $\mathcal{J}(t) = 0$. The system will oscillate at the frequency ω_π , $\exists \angle L_O(j\omega_\pi) = -180^\circ$. When we apply the injected signal at frequency ω_o , the self-oscillation with frequency ω_π is not desirable, because in general the Triple Input Describing Function (T.I.D.F.) and the system properties are more complicated if both periodic signals are present.

The injected signal must "quench" the self-oscillation. It has been shown [12] that for saturating non-linearities the quenching condition is

$$-L_O(j\omega_\pi) = \frac{M_O}{M_f} |L_f(j\omega_\pi)| < \rho \quad (3.2-9)$$

Which actually means a minimum gain margin condition for the loop transmission. For the ideal relay $\rho = 1.49$. Another condition for self-oscillation quenching is presented at the end of Section 3.4-2.

3.3 Mathematical Relations

Some relations will be developed in this section. These relations will be helpful in proofs, synthesis procedure and results interpretations. Suppose in Figure 3.1-1, $d(t) = n(t) = r(t) = 0$, and $L(j\omega) = G_1 G_2 P(j\omega)$ defined and known. We assume the system has achieved its steady state response due only to the injected signal $\mathcal{J}(t)$, with first harmonic representation $\mathcal{J}(t) = A_o \sin(\omega_o t)$. The oscillating input to the non-linearity is denoted by $X(j\omega_o)$, then:

$$X(j\omega_o) = \frac{-I(j\omega_o) L(j\omega_o)}{1 + N_o L(j\omega_o)} \quad (3.3-1)$$

Where the phasor $I(j\omega_o)$ can represent $A_o \sin \omega_o t$, and at $j\omega_o$

$$X_o(j\omega_o) = A e^{j\varphi} \quad (3.3-2)$$

Then:

$$A e^{j\varphi} = \frac{-A_o L(j\omega_o)}{1 + N_o L(j\omega_o)} \quad (3.3-3)$$

or

$$A + A N_o L(j\omega_o) = -A_o e^{-j\varphi} L(j\omega_o) \quad (3.3-4)$$

Replacing N_o by its value in Equation 3.2-1, we get:

$$\begin{aligned} A + M_o L(j\omega_o) &= -A_o e^{-j\varphi} L(j\omega_o) \\ \frac{A}{A_o} + \frac{M_o}{A_o} L(j\omega_o) &= -L(j\omega_o) e^{-j\varphi} \end{aligned} \quad (3.3-5)$$

If $L(j\omega_0) = G_1 G_2 P(j\omega_0)$, A_0 and M_0 are known, A and φ can be calculated, which define the oscillating input to the non-linearity. Equation 3.3-5 is solved graphically in Figure 3.3-1.

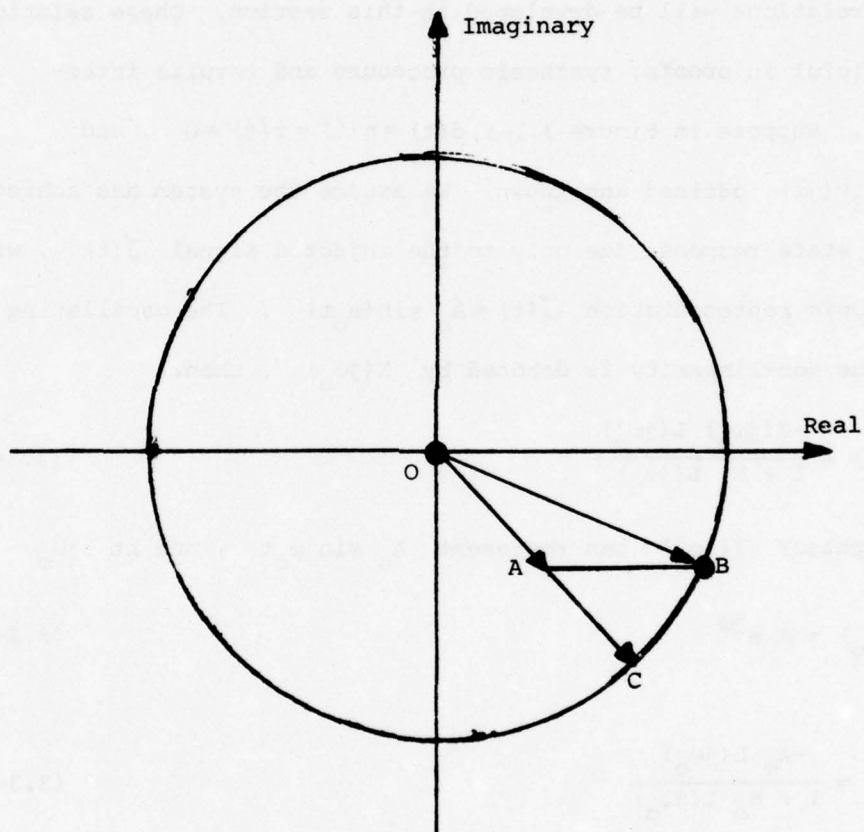


Figure 3.3-1 - Graphical Solution of Equation 3.3-5.

\vec{OC} represents the complex number $L(j\omega_0)$, the linear part of the loop transmission which is assumed known. In Equation 3.3-5 a real positive number has to be added to $L(j\omega_0) \cdot \frac{M_0}{A_0}$ ($= \vec{OA}$ in Figure 3.3.1)

to get a complex number with amplitude $|L(j\omega_o)|$. Graphically this is done by tracing from A a parallel line to the real axis, until it intersects the circle with radius $|L(j\omega_o)|$ at B. \vec{OB} is the complex number $-L(j\omega_o)e^{-j\varphi}$ and \vec{AB} is the real number $\frac{A}{A_o}$. In this way φ and $\frac{A}{A_o}$ are graphically calculated. The analytical solution is also developed. Let:

$$L(j\omega_o) = |L(j\omega_o)| e^{j\theta} \quad (3.3-6)$$

So, based on Equation 3.3-5

$$\left\{ \left(\frac{A}{A_o} + \frac{M_o}{A_o} |L(j\omega_o)| \cos \theta \right) \right\}^2 + \left\{ \frac{M_o}{A_o} |L(j\omega_o)| \sin \theta \right\}^2 = |L(j\omega_o)|^2 \quad (3.3-7)$$

$$\begin{aligned} \left(\frac{A}{A_o} \right)^2 + 2 \left(\frac{A}{A_o} \right) \cdot \left(\frac{M_o}{A_o} \right) |L(j\omega_o)| \cos \theta + \left(\frac{M_o}{A_o} \right)^2 |L(j\omega_o)|^2 \cos^2 \theta + \\ \left(\frac{M_o}{A_o} \right)^2 |L(j\omega_o)|^2 \sin^2 \theta = |L(j\omega_o)|^2 \end{aligned} \quad (3.3-8)$$

Or:

$$\left(\frac{A}{A_o} \right)^2 + 2 \left(\frac{M_o}{A_o} \right) \cdot |L(j\omega_o)| \cos \theta \cdot \left(\frac{A}{A_o} \right) + \left(\frac{M_o^2}{A_o^2} - 1 \right) |L(j\omega_o)|^2 = 0 \quad (3.3-9)$$

From which:

$$\frac{A}{A_o} = |L(j\omega_o)| \left(-\frac{M_o}{A_o} \cos \theta \pm \sqrt{1 - \left(\frac{M_o}{A_o} \right)^2 \sin^2 \theta} \right) \quad (3.3-10)$$

$\frac{A}{A_o}$ must be a real positive number.

We will discuss the several possibilities for a real positive solution for $\frac{A}{A_o}$ in Equation 3.3-10.

Case 1 $\cos \theta \geq 0$ (3.3-11)
 $-\pi/2 \leq \theta \leq \pi/2$

Subcase 1a $\frac{M_O}{A_O} < 1$ (3.3-12)

In this subcase we can write

$$\sqrt{1 - \left(\frac{M_O}{A_O}\right)^2 \sin^2 \theta} > \sqrt{1 - \sin^2 \theta} = \cos \theta > \frac{M_O}{A_O} \cos \theta \quad (3.3-13)$$

So in Equation 3.3-10

$$\sqrt{1 - \left(\frac{M_O}{A_O}\right)^2 \sin^2 \theta} > \frac{M_O}{A_O} \cos \theta$$

and there is always a unique real positive solution for $\frac{A}{A_O}$.

$$\frac{A}{A_O} = |L(j\omega_O)| \left(\sqrt{1 - \left(\frac{M_O}{A_O}\right)^2 \sin^2 \theta} - \frac{M_O}{A_O} \cos \theta \right) \quad (3.3-14)$$

which is the solution of Equation 3.3-10 for Subcase 1a.

Subcase 1b $\frac{M_O}{A_O} = 1$ (3.3-15)

In this subcase we can write:

$$\sqrt{1 - \left(\frac{M_O}{A_O}\right)^2 \sin^2 \theta} = \sqrt{1 - \sin^2 \theta} = \cos \theta = \frac{M_O}{A_O} \cos \theta \quad (3.3-16)$$

So

$$\frac{A}{A_O} = |L(j\omega_O)| \left(-\frac{M_O}{A_O} \cos \theta \pm \frac{M_O}{A_O} \cos \theta \right) \quad (3.3-17)$$

which provide

$$\frac{A}{A_O} = 0 \quad (3.3-18)$$

$$\frac{A}{A_0} = |L(j\omega_0)| (-2 \cos \theta) \quad (3.3-19)$$

Since $\cos \theta > 0$, the solution given in Equation 3.3-19 is negative and there is no real positive solution for $\frac{A}{A_0}$ in Subcase 1b.

Subcase 1c $\frac{M_0}{A_0} > 1 \quad (3.3-20)$

In this subcase, if $\frac{M_0}{A_0} \sin \theta > 1$, then $1 - \left(\frac{M_0}{A_0} \sin \theta\right)^2 < 0$

and there is no real solution for Equation 3.3-10. If $\frac{M_0}{A_0} \sin \theta \leq 1$ then

$$\sqrt{1 - \left(\frac{M_0}{A_0}\right)^2 \sin^2 \theta} < \sqrt{1 - \sin^2 \theta} = \cos \theta < \frac{M_0}{A_0} \cos \theta$$

In Equation 3.3-10

$$-\frac{M_0}{A_0} \cos \theta \pm \sqrt{1 - \left(\frac{M_0}{A_0}\right)^2 \sin^2 \theta} < 0 \quad (3.3-21)$$

and there is no real positive solution for $\frac{A}{A_0}$ in Subcase 1c.

To summarize Case 1, where $-\pi/2 \leq \theta \leq \pi/2$, the only possible real positive solution for $\frac{A}{A_0}$ in Equation 3.3-10 exists when the injected signal A_0 has a higher amplitude than the non-linearity output oscillation signal M_0 , i.e. $A_0 > M_0$ or $\frac{M_0}{A_0} < 1$.

We can see in Figure 3.3-2 the same results of Case 1, based on the graphical solution. In this figure \vec{OB} represents a typical case when $-\frac{\pi}{2} \leq \theta \leq \frac{\pi}{2}$. Subcases 1a, 1b and 1c are represented respectively by \vec{OA} , \vec{OB} and \vec{OC} . One can see that only for Subcase 1a there is a possible positive solution, represented by \vec{AD} , which is $\frac{A}{A_0}$.

This corresponds to Subcase 1a. \vec{OB} and \vec{OC} represent Subcases 1b and 1c, and there is no possible positive solution for $\left| \frac{A}{A_0} \right|$.

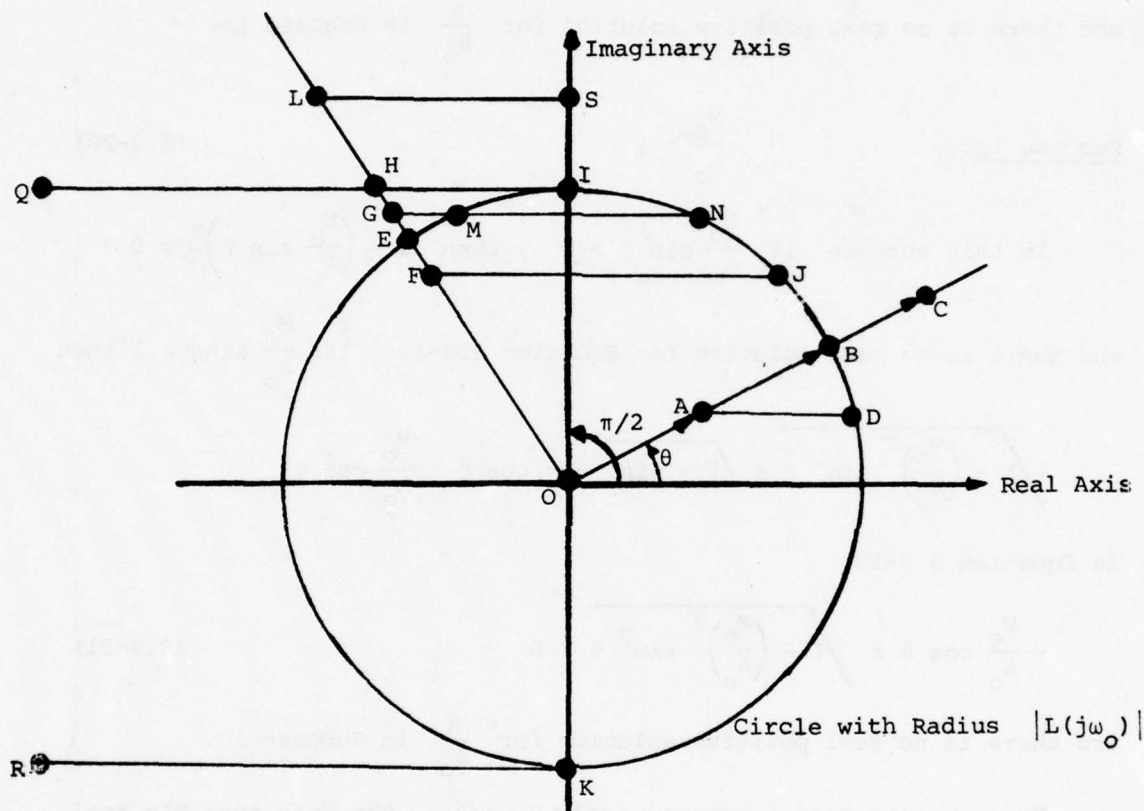


Figure 3.3-2 - Graphical Discussion of Equation 3.3-10

Case 2

$$\cos \theta < 0$$

$$(3.3-22)$$

$$\frac{\pi}{2} < \theta < \frac{3\pi}{2}$$

Subcase 2a

$$\frac{M_o}{A_o} \leq 1$$

(3.3-23)

In this subcase

$$\sqrt{1 - \left(\frac{M_0}{A_0}\right)^2 \sin^2 \theta} \geq \sqrt{1 - \sin^2 \theta} = |\cos \theta| \geq \frac{M_0}{A_0} |\cos \theta|$$

So Equation 3.3-10

$$\left| \frac{M_O}{A_O} \right| (-\cos \theta) = \left| \frac{M_O}{A_O} \right| |\cos \theta| \leq \sqrt{1 - \left| \frac{M_O}{A_O} \right|^2 \sin^2 \theta} \quad (3.3-24)$$

and there will always be only one real positive solution for $\left| \frac{A}{A_O} \right|$.

Subcase 2b

$$\left| \frac{M_O}{A_O} \right| > 1 \quad (3.3-25)$$

$$\left| \frac{M_O}{A_O} \right| |\sin \theta| < 1$$

In this subcase $\sqrt{1 - \left| \frac{M_O}{A_O} \right|^2 \sin^2 \theta}$ is real and we can write:

$$\sqrt{1 - \left| \frac{M_O}{A_O} \right|^2 \sin^2 \theta} < \sqrt{1 - \sin^2 \theta} = |\cos \theta| < \left| \frac{M_O}{A_O} \right| |\cos \theta|$$

and there will be two positive real solutions for $\left| \frac{A}{A_O} \right|$ in Equation 10. They are (since $-\cos \theta = |\cos \theta|$):

$$\left| \frac{A}{A_O} \right| = |L(j\omega_O)| \left(\left| \frac{M_O}{A_O} \right| |\cos \theta| \pm \sqrt{1 - \left| \frac{M_O}{A_O} \right|^2 \sin^2 \theta} \right) \quad (3.2-26)$$

Subcase 2c

$$\left| \frac{M_O}{A_O} \right| > 1 \quad (3.2-27)$$

$$\left| \frac{M_O}{A_O} \right| |\sin \theta| = 1$$

In this subcase $\sqrt{1 - \left| \frac{M_O}{A_O} \right|^2 \sin^2 \theta} = 0$, and Equation 10 provides two identical positive solutions for $\left| \frac{A}{A_O} \right|$. In this subcase:

$$\left| \frac{A}{A_O} \right| = -|L(j\omega_O)| \left| \frac{M_O}{A_O} \right| \cos \theta \quad (3.2-28)$$

Subcase 2d

$$\left| \frac{M_o}{A_o} \right| > 1$$

(3.3-29)

$$\left| \frac{M_o}{A_o} \right| |\sin \theta| > 1$$

In this subcase $\sqrt{1 - \left| \frac{M_o}{A_o} \right|^2 \sin^2 \theta}$ is an imaginary number and there is no positive real solution for $\left| \frac{A}{A_o} \right|$ in Equation 10.

In Figure 3.3-2 the results of Subcases 2a, 2b, 2c, 2d are represented by \vec{OF} , \vec{OG} , \vec{OH} and \vec{OL} respectively. In this figure the limits of $\left| \frac{M_o}{A_o} \right| L(j\omega_o)$, which provide a real positive solution for $\left| \frac{A}{A_o} \right|$ in Equation 10, are also plotted and defined by the segments \overline{QI} , \overline{IK} , \overline{KR} .

The phase angle " φ " in Equation 3.3-5 still has to be calculated. For reference, Equation 3.3-5 is rewritten here:

$$\left| \frac{A}{A_o} \right| + \left| \frac{M_o}{A_o} \right| L(j\omega_o) = -L(j\omega_o) e^{j\varphi}$$

So

$$\left| \frac{A}{A_o} \right| + \left| \frac{M_o}{A_o} \right| L(j\omega_o) = \angle -L(j\omega_o) e^{-j\varphi}$$

But

$$\angle -L(j\omega_o) e^{-j\varphi} = \pi + \angle L(j\omega_o) e^{-j\varphi} = \pi + \theta - \varphi$$

and

$$\text{tg} \left(\angle -L(j\omega_o) e^{-j\varphi} \right) = \text{tg} \left(\left| \frac{A}{A_o} \right| + \left| \frac{M_o}{A_o} \right| L(j\omega_o) \right) \quad (3.3-30)$$

$$\operatorname{tg} \left(\frac{\left| \frac{A}{A_0} \right| + \left| \frac{M_0}{A_0} \right| L(j\omega_0)}{\operatorname{Re} \left[\left| \frac{A}{A_0} \right| + \left| \frac{M_0}{A_0} \right| L(j\omega_0) \right]} \right) = \frac{\operatorname{Im} \left[\left| \frac{A}{A_0} \right| + \left| \frac{M_0}{A_0} \right| L(j\omega_0) \right]}{\operatorname{Re} \left[\left| \frac{A}{A_0} \right| + \left| \frac{M_0}{A_0} \right| L(j\omega_0) \right]} \quad (3.3-32)$$

Combining Equations 3.3-30, 3.3-31, 3.3-32, we can write

$$\operatorname{tg}(\theta - \varphi) = \frac{\operatorname{Im} \left[\left| \frac{A}{A_0} \right| + \left| \frac{M_0}{A_0} \right| L(j\omega_0) \right]}{\operatorname{Re} \left[\left| \frac{A}{A_0} \right| + \left| \frac{M_0}{A_0} \right| L(j\omega_0) \right]}$$

Due to Equation 3.3-30, we can also write:

$$\operatorname{tg}(\theta - \varphi) = \frac{\operatorname{Im} \left[\left| \frac{A}{A_0} \right| + \left| \frac{M_0}{A_0} \right| L(j\omega_0) \right]}{\operatorname{Re} \left[-L(j\omega_0) e^{-j\varphi} \right]} =$$

or

$$\operatorname{tg}(\theta - \varphi) = \frac{\left| \frac{M_0}{A_0} \right| |L(j\omega_0)| \sin \theta}{-|L(j\omega_0)| \cos(\theta - \varphi)} =$$

$$\sin(\theta - \varphi) = -\left| \frac{M_0}{A_0} \right| \sin \theta$$

$$\theta - \varphi = \sin^{-1} \left[-\left| \frac{M_0}{A_0} \right| \sin \theta \right]$$

$$\varphi = \theta - \sin^{-1} \left[-\left| \frac{M_0}{A_0} \right| \sin \theta \right] \quad (3.3-32)$$

Equation 3.3-32 gives the solution for φ in Equation 3.3-32. As expected, due to the saturating non-linearity, φ is not a function of the magnitude $|L(j\omega_0)|$ but only of the angle $\angle L(j\omega_0) = \theta$. The graphical solution for the angle φ has already been presented in Figure 3.3-1.

3.4 Mathematical Relations Interpretation

The relations obtained in Section 3.3 will be interpreted in this section. Basic properties will be pointed out as a result of these relations. When necessary, physical interpretation of the results will be given to explain some "strange results" obtained.

3.4-1 Zero Sensitivity Property of the E.E.A.S. to Pure Gain Changes of the Plant P

We recall Equation 3.3-5:

$$\left| \frac{A}{A_o} \right| + L(j\omega_o) \left| \frac{M_o}{A_o} \right| = -L(j\omega_o) e^{-j\varphi}$$

But $L(j\omega_o) = G_1 G_2 P(j\omega_o)$, $P(j\omega) \triangleq K P_h(j\omega) \forall \omega$

So,

$$|A| + |M_o| \left[G_1 G_2 K P_h(j\omega_o) \right] = - \left[G_1 G_2 K P_h(j\omega_o) \right] e^{-j\varphi} |A_o|$$

$$\left| \frac{A}{K} \right| = - \left[G_1 G_2 P_h(j\omega_o) \right] \left[|A_o| e^{-j\varphi} + |M_o| \right] = \text{constant} \quad (3.4-1)$$

Equation 3.4-1 shows that the factor $\left| \frac{A}{K} \right|$ is independent of K itself, because: A_o , the injected signal is constant. φ is defined by $\angle L(j\omega_o)$, M_o and A_o (Equation 3.3-32). M_o is defined completely by the non-linearity saturating level used. This means that

when $K = K_{\max} = K_2$, A will have its maximum value $A = A_{\max} = A_2$.

When $K = K_{\min} = K_1$, A will have its minimum value $A = A_{\min} = A_1$.

The loop transmission for the forced and disturbance signals is (Figure 3.1 and Equations 3.2-1 - 3.2-5):

$$L_f(j\omega) = \frac{L_o}{2} = \frac{M_o}{2} G_1 G_2 P_h(j\omega) \times \frac{K}{A} \quad (3.4-2)$$

and is consequently independent of K , i.e., the EEAS properly designed also has zero sensitivity properties for pure gain changes of the plant. This property exists only if the injected signal is applied at any point between the non-linearity output and the plant input. To prove so, we will make another possible block diagram for the EEAS structure in Figure 3.4-1, where

$$G_{21}(s) \times G_{22}(s) = G_2(s) \quad (3.4-3)$$

The injected signal is applied at the input to $G_{22}(s)$. The structure represented in Figure 3.1-1 is a special case of the structure represented in Figure 3.4-1.

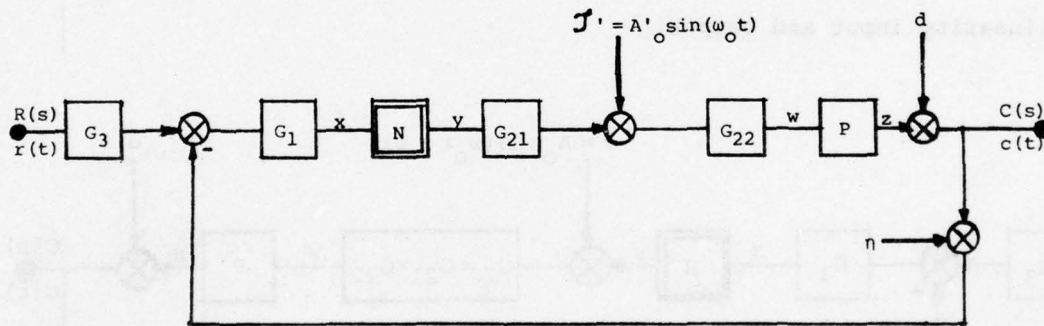


Figure 3.4-1 - Generalized EEAS

$G_{21}(s)$ being a linear time invariant compensation, the injected signal $J' = A' \sin(\omega_0 t)$ could be applied as an equivalent signal at the input to G_{21} .

$$I(j\omega_0) = \frac{I'(j\omega_0)}{G_{21}(j\omega_0)} \quad (3.4-4)$$

Where

$$I(j\omega_o) = |\mathcal{L}[\mathcal{J}(t)]|_{s=j\omega_o}$$

$$I'(j\omega_o) = |\mathcal{L}[\mathcal{J}'(t)]|_{s=j\omega_o}$$

The equivalent injected signal is

$$\mathcal{J} = A \sin(\omega_o t - \psi)$$

Where

$$A = \frac{A'_o}{|G_{21}(j\omega_o)|} \quad (3.4-5)$$

$$\psi = \angle G_{21}(j\omega_o)$$

So, the systems represented in Figures 3.4-1 and 3.4-2 are equivalent in all aspects, regarding overall performance and signal levels at the non-linearity input and output.

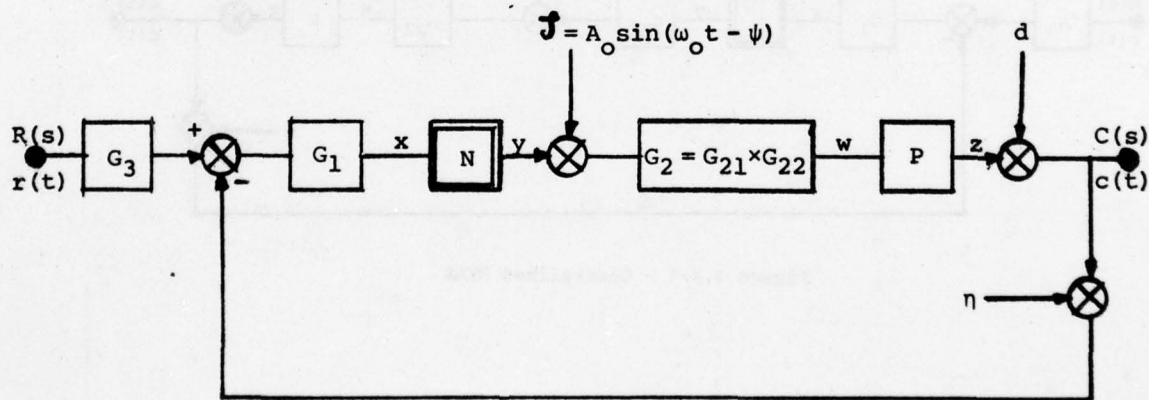


Figure 3.4-2 - Equivalent System for the Generalized EEAS

But the system represented in Figure 3.4-2 is the EEAS itself, which proves that if the injected signal is applied at any point in the loop between the non-linearity output and the plant, the zero

sensitivity property to pure gain changes is kept.

Let us assume now that the injected signal is applied at any point in the loop between the system output and the input to the non-linearity. The block-diagram of this configuration is represented in Figure 3.4-3.

G_{11} and G_{12} are linear time invariant compensations, such that

$$G_{11} \times G_{12} = G_1 \quad (3.4-6)$$

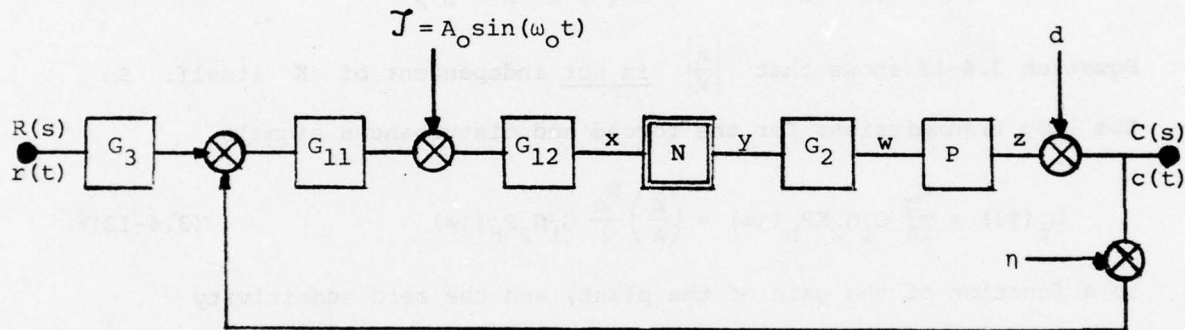


Figure 3.4-3 - Injected signal applied between the system output and the non-linearity

In this case, assuming the system has achieved its steady state oscillation due to the injected signal

$$x_0 = A \sin(\omega_0 t + \varphi)$$

$$J = A_0 \sin(\omega_0 t) \quad (3.4-7)$$

$$y_0 = M_0 \sin(\omega_0 t + \varphi)$$

We can write:

$$|X(j\omega_0)| = \left| \frac{I(j\omega_0) G_{12}(j\omega_0)}{1 + L_0(j\omega_0)} \right| \quad (3.4-8)$$

or

$$X(j\omega_o) = I(j\omega_o) \cdot G_{12}(j\omega_o) - Y(j\omega_o) \cdot G_2^{KP_h} G_{11} G_{12}(j\omega_o) \quad (3.4-9)$$

or

$$|A| e^{j(\omega_o t + \varphi)} = |A_o| e^{j(\omega_o t)} \cdot G_{12}(j\omega_o) - |M_o| e^{j(\omega_o t + \varphi)} \cdot (G_1 G_2^{KP_h}(j\omega_o)) \quad (3.4-10)$$

$$|A| e^{j\varphi} = |A_o| \cdot G_{12}(j\omega_o) - |M_o| e^{j\varphi} (G_1 G_2^{KP_h}(j\omega_o)) \quad (3.4-11)$$

or

$$\left| \frac{A}{K} \right| = \left| \frac{A_o}{K} \right| G_{12}(j\omega_o) e^{-j\varphi} - |M_o| (G_1 G_2^{KP_h}(j\omega_o)) \quad (3.4-12)$$

Equation 3.4-12 shows that $\left| \frac{A}{K} \right|$ is not independent of K itself. So the loop transmissions for the forced and disturbances signals

$$L_f(j\omega) = \frac{M_o}{2A} G_1 G_2^{KP_h}(j\omega) = \left(\frac{K}{A} \right) \frac{M_o}{2} G_1 G_2^{P_h}(j\omega) \quad (3.4-13)$$

is a function of the gain of the plant, and the zero sensitivity property is not kept when the injected signal is applied as in Figure 3.4-3.

A last remark - if the injected signal would have its amplitude variable and proportional to the gain of the plant K , then $\left| \frac{A_o}{K} \right|$ in Equation 3.4-12 would be a constant value and zero sensitivity properties would be kept. For more details see Section 6.

3.4-2 Physical Interpretation of the Mathematical Relations Developed

In Section 3.3 some relations were developed, which result mainly from the solution of Equation 3.3-10. The solution of this equation, depending on the several parameters, sometimes gives "strange results". If the signal $\mathcal{J} = A_o \sin(\omega_o t)$ is injected at a certain point in the loop, we "expect" to have a well defined periodic signal at any point

of the loop, including the non-linearity input.

The discussion of Equation 3.3-10, which provides the solution for the amplitude A of the oscillating signal at the non-linearity input, ($x_o = A \sin(\omega_o t + \varphi)$) shows that in some cases we have one defined value for A (as "expected"). In other cases there are two possible values for A , which mean "two oscillations" at the same frequency. And finally, in some cases there is no possible value for A , which means there is "no oscillation" component at the non-linearity input even when the injected signal is applied.

The two last possibilities seem rather "strange", and we will give a physical interpretation for these results. We first repeat Equation 3.3-10

$$\left| \frac{A}{A_o} \right| = |L(j\omega_o)| \left(-\left| \frac{M_o}{A_o} \right| \cos \theta \pm \sqrt{1 - \left| \frac{M_o}{A_o} \right|^2 \sin^2 \theta} \right) \quad (3.4-14)$$

and represent in Figure 3.4-4 the results of the several possible cases discussed in Section 3.3.

The independent variable in Figure 3.4-4 is the angle θ as expressed in Equation 3.3-6 $\theta = \angle G_1 G_2 P(j\omega_o) = \angle L(j\omega_o)$. In Figure 3.4-5, the several possibilities are presented as a table, with all cases involved.

We plot the same results, having $\left| \frac{A_o}{M_o} \right|$ as a dependent variable, instead of $\left| \frac{M_o}{A_o} \right|$, in Figure 3.4-6.

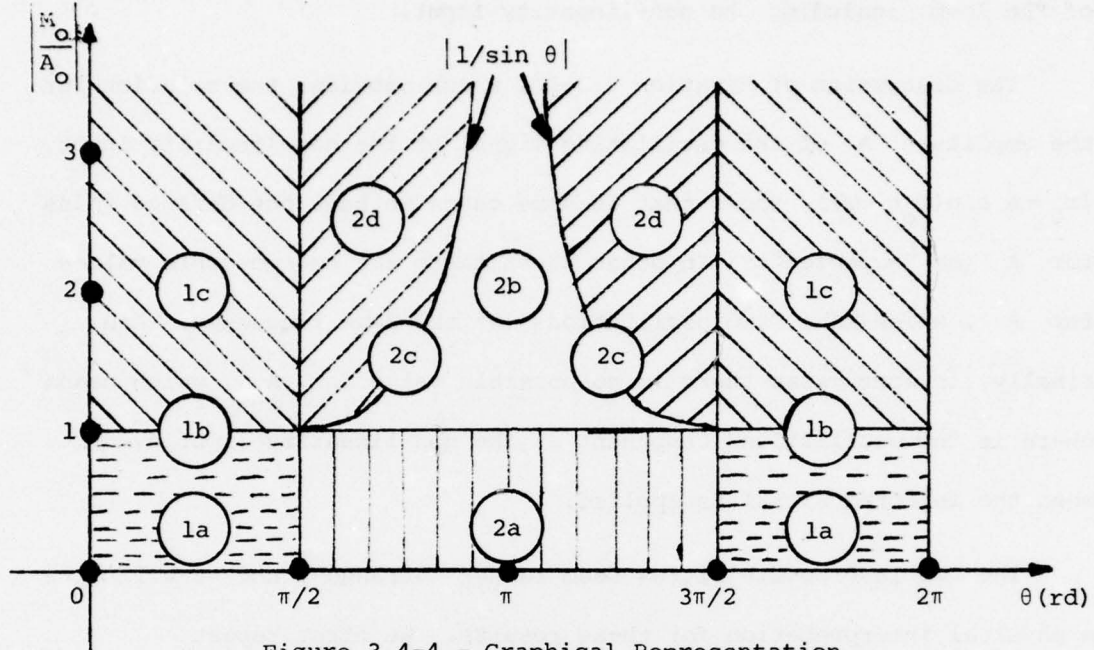


Figure 3.4-4 - Graphical Representation
Discussion of Equation 3.3-10

Case	θ	$\left \frac{M_O}{A_O} \right $	$\left \frac{A_O}{M_O} \right $	Number of real positive solutions for A
1a	$\frac{\pi}{2} \geq \theta \geq \frac{\pi}{2} (= \frac{3}{2})$	< 1	> 1	1
1b	"	$= 1$	$= 1$	0
1c	"	> 1	< 1	0
2a	$\frac{\pi}{2} < \theta < \frac{3\pi}{2}$	≤ 1	≥ 1	1
2b	"	$\begin{matrix} > 1 \\ < \frac{1}{ \sin \theta } \end{matrix}$	$\begin{matrix} < 1 \\ > \frac{1}{ \sin \theta } \end{matrix}$	2
2c	"	$= \frac{1}{ \sin \theta }$	$= \frac{1}{ \sin \theta }$	1
2d	"	$\begin{matrix} > 1 \\ > \frac{1}{ \sin \theta } \end{matrix}$	$\begin{matrix} < 1 \\ < \frac{1}{ \sin \theta } \end{matrix}$	0

Figure 3.4-5 Several cases for oscillating component determination

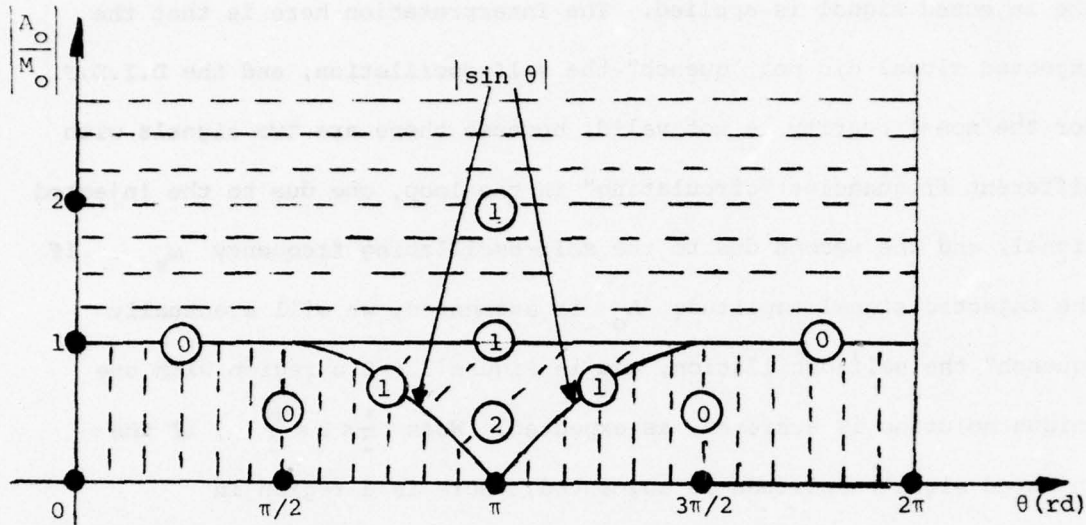


Figure 3.4-6 - Graphical Representation
Discussion of Results - Equation 3.3-10

In Figure 3.4-6 the encircled numbers in each "region" represent the existing number of solutions in the several cases, resumed in the table of Figure 3.4-5.

The "strange" results can now be physically explained. First notice in Figure 3.4-6 that for $\theta = \pi$ and if $\left| \frac{A_O}{M_O} \right| = 0$, there is one solution for Equation 3.3-10. $\left| \frac{A_O}{M_O} \right| = 0$ means there is no injected signal, and the system self-oscillates at the frequency ω_π such that $\theta = \angle L_O(j\omega_\pi) = \pi$. In this case we are back to the SOAS. For any $\theta \neq \pi$, when $\left| \frac{A_O}{M_O} \right| = 0$, there is no solution for Equation 3.3-10, which defines the amplitude and phase of the oscillating component due to injected signal. If there is no injected signal ($A_O = 0$), the system self-oscillates at ω_π .

Suppose now we inject a very small amplitude for $|A_O|$. For any $\theta \neq \pi$, there is still "no solution" for Equation 3.3-7, even when

the injected signal is applied. The interpretation here is that the injected signal did not "quench" the self-oscillation, and the D.I.D.F. for the non-linearity is not valid, because there are two signals with different frequencies "circulating" in the loop, one due to the injected signal, and the second due to the self-oscillating frequency ω_{π} . If the injected signal amplitude A_o is augmented, we will eventually "quench" the self-oscillation, and in Figure 3.4-6 a region with one unique solution is achieved, as expected. When $\frac{\pi}{2} < \theta < \frac{3\pi}{2}$, if the injected signal amplitude is augmented, there is a region in Figure 3.4-6 with two different solutions for the amplitude signal with the same frequency. The physical interpretation is that one of them is unstable and only the signal with the largest amplitude exists.

The same results could be obtained (for φ) by using the Nichol's chart as in Figure 3.4-7. Based on the EEAS structure shown in Figure 3-1 we can write:

$$Y(j\omega_o) = - \frac{I(j\omega_o) L_o(j\omega_o)}{1 + L_o(j\omega_o)} \quad (3.4-15)$$

But

$$|Y(j\omega_o)| = |M_o| \quad (3.4-16)$$

And

$$|I(j\omega_o)| = |A_o| \quad (3.4-17)$$

Substituting in Equation 3.4-15, we get:

$$\left| \frac{M_o}{A_o} \right| = \left| \frac{L_o(j\omega_o)}{1 + L_o(j\omega_o)} \right| \quad (3.4-18)$$

In the Nichol's chart, shown in Figure 3.4-7, the straight lines represent L , the open loop characteristics (horizontal lines have constant amplitude, scaled in dB; vertical lines have constant phase

angles, scaled in degrees), and the curved lines represent constant amplitude (scaled in dB) and constant phase (scaled in degrees) of the closed loop $\frac{L}{(1+L)}$.

We notice that if $\left| \frac{M_O}{A_O} \right| < 1$, or based on Equation 3.4-18, $\left| \frac{L_O(j\omega_O)}{1+L_O(j\omega_O)} \right| < 0$ dBs, which are represented by curved contours, there is only one value of $L_O(j\omega_O)$ for each value of θ .

For $-\frac{\pi}{2} \leq \theta \leq \frac{\pi}{2}$ there is no possibility of having

$\left| \frac{L_O(j\omega_O)}{1+L_O(j\omega_O)} \right| > 0$ dBs, which means that for $\left| \frac{M_O}{A_O} \right| = \left| \frac{L_O(j\omega_O)}{1+L_O(j\omega_O)} \right| > 1$

there is no solution for Equation 3.4-18. As an example, in Figure 3.4-7

the vertical line representing $\theta = -60^\circ$ is drawn more heavily. This

line intercepts the closed loop $\left(\frac{L}{1+L} \right)$ contours of $\left| \frac{M_O}{A_O} \right|$ with values < 0 dBs, which means $\left| \frac{M_O}{A_O} \right| < 1$.

For $\frac{\pi}{2} < \theta < \frac{3\pi}{2}$, if $\left| \frac{M_O}{A_O} \right| > 1$ (> 0 dBs), for each θ there are two possible solutions for Equation 3.4-18. As an example, in

Figure 3.4-7 the line representing $\theta = -160^\circ$ is also redrawn and if we

consider $\frac{M_O}{A_O} = 2$ ($\triangleq 6$ dB), two possible solutions are represented by

A and B in the same figure. When $\left| \frac{M_O}{A_O} \right| = -4$ dB (< 0 dB) there is only one solution, represented by C.

Figure 3.4-8 represents the limit cycle build-up of a typical EEAS.

The example used here is that one in Section 3.5, in which the

synthesized open loop transmission has been decreased by 6 dB.

In this case $\theta \approx -350^\circ$ and $\frac{M_O}{A_O} \approx 0.9$ and there is a unique solution.

Figure 3.4-9 represents the limit cycle build-up when A_O is half of

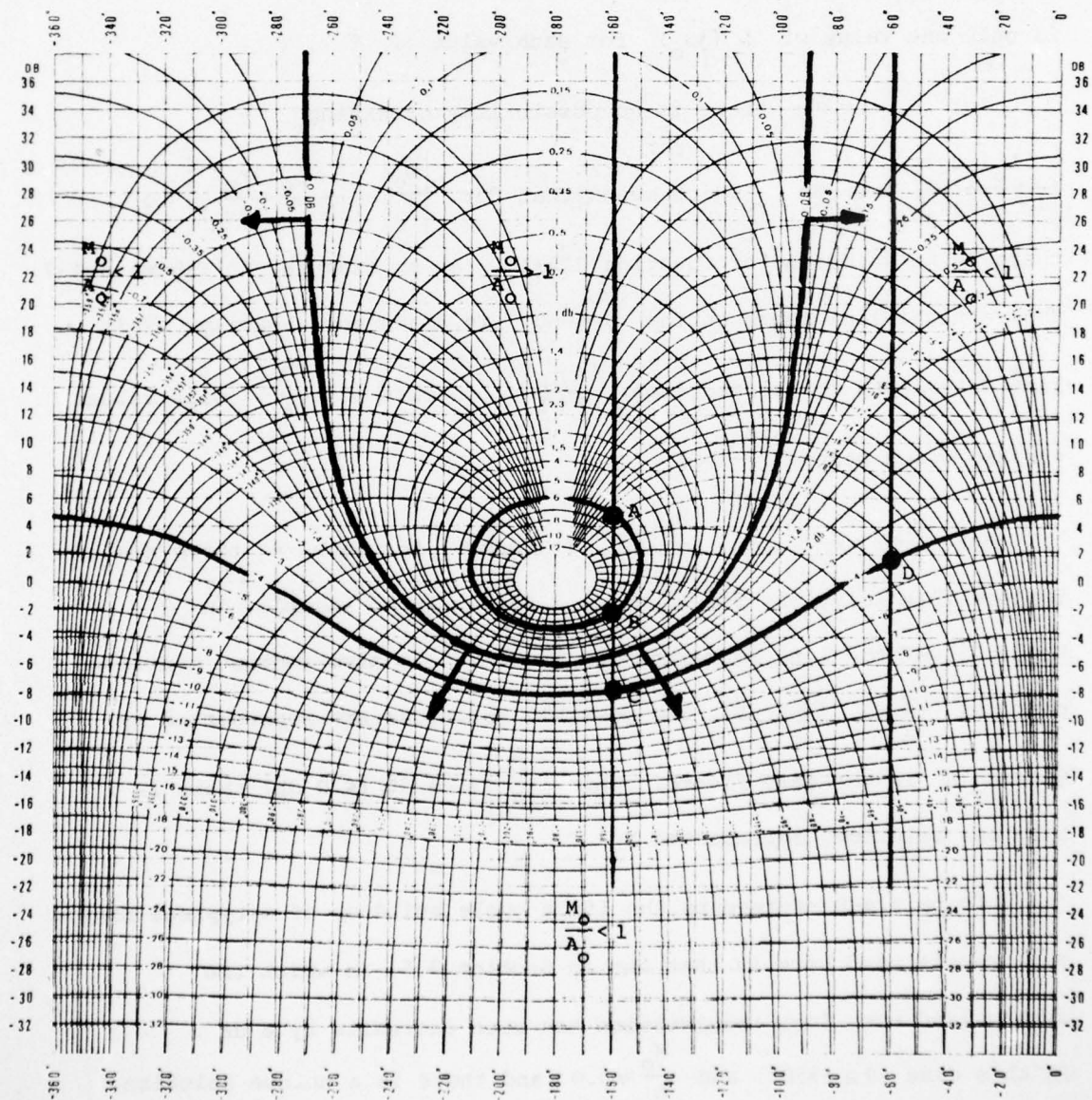


Figure 3.4-7 - Nychol's Chart

Possible solutions for oscillating component determination

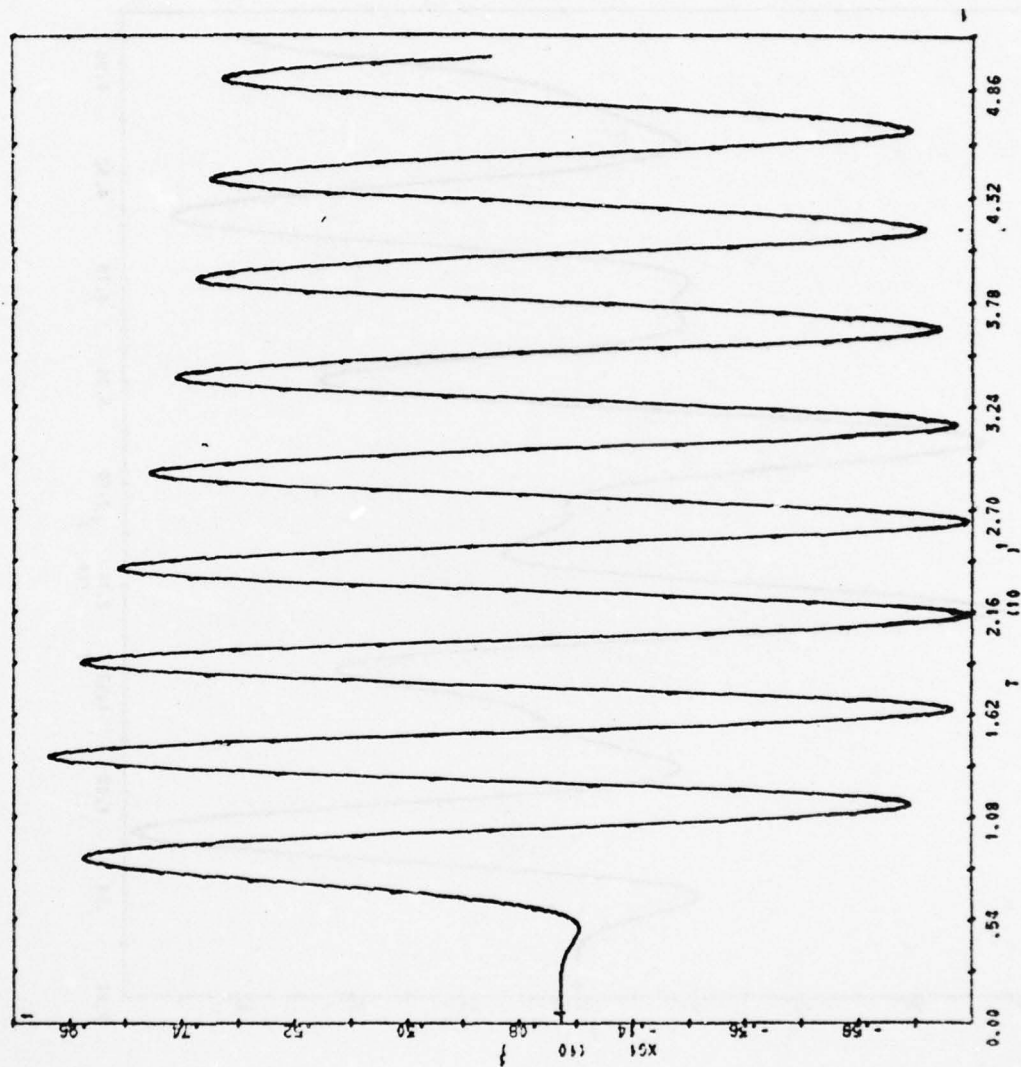


Figure 3.4-8 - Limit Cycle Build-up for a Typical EEAS

XG_1 is the input to the non-linearity

T is time in seconds

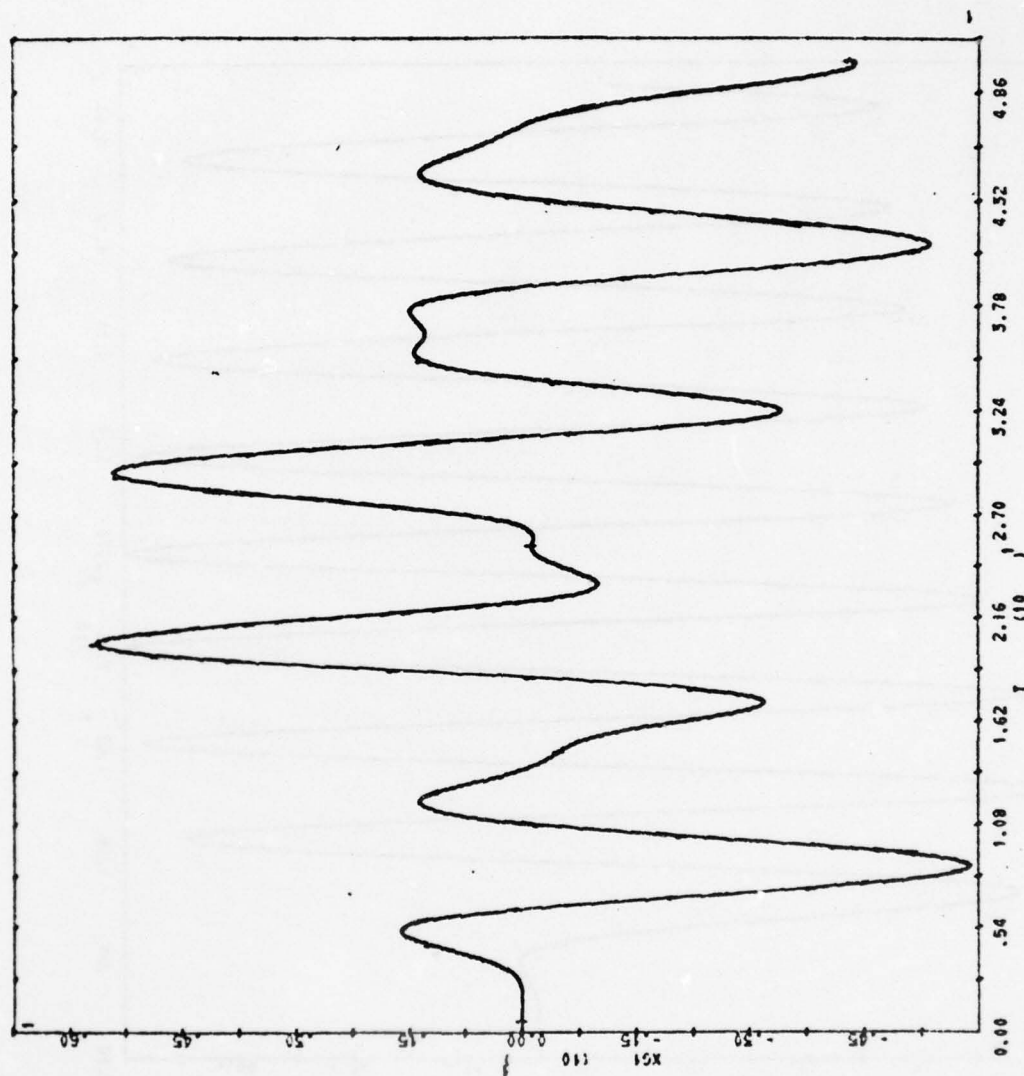


Figure 3.4-9 - EEAS - Two Oscillations in the Loop (ω_0 and ω_π)

XG1 is the input to the non-linearity

T is time in seconds

AD-A046 011

COLORADO UNIV BOULDER SYSTEMS ENGINEERING LAB
SYNTHESIS OF OSCILLATING ADAPTIVE SYSTEMS.(U)
JUL 77 A SHAPIRO, I HOROWITZ

F/G 9/4

UNCLASSIFIED

2 OF 4

AD
A046011

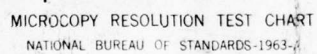


AFOSR-76-2946

AFOSR-TR-77-1223

NL





MICROCOPY RESOLUTION TEST CHART
NATIONAL BUREAU OF STANDARDS-1963-A

the previous value. In this case $\frac{M_o}{A_o} \approx 1.8$ (> 0 dBs), and there is no solution, since $\theta \approx -350^\circ$. The limit cycle "build-up" is composed of two different frequencies, one due to the injected signal and the second due to the self-oscillation. The DIDF model for the non-linearity is not valid. In both figures the non-linearity input is represented.

3.4-3 EEAS Sensitivity to Dynamic Changes of the Plant

It has been shown that both the EEAS and the SOAS have the zero sensitivity property to pure gain changes of the plant. It was also shown (Section 2.4) that for the SOAS, if the plant $P(j\omega) = KP_h(j\omega)$ changes its dynamics characteristics ($P_h(j\omega)$ changes), then the oscillating frequency ω_o changes in such a manner that

$$\angle G_1 G_2 P_h(j\omega_o) = -180^\circ \quad (3.4-19)$$

is satisfied.

The situation is different for the EEAS, since the oscillating frequency ω_o is that of the injected signal, if "quenching" is achieved. What happens when the plant phase $\angle P_h(j\omega_o)$ changes?

The non-linearity used here is such that its representation is a pure gain with zero phase.

Repeating Equation 3.4-18

$$\left| \frac{M_o}{A_o} \right| = \left| \frac{L_o(j\omega_o)}{1 + L_o(j\omega_o)} \right| \quad (3.4-20)$$

M_o and A_o are fixed. Thus as the plant changes its phase angle $\angle P(j\omega_o)$, $L_o(j\omega_o)$ follows this change in open loop along the

contour defined by $\left| \frac{M_o}{A_o} \right| = \left| \frac{L_o(j\omega_o)}{1 + L_o(j\omega_o)} \right| = \text{constant}$. As an example,

if $L_O(j\omega_o)$ is represented in Figure 3.4-7 at D ,

$\left(\left| \frac{L_O(j\omega_o)}{1+L_O(j\omega_o)} \right| = -4 \text{ dB} , \angle L_O(j\omega_o) = -60^\circ \right)$ and there is a change in the phase of the plant at ω_o of -100° , the new $L_O(j\omega_o)$ is represented at C $\left(\left| \frac{L_O(j\omega_o)}{1+L_O(j\omega_o)} \right| = -4 \text{ dB} , \angle L_O(j\omega_o) = -160^\circ \right)$.

Suppose now a situation where $\left| \frac{M_O}{A_O} \right| > 1$, as represented by B $\left(\left| \frac{L_O(j\omega_o)}{1+L_O(j\omega_o)} \right| = +6 \text{ dB} , \angle L_O(j\omega_o) = -160^\circ \right)$, and there is a change in the phase of the plant at ω_o of $+100^\circ$. At $\angle L_O(j\omega_o) = -160^\circ + 100^\circ = -60^\circ$ there is no possible solution for $\left| \frac{M_O}{A_O} \right| = \left| \frac{L_O(j\omega_o)}{1+L_O(j\omega_o)} \right| = +6 \text{ dB}$, so the system would eventually begin to self-oscillate and the DIDF representation for the non-linearity is not valid anymore. This is true for a static saturating non-linearity, where the change in phase of the plant at ω_o is reflected directly as a change in θ , the phase of the loop transmission at the frequency ω_o .

This is not necessarily true if a dynamic saturating non-linearity would be used, represented by its amplitude and phase. This could open new possibilities for design and "insensitivity" to $P(j\omega_o)$ changes (and perhaps also to $P(j\omega)$ changes). No work has been done on this subject, but a possible non-linearity is a relay with hysteresis, as in Figure 3.4-10. The DIDF is [12]

$$\begin{aligned} N_f &= \frac{B}{\pi x_f} \left[\sin^{-1} \left(\frac{\delta + x_f}{A} \right) - \sin^{-1} \left(\frac{\delta - x_f}{A} \right) \right] \\ N_o &= \frac{2B}{\pi A} \left[\sqrt{1 - \left(\frac{\delta + x_f}{A} \right)^2} + \sqrt{1 - \left(\frac{\delta - x_f}{A} \right)^2} \right] - j \frac{4D\delta}{\pi A^2} \end{aligned} \quad (3.4-21)$$

Probably the constraints would also have to be changed, so quasi-linearity conditions are kept. From now on we will consider only changes in the overall gain of the plant.

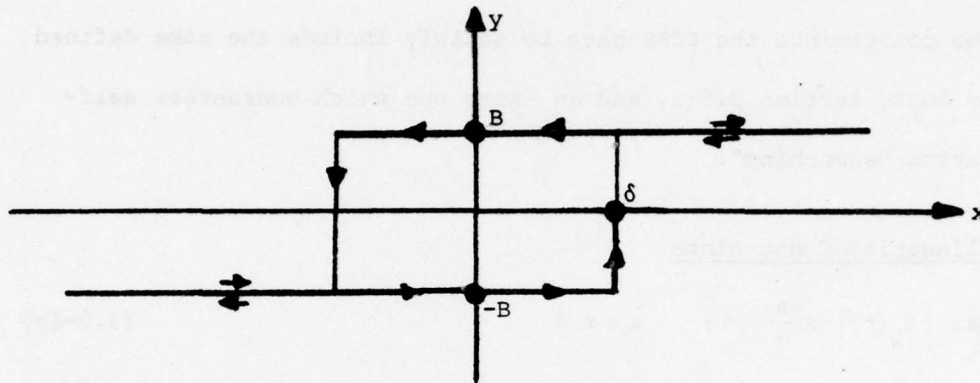


Figure 3.4-10 - Relay with hysteresis representation

3.5 Synthesis Procedure for the EEAS

In this section a synthesis procedure for the EEAS will be derived. It is assumed uncertainly only in plant gain K in $P(s) = KP_h(s)$, $K_1 \leq K \leq K_2$. The non-linearity used is an ideal relay. This synthesis procedure will allow the designer to satisfy the specifications and constraints, and optimize the noise effect as defined for the SOAS and in Appendix I.

3.5-1 Specifications and Data

It is assumed that the set of specifications and data listed below are known or can be estimated.

- Desired Command Input Response
- Disturbance Attenuation
- The Plant
- Extreme Command Input
- Extreme Disturbance Input

The meanings and comments given in Section 2.5-1 for the SOAS are valid for the EEAS.

3.5-2 The Constraints

The constraints the EEAS have to satisfy include the same defined for the SOAS, Section 2.5-2, and an extra one which guarantees self-oscillating "quenching".

Quasi-linearity Constraints

$$\max_t |x_i(t)| \leq \frac{A}{\alpha} \quad ; \quad i=r,d \quad (3.5-1a)$$

$$\omega_{bi} \leq \frac{\omega_o}{\beta} \quad ; \quad i=r,d \quad (3.5-1b)$$

$$\alpha = 3 \quad (3.5-1c)$$

$$\beta = 3 \quad (3.5-1d)$$

These conditions, if satisfied, permit us to write:

$$x = x_o + x_r + x_d \quad (3.5-2a)$$

$$y = y_o + y_r + y_d \quad (3.5-2b)$$

$$y_i = N_i x_i \quad (3.5-2c)$$

$$N_f = N_r = N_d = \frac{M_f}{A} \quad (= \frac{2B}{A} \text{ for ideal relay}) \quad (3.5-2d)$$

$$N_o \approx \frac{M_o}{A} = \frac{2M_f}{A} \quad (= \frac{4B}{A} \text{ for ideal relay}) \quad (3.5-2e)$$

B is the saturating level of the ideal relay, as the non-linearity (Figure 3.5-1).

Self-oscillation "Quenching"

Sufficient condition for limit cycle quenching is known [12] using the two sinusoid input describing function (T.S.I.D.F.). The

result is the condition:

$$L_o(j\omega_\pi) < \rho \quad (3.5-3a)$$

$$L_f(j\omega_\pi) < \frac{\rho}{2} \quad (3.5-3b)$$

$$\rho = 1.49 \text{ for an ideal relay} \quad (3.5-3c)$$

This constraint is given clearly in terms of the loop transmission gain margin, since ω_π is such that $\angle L_o(j\omega_\pi) = \angle L_f(j\omega_\pi) = -180^\circ$. The

"quenching" condition automatically takes care that $\left| \frac{L_o(j\omega_o)}{1 + L_o(j\omega_o)} \right|$ has a "possible" solution as mentioned at the end of Section 3.4.

Maximum Plant Output Oscillation

Finally

$$[c_o(t)]_{\max} \leq m \quad (3.5-4a)$$

or (Figure 3.5-1)

$$\frac{A_o |G_2 K P_h(j\omega_o)|}{|1 + L_o(j\omega_o)|} \leq m \quad (3.5-4b)$$

3.5-3 Synthesis Procedure (Smooth Solution)

The basic EEAS structure is drawn again in Figure 3.5-1, with non-linear element and ideal relay whose saturation level is B . As in the SOAS, there are two loop transmissions. $L_o, L_f = L_r, L_d$, if x_r, x_d are relatively slow aperiodic signals due to the command and disturbance inputs. L_f is valid for frequencies less than $\frac{\omega_o}{\beta} \approx \frac{\omega_o}{3}$.

Then

$$L_f(j\omega) = N_f G_1 G_2 K P_h(j\omega) \quad (3.5-5a)$$

$$N_f = \frac{2B}{\pi A} \text{ (for the ideal relay)} \quad (3.5-5b)$$

$$L_o(j\omega) = N_o G_1 G_2 K P_h(j\omega) \quad (3.5-5c)$$

$$N_o = \frac{4B}{\pi A} \quad (\text{for the ideal relay}) \quad (3.5-5d)$$

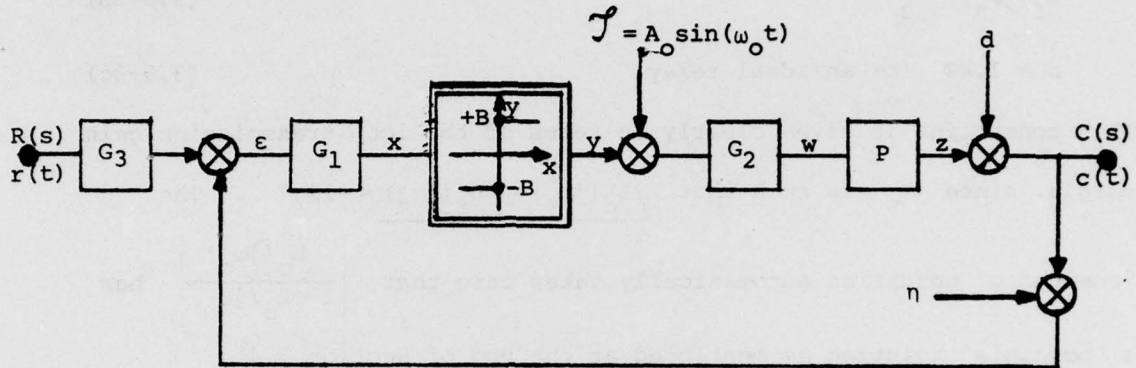


Figure 3.5-1 - Basic EEAS Structure
Non-linearity - Ideal Relay

First some relations will be derived based on the desired transmission for the command input, and on the extreme command input. All these relations are derived under the assumption that a "smooth" solution is used as discussed in Section 2.5-3 and Appendix II.

$$T_r(j\omega) = \frac{C_r}{R}(j\omega) = G_3(j\omega) \cdot \frac{L_f(j\omega)}{1 + L_f(j\omega)} \quad (3.5-6)$$

$$X_r(j\omega) = \frac{C_r(j\omega)}{N_f G_2 K P_h(j\omega)} \quad (3.5-7)$$

Substituting $C = RT_f$, $N_f = \frac{M_f}{A}$ in Equation 3.5-7, gives

$$\frac{X_r}{A}(j\omega) = \frac{RT_r(j\omega)}{M_f G_2 K P_h(j\omega)} \quad (3.5-8)$$

Equation 3.5-8 provides a relation defined in the frequency domain. The quasi-linearity constraint defined in Equation 3.5-1a gives a relation in the time domain

$$\frac{|x_r(t)|}{A} \leq \frac{1}{\alpha} = \frac{1}{3} \quad (3.5-9)$$

which has the same variables in the left side as in Equation 3.5-8.

Condition 3.5-9 is the most difficult to satisfy when:

- a) A has its minimum value. A has its minimum value when the plant has its minimum gain $K = K_{\min} = K_1$. This has already been shown in Equation 3.4-1. In this case $A = A_{\min} = A_1$.
- b) $x_r(t)$ has its maximum value. This will happen when the command input has its extreme value $r_e(t)$. This is the main reason the extreme command input has to be defined, as mentioned in Section 3.5-1.

Again as in the SOAS, we translate the time-domain condition expressed in Equation 3.5-9 as a frequency domain condition. Assuming $x_r(t)$ has a "smooth" shape, and using the results of Appendix II, if

$$\frac{|x_r(t)|}{A} \leq \frac{1}{\alpha} \quad (3.5-10a)$$

then

$$\left| \frac{x_r(j\omega)}{A} \right| \leq \left| \frac{1}{\alpha\omega} \right| \quad \forall \omega \quad (3.5-10b)$$

Returning to Equations 3.5-8 and 10b and replacing the parameters giving the most difficult conditions ($A = A_1$, $K = K_1$, $R(j\omega) = R_e(j\omega)$)

$$\left| \frac{x_r(j\omega)}{A_1} \right| = \left| \frac{R_e T_r(j\omega)}{M_f G_2 K_1 P_h(j\omega)} \right| \quad \omega \leq \frac{\omega_o}{\beta} \quad (3.5-11)$$

$$\left| \frac{x_r(j\omega)}{A_1} \right| \leq \left| \frac{1}{\alpha\omega} \right| \quad \forall \omega \quad (3.5-12)$$

or

$$\left| \frac{x_r(j\omega)}{A_1} \right| = \left| \frac{R_e T_r(j\omega)}{M_f G_2 K_1 P_h(j\omega)} \right| \leq \left| \frac{1}{\alpha\omega} \right|$$

or

$$\left| M_f G_2 K_2 P_h(j\omega) \right| \geq \frac{K_2}{K_1} \cdot \alpha \cdot \omega \left| R_e T_r(j\omega) \right| \quad \forall \quad \omega < \frac{\omega_o}{\beta} \quad (3.5-13)$$

A similar expression to 3.5-13 is derived for the extreme disturbance at the plant output. In Figure 3.5-1, due to the disturbance D ,

$$Z_d(j\omega) = -D(j\omega) \cdot \frac{L_f(j\omega)}{1 + L_f(j\omega)} \quad \omega \leq \frac{\omega_o}{\beta} \quad (3.5-14)$$

$$X_d(j\omega) = \frac{Z_d(j\omega)}{N_f G_2 K P_h(j\omega)} = \frac{-D(j\omega)}{N_f G_2 K P_h(j\omega)} \cdot \frac{L_f(j\omega)}{1 + L_f(j\omega)} \quad \omega \leq \frac{\omega_o}{\beta} \quad (3.5-15)$$

From here on until Equation 3.5-19 we follow the same reasoning used in the development of Equation 3.5-13 for the command input.

Substituting $N_f = \frac{M_f}{A}$ in Equation 3.5-15

$$\frac{X_d}{A}(j\omega) = \frac{-D(j\omega)}{M_f G_2 K P_h(j\omega)} \cdot \frac{L_f(j\omega)}{1 + L_f(j\omega)} \quad (3.5-16)$$

The constraint $\max_t |x_d(t)| \leq \frac{A}{\alpha}$ (Equation 3.5-1a) has to be satisfied, and the most difficult conditions to satisfy it are at $A = A_{\min} = A_1$, and consequently $K = K_{\min} = K_1$, and when $D(j\omega) = D_e(j\omega)$. Using again the results of Appendix II for smooth $x_d(t)$, if

$$\frac{|x_d(t)|}{A} \leq \frac{1}{\alpha} \quad (3.5-17a)$$

then

$$\frac{|X_d(j\omega)|}{A} \leq \left| \frac{1}{\alpha \omega} \right| \quad (3.5-17b)$$

Substituting in Equation 3.5-16

$$\left| \frac{X_d}{A_1}(j\omega) \right| = \left| \frac{D_e(j\omega)}{M_f G_2 K_1 P_h(j\omega)} \right| \left| \frac{L_f(j\omega)}{1 + L_f(j\omega)} \right| \leq \frac{1}{\alpha \omega} \quad \forall \quad \omega \leq \frac{\omega_o}{\beta} \quad (3.5-18)$$

or

$$\left| M_f G_2 K_2 P_h(j\omega) \right| \geq \frac{K_2}{K_1} \cdot \alpha \cdot \omega \left| D_e(j\omega) \cdot \frac{L_f(j\omega)}{1 + L_f(j\omega)} \right| \quad \forall \omega \leq \frac{\omega_0}{\beta} \quad (3.5-19)$$

There is a difference in the explicitness of Equation 3.5-19 if compared with 3.5-13. In 3.5-13 the right side of the inequality is completely defined apart the "far-off" poles and zeros that can be added to the nominal $T_f(j\omega)$. In Equation 3.5-19 $L_f(j\omega)$ is unknown, being the most important result of the system synthesis. Let us leave this subject for the time being and let us work out some useful relations related to the specified disturbance attenuation. The specified minimum disturbance attenuation provides bounds on $L_f(j\omega)$ for each frequency. Based on Figure 3.5-1,

$$\left| T_d(j\omega) \right| = \left| \frac{C_d(j\omega)}{D(j\omega)} \right| = \left| \frac{1}{1 + L_f(j\omega)} \right| \leq \left| T_d^{min}(j\omega) \right| \quad (3.5-20)$$

The same technique [1] used for the SOAS (Section 2.5-3) will be used. Figures 2.5-3,4,5 are valid also for the EEAS.

The second constraint that has to be satisfied is the self-oscillation quenching (Section 3.5-2, Equation 3.5-3).

$$\left| L_f(j\omega_\pi) \right| < \frac{\rho}{2} = \frac{1.49}{2} \quad (-2.56 \text{ dB}) \quad (3.5-21)$$

This is equivalent to a minimum gain margin for $L_f(j\omega)$ of 2.56 dB.

In general the disturbance attenuation requirement is more "severe" than the "quenching" demand, since the disturbance attenuation due to the "quenching" demand is

$$\left| T_d(j\omega_\pi) \right|_{GM=2.56 \text{ dB}} \cong 10 \text{ dB} \quad (3.5-22)$$

which is not very common, since it means that the effect of disturbances at ω_π is allowed to be about three times the disturbance itself (If $|D(j\omega_\pi)|$ is small enough, it might be allowed).

The third constraint to be satisfied is the maximum allowable plant output oscillation amplitude (Figure 3.5-1 and Equation 3.5-4).

$$|C_o(j\omega_o)| = A_o \frac{|G_2 K P_h(j\omega_o)|}{|1 + L_o(j\omega_o)|} \quad (3.5-23)$$

The maximum amplitude of oscillation occurs when $K = K_{\max} = K_2$, giving

$$|C_o(j\omega_o)|_{\max} = \frac{A_o |G_2 K_2 P_h(j\omega_o)|}{|1 + L_o(j\omega_o)|} \leq m \quad (3.5-24)$$

or

$$|G_2 K_2 P_h(j\omega_o)| \leq \frac{m |1 + L_o(j\omega_o)|}{A_o} \quad (3.5-25)$$

But (Equation 3.4-20)

$$\frac{M_o}{A_o} = \frac{|L_o(j\omega_o)|}{|1 + L_o(j\omega_o)|}$$

So

$$\frac{|1 + L_o(j\omega_o)|}{A_o} = \frac{|L_o(j\omega_o)|}{M_o} = \frac{|L_o(j\omega_o)|}{M_o} \times M_f \times \frac{1}{M_f}$$

and

$$\frac{|1 + L_o(j\omega_o)|}{A_o} = \frac{|L_f(j\omega_o)|}{M_f} \quad (3.5-26)$$

Substituting in Equation 3.5-25

$$|M_f G_2 K_2 P_h(j\omega_o)| \leq m |L_f(j\omega_o)| \quad (3.5-27)$$

Now we will extrapolate Equations 3.5-11 and 18 for $\omega = \omega_o$. This extrapolation is valid as per Appendix III, and was also used in the SOAS synthesis (Section 2.5, Equations 2.5-27,30). The same is valid for Equations 3.5-32,35.

$$\frac{|x_r(j\omega_o)|}{A_1} \approx \frac{|R_e T_r(j\omega_o)|}{|M_f G_2 K_1 P_h(j\omega_o)|} \quad (3.5-28)$$

$$\frac{|x_d(j\omega_o)|}{A_1} \approx \frac{|D_e(j\omega_o)|}{|M_f G_2 K_1 P_h(j\omega_o)|} \times \frac{|L_f(j\omega_o)|}{|1 + L_f(j\omega_o)|} \quad (3.5-29)$$

Substituting Equation 3.5-27 in 28 and 29

$$\left| \frac{x_r}{A_1}(j\omega_o) \right| \geq \frac{K_2}{K_{1m}} \left| \frac{T_r R_e}{L_f}(j\omega_o) \right| \quad (3.5-30)$$

$$\left| \frac{x_d}{A_1}(j\omega_o) \right| \geq \frac{K_2}{K_{1m}} \left| \frac{D_e(j\omega_o)}{1 + L_f(j\omega_o)} \right| \quad (3.5-31)$$

But

$$\left| T_d(j\omega_o) \right| \approx \left| \frac{1}{1 + L_f(j\omega_o)} \right| \quad (3.5-32)$$

So

$$\left| \frac{x_d}{A_1}(j\omega_o) \right| \geq \frac{K_2}{K_{1m}} \left| D_e T_d(j\omega_o) \right| \quad (3.5-33)$$

Again as in the SOAS, $\frac{K_2}{K_1}$, the main reason for using an adaptive system instead of a linear time invariant system, reappears as a factor defining the oscillating frequency. The reason for this "reappearance" is the same as for the SOAS.

Notice that Equations 3.5-30 and 33 are similar to their equivalent equations obtained for the SOAS (Equations 2.5-29,30) when in this case

$\left| L_f(j\omega_o) \right|_{\text{SOAS}} = \frac{1}{2}$ and $\left| T_d(j\omega_o) \right|_{\text{SOAS}} \triangleq \left| \frac{1}{1 + L_f(j\omega_o)} \right| = 2$. Here lies the main advantage of the EEAS when compared to the SOAS, since the connection between the oscillating frequency and the system bandwidth has been broken.

Equations 3.5-30 and 33 could be combined in one equation, which can provide a good graphical sketch for a better understanding of the problem. In Equation 3.5-30

$$Z_{er}(j\omega_o) = T_r R_e(j\omega_o) \quad (3.5-34)$$

where $Z_{er}(j\omega_o)$ is the extreme plant output due to the extreme command input $R_e(j\omega)$ at the frequency ω_o .

In Equation 3.5-33, and Figure 3.5-1,

$$|D_e T_d(j\omega_o)| \approx \left| \frac{D_e}{1 + L_f(j\omega_o)} \right| \cdot \left| \frac{L_f(j\omega_o)}{L_f(j\omega_o)} \right| = \left| \frac{Z_{ed}(j\omega_o)}{L_f(j\omega_o)} \right| \quad (3.5-35)$$

where $Z_{ed}(j\omega_o)$ is the extreme plant output due to the extreme disturbance signal $D_e(j\omega)$ at the frequency ω_o . Substituting Equations 3.5-34 and 35 in 30 and 33

$$\left| \frac{X_f}{A_1}(j\omega_o) \right| \geq \frac{K_2}{K_1 m} \left| \frac{Z_e}{L_f}(j\omega_o) \right| \quad (3.5-36)$$

where X_f represents the forced signal at the non-linearity input and Z_e is the extreme plant output, due to either the extreme command or extreme disturbance signals.

For a smooth shape of $x(t)$, as per Equations 3.5-12 and 17,

$$\left| \frac{X_f}{A_1}(j\omega) \right| \leq \left| \frac{1}{\alpha\omega} \right| \quad (3.5-37)$$

Combining with Equation 3.5-36

$$\begin{aligned} \left| \frac{1}{\alpha\omega} \right|_{\omega_o} &\geq \frac{K_2}{K_1 m} \left| \frac{Z_e}{L_f}(j\omega_o) \right| \\ \text{or} \quad |L_o(j\omega_o)| &= 2 |L_f(j\omega_o)| \geq \frac{2\alpha K_2}{m K_1} |\omega_o Z_e(j\omega_o)| \end{aligned} \quad (3.5-38)$$

A typical sketch representing Equation 3.5-38 is shown in Figure 3.5-2, where ω_o , the oscillation frequency, is graphically determined, as the intersection of curves $L_o(j\omega)$ and $\frac{2\alpha K_2}{m K_1} \cdot |\omega_o Z_e(j\omega_o)|$. ω_o is the smallest frequency satisfying Equation 3.5-38.

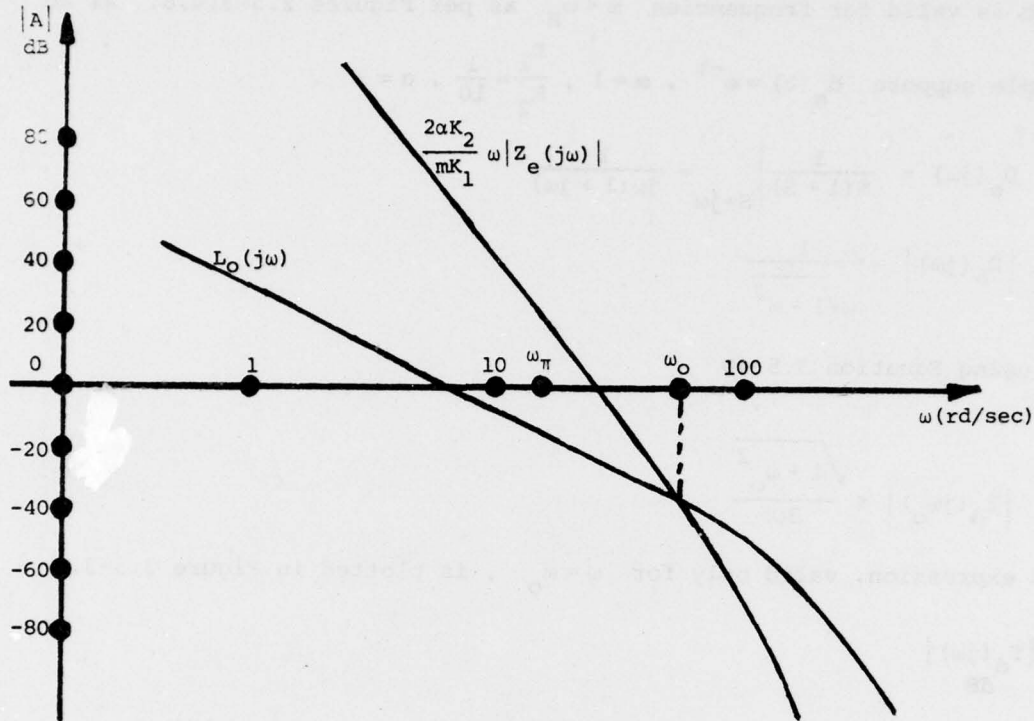


Figure 3.5-2 - Typical sketch for oscillation frequency determination

EEAS - Smooth case of $\frac{X_f}{A_1}(j\omega)$

This graphical solution only gives an insight of the problem, since $Z_e(j\omega_o)$ and $L_o(j\omega_o)$ are still unknown. Some more relations are derived. Comparing Equation 3.5-19 extrapolated for $\omega = \omega_o$ and Equation 3.5-27,

$$\frac{K_2}{K_1} \alpha \omega_o \frac{|D_e(j\omega_o)L_f(j\omega_o)|}{|1 + L_f(j\omega_o)|} \leq |M_f G_2 K_2 P_h(j\omega_o)| \leq m |L_f(j\omega_o)| \quad (3.5-39)$$

or comparing the two extreme terms of inequality 39

$$T_d(j\omega_o) = \left| \frac{1}{1 + L_f(j\omega_o)} \right| \leq \frac{mK_1}{\alpha K_2 \omega_o |D_e(j\omega_o)|} \quad (3.5-40)$$

Equation 3.5-40 gives a constraint, valid only for $\omega = \omega_o$, and it is equivalent to the one given by the specified disturbance attenuation,

which is valid for frequencies $\omega < \omega_H$ as per Figures 2.5-3,4,5. As an example suppose $d_e(t) = e^{-t}$, $m=1$, $\frac{K_1}{K_2} = \frac{1}{10}$, $\alpha=3$.

$$D_e(j\omega) = \left. \frac{1}{s(1+s)} \right|_{s=j\omega} = \frac{1}{j\omega(1+j\omega)}$$

$$|D_e(j\omega)| = \frac{1}{\omega\sqrt{1+\omega^2}}$$

and using Equation 3.5-40

$$|T_d(j\omega_o)| \leq \frac{\sqrt{1+\omega_o^2}}{30}$$

This expression, valid only for $\omega = \omega_o$, is plotted in Figure 3.5-3.

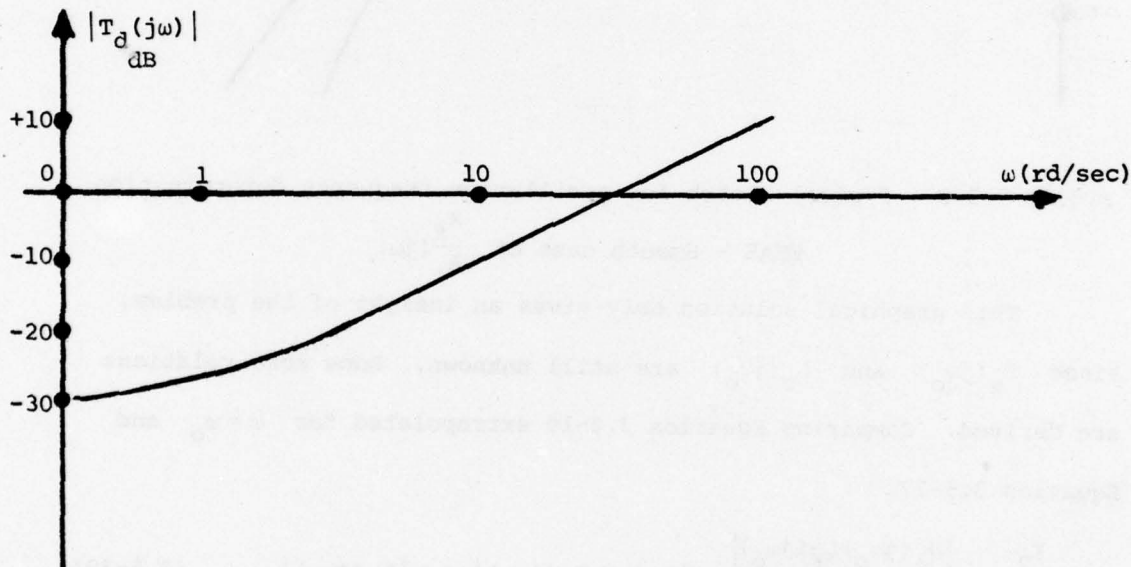


Figure 3.5-3 - Typical "Disturbance Attenuation" at ω_o

The bounds of $L_f(j\omega_o)$ satisfying the "disturbance attenuation" requirements at ω_o are plotted in Figure 3.5-4, using the same technique as explained in Section 2.5-3, Figures 2.5-3,4,5.

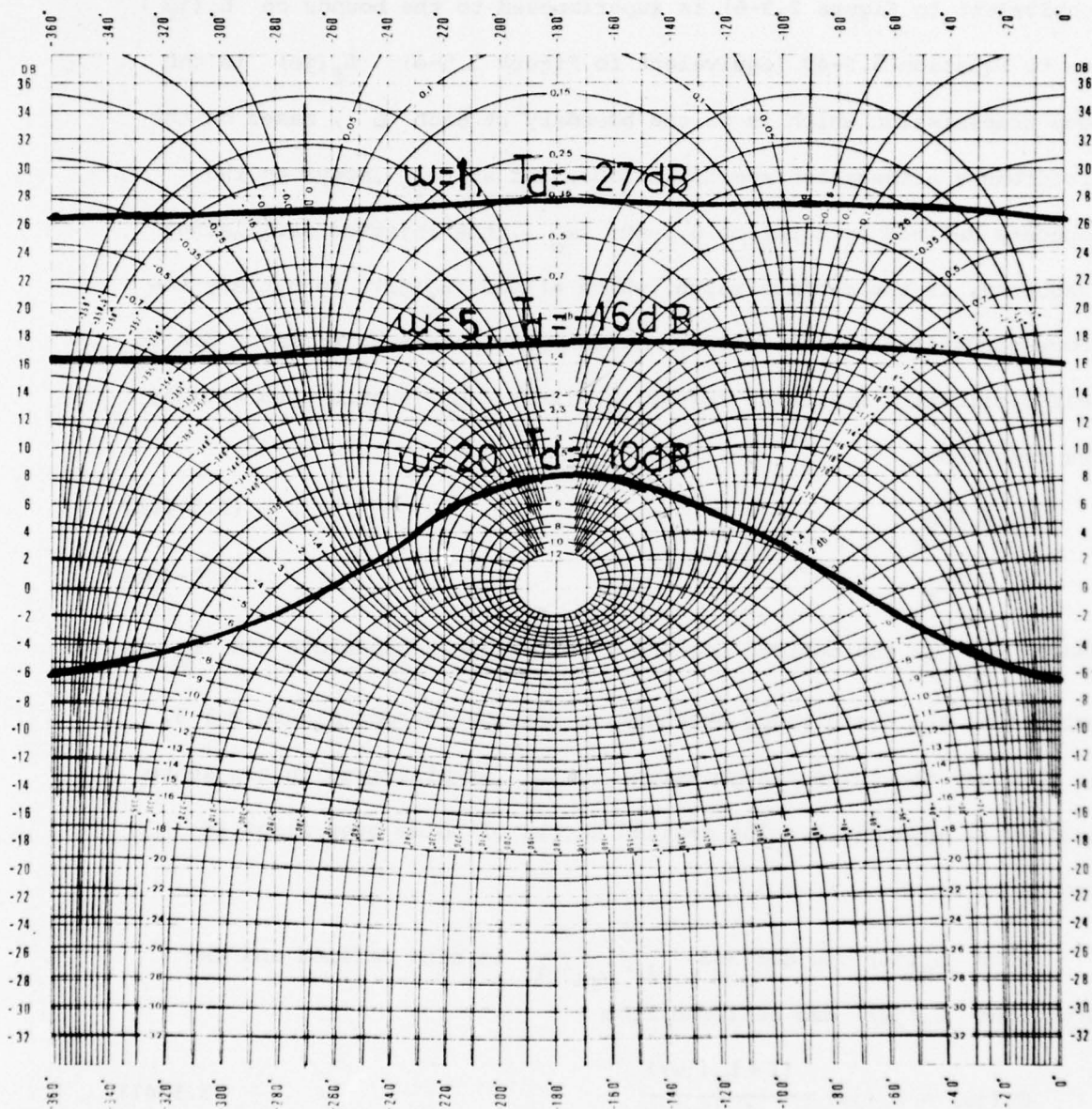


Figure 3.5-4 - Nychol's plot for bounds on $L_f(j\omega_0)$
(Related to Figure 3.5-3)

Notice in Figures 3.5-3 and 4, bounds have been plotted for several frequencies. Only one of these bounds has to be satisfied - the one related to ω_o . Now $L_f(j\omega)$ can be defined. In the same Nichol's chart the bounds on $L_f(j\omega)$, due to the specified disturbance attenuation (equivalent to Figure 2.3-6), is superimposed to the bounds on $L_f(j\omega_o)$ due to Equation 3.5-40 (equivalent to Figure 3.5-4). $L_f(j\omega)$ is the loop transmission which is on the boundary at each ω , based on the disturbance attenuation specifications, and at ω_o , stays on the boundary defined by Equation 3.5-40; ω_o , the injected oscillating frequency, is the minimum value which allows $L_f(j\omega)$ to satisfy the above conditions and to satisfy minimum gain margin requirement due to self-oscillation quenching (Equation 3.2-8). ω_o should also satisfy the relations:

$$\omega_o \geq \beta\omega_{T_r} \quad (3.5-40a)$$

$$\omega_o \geq \beta\omega_H \quad (3.5-40b)$$

Where ω_{T_r} is the desired command input response bandwidth and ω_H is related to the disturbance attenuation response as per Figure 2.5-3. In this way the noise transmission $T_n(j\omega)$ is minimized in the sense defined in Appendix I. The desired excess of poles over zeros in L_f should be known.

Once $L_f(j\omega)$ is defined, $\frac{L_f(j\omega)}{1+L_f(j\omega)}$ is also defined and the prefilter $G_3(j\omega)$ can be found from

$$G_3(j\omega) = T_r(j\omega) \times \frac{(1+L_f(j\omega))}{L_f(j\omega)} \quad (3.5-41)$$

This expression is derived directly from Equation 3.5-6.

Next $M_f G_2 K_2 P_h(j\omega)$ is to be defined - it satisfies inequalities 3.5-13 and 19 repeated here:

$$|M_f G_2 K_2 P_h(j\omega)| \geq \frac{K_2}{K_1} \cdot \alpha \cdot \omega \cdot |R_e T_r(j\omega)| \quad (3.5-42)$$

$$|M_f G_2 K_2 P_h(j\omega)| \geq \frac{K_2}{K_1} \cdot \alpha \cdot \omega \cdot \left| D_e(j\omega) \times \frac{L_f(j\omega)}{1 + L_f(j\omega)} \right| \quad (3.5-43)$$

And at ω_o , based on Equation 3.5-27

$$|M_f G_2 K_2 P_h(j\omega_o)| \leq m |L_f(j\omega_o)| \quad (3.5-44)$$

Once $M_f G_2 K_2 P_h(j\omega)$ and $L_f(j\omega)$ are known, it is possible to determine

$$\frac{G_1(j\omega)}{A_2} = \frac{L_f(j\omega)}{M_f G_2 K_2 P_h(j\omega)} \quad (3.5-45)$$

The ideal relay saturation level $B = \frac{M_f \pi}{2}$ and A_2 are chosen available voltages, and in practice should be chosen as large as possible. The injected signal amplitude $\mathcal{J} = A_o \sin(\omega_o t)$ is given by

$$A_o = M_o \left| \frac{1 + L_o(j\omega_o)}{L_o(j\omega_o)} \right| \quad \text{as per Equation 3.4-18.}$$

Before we proceed on the numerical example, Equation 3.5-38 is repeated:

$$|L_o(j\omega_o)| \geq \frac{2\alpha K_2}{mK_1} |\omega_o Z_e(j\omega_o)| \quad (3.5-46)$$

As per Figure 3.5-2, since $\omega_o > \omega_\pi$, we assume $|L_o(j\omega_o)| < |L_o(j\omega_\pi)|$.

Suppose now $L_f(j\omega_o)$ (and also $L_o(j\omega_o) = 2L_f(j\omega_o)$) have very large magnitude. In this case Equation 3.5-46 is much easier to satisfy, reducing the possible oscillation frequency ω_o . This is shown in Figure 3.5-5, and also in the numerical example, Section 3.6. In Figure 3.5-5 three possible solutions for $L_o(j\omega_o)$ are plotted with their corresponding oscillation frequencies. L_{o1} is the case where

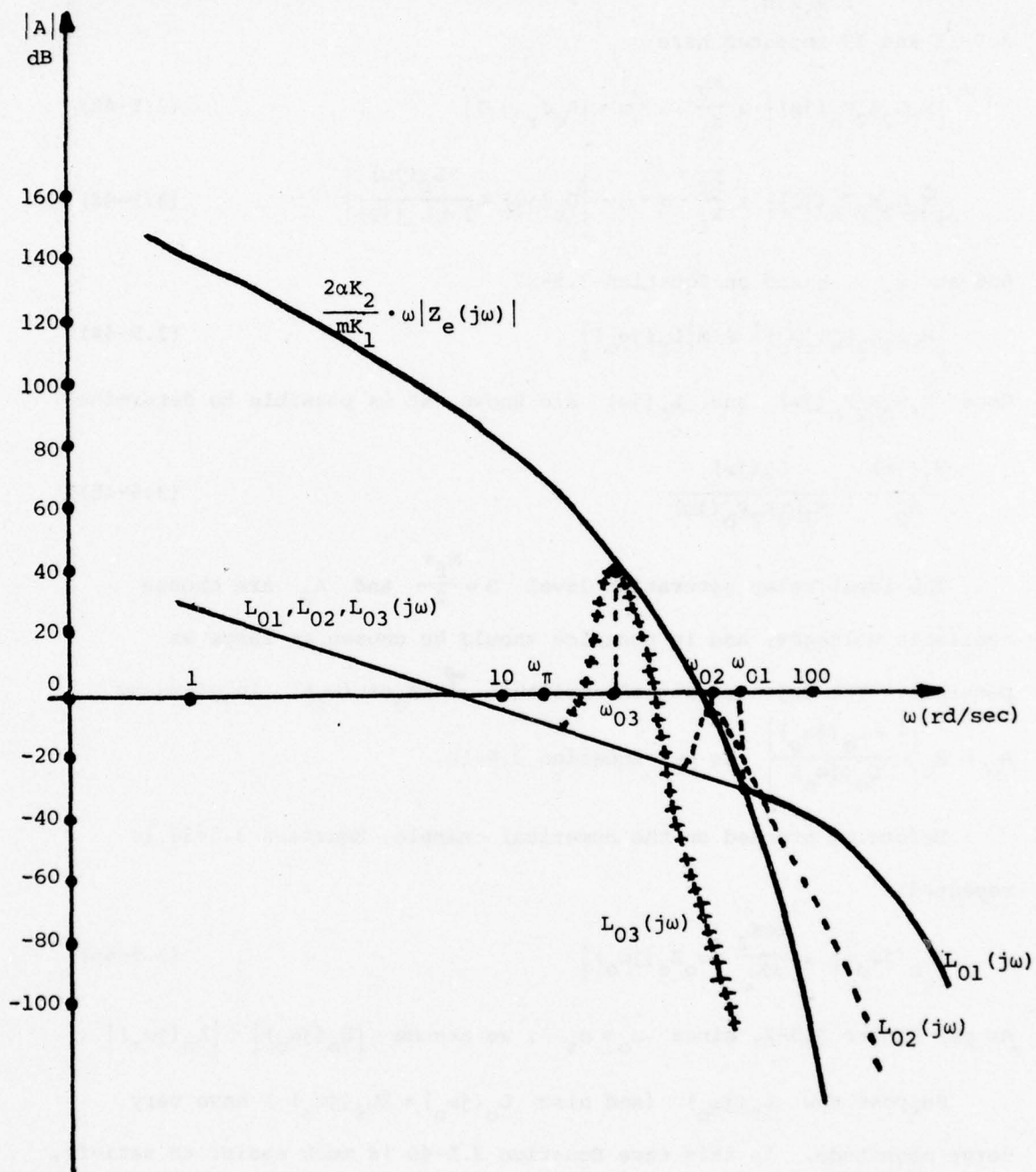


Figure 3.5-5 - Comparison between a "smooth" and possible "non-smooth" cases.

EEAS loop transmission ($\frac{X_f}{A}(j\omega)$ is "smooth")

the loop transmission is a "smooth" one, L_{02} is the case where the loop transmission has a "non-smooth" shape but still $|L_{02}(j\omega_0)| < 1$, and finally in $L_{03}(j\omega)$ the loop transmission has a "non-smooth" shape and $|L_{03}(j\omega_0)| > 1$. In this last case special attention should be taken to have enough gain margin at $\phi = -(180^\circ + n \times 360^\circ)$, to quench any other possible self-oscillation.

In Figure 3.5-5, ω_{01} , ω_{02} , ω_{03} represent the oscillation frequency for L_{01} , L_{02} , L_{03} .

3.6 Numerical Example for the EEAS

In this numerical example the procedure outlined in 3.5-5 is followed.

Specifications and Constraints

- Desired Command Response -

$$T_r(s) = \frac{1}{1 + \frac{2 \cdot 5}{.1} s + \frac{s^2}{.1^2}} \times \phi(s)$$

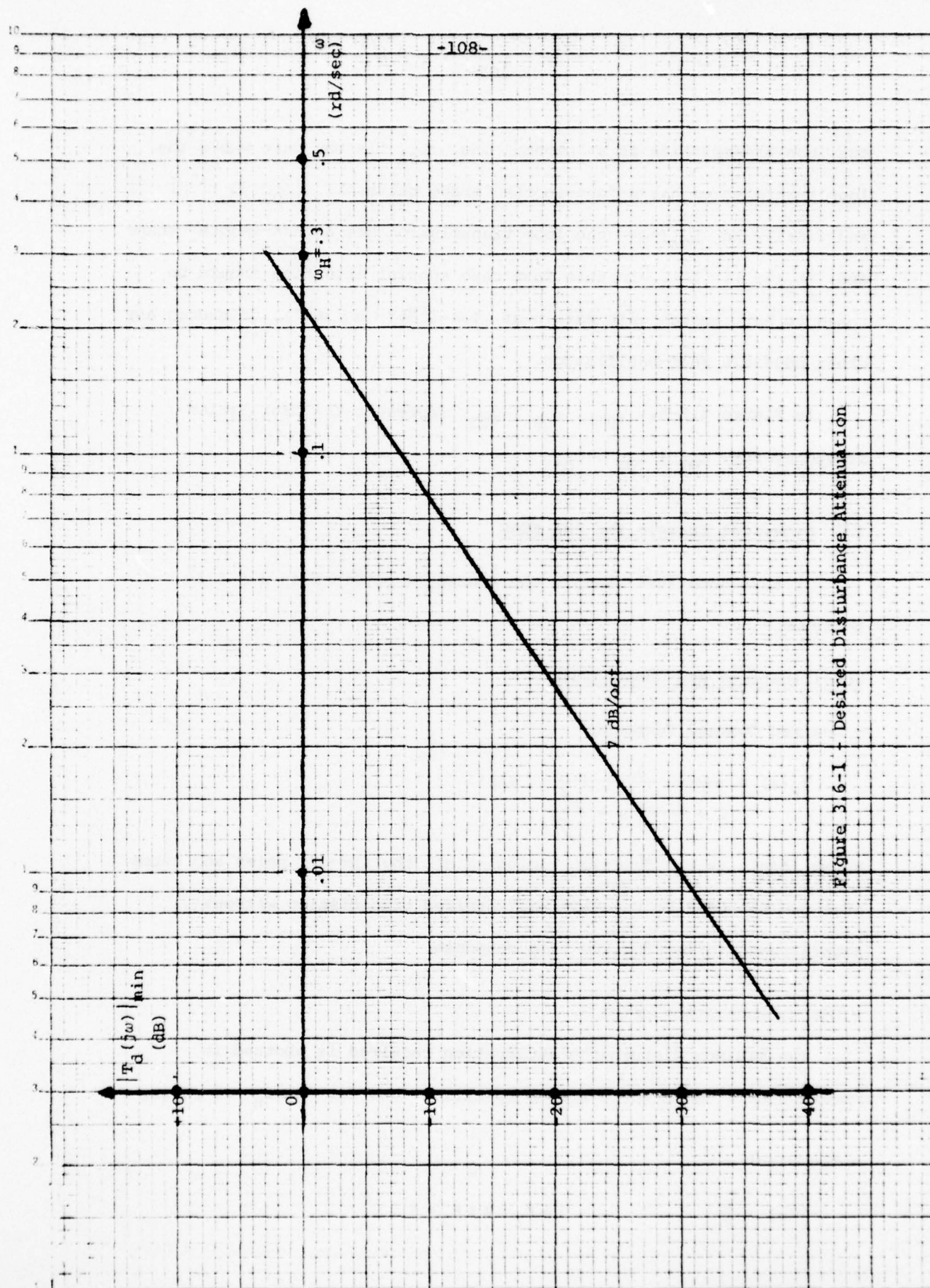
Where $\phi(s)$ is the function including all the far-off poles and zeros that can be added to the "nominal" desired transmission without significantly affecting the time response.

- Disturbance Attenuation -

The minimum disturbance attenuation required is plotted in Figure 3.6-1. Note there are no specifications for $\omega \geq \omega_H = .3$ rad/sec.

- The Plant -

$$P(s) = \frac{K}{s} \quad 1 = K_1 \leq K \leq K_2 = 5$$



- Extreme Command Input -

$$r_e(t) = 75 \cdot \mu(t) \rightarrow R_e(s) = \frac{75}{s}$$

- Extreme Disturbance Input -

$$d_e(t) = (1 - e^{-t/3})\mu(t) \rightarrow D_e(s) = \frac{1}{s(1+3s)}$$

Find also the maximum allowable step disturbance (which is supposed not to be oscillatory).

- Quasi-linear Constraints -

The used parameters are $\alpha = \beta = 3$, so

$$\left| \frac{x_r(t)}{A} \right| \leq \frac{1}{3}, \quad \left| \frac{x_d(t)}{A} \right| \leq \frac{1}{3}, \quad \omega_{br} \leq \frac{\omega_o}{3}, \quad \omega_{bd} \leq \frac{\omega_o}{3}.$$

- Plant Output Oscillation -

$$|C_o(t)| \leq m = 1$$

- Limit Cycle Quenching -

In Equation 3.2-8 we take $\rho = 1$, so

$$|L_o(j\omega_\pi)| < 1 \quad \text{and} \quad |L_f(j\omega_\pi)| < \frac{1}{2}$$

- Excess of Poles over Zeros -

$L_f(j\omega)$ is to have an excess of 9 poles over zeros.

The Solution

In the Nichol's chart (Figure 3.6-2) all the existing bounds of $L_f(j\omega)$ are plotted. They are due to:

1. Disturbance attenuation specifications as per Figure 3.6-1, and valid for $\omega \leq .3$ rad/sec.

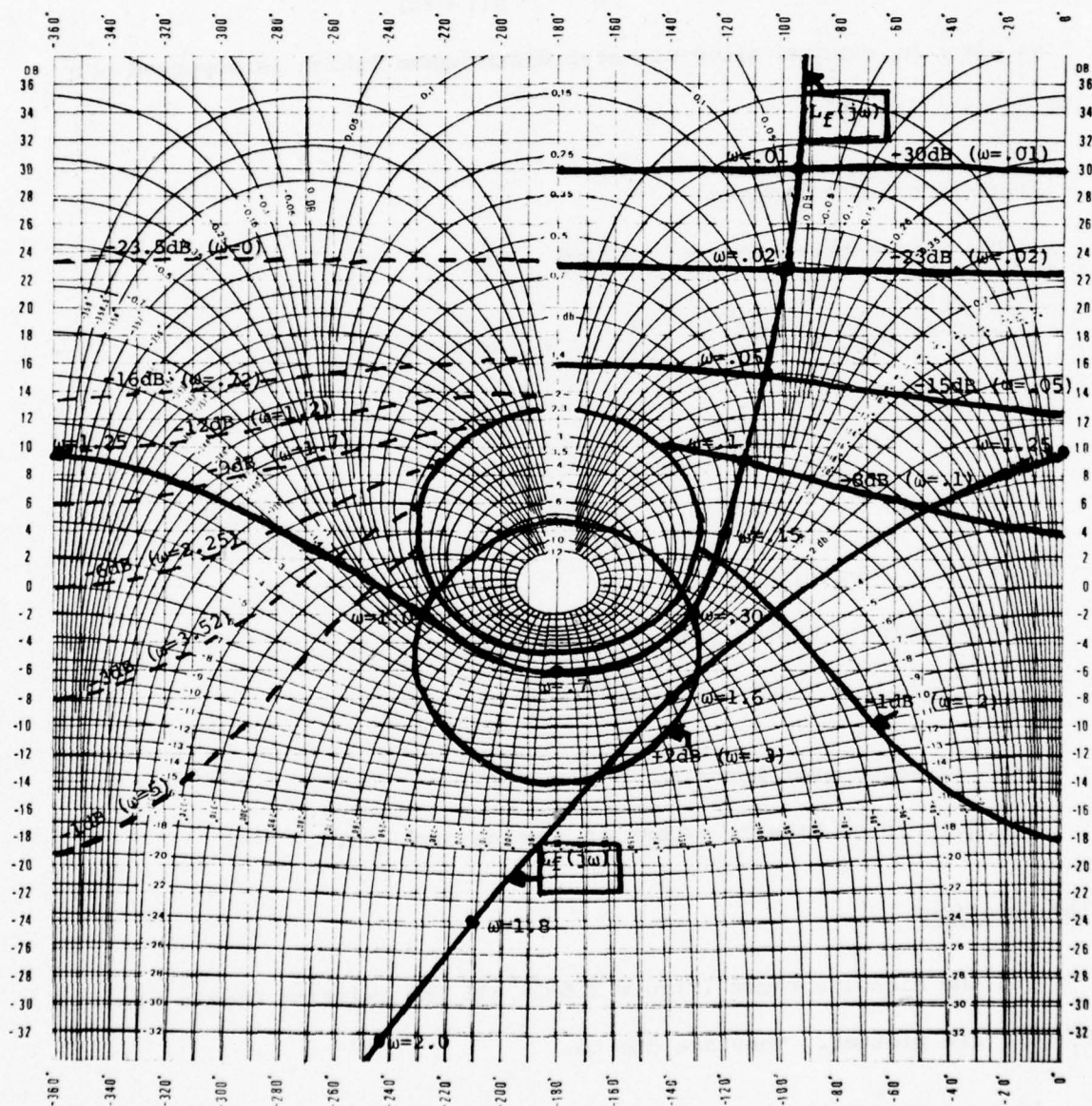


Figure 3.6-2 - EEAS Numerical Example
Bounds on $L_f(j\omega)$ and Solution

2. The condition due to Equation 3.5-40 can be viewed as an "equivalent disturbance attenuation", and is valid only for the oscillating frequency ω_o . Since ω_o is unknown, it is necessary to plot this "equivalent disturbance" bound for several frequencies.
3. $L_f(j\omega_\pi) < \frac{1}{2}$ (to avoid self-oscillation). It is a minimum gain margin demand.
4. The step response, as requested, should not be oscillatory. A good engineering solution is not to allow $\left| \frac{L_f(j\omega)}{1 + L_f(j\omega)} \right| > 2.3 \text{ dB}$.

All these bounds are plotted in Figure 3.6-2. First, the constraints on $L_f(j\omega)$ due to the disturbance attenuation specifications are plotted based on the technique explained in Section 2.5-3, Figures 2.5-3,4,5. The bounds on $L_f(j\omega)$ are plotted for a certain number of frequencies.

ω (rd/sec)	$ T_d(j\omega) _{\min}$ (dB)
.01	-30
.02	-23
.05	-15
.10	- 8
.20	- 1
.30	+ 2

These bounds are plotted, and for each bound its associated frequency and desired disturbance attenuation are pointed out. Next Equation 3.5-40 provides a bound on $|L_f(j\omega_o)|$, as

$$|T_d(j\omega_o)| = \left| \frac{1}{1 + L_f(j\omega_o)} \right| \leq \frac{mK_1}{\alpha K_2 \omega_o D_e(j\omega_o)}$$

Since ω_o is unknown, we will have bounds for several frequencies but need to be satisfied only at ω_o . Substituting the values by the given data $\left(m=1, \alpha=3, \frac{K_2}{K_1}=5, D_e(j\omega) = \frac{1}{j\omega(1+3j\omega)} \right)$.

$$|T_d(j\omega_o)|_{\min} = \frac{\sqrt{1+9\omega_o^2}}{15}$$

which provides the following table:

ω_o (rd/sec)	$T_d(j\omega_o)$ (dB)
0	-23.5
.37	-20.0
.72	-16.0
1.2	-12.0
1.7	- 9.0
2.25	- 6.0
3.52	- 3.0

These bounds are plotted with their associated frequencies and desired disturbance attenuation marked. Note that if the extreme disturbance was a unit step, $d'_e(t) = u(t)$, the limit

$$|T_d(j\omega_o)|_{\min} = -23.5 \text{ dB} \left(\frac{mK_1}{\alpha K_2} = \frac{1}{15} \right) \text{ independently of the frequency}$$

(which corresponds in the present case for $\omega = 0$). Next $|L_f(j\omega_\pi)| < \frac{1}{2}$ is also marked as the point A, with 6 dB gain margin at the angle -180° . Finally $\left| \frac{L_f(j\omega)}{1+L_f(j\omega)} \right| < 2.3 \text{ dB}$ is also plotted in the Nichols chart.

Once all the bounds have been plotted in the Nichols chart, $L_f(j\omega)$ is derived, based on the technique developed by Horowitz [5], and summarized in Appendix I.

There are still two conditions to be satisfied:

$$\omega_o \geq \beta \omega_{bf} = 3 \times .1 = .3 \text{ rd/sec}$$

$$\omega_o \geq \beta \omega_{bd} = 3 \times .3 = .9 \text{ rd/sec}$$

The derived $L_f(s)$ in our case is:

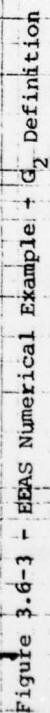
$$L_f(s) = \frac{.2 \left(1 + \frac{s}{.35}\right)^2 \left(\omega = 1.5\right) \left(\zeta = .5\right)}{s \left(1 + \frac{s}{.15}\right) \left(\omega = 1.25\right) \left(\zeta = .025\right) \left(1 + \frac{s}{1.5}\right) \left(\omega = 1.5\right)^2 \left(\zeta = 1\right) \left(\omega = 1.5\right)^2 \left(\zeta = .3\right)}$$

which is also plotted in Figure 3.6-2, where the oscillation frequency $\omega_o = 1.25 \text{ rd/sec}$. Notice that one of the poles has already a very small damping factor ($\zeta = .025$). In case the extreme disturbance was a unit step input, and the same oscillation frequency is kept, a solution for $L'_f(j\omega)$ is "available" by keeping the same $L_f(s)$; the only change is in substituting the already low damping factor for the complex pole ($\omega = 1.25$, $\zeta = .025$) by an even lower damping factor ($\omega = 1.25$, $\zeta = .006$) to satisfy the demands of $L_f(j\omega_o)$ as per Equation 3.5-40. Notice also that if a smooth loop transmission (relate to Figure 3.5-5) is considered, then the oscillation frequency could not be less than 4-5 rd/sec. in the case being treated, where an "exponential" disturbance is applied. In the case of a "step" disturbance, no "smooth" loop transmission gives a solution for the problem.

$L_f(j\omega)$ being defined, so is $\frac{|L_f(j\omega)|}{|1 + L_f(j\omega)|}$. Now, the limits of $|M_f G_2 K_2 P_h(j\omega)|$ due to the disturbance input, as per Equation 3.5-43, can be set.

$$M_f G_2 K_2 P_h(j\omega) \geq \frac{K_2}{K_1} \cdot \alpha \cdot \omega \cdot \left| D_e(j\omega) \cdot \frac{L_f(j\omega)}{(1 + L_f(j\omega))} \right|$$

Substituting $\frac{K_2}{K_1}$, α , $D_e(j\omega)$ as defined in this problem,



$$|M_f G_2 K_2 P_h(j\omega)| \geq 15 \left| \frac{1}{\sqrt{1+9\omega^2}} \right| \left| \frac{L_f(j\omega)}{1+L_f(j\omega)} \right|$$

We first draw $\left| \frac{L_f(j\omega)}{1+L_f(j\omega)} \right|$ in Figure 3.6-3. Next, $\frac{15}{\sqrt{1+9\omega^2}} \times \left| \frac{L_f(j\omega)}{1+L_f(j\omega)} \right|$

is plotted. Then, the "nominal" desired transmission function

$$T_r(s) = \frac{1}{1 + \frac{2 \times .5}{.1} s + \frac{s^2}{.1^2}} = \quad , \text{ is plotted. Far-off poles and zeros can}$$

be added to this nominal transmission.

All the poles and zeros of $\frac{L_f(s)}{1+L_f(s)}$ are considered as far-off

poles and zeros of $T_r(s)$. This is valid since for all

$$\omega < 3\omega_o = 3.75 \text{ rd/sec} , \quad \left| \frac{L_f(s)}{1+L_f(s)} \right| \approx 1 . \text{ This makes:}$$

$$T_r(s) = \frac{1}{\left(\begin{smallmatrix} \omega_n = .1 \\ \zeta = .5 \end{smallmatrix} \right)} \times \frac{L_f(s)}{1+L_f(s)}$$

with

$$G_3(s) = \frac{1}{\left(\begin{smallmatrix} \omega_n = .1 \\ \zeta = .5 \end{smallmatrix} \right)}$$

Next the real transmission $T_r(s)$ is plotted, and so the limit for

$M_f G_2 K_2 P_h(s)$ as per Equation 3.5-42.

$$|M_f G_2 K_2 P_h(j\omega)| \geq \frac{K_2}{K_1} \cdot \alpha \cdot \omega \cdot |R_e T_r(j\omega)|$$

Substituting the values of this example

$$|M_f G_2 K_2 P_h(j\omega)| \geq 1.125 |T_r(j\omega)|$$

which is also plotted in Figure 3.6-3.

$|M_f G_2 K_2 P_h(j\omega)|$ has to have a magnitude (at all frequencies) which satisfies both conditions, due to the extreme disturbance and to

the extreme input. $|M_f G_2 K_2 P_h(j\omega_o)|$ has to satisfy also the condition given by Equation 3.5-44, which guarantees a maximum oscillation level at the plant output ($\leq m$).

$$|M_f G_2 K_2 P_h(j\omega_o)| \leq m |L_f(j\omega_o)| = 1 \times 2.8 = 2.8$$

This constraint is automatically satisfied if

$$|M_f G_2 K_2 P_h(j\omega_o)| = \frac{15}{\sqrt{1+9\omega_o^2}} \times \left| \frac{L_f(j\omega_o)}{1+L_f(j\omega_o)} \right|, \text{ since based on Equation 3.5-39}$$

$$\frac{K_2}{K_1} \cdot \alpha \cdot \omega_o \cdot |D_e(j\omega_o)| \left| \frac{L_f(j\omega_o)}{1+L_f(j\omega_o)} \right| = |M_f G_2 K_2 P_h(j\omega_o)| = m |L_f(j\omega_o)|$$

and $\left| \frac{1}{1+L_f(j\omega_o)} \right| = \frac{mK_1}{\alpha K_2 \omega_o D_e(j\omega_o)}$ has been satisfied.

On the other hand, the limit of $|M_f G_2 K_2 P_h(j\omega_o)|$ due to the command input, is lower than the limit of $|M_f G_2 K_2 P_h(j\omega_o)|$ due to the disturbance input, so all the conditions are satisfied. In the opposite case there are two possibilities; either add some more far-off poles to G_3 (this means some extra far-off poles to T_r), until $|M_f G_2 K_2 P_h(j\omega_o)|$ due to the command signal equals or is lower than the limit due to the disturbance, or in case no more extra far-off poles are allowed, the oscillation frequency should be increased.

To avoid the complexity of the functions, we try to use as many as possible zeros and poles of L_f . We choose

$$M_f G_2 K_2 P(s) = \frac{112 \cdot \left(\begin{smallmatrix} \omega = 1.5 \\ \zeta = .5 \end{smallmatrix} \right)}{s \left(1 + \frac{s}{.15} \right) \left(\begin{smallmatrix} \omega = 1.5 \\ \zeta = 1 \end{smallmatrix} \right)^2 \left(1 + \frac{s}{1.5} \right)}$$

so

$$|M_f G_2 K_2 P(j\omega_o)| = 2.6$$

Now we can define

$$\frac{G_1}{A_2}(s) = \frac{L_f(s)}{M_f G_2 K_2 P(s)} = \frac{1}{560} \frac{\left(1 + \frac{s}{.35}\right)^2}{\left(\omega = 1.25\right) \left(\omega = 1.5\right)^2 \left(\zeta = .025\right) \left(\zeta = .3\right)}$$

If we take $B = 20 \pi$, then $M_f = \frac{2B}{\pi} = 40$, and considering the extreme plant $K_2 P(s) = \frac{5}{s}$, $M_f K_2 P = \frac{200}{s}$, we get

$$G_2(s) = \frac{.56 \left(\omega = 1.5\right) \left(\zeta = .5\right)}{\left(1 + \frac{s}{.15}\right) \left(\omega = 1.5\right)^2 \left(\zeta = 1\right) \left(1 + \frac{s}{1.5}\right)}$$

Choosing $A_2 = 50$ (so $A_1 = 10$)

$$G_1 = \frac{.091 \left(1 + \frac{s}{.35}\right)^2}{\left(\omega = 1.25\right) \left(\omega = 1.5\right)^2 \left(\zeta = .025\right) \left(\zeta = .3\right)}$$

$G_3(s)$ has already been determined

$$G_3(s) = \frac{1}{1 + \frac{2 \times .5}{.1} s + \frac{s^2}{.1^2}}$$

The injected signal $\mathcal{J} = A_o \sin(\omega_o t)$ has a frequency $\omega_o = 1.25$ rd/sec and its amplitude is available from

$$\left| \frac{M_o}{I_o} \right| = \left| \frac{L_o(j\omega_o)}{1 + L_o(j\omega_o)} \right| = (-1.4 \text{ dB}) = (.85)$$

Observation - $\left| \frac{L_o(j\omega_o)}{1 + L_o(j\omega_o)} \right|$ is measured in the Nichols chart when

$$L_f(j\omega_o) = \frac{L_o(j\omega_o)}{2}, \text{ so}$$

$$I_o = \frac{M_o}{.85} = \frac{\frac{4B}{\pi}}{.85} = \frac{\frac{4 \times 20 \pi}{\pi}}{.85} = \frac{80}{.85} = 94.116$$

Hence the injected signal is

$$\mathcal{J}(t) = 94 \sin(1.25 t)$$

Simulation Results

The numerical example has been simulated on a CDC computer.

Figures 3.6-4 - 3.6-6 represent the signals for several gains of the plant ($K=1, 10, 100$ respectively) when an extreme command input is applied. Subscript a represents the plant output, and subscript b represents the non-linearity input.

Figures 3.6-7 - 3.6-9 represent signals for several gains of the plant ($K=1, 10, 100$ respectively) when the extreme disturbance input is applied. Subscripts a and b represent plant output and non-linearity input respectively.

Finally simulations were also performed when a step disturbance is applied (conditions are more severe than prescribed by specifications).

Figures 3.6-10 - 3.6-12 represent signals for several gains of the plant ($K=1, 10, 100$ respectively) when this step disturbance is applied. Subscripts a and b represent plant output and non-linearity input respectively.

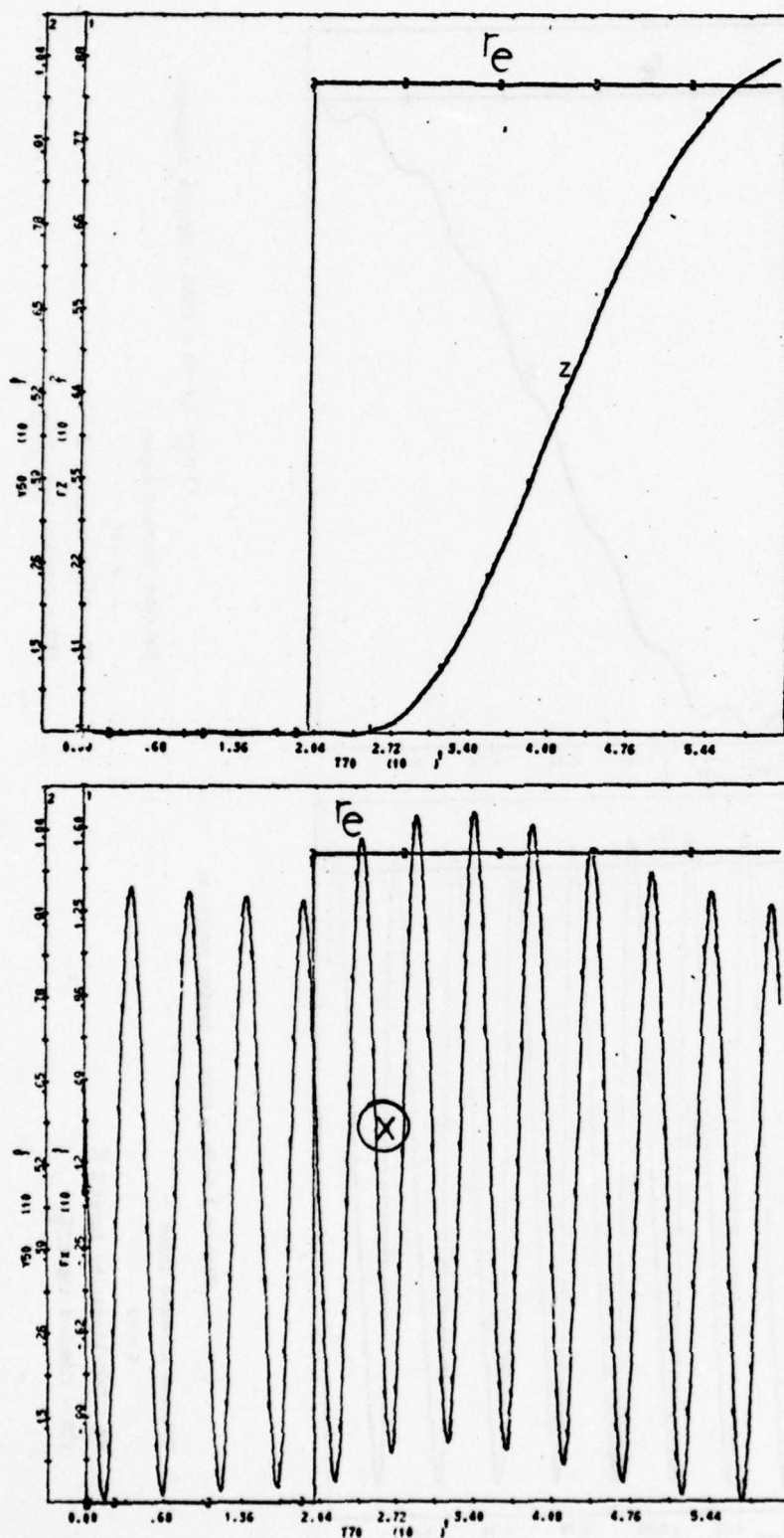


Figure 3.6-4a

EEAS - System Response
Extreme Command Input
K = 1

Figure 3.6-4b

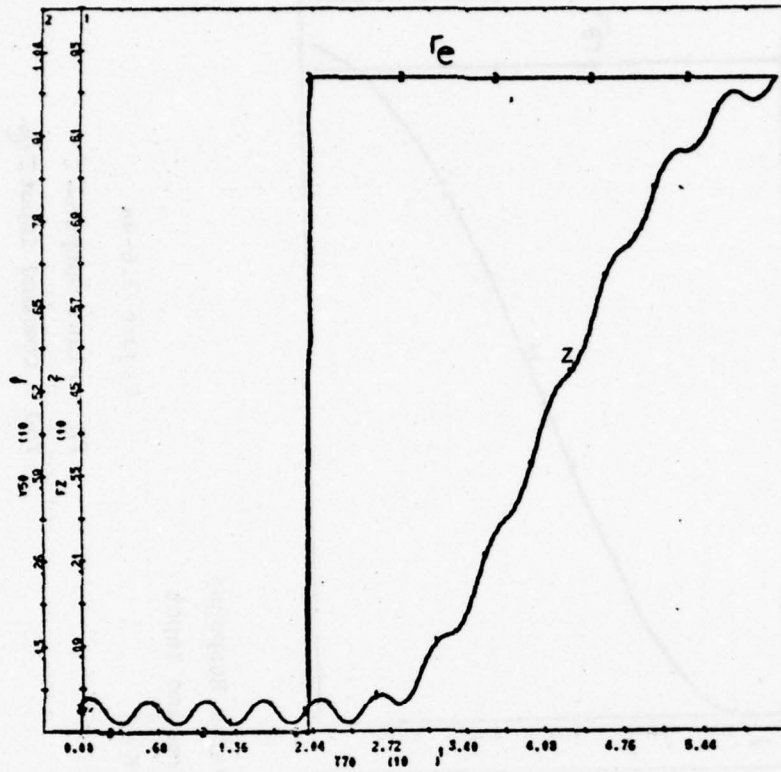


Figure 3.6-5a - EEAS - System Response

Extreme Command Input

K = 10

FZ - Plant Output = Z

Y50 - Command Input = Y50

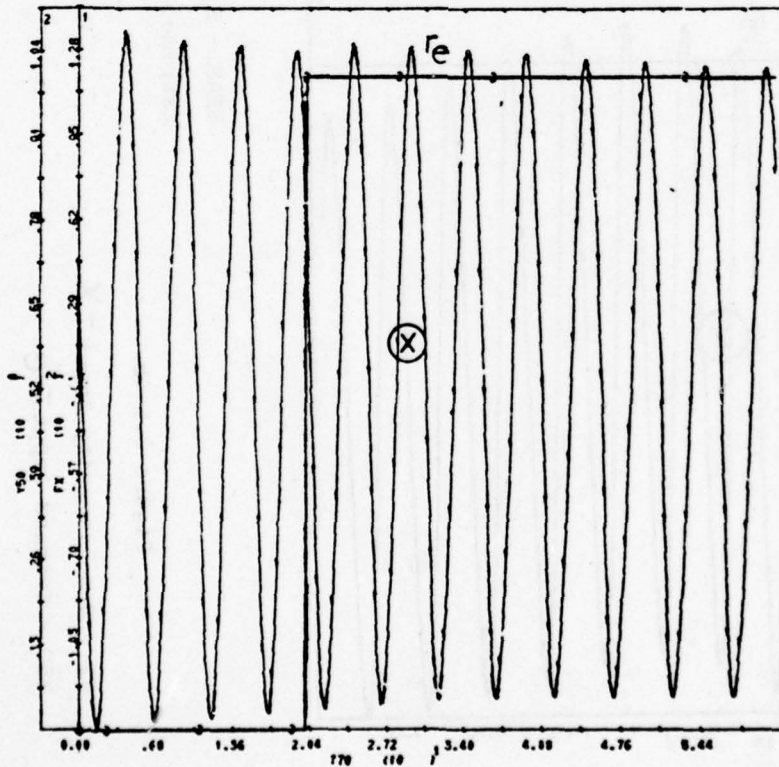


Figure 3.6-5b - EEAS - System Response

Extreme Command Input

K = 10

FX - Non-linearity Input = FX

Y50 - Command Input = Y50

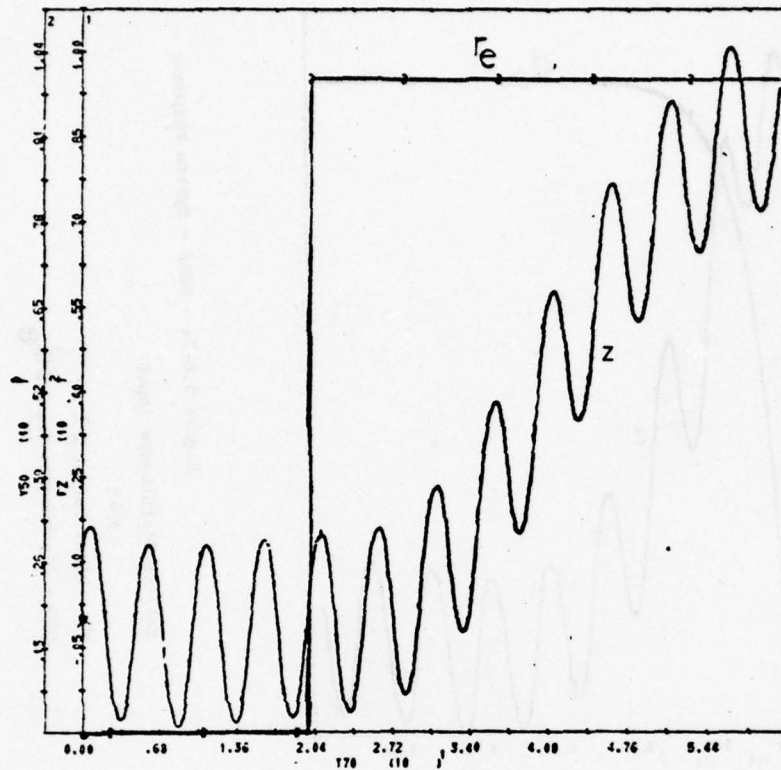


Figure 3.6-6a - EEAS - System Response

Extreme Command Input

$K = 100$

FZ - Plant Output $= z$

Y50 - Command Input $= e$

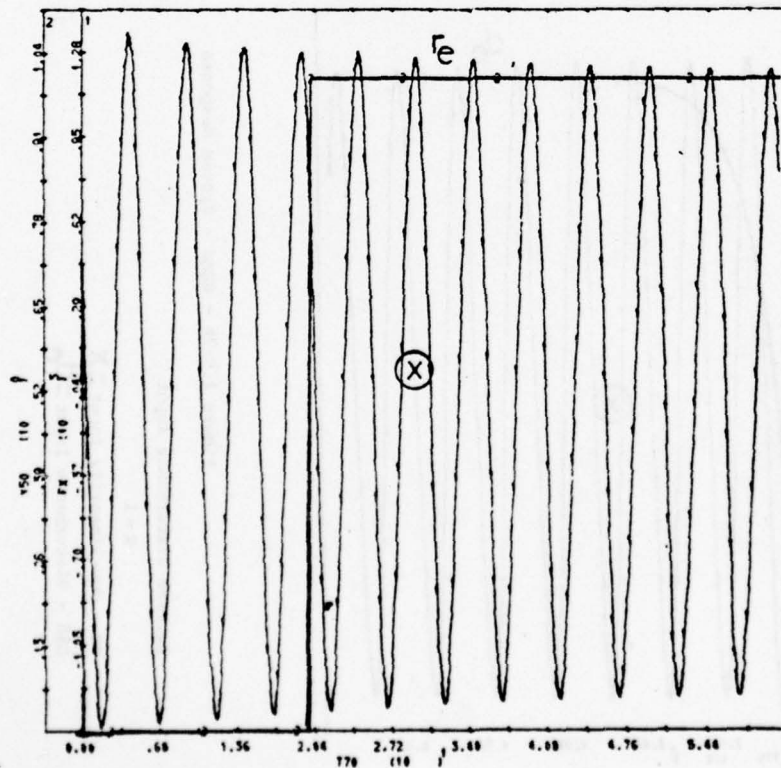


Figure 3.6-6b - EEAS - System Response

Extreme Command Input

$K = 100$

FX - Non-linearity Input $= x$

Y50 - Command Input $= e$

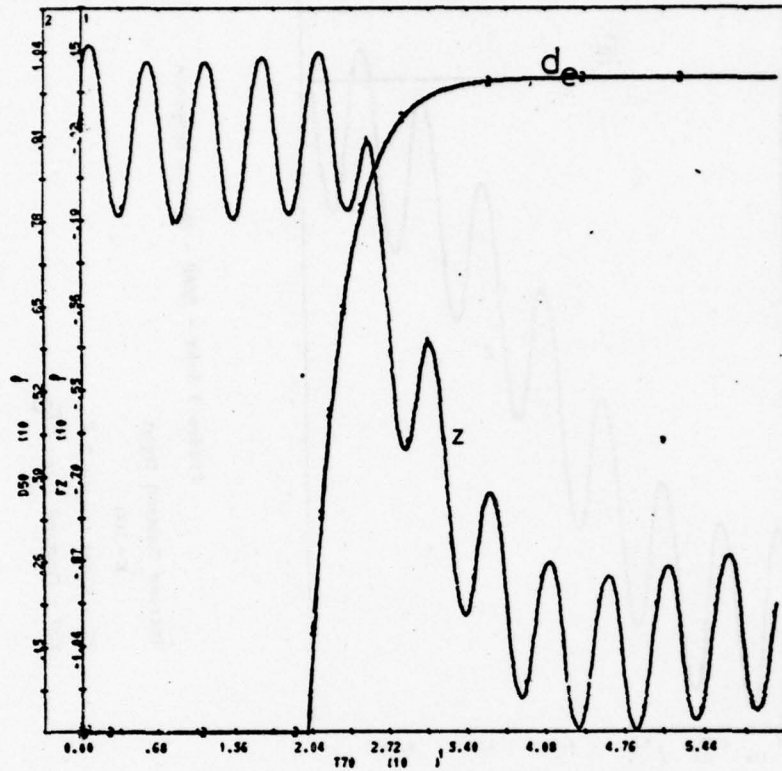


Figure 3.6-7a - EEAS - System Response

Extreme Disturbance Input

 $K = 1$

FZ - Plant Output = Z

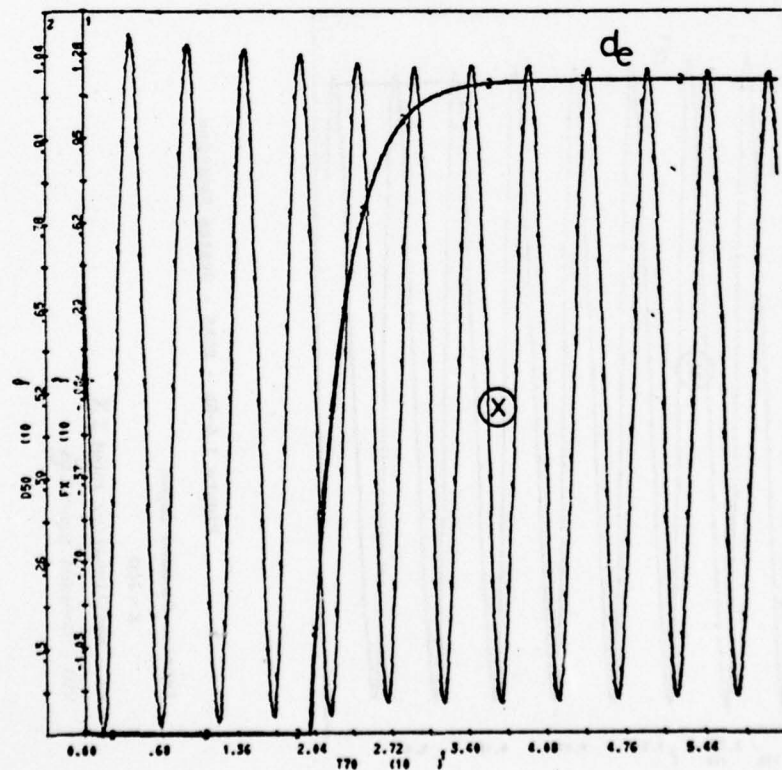
D50 - Disturbance Input = d_e 

Figure 3.6-7b - EEAS - System Response

Extreme Disturbance Input

 $K = 1$

FX - Non-linearity Input = X

D50 - Disturbance Input = d_e

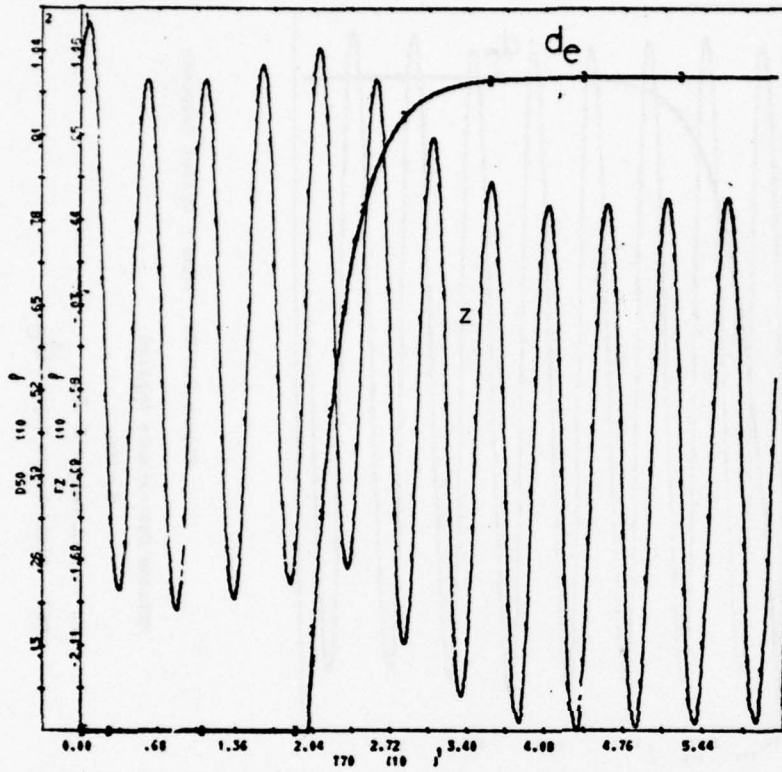


Figure 3.6-8a - EEAS - System Response

Extreme Disturbance Input

$K = 10$

FZ - Plant Output $= Z$

$D50$ - Disturbance Input $= de$

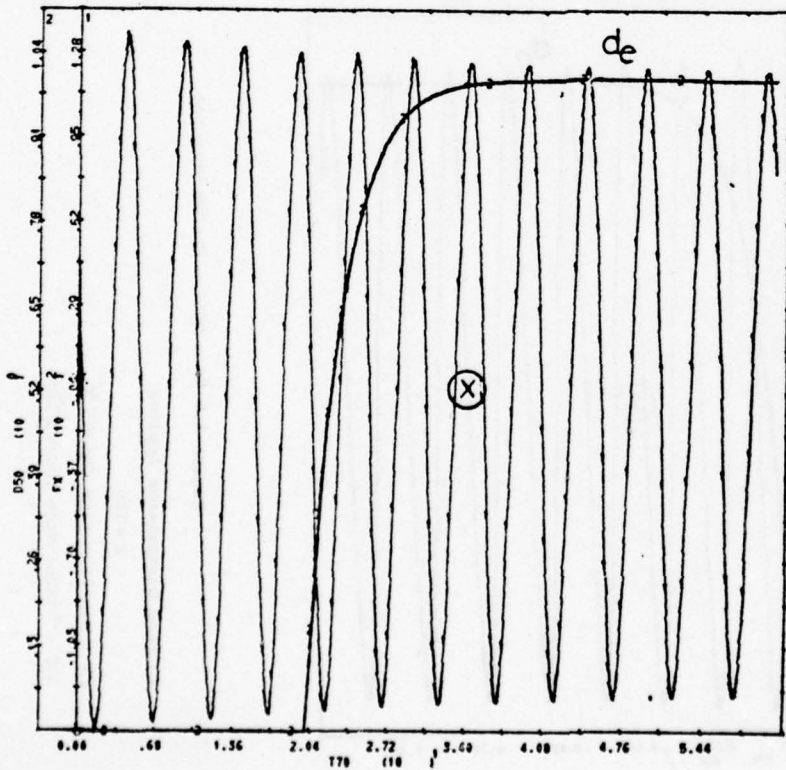


Figure 3.6-8b - EEAS - System Response

Extreme Disturbance Input

$K = 10$

FX - Non-linearity Input $= X$

$D50$ - Disturbance Input $= de$

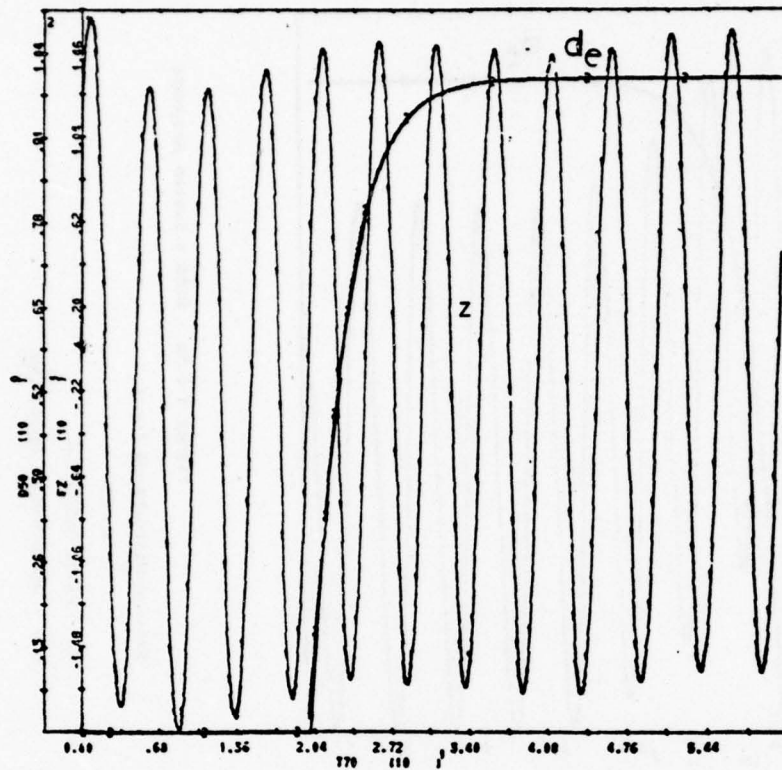


Figure 3.6-9a - EEAS - System Response

Extreme Disturbance Applied

$K = 100$

FZ - Plant Output = Z

D50 - Disturbance Input = d_e

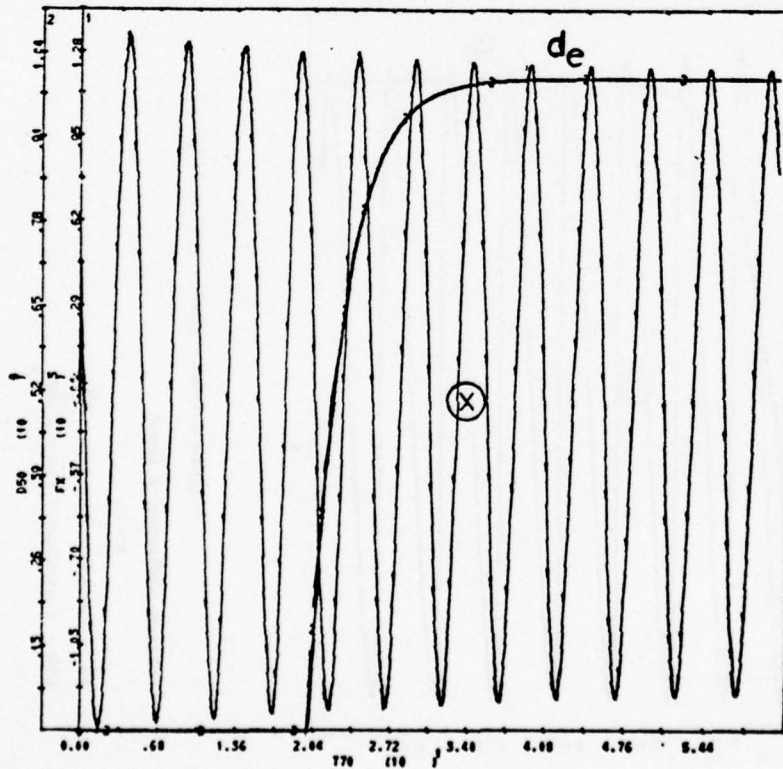


Figure 3.6-9a - EEAS - System Response

Extreme Disturbance Applied

$K = 100$

FX - Non-linearity Input = X

D50 - Disturbance Input = d_e

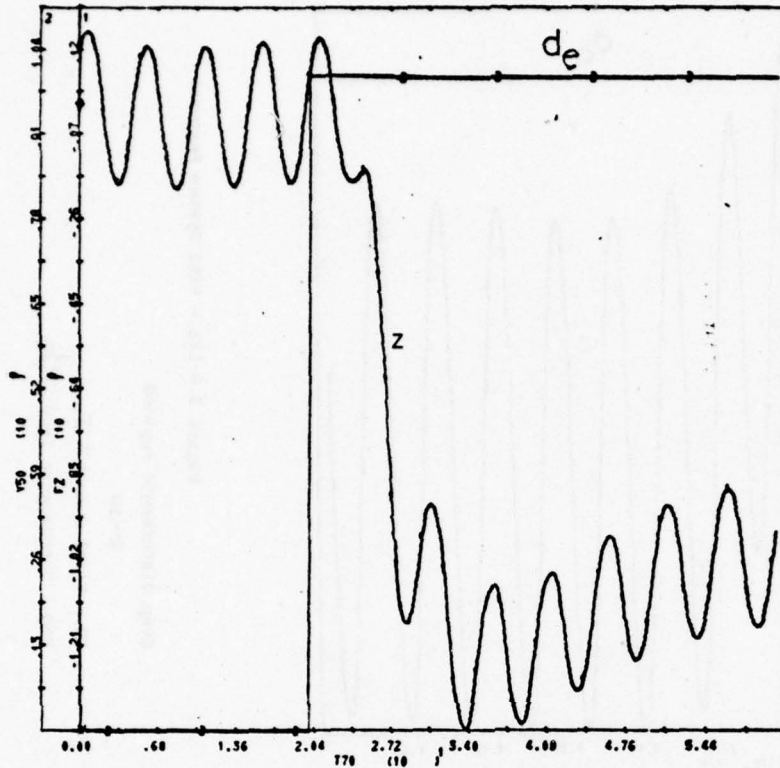


Figure 3.6-10a - EEAS - System Response

Step Disturbance Applied

$K = 1$

FZ - Plant Output $\hat{=}$ Z

Y50 - Disturbance Input $\hat{=}$ de

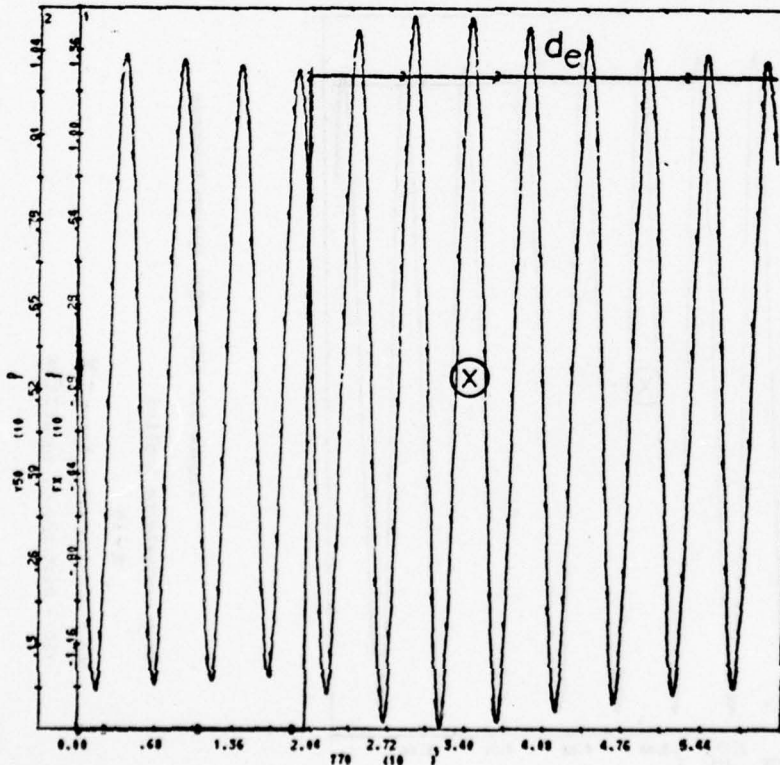


Figure 3.6-10b - EEAS - System Response

Step Disturbance Applied

$K = 1$

FX - Non-linearity Input $\hat{=}$ X

Y50 - Disturbance Input $\hat{=}$ de

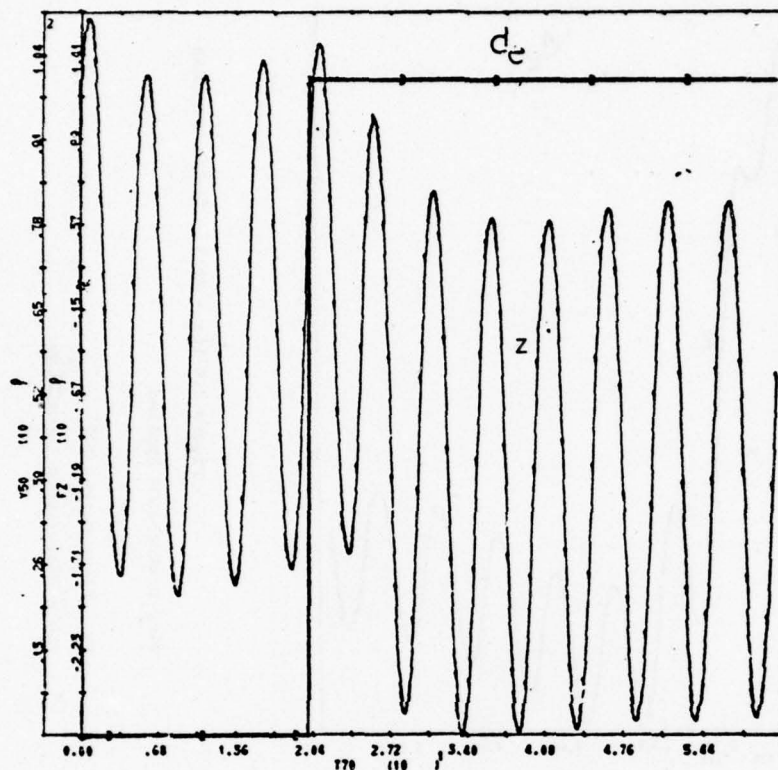


Figure 3.6-11a - EEAS System Response

Step Disturbance Applied

$K = 10$

FZ - Plant Output = Z

Y50 - Disturbance Input = d_e

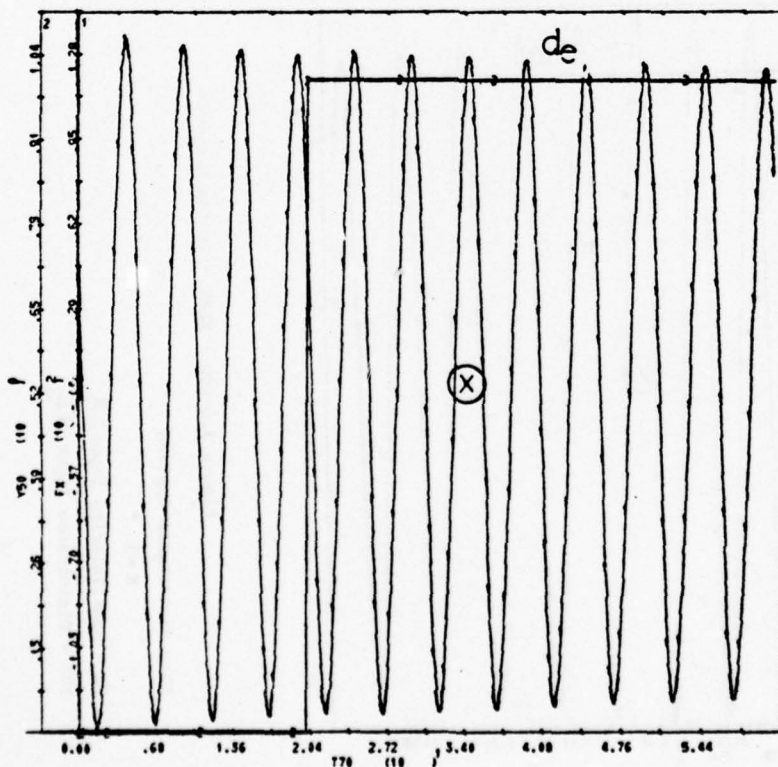


Figure 3.6-11b - EEAS System Response

Step Disturbance Applied

$K = 10$

FX - Non-linearity Input = X

Y50 - Disturbance Input = d_e

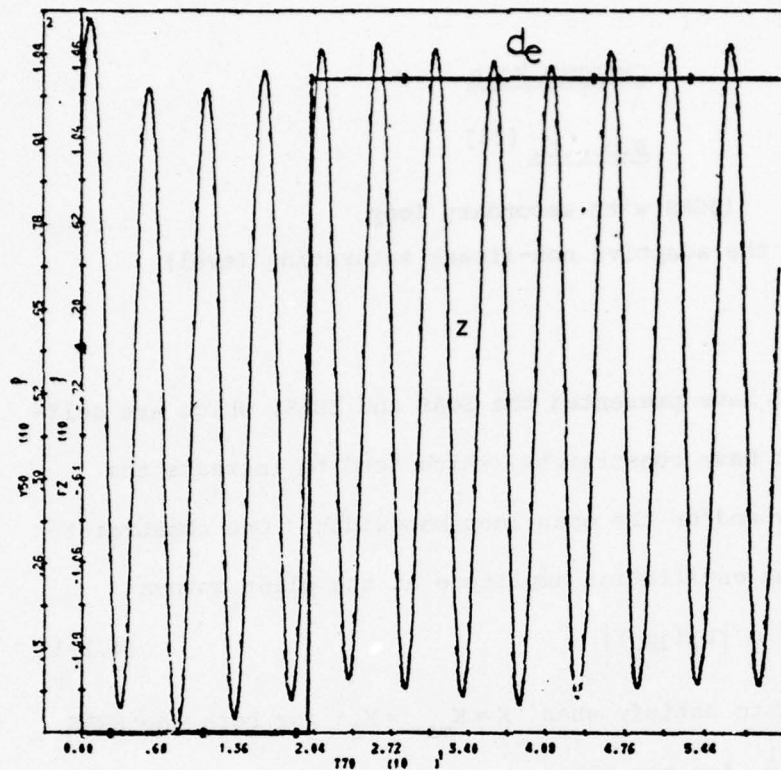


Figure 3.6-12a - EEAS System Response

Step Disturbance Applied

K = 100

PZ - Plant Output = Z

Y50 - Disturbance Input = de

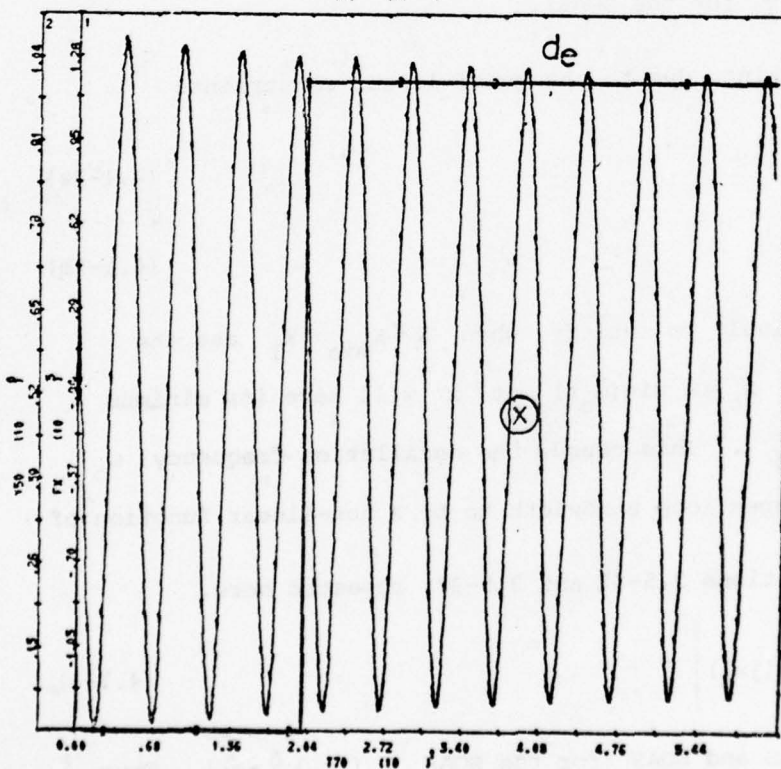


Figure 3.6-12b - EEAS System Response

Step Disturbance Applied

K = 100

PX - Non-linearity Input = X

Y50 - Disturbance Input = de

CHAPTER FOUR

S.O.A.L. [25]

(SOAS with secondary loop
controlling the adaptive non-linear saturating level)

4.1 General

Chapters 2 and 3 have presented the SOAS and EEAS, which are self-adaptive systems, but have constraints which tend to increase the oscillating frequency and/or the open loop bandwidth. One constraint defined by the maximum oscillation amplitude at the plant output

$$|M_f G_2 K P_h(j\omega_o)| \leq m |L_f(j\omega_o)| \quad (4.1-1)$$

is the most difficult to satisfy when $K = K_{\max} = K_2$ for both the EEAS and SOAS ($L_f(j\omega_o) \triangleq -\frac{1}{2}$ for the SOAS).

The other constraint, due to the quasi-linear constraints

$$\frac{x_r}{A}(t) \leq \frac{1}{\alpha} \quad (4.1-2a)$$

$$\frac{x_d}{A}(t) \leq \frac{1}{\alpha} \quad (4.1-2b)$$

will be the most difficult to satisfy, when $K = K_{\min} = K_1$ and the oscillating component $x_o = A \sin(\omega_o t)$ at x will have its minimum amplitude $A = A_{\min} = A_1$. This causes the oscillation frequency ω_o and consequently the open loop bandwidth to be a non-linear function of $\frac{K_2}{K_1}$, by means of relations 2.5-37 and 3.5-37, repeated here.

$$\left| \frac{x_f}{A_1}(j\omega_o) \right| \geq \frac{K_2}{K_1 m} \left| \frac{z_e}{L_f}(j\omega_o) \right| \quad (4.1-3)$$

valid for both the EEAS and SOAS (for the SOAS $L_f(j\omega_o) \triangleq -\frac{1}{2}$). Thus

the main factor $\frac{K_2}{K_1}$ we tried to eliminate, reappears in the adaptive systems in the expression defining the loop transmission bandwidth. This reappearance is inherent in the SOAS and EEAS, because the adaptive property exists due to K being tracked by the amplitude A , which in turn causes the non-linear element to vary its gain N_f inversely with A .

Note that constraints 4.1-1,2 are such that the system (EEAS or SOAS) is overdesigned at any non-extreme value of the plant gain.

The idea of the SOAS is to eliminate the factor $\frac{K_2}{K_1}$ in Equation 4.1-3. This factor appeared because A in $x_o = A \sin(\omega_o t)$ was used to make $N_f = \frac{2B}{\pi A}$ inversely proportional to K . In the SOAL, A is kept (or at least tried to be kept) constant, and instead, the saturating level B in $N_f = \frac{B}{A}$ tracks K , i.e., B is made inversely proportional to the plant gain K .

Since the value of K itself is unknown, K cannot be directly tracked. The technique used in the SOAL is to adjust B so as to force A to be constant, as shown in Figure 4.1-1. A is measured and compared to a reference A_r . The difference (error) passes through a compensation network $\psi(s)$, whose output controls B .

The point chosen for measuring the oscillation level, which indirectly gives the plant gain, is x , the input to N for two main reasons. First, the system is designed to meet quasi-linearity constraints at x , so

$$|x_f(t)| < \frac{A}{3} \quad \text{and} \quad (4.1-4)$$

$$\max_t |x(t)| = A + |x_f(t)| = \frac{4A}{3} \quad (4.1-5)$$

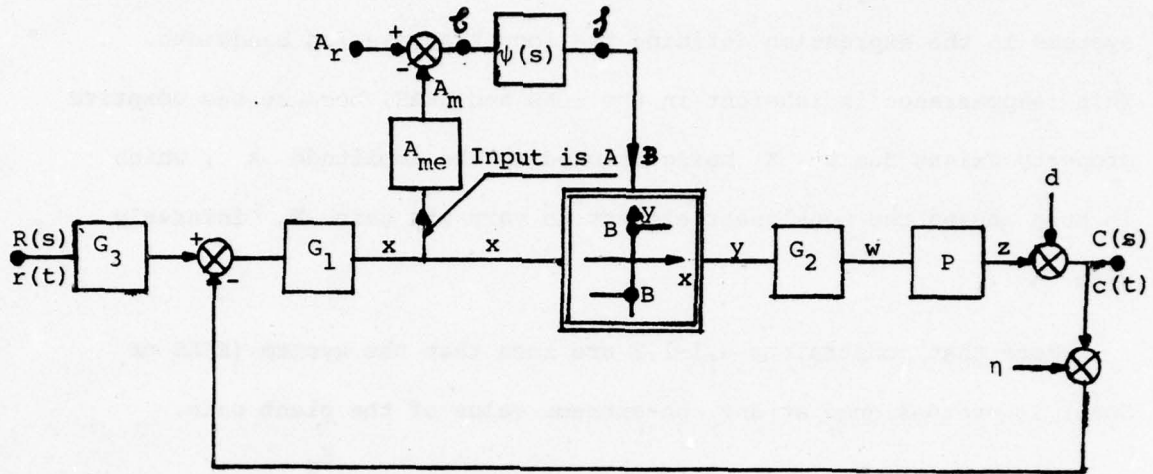


Figure 4.1-1 - SOAL Structure - Non-linearity - Ideal Relay

This means that if A is measured by the maximum (peak) value of $x(t)$, the maximum possible relative error is $\frac{1}{3}$. In reality the error in measuring A is much smaller in a peak to peak detector measurement, because x_f is slow relative to x_o , so the x_f component practically disappears, except for the change in x_f in half an oscillation period. A priori, Equation 2.5-5 requires this change to be small. Also, $x(t)$ crosses the zero value twice per cycle, which is useful for measurement purposes.

Next, due to the low pass band characteristics of $G_1 G_2 K P(j\omega)$, $x_o(t)$ is supposed to have a "very" sinusoidal shape, which also helps in the amplitude A measurement and consequently in the plant gain identification accuracy.

In Figure 4.1-1 there are "two loops". The main loop is defined by $L_f(j\omega) = G_1 G_2 N_f K P_h(j\omega)$, which is the same as for the SOAS and EEAS, controlling the forced signals. The secondary loop, which adjusts the relay saturation level, is not "an instantaneous" loop, and its dynamics and stability problems must be analyzed. This is done in Section 4.2.

4.2 The Stability and Dynamics of the Secondary loop - SOAL

The dynamics and stability of the secondary loop can be obtained by using the technique ^[4] of the "Fundamental Feedback Equation", which incidentally demonstrates the power of this concept.

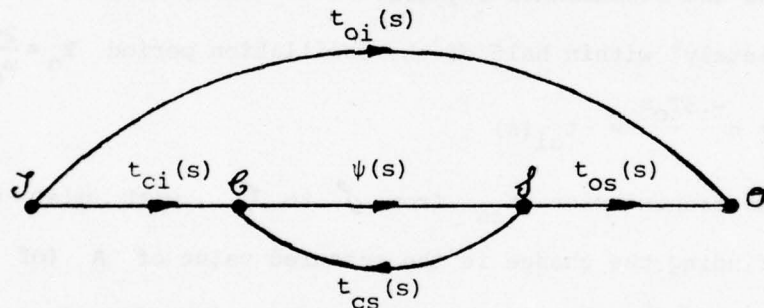


Figure 4.2-1 - Fundamental Feedback Equation

$$\frac{O}{J}(s) \triangleq t_{oi}(s) + t_{ci}(s) t_{os}(s) \frac{\psi(s)}{1 - \psi t_{cs}(s)} \quad (4.2-1)$$

\mathcal{G} is the controlling variable

\mathcal{J} is the controlled source (controlled variable)

In Figure 4.1-1 consider the independent input as a change in A , and the output as change in B . The controlling variable \mathcal{G} and the controlled source \mathcal{J} are explicitly marked. The several transmissions

of the secondary loop are calculated.

$$t_{oi}(s) = \left. \frac{\Delta B}{\Delta A}(s) \right|_{\psi(s)=0} = 0 \quad (4.2-2)$$

The "leakage" transmission t_{oi} is obtained by setting $\psi(s)=0$ in Equation 4.2-1. There is no change in the saturation level B , so $t_{oi}(s) = 0$.

$$t_{ci}(s) = \left. \frac{\mathcal{C}}{\mathcal{J}}(s) \right|_{\psi(s)=0} = -A_{me}(s) \quad (4.2-3)$$

$A_{me}(s)$ in Figure 4.1-1 represents the measurement dynamics of A from the signal x . The technique used in the SOAL is a "peak to peak" detector which measures the extreme values of x .

As previously noted, this technique minimizes the measurement error due to the command and disturbance signals. This measurement is done

"almost completely" within half of the oscillation period $T_o = \frac{2\pi}{\omega_o}$, so

$$A_{me}(s) = e^{-.5T_o s} = -t_{ci}(s) \quad (4.2-4)$$

Next, the transmission t_{cs} from \mathcal{J} to \mathcal{C} , with $\psi(s)=0$, is obtained by finding the change in the measured value of A (of x_o) due to a unit change in B . This transmission is composed of two parts. The first one, t_{cs1} , represents the dynamics of the limit cycle build up in the primary loop (SOAS case). The second part, t_{cs2} , is again the block A_{me} . Hence

$$t_{cs}(s) = t_{cs1}(s) \times t_{cs2}(s) \quad (4.2-5)$$

$$t_{cs2}(s) = -e^{-.5T_o s}$$

$t_{cs1}(s)$, which represents the dynamics of the SOAS limit cycle buildup, can be approximated (Appendix IV) by

$$t_{cs1}(s) = \frac{\Delta A}{\Delta B}(s) \Big|_{SOAS} \approx \left| \frac{4}{\pi} G_1 G_2 K P_h(j\omega_o) \right| \times \frac{\frac{L_f(s)}{3}}{1 + \frac{L_f(s)}{3}} \quad (4.2-6)$$

This approximation suits the synthesis technique used and is valid for $L_f(s)$ of type 1. Equation 4.2-6 essentially means that in case of a change of ΔB , the final value of ΔA is $\Delta B \left| \frac{4}{\pi} G_1 G_2 K P_h(j\omega_o) \right|$ and the dynamics of this build up is very close to the dynamics of $\frac{L_f(s)/3}{1 + L_f(s)/3}$.

So

$$t_{cs}(s) = - \left| \frac{4}{\pi} G_1 G_2 K P_h(j\omega_o) \right| \cdot \frac{L_f(s)/3}{1 + L_f(s)/3} \cdot e^{-.5T_o s} \quad (4.2-7)$$

Finally the transmission $t_{os}(s)$ which is the transmission from Δ to the output ΔB is 1.

$$t_{os}(s) = 1 \quad (4.2-8)$$

Substituting Equations 4.2-2,4,7,8 in 1,

$$\frac{\Delta B}{\Delta A}(s) = \frac{-\psi(s) e^{-.5T_o s}}{1 + \left| \frac{4}{\pi} G_1 G_2 P_h(j\omega_o) \right| K e^{-.5T_o s} \left(\frac{L_f(s)/3}{1 + L_f(s)/3} \right) \psi(s)} \quad (4.2-9)$$

where the secondary loop transmission L_s ,

$$L_s(s) = \left| \frac{4}{\pi} G_1 G_2 P_h(j\omega_o) \right| K e^{-.5T_o s} \left(\frac{L_f(s)/3}{1 + L_f(s)/3} \right) \psi(s) \quad (4.2-10)$$

In Equation 4.2-10, the maximum L_s crossover frequency is less than approximately $\frac{\omega_o}{3}$, because of the existing pure delay of $.5T_o$, which adds -60° at $\frac{\omega_o}{3}$, and one must allow say 30° phase margin - leaving badly needed 90° for $|L_s|$ reduction.

It is very interesting to see how the uncertainty in the plant gain factor K has now reappeared in the secondary loop (after being eliminated from the main loop), by the presence of K in the denominator

in Equation 4.2-9. Hence this secondary loop must be designed to be stable over the entire range of variation of K . We have transferred the problem from the main loop to the secondary loop. This means that the maximum crossover frequency of the secondary loop L_S is limited by $\frac{\omega_0}{3}$ at $K = K_{\max} = K_2$. The maximum crossover frequency at $K = K_{\min} = K_1$ may be much smaller than $\frac{\omega_0}{3}$, and it means that at $K = K_{\min} = K_1$, the dynamics of the adjustment (secondary) loop can be quite slow, i.e. at K_1 the B adjustment mechanism is relatively slow.

4.3 Mathematical Relations

Suppose in Figure 4.1-1 $r(t) = d(t) = \eta(t) = 0$, K' is constant in $P(s) = K'P_h(s)$, the system has achieved its steady state limit cycle $x_0 = A \sin(\omega_0 t)$, and the secondary loop has also achieved its steady state value with the relay saturation level B' . It is possible to write for the main loop

$$L'_o(j\omega_0) = \frac{4B'}{\pi A} \cdot G_1 G_2 K' P_h(j\omega_0) = -1 \quad (4.3-1)$$

So, the loop transmission for the command input and disturbance signal, if the quasi-linear constraints are not violated, is:

$$L'_f(s) = \frac{2B'}{\pi A} \cdot G_1 G_2 K' P_h(s) \quad (4.3-2)$$

Suppose now the plant gain changes instantaneously from K' to K'' , so $P(s) = K''P_h(s)$. There is a change in the amplitude of oscillation at x , which is sensed and corrected in a manner explained in Section 4.2. After a certain transient, the relay achieves a new steady state. Assuming the secondary loop L_S is of type 1, x_0 (in the main loop) is back to its previous value $= A \sin(\omega_0 t)$, with the same

amplitude and frequency as before. In this case

$$L''_o(j\omega_o) = \frac{4B''}{\pi A} \cdot G_1 G_2 K'' P_h(j\omega_o) = -1 \quad (4.3-3)$$

So the forced loop transmission is:

$$L''_f(s) = \frac{2B''}{\pi A} \cdot G_1 G_2 K'' P_h(s) \quad (4.3-4)$$

Comparing Equations 4.3-1 and 3,

$$B'K' = B''K'' = BK = \text{constant} \quad (4.3-5a)$$

$$BK = \frac{\pi A}{4G_1 G_2 P_h(j\omega_o)} = \text{constant} \quad (4.3-5b)$$

Substituting in Equations 4.3-2 and 3, we get

$$L'_f(s) = L''_f(s) = L_f(s) = \frac{G_1 G_2 P_h(s)}{2 |G_1 G_2 P_h(j\omega_o)|} \quad (4.3-6)$$

which is similar to expression 2.3-9 and depicts the zero sensitivity property to pure gain changes of the plant.

We now see the advantage of the SOAL over the SOAS. Since A is constant, the quasi-linear condition $\left| \frac{x_r}{A}(t) \right| < \frac{1}{\alpha}$, $\left| \frac{x_d}{A}(t) \right| < \frac{1}{\alpha}$ is independent of the gain factor K of the plant, whereas in the SOAS A is a function of K , so $A = A_{\min} = A_1$, corresponding to $K = K_{\min} = K_1$ was used. Also in the SOAL

$$|C_o(j\omega_o)| = \frac{A}{|G_1(j\omega_o)|}$$

with A and $|G_1(j\omega_o)|$ constants, so there is no "most difficult" case to satisfy in $|C_o(t)| \leq m$, whereas in the SOAS the "most difficult" case to satisfy was at $K = K_{\max} = K_2$. These two constraints resulted in $\frac{K_2}{K_1}$ appearing in Equation 2.5-37, and forcing ω_o to be "large" in the SOAS (and EEAS). In the SOAL, $\frac{K_2}{K_1}$ has been eliminated as a factor influencing $(\omega_o)_{\min}$.

4.4 SOAL Sensitivity to Uncertainty in Plant Dynamics

If there is uncertainty in the plant dynamics (poles and zeros), the loop transmission and the oscillation frequency ω_o are affected because

$$L_o(j\omega_o) = \frac{4B}{\pi A} \cdot G_1 G_2 K P_h(j\omega_o) = -1 \quad (4.4-1)$$

In the SOAL, A remains constant. The only change considered in this study is the plant overall gain K . A generalization of the synthesis method developed, which would include dynamic changes of the plant, can be developed using the technique of Horowitz and Sidi [1] for linear systems.

4.5 Synthesis Procedure for the SOAL

A synthesis procedure is developed for the SOAL, similar to that for the SOAS.

4.5-1 Specifications and Data

As for the SOAS (c.f. 2.5-1),

$$\begin{aligned} T_r(j\omega) &\triangleq \frac{C_r}{R}(j\omega) = G_3(j\omega) \frac{L_f(j\omega)}{1 + L_f(j\omega)} \quad ; \quad \omega_o \geq \beta\omega_r \\ |T_d(j\omega)| &\triangleq \left| \frac{C_d}{D}(j\omega) \right| = \left| \frac{1}{1 + L_f(j\omega)} \right| \leq |T_{d \min}(j\omega)| \quad ; \quad \omega_o \geq \beta\omega_d \quad (4.5-1) \\ P(j\omega) &= K P_h(j\omega) \quad ; \quad K_{\min} = K_1 \leq K \leq K_2 = K_{\max} \end{aligned}$$

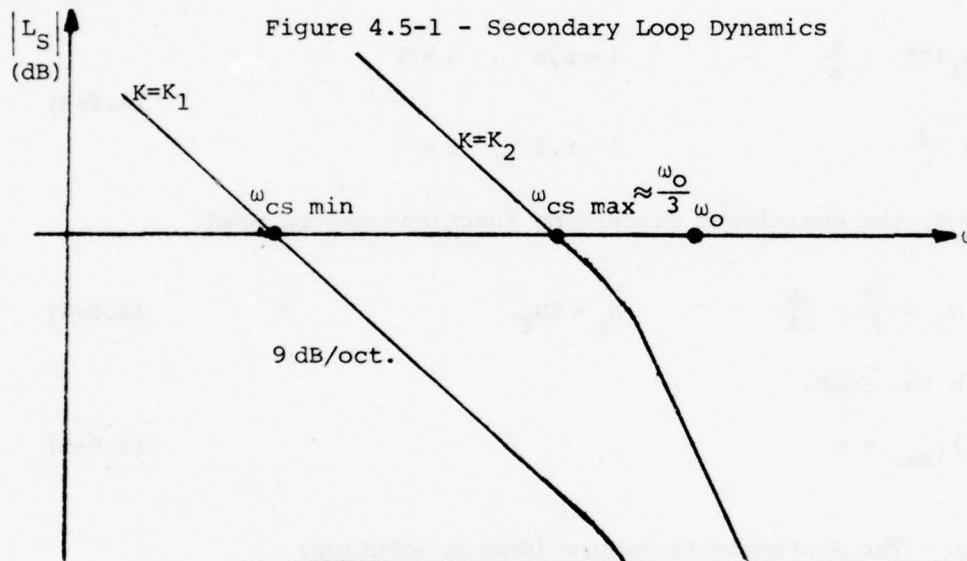
The extreme command input $r_e(t) \rightarrow R_e(s)$

The extreme disturbance input $d_e(t) \rightarrow D_e(s)$

In addition to the above (same as for the SOAS) specifications, there exists a complementary specification to be defined for the SOAL. The following paragraph covers it.

Dynamics of the Adjustment Loop

The dynamics of the adjustment loop change with the value of the gain of the plant (Section 4.2). When the plant has its maximum gain K_2 , the maximum possible crossover frequency of the adjustment loop is about $\frac{\omega_0}{3}$. When the plant has its minimum gain, the bandwidth of the adjustment loop decreases accordingly to the variation of K and the "shaping" of L_f and ψ .



Assuming the loop has been properly designed (in the frequency range $\omega_{cs \min} - \omega_{cs \max}$, the average slope is 9 dB/oct.), and $\omega_{cs \max} \approx \frac{\omega_0}{3}$, Then (see Equation 4.2-9),

$$\frac{20 \log_{10} \left(\frac{K_2}{K_1} \right)}{20 \log_{10} \left(\frac{\omega_{cs \max}}{\omega_{cs \min}} \right)} \approx \frac{9}{6} = \frac{3}{2}$$

$$\omega_{cs \min} \approx \omega_{cs \max} \left(\frac{K_1}{K_2} \right)^{2/3} \approx \frac{\omega_0}{3} \left(\frac{K_1}{K_2} \right)^{2/3} \quad (4.5-2)$$

Actually, one could include in the specifications list a minimum dynamic

response for the adjustment loop (when $K = K_1$), and this might require increasing ω_0 , as per Equation 4.5-2. We assume there is no such requirement, and the adjustment loop should have its possible crossover frequency maximized.

4.5-2 The Constraints

The constraints on the SOAL are the same as (c.f. 3.5-2) on the SOAS, i.e.,

$$\begin{aligned} \max_t |x_i(t)| &\leq \frac{A}{\alpha} & i = r, d, \quad \alpha = 3 \\ \omega_{bi} &\leq \frac{\omega_0}{\beta} & i = r, d, \quad \beta = 3 \end{aligned} \quad (4.5-3)$$

If satisfied, the dual-input describing functions can be used.

$$N_f = N_d = \frac{M_f}{A} = \frac{2B}{\pi A} \quad N_o = 2N_f \quad (4.5-4)$$

Also, as in the SOAS,

$$|C_o(t)|_{\max} \leq m \quad (4.5-5)$$

4.5-3 SOAL - The Synthesis Procedure (Smooth Solution)

The SOAL structure is pictured again in Figure 4.5-2 with loop transmissions

$$L_f(j\omega) = N_f G_1 G_2 K P_h(j\omega) \quad , \quad N_f = \frac{M_f}{A} = \frac{2B}{A} \quad (4.5-6)$$

which is valid for $\omega \leq \frac{\omega_0}{\beta}$ for both the forced and disturbance signals and

$$L_o(j\omega_o) = N_o G_1 G_2 K P_h(j\omega_o) \quad , \quad N_o = \frac{M_o}{A} = \frac{4B}{\pi A} \quad (4.5-7)$$

which is valid only at $\omega = \omega_o$.

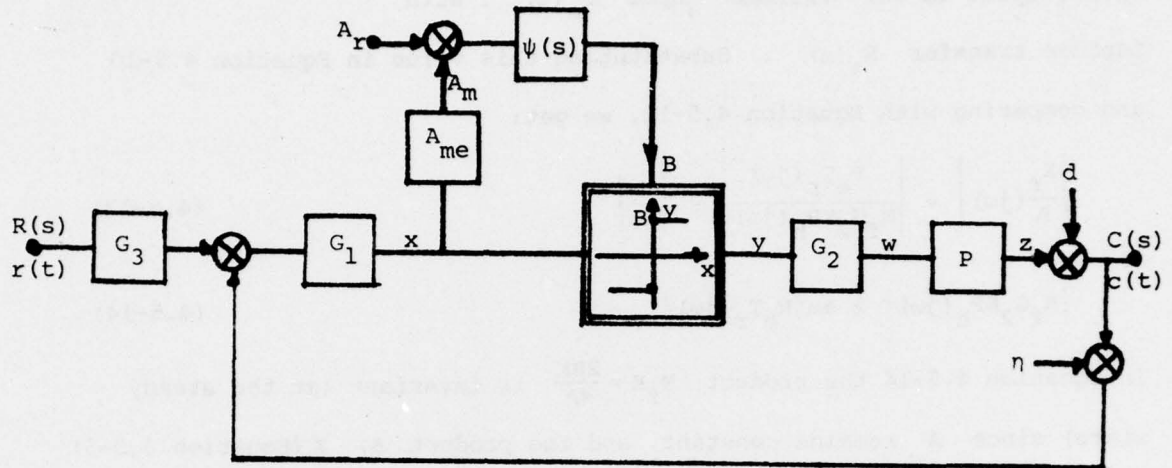


Figure 4.5-2 - SOAL Structure

Following the same reasoning as for the SOAS (Equations 2.5-8 - 13), we get:

$$T_r(j\omega) \triangleq \frac{C_r}{R}(j\omega) = \frac{G_3 L_f(j\omega)}{1 + L_f(j\omega)} \quad (4.5-8)$$

$$X_r(j\omega) = \frac{C_r(j\omega)}{N_f G_2^{KP_h}(j\omega)} \quad (4.5-9)$$

$$\frac{X_r}{A}(j\omega) = \frac{R T_r(j\omega)}{M_f G_2^{KP_h}(j\omega)} \quad (4.5-10)$$

Repeating the quasi-linearity condition

$$\left| \frac{x_r}{A}(t) \right| \leq \frac{1}{\alpha} = \frac{1}{3} \quad (4.5-11)$$

which, for a "smooth shape", has a correspondent limit:

$$\left| \frac{X_r}{A}(j\omega) \right| \leq \frac{1}{\alpha(\omega)} = \frac{1}{3\omega} \quad \forall \omega \quad (4.5-12)$$

From this point on, there is a difference between the SOAS and the SOAL, since there is no "most difficult" situation to satisfy Equation 4.5-11 with regard to the plant gain. There is the "most difficult" situation

with respect to the "extreme" input $r_e(t)$, with Laplace transfer $R_e(s)$. Substituting this value in Equation 4.5-10 and comparing with Equation 4.5-12, we get:

$$\left| \frac{X_r}{A}(j\omega) \right| = \left| \frac{R_e T_r(j\omega)}{M_f G_2 K P_h(j\omega)} \right| \leq \left| \frac{1}{\alpha \omega} \right| \quad (4.5-13)$$

So

$$|M_f G_2 K P_h(j\omega)| \geq \alpha \omega |R_e T_r(j\omega)| \quad (4.5-14)$$

In Equation 4.5-14 the product $M_f K = \frac{2BK}{\pi A}$ is invariant (at the steady state) since A remains constant, and the product $B \cdot K$ (Equation 4.3-5) is also constant.

Inequality 4.5-14 assures non violation of quasi-linearity constraints due to command input signals for $K_1 \leq K \leq K_2$. An expression similar to Equation 4.5-14 is obtained for the extreme disturbance input.

$$Z_d(j\omega) = -D(j\omega) \frac{L_f(j\omega)}{1 + L_f(j\omega)} \quad (4.5-15)$$

Then

$$X_d(j\omega) = \frac{Z_d(j\omega)}{N_f G_2 K P_h(j\omega)} = \frac{-D(j\omega)}{N_f G_2 K P_h(j\omega)} \cdot \frac{L_f(j\omega)}{1 + L_f(j\omega)} \quad (4.5-16)$$

But $N_f = \frac{M_f}{A}$, so

$$\frac{X_d}{A}(j\omega) = \frac{-D(j\omega)}{M_f G_2 K P_h(j\omega)} \cdot \frac{L_f(j\omega)}{1 + L_f(j\omega)} \quad (4.5-17)$$

$$\left| \frac{X_d}{A}(j\omega) \right| \leq \frac{1}{\alpha \omega} = \frac{1}{3\omega} \quad (4.5-18)$$

Hence

$$|M_f G_2 K P_h(j\omega)| \geq \alpha \cdot \omega \cdot |D_e(j\omega)| \left| \frac{L_f(j\omega)}{1 + L_f(j\omega)} \right| \quad (4.5-19)$$

Notice that in Equation 4.5-19, $D(j\omega)$ has been replaced by its extreme value $D_e(j\omega)$, which is the only parameter that can assume

different values, so its "most difficult" value has been chosen.

Inequality 4.5-19 being satisfied assures non violation of quasi-linearity constraints due to the disturbance input. There is a difference in the explicitness of Equations 4.5-14 and 19, because T_r is "almost" completely defined (except possibly for more "far-off" poles and zeros which may be added), while $L_f(j\omega)$ is unknown.

We use the Nichol's chart technique here just as in the SOAS, as explained in Section 2.5-3, Figures 2.5-4,5, to plot the bounds on L_f due to the disturbance attenuation specifications.

Next we will develop an expression assuring the plant output oscillation level, to be \leq the limit m . We have

$$|C_o(j\omega_o)| = |M_o G_2 K P_h(j\omega_o)| = |2M_f G_2 K P_h(j\omega_o)| \leq m \quad (4.5-20)$$

Again, there is no "most difficult" case to satisfy Equation 4.5-20,

since $M_f K = \frac{2BK}{\pi A}$ is constant (as per Equation 4.3-5).

Recalling Equations 4.5-13 and 17, and replacing ω by ω_o , we get

$$\left| \frac{X_r}{A}(j\omega_o) \right| = \left| \frac{R_e T_r(j\omega_o)}{M_f G_2 K P_h(j\omega_o)} \right| \quad (4.5-21)$$

$$\left| \frac{X_d}{A}(j\omega_o) \right| = \left| \frac{D_e(j\omega_o)}{M_f G_2 K P_h(j\omega_o)} \right| \times \left| \frac{L_f(j\omega_o)}{1 + L_f(j\omega_o)} \right| = \left| \frac{D_e(j\omega_o)}{M_f G_2 K P_h(j\omega_o)} \right| \quad (4.5-22)$$

because $L_f(j\omega_o) = -\frac{1}{2}$, and $\left| \frac{L_f(j\omega_o)}{1 + L_f(j\omega_o)} \right| = 1$. Substituting

Equation 4.5-20 into 21 and 22,

$$\left| \frac{X_r}{A}(j\omega_o) \right| = \left| \frac{R_e T_r(j\omega_o)}{M_f G_2 K P_h(j\omega_o)} \right| \geq \frac{2}{m} |T_r R_e(j\omega_o)| \quad (4.5-23)$$

$$\left| \frac{X_d}{A}(j\omega_o) \right| = \left| \frac{D_e(j\omega_o)}{M_f G_2 K P_h(j\omega_o)} \right| \geq \frac{2}{m} |D_e(j\omega_o)| \quad (4.5-24)$$

which are non-linear functions defining $(\omega_o)_{\min}$ for "smooth" $x_r(j\omega)$, $x_d(j\omega)$. It is important to note that the factor $\frac{K_2}{K_1}$ present in the SOAS case (Equations 2.5-29,30) has disappeared. This is a great advantage of the SOAL over the SOAS, but the price paid is in the dynamics of the secondary loop which becomes very slow at $K=K_1$, especially for large $\frac{K_2}{K_1}$.

We could also write:

$$Z_{er}(j\omega_o) = R_e(j\omega_o) \times T_r(j\omega_o) \quad (4.5-25)$$

where the $Z_{er}(j\omega_o)$ represents the extreme plant output, due to the extreme command input $r_e(t)$. Equation 4.5-23 becomes:

$$\left| \frac{x_r}{A}(j\omega_o) \right| \geq \frac{2}{m} |Z_{er}(j\omega_o)| \quad (4.5-26)$$

In the same way

$$|Z_{ed}(j\omega_o)| = D_e(j\omega_o) \times \left| \frac{L_f(j\omega_o)}{1+L_f(j\omega_o)} \right| = D_e(j\omega_o) \quad (4.5-27)$$

where $Z_{ed}(j\omega)$ is the extreme plant output, due to the extreme disturbance $d_e(t)$. Equation 4.5-24 becomes

$$\left| \frac{x_d}{A}(j\omega_o) \right| \geq \frac{2}{m} |Z_{ed}(j\omega_o)| \quad (4.5-28)$$

Equations 4.5-26,28 can be combined into

$$\left| \frac{x_f}{A}(j\omega_o) \right| \geq \frac{2}{m} |Z_e(j\omega_o)| \quad (4.5-29)$$

where x_f represents the forced signal at the non-linearity input, and $Z_e(j\omega)$ is the extreme plant output, due to either the command or disturbance input. Since x_f is "smooth"

$$\left| \frac{x_f}{A}(j\omega) \right| \leq \frac{1}{3\omega} \quad ; \quad \frac{2}{m} |Z_e(j\omega_o)| \leq \left| \frac{x_f}{A}(j\omega_o) \right| \leq \frac{1}{3\omega_o} \quad (4.5-30)$$

A typical situation is shown in Figure 4.5-3, and compared with the SOAS case for the same problem specifications. The SOAS ω_o value is $\omega_{o1} = 100 \text{ rd/sec} > \omega_{o2}(\text{SOAL}) = 12 \text{ rd/sec}$.

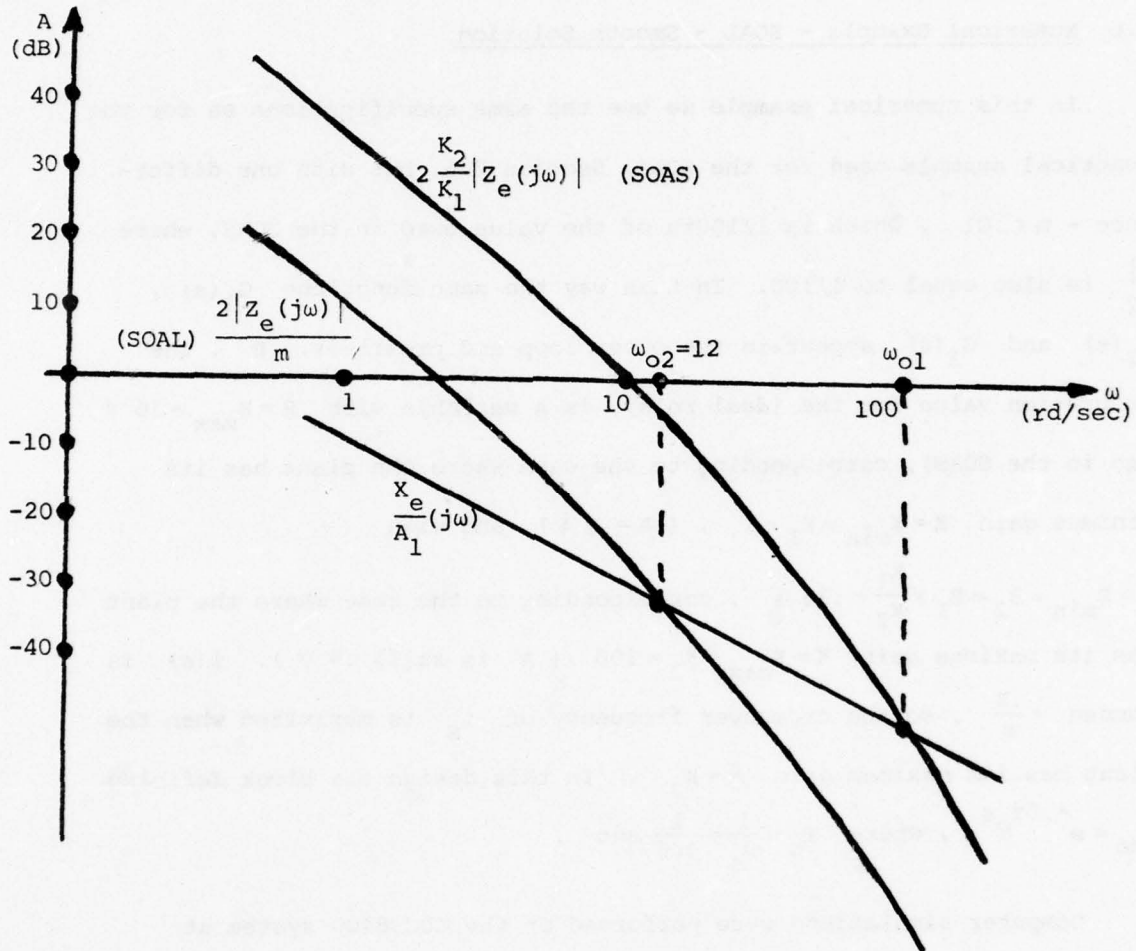


Figure 4.5-3 - SOAL - Oscillation Frequency Determination

As in the SOAS, there may be no solution for some disturbance signals, but for the same specifications and constraints, the level of disturbances for which a solution is available in the SOAL, is $\sqrt{\frac{K_2}{K_1}}$ times as great as in the SOAS. This can be a significant factor.

The technique used for definition of $L_f(j\omega)$ and ω_o is identical to the one defined for the SOAS. Only $\psi(s)$ is left to define, in the

secondary loop. As noted earlier, $\psi(s)$ is chosen to achieve a satisfactory secondary loop L_S , with maximum possible crossover frequency.

4.6 Numerical Example - SOAL - Smooth Solution

In this numerical example we use the same specifications as for the numerical example used for the SOAS, Section 2.6, but with one difference - $m \leq .01$, which is 1/100th of the value used in the SOAS, where $\frac{K_1}{K_2}$ is also equal to 1/100. In this way the same functions $G_1(s)$, $G_2(s)$ and $G_3(s)$ appear in the outer loop and prefilter. B , the saturation value for the ideal relay, is a variable with $B = B_{\max} = 16 \pi$ (as in the SOAS), corresponding to the case where the plant has its minimum gain $K = K_{\min} = K_1 = 1$, ($A = .5 \text{ V}$), and with $B = B_{\min} = B_2 = B_1 \times \frac{K_1}{K_2} = .16 \pi$, corresponding to the case where the plant has its maximum gain $K = K_{\max} = K_2 = 100$ (A is still $.5 \text{ V}$). $\psi(s)$ is chosen $= \frac{.4}{s}$, so the crossover frequency of L_S is maximized when the plant has its maximum gain $K = K_2$. In this design the block defining $A_{me} = e^{-.5T_0 s}$, where $T_0 = \frac{1}{\omega_0} = \frac{1}{4.6} \text{ sec}$.

Computer simulations were performed on the CDC 6400 system at University of Colorado, using "Mimic" program. Two types of runs were performed. First, the gain of the plant is changed (with different initial gain values) and no command or disturbance inputs are considered. The dynamics of the adjustment loop changes accordingly. The gain is changed abruptly from K_{in} to K_{fi} . The table below gives the list of the simulations performed.

Figure	K_{in}	K_{fi}	R	D
4.6-1	100	50	0	0
4.6-2	50	25	0	0
4.6-3	10	5	0	0
4.6-4	2	1	0	0

Table 1 - Simulations performed - Gain changes

In these figures only two variables are shown; sub a depicts $x_o(t)$ (the input to the non-linearity) and the plant gain K ; sub b depicts B (the non-linearity saturation level) and K . Note in Figure 4.6-1 that when $K_{in} = 100$, $K_{fi} = 50$, the new steady state is achieved after about 5 oscillations, while in Figure 4.6-4, $K_{in} = 2$, $K_{fi} = 1$, the dynamics of adjustment are very slow.

The second group of runs shows the system response to command and disturbance inputs, when extreme values are applied for fixed plant gain values. The table below summarized the simulations done.

Figure	K	R	D
4.6-5	100	R_e	0
4.6-6	10	R_e	0
4.6-7	1	R_e	0
4.6-8	100	0	D_e
4.6-9	10	0	D_e
4.6-10	1	0	D_e

Table 2 - Simulations performed.

System response to command and disturbances

and the input to the non-linearity.

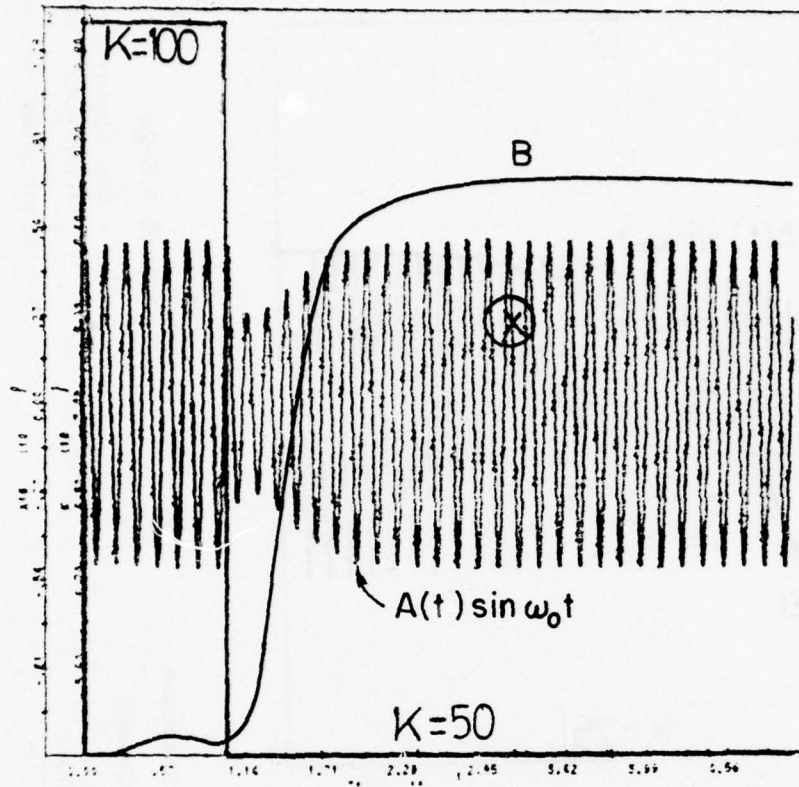


Figure 4.6-la
X 18 - Non-linearity
Input $-X$
K - Plant Gain

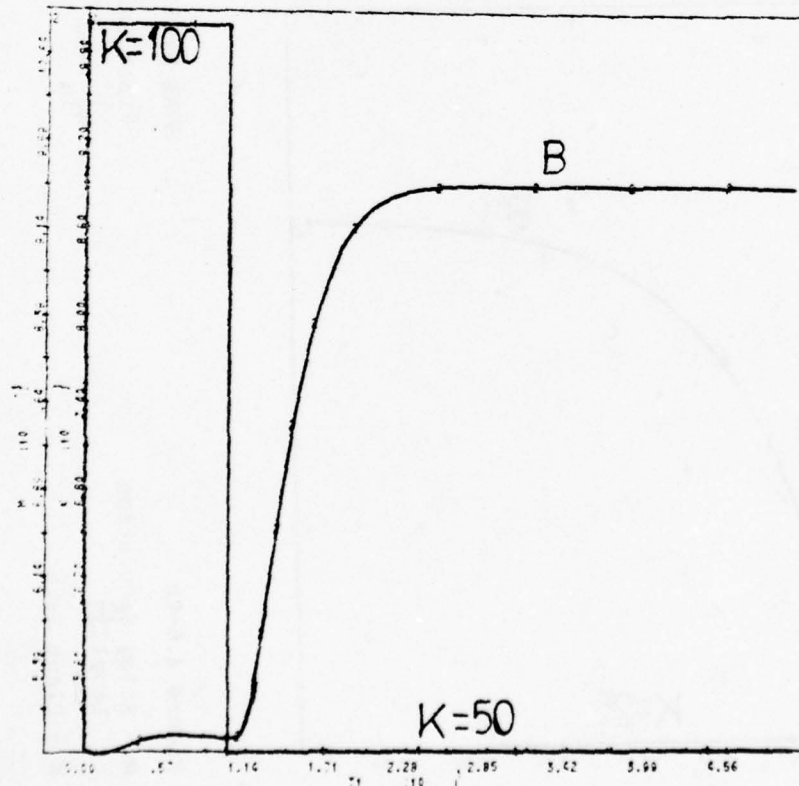


Figure 4.6-lb
M - Relay Saturation
Level $-B$
K - Plant Gain

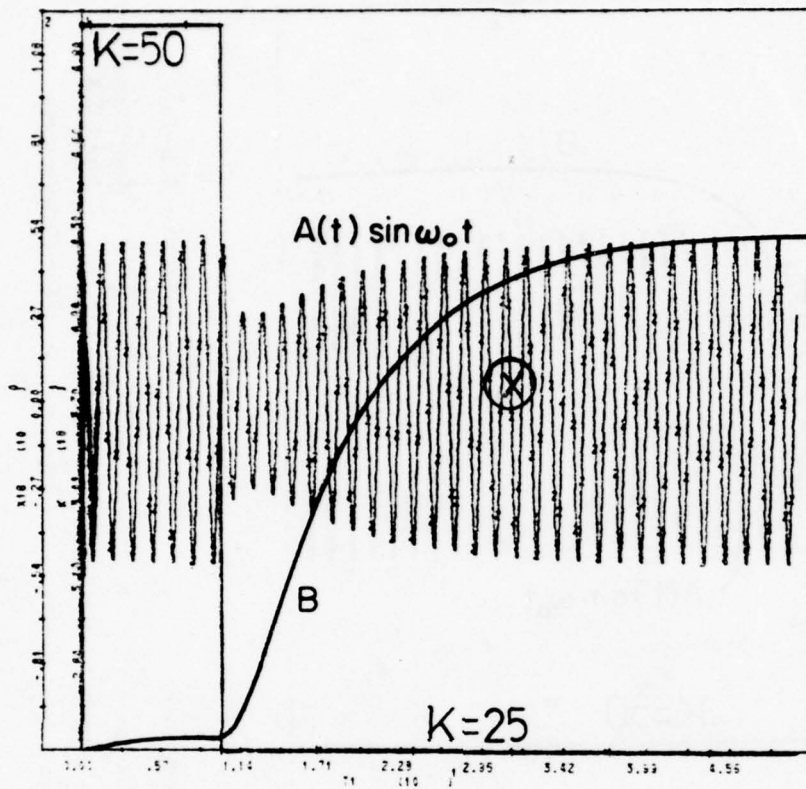
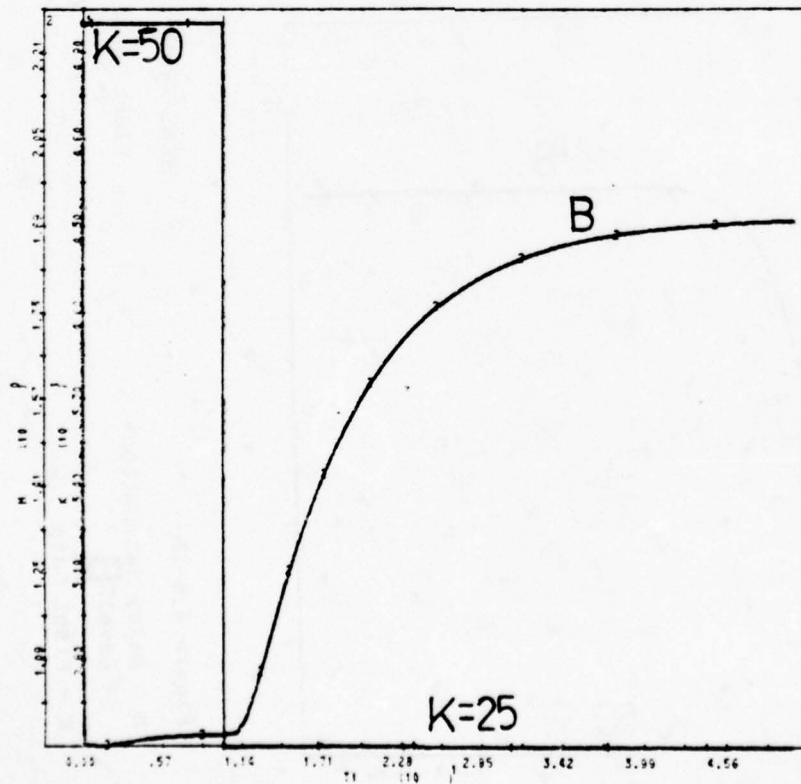


Figure 4.6-2a
X 18 - Non-linearity
Input - X
K - Plant Gain



SOAL System Response
Plant Gain Change
 $K_{in} = 50$ $K_{fi} = 25$

Figure 4.6-2b
M - Relay Saturation
Level - B
K - Plant Gain

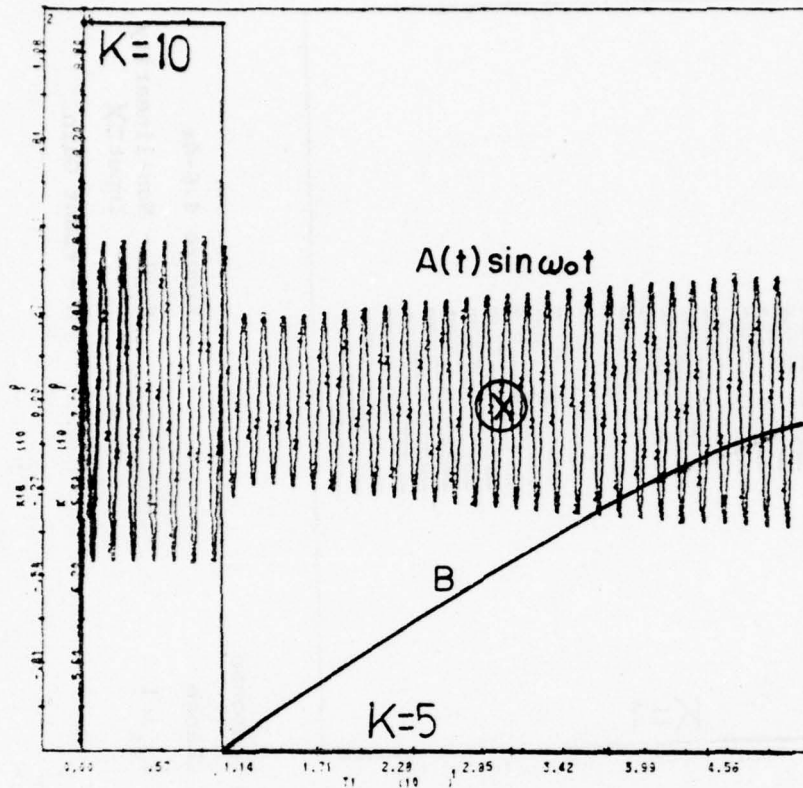
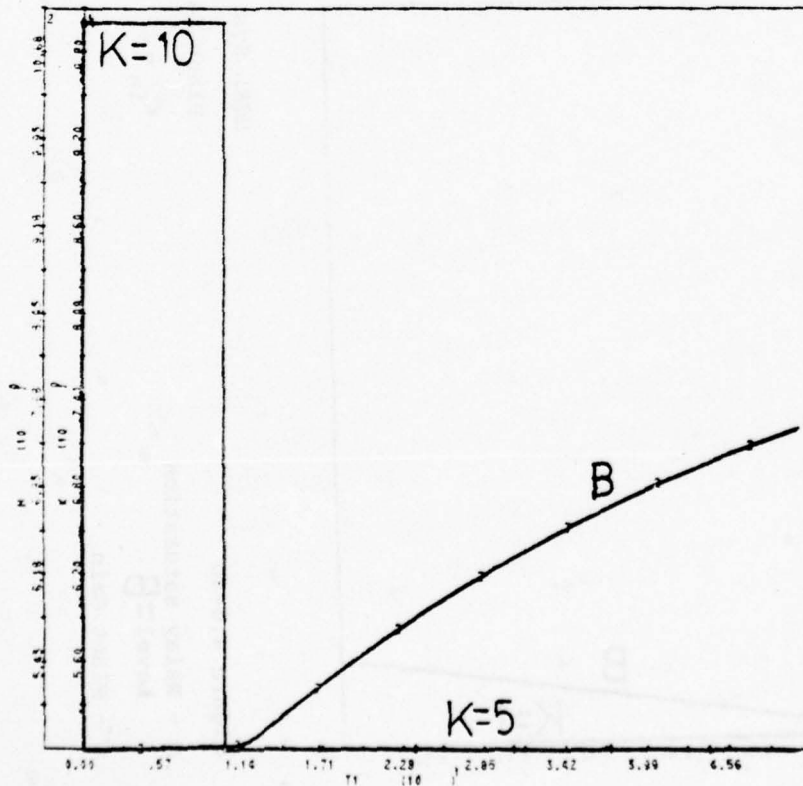


Figure 4.6-3a
X 18 - Non-linearity
Input = X
K - Plant Gain



SOAL System Response
Plant Gain Change
 $K_{in} = 10$ $K_{fi} = 5$

Figure 4.6-3b
M - Relay Saturation
Level = B
K - Plant Gain

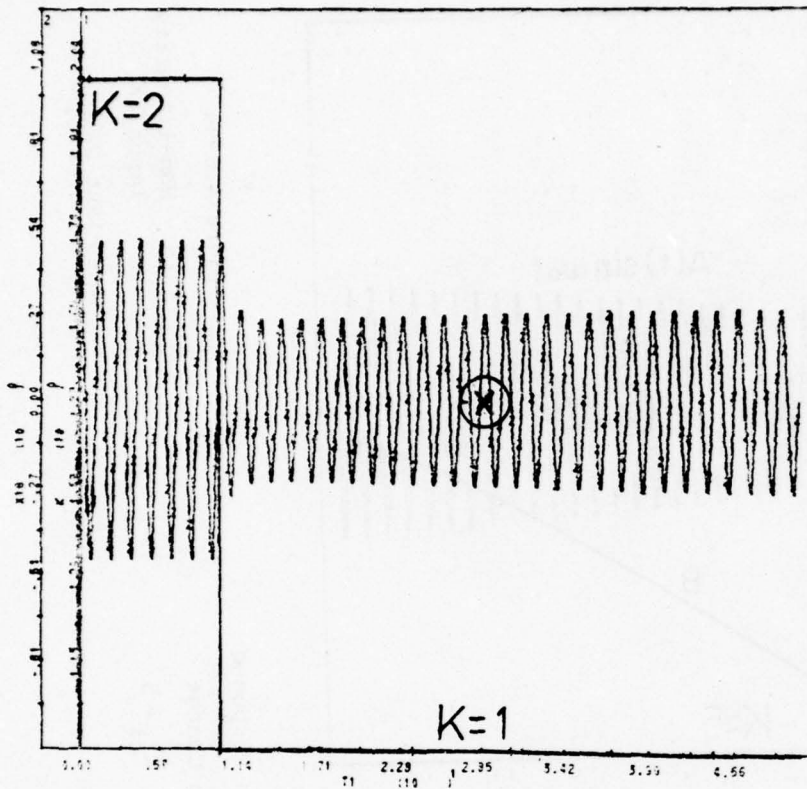


Figure 4.6-4a
 X - Non-linearity
 Input $\approx X$
 K - Plant Gain

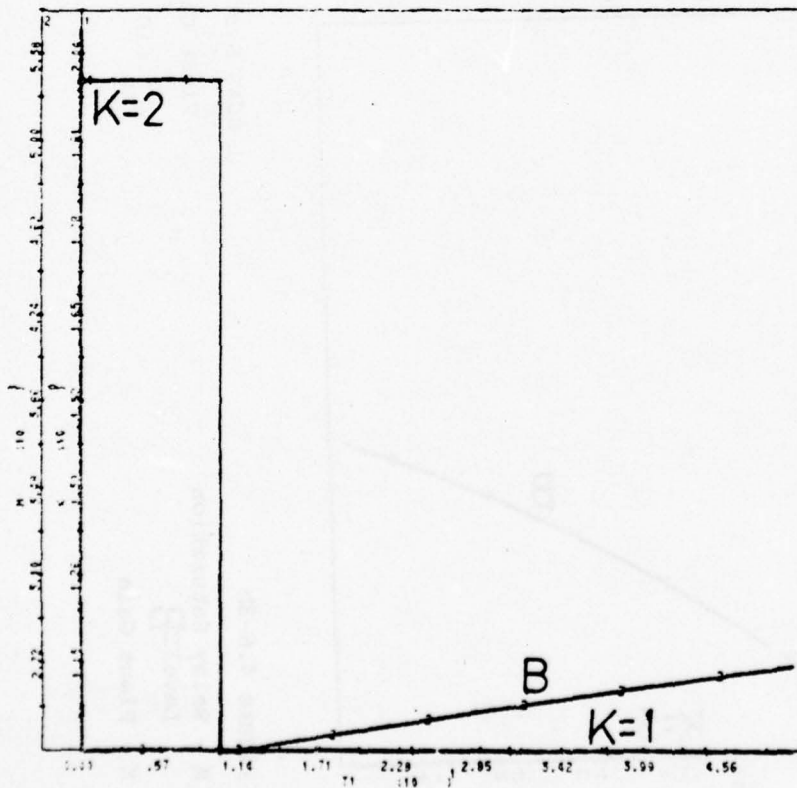


Figure 4.6-4b
 M - Relay saturation
 Level $= B$
 K - Plant Gain

SOAL System Response

Plant Gain Change

$K_{in} = 2$ $K_{fi} = 1$

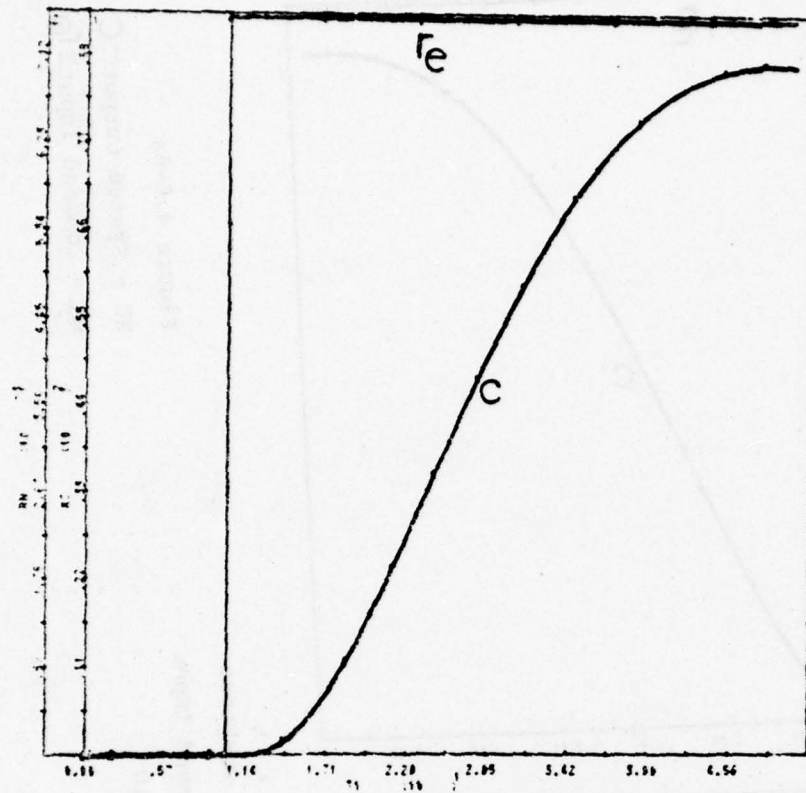
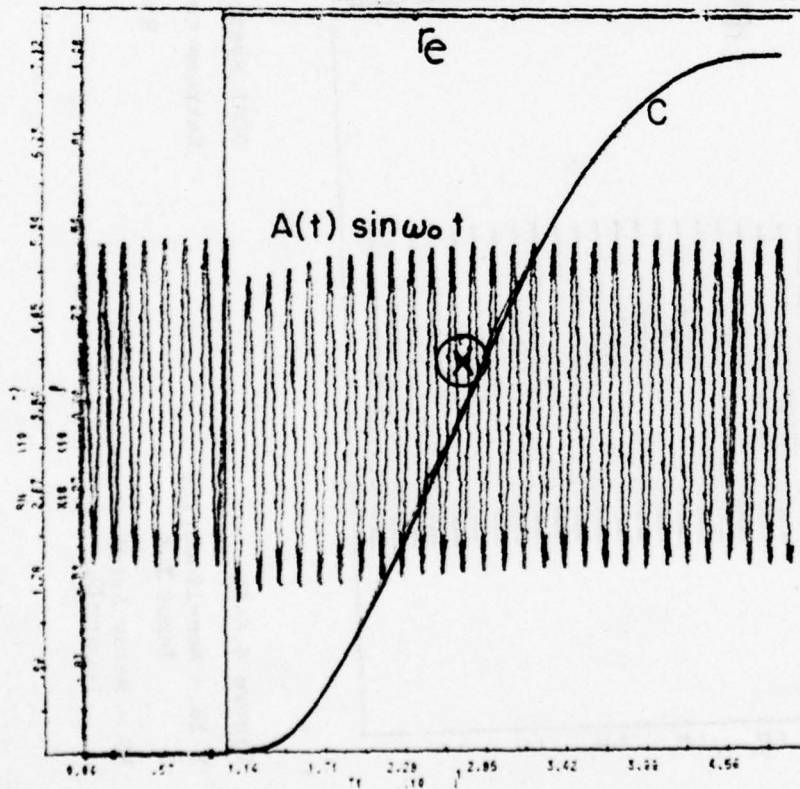
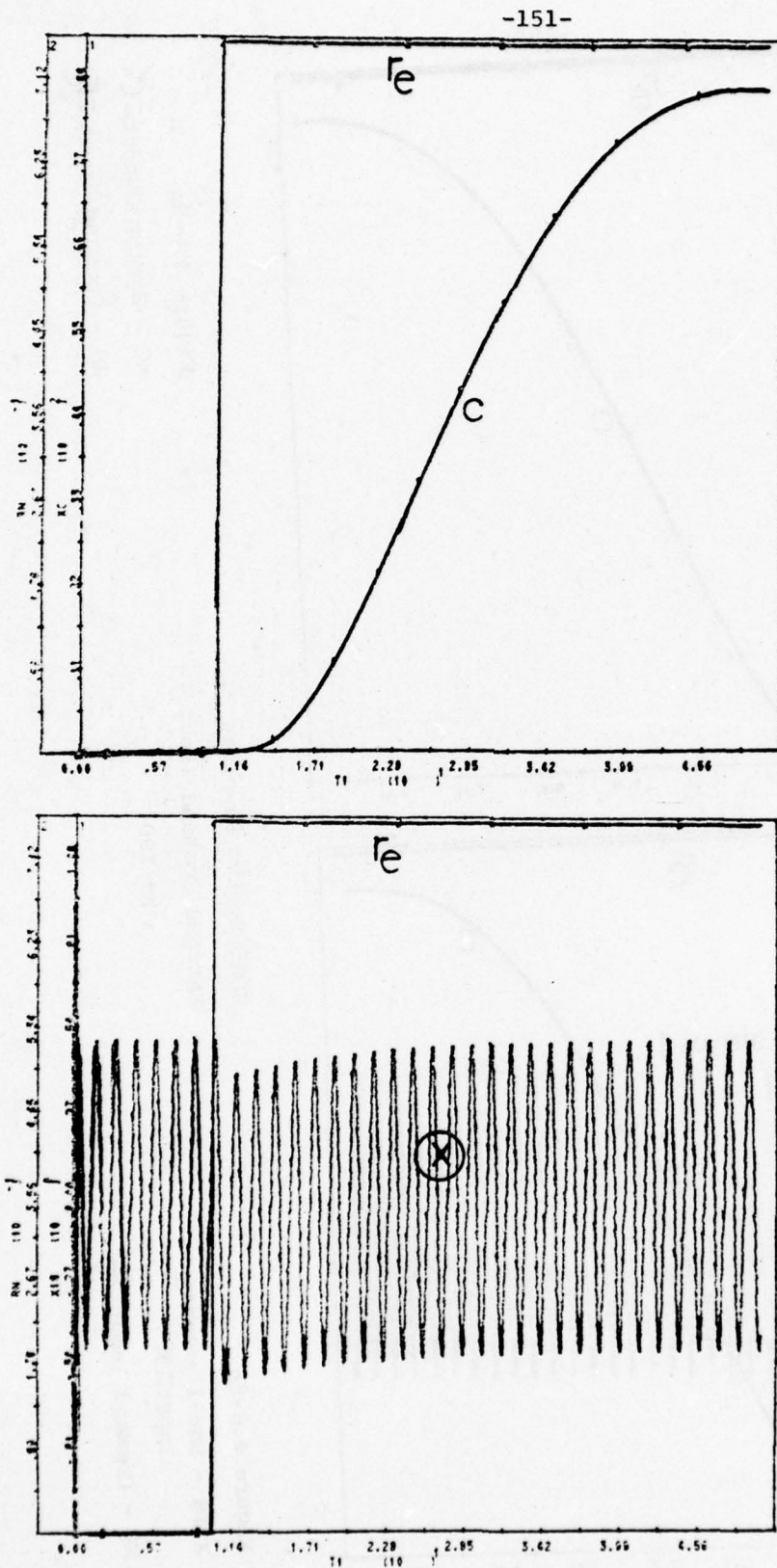


Figure 4.6-5a
 XC - System Output $= C$
 RN - Command Input $= RN$



SOAL System Response
 Extreme Command Input
 $K = 100$

Figure 4.6-5b
 X 18 - Non-linearity
 Input $= X$
 RN - Command Input $= RN$



SOAL System Response
Extreme Command Input

$K = 10$

Figure 4.6-6a
XC - System Output = C
RN - Command Input = e

Figure 4.6-6b
X 18 - Non-linearity
Input = X
RN - Relay Saturation
Level = e

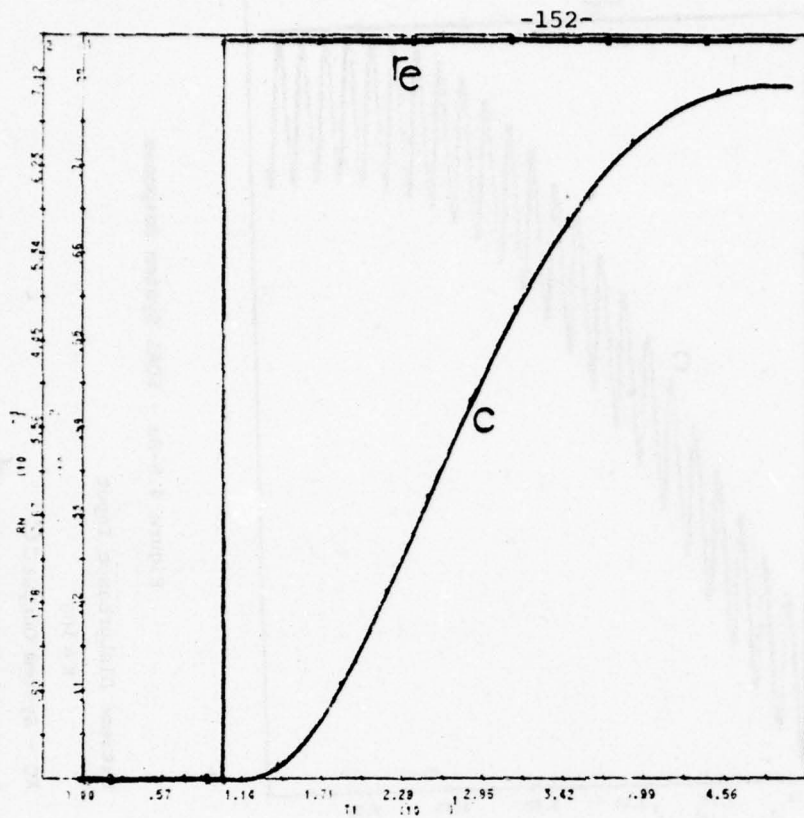


Figure 4.6-7a
XC - System Output = C
RN - Command Input = e

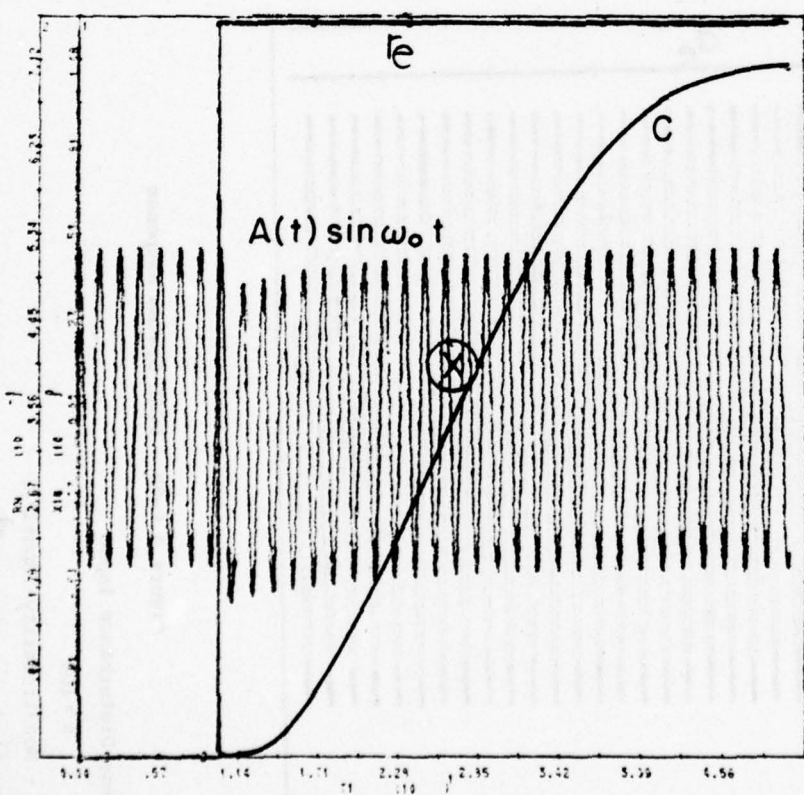


Figure 4.6-7b
X18 - Non-linearity
Input = X
RN - Command Input = e

SOAL System Response
Extreme Command Input
K = 1

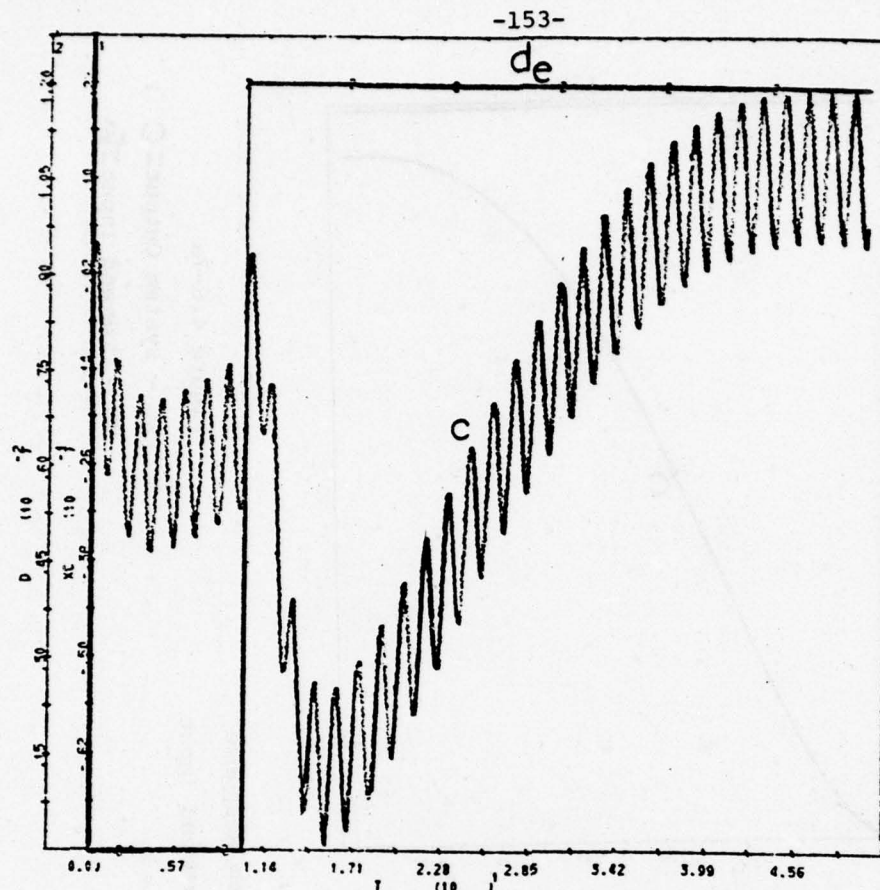


Figure 4.6-8a - SOAL System Response

Extreme Disturbance Input

$K = 100$

XC - System Output $= C$

D - Applied Disturbance $= d_e$

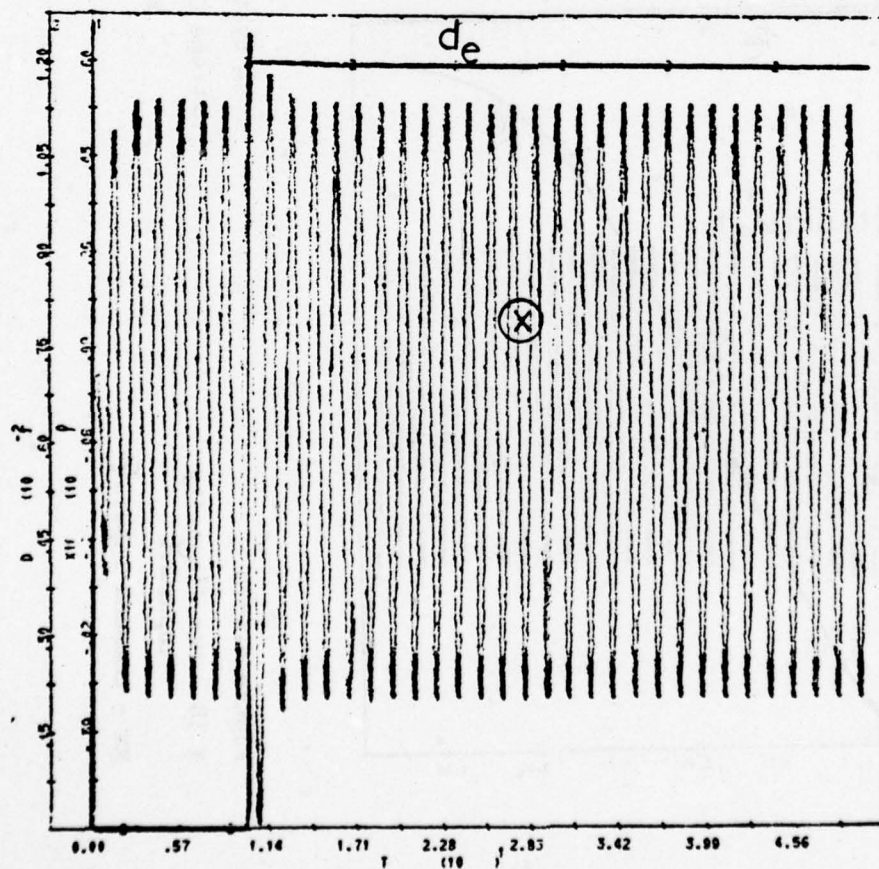


Figure 4.6-8b - SOAL System Response

Extreme Disturbance Input

$K = 100$

X 18 - Non-linearity Input $= X$

D - Applied Disturbance $= d_e$

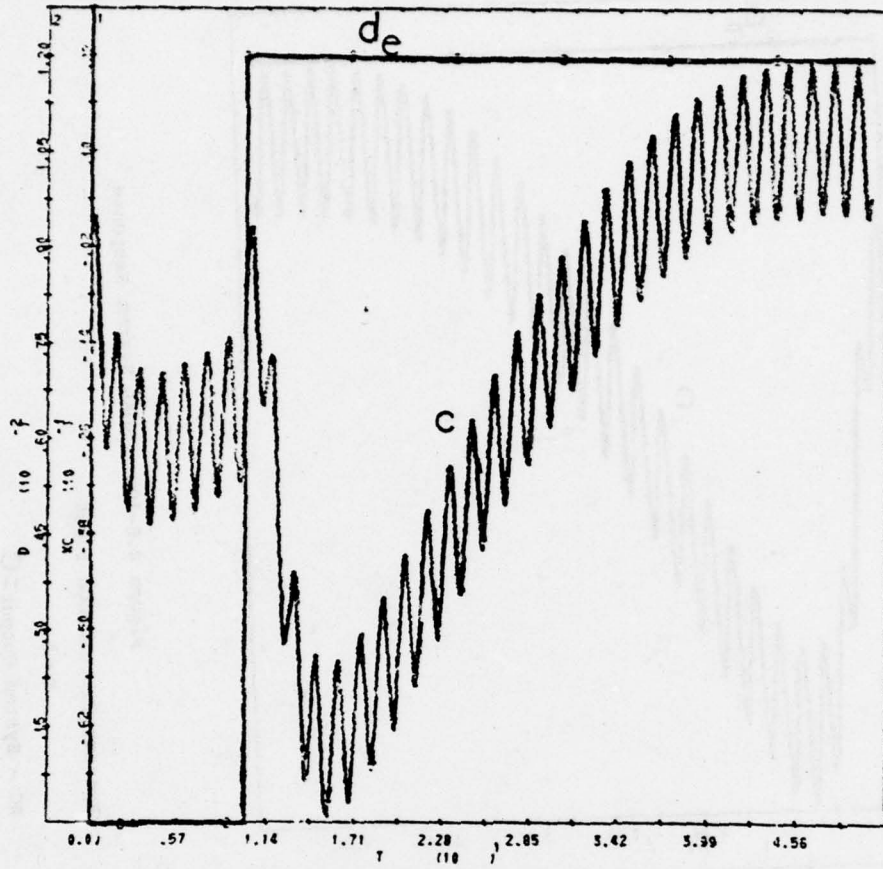


Figure 4.6-9a - SOAL System Response

Extreme Disturbance Input

$K = 10$

XC - System Output = C

D - Applied Disturbance = d_e

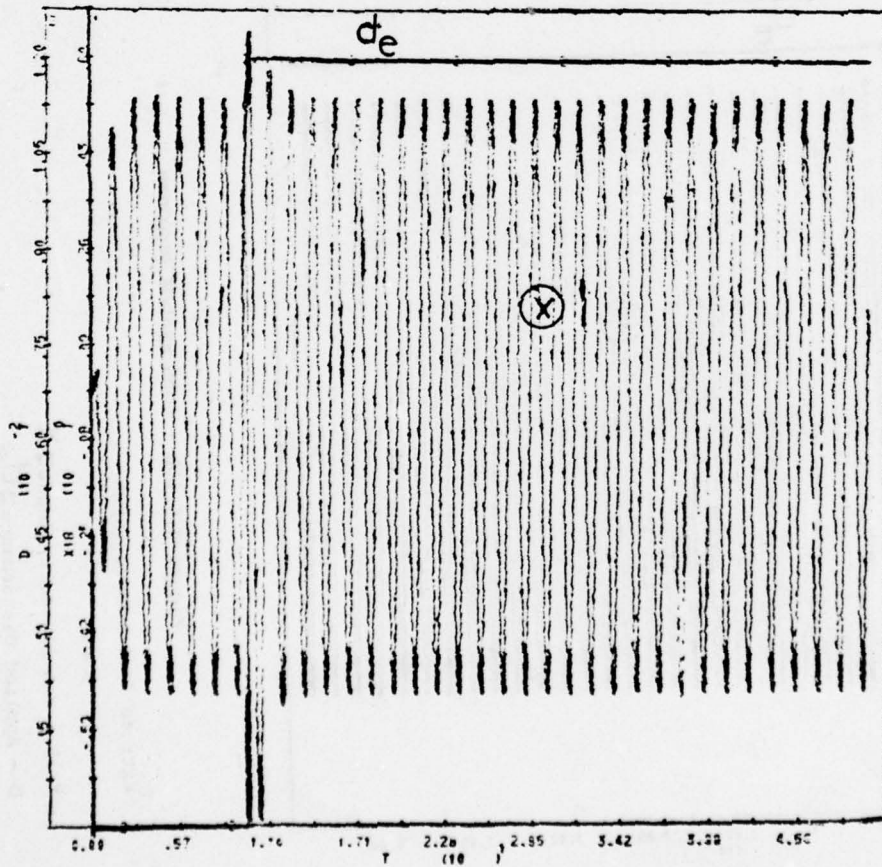


Figure 4.6-9b - SOAL System Response

Extreme Disturbance Input

$K = 10$

X 18 - Non-linearity Input = X

D - Applied Disturbance = d_e

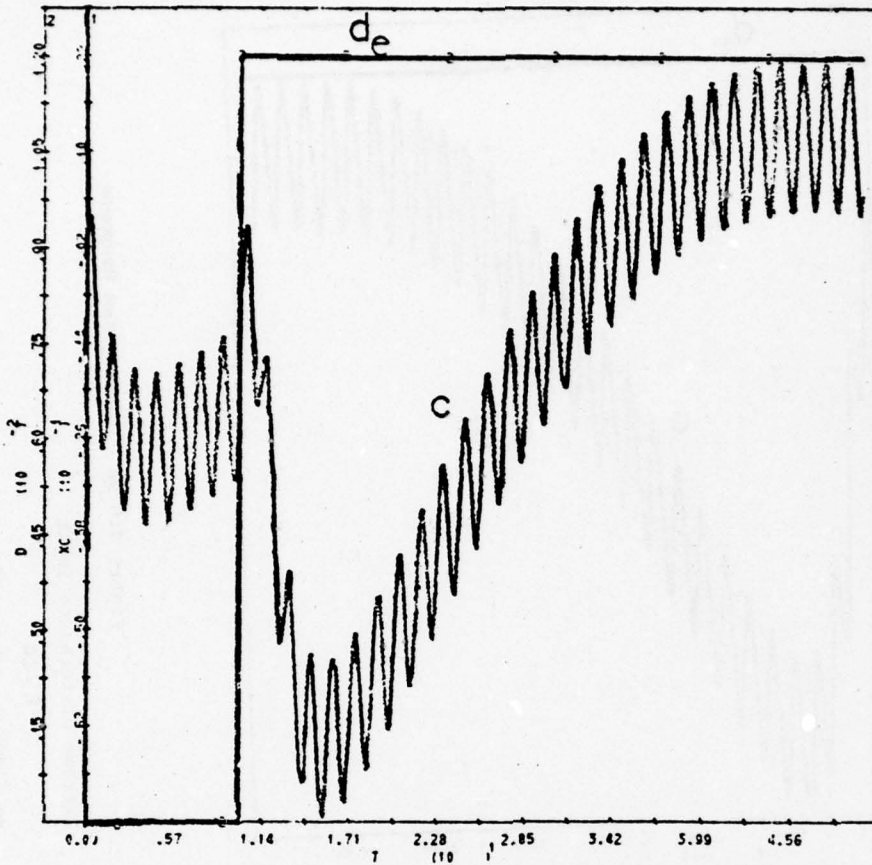


Figure 4.6-10a - SOAL System Response

Extreme Disturbance Input

$K = 1$

XC - System Output = C

D - Applied Disturbance = d_e

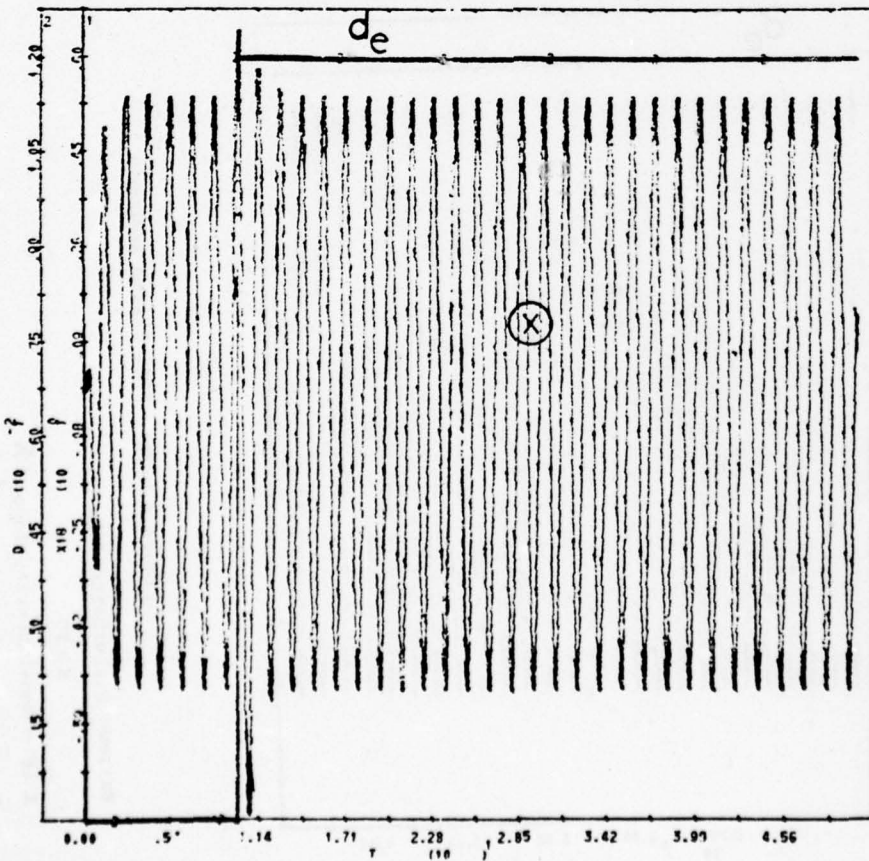


Figure 4.6-10b - SOAL System Response

Extreme Disturbance Input

$K = 1$

X 18 - Non-linearity Input = X

D - Applied Disturbance = d_e

4.7 Comparison with the Minneapolis-Honeywell System

It is worth noting the differences between the SOAL and the final Minneapolis-Honeywell (MH) adaptive flight control 2-loop design used in the X-15 [21]. The basic philosophy of the MH and SOAL designs is identical, i.e. to use the oscillating component amplitude measurement in order to change the gain in the main loop, such that in the steady-state, the oscillating amplitude is constant. However, the means of execution are radically different.

In the MH design, the oscillation is measured near or at the system output, where it is not large relative to the other signal components. A band-pass filter centered at ω_0 is therefore needed, introducing an additional very significant lag in the second loop [27]. Other signals, such as command and especially fast disturbance signals, also excite the band-pass filter. If its bandwidth is therefore decreased, its effective time constant is increased since the latter is inversely proportional to the bandwidth [27]. A disturbance signal may thus conceivably be interpreted as a plant gain change. In addition, the narrower the band of the filter, the more sensitive it is to changes in the oscillating frequency.

Finally, the output of the band-pass amplifier must be measured and compared with a reference - exactly as in the SOAL. Thus, the band pass filter has been eliminated in the SOAL. In the SOAL, the measurement of the oscillation is made at a point where it is inherently the dominant signal. Peak to peak measurement decreases the sensitivity to other signals, providing they are relatively constant over half a period. Finally, it is important to note that no analytic design theory was made available by the Minneapolis-Honeywell effort.

CHAPTER FIVE

S.O.A.N.L.

(SOAL with non-linearity in the secondary loop)

5.1 General

Chapter 4 dealt with the SOAL structure, which has some important advantages over the SOAS structure. The SOAL succeeded in eliminating the factor $\frac{K_{\max}}{K_{\min}}$ from the outer (adaptive) loop. But the factor $\frac{K_{\max}}{K_{\min}}$ reappeared in the secondary loop which determines the rate of adaptation of the system. The latter is given by Equation 4.2-9, repeated here.

$$\frac{\Delta B}{\Delta A}(s) = \frac{-\psi(s) e^{-.5T_o s}}{1 + \left| \frac{4}{\pi} G_1 G_2 P_h(j\omega_o) \right| K e^{-.5T_o s} \left(\frac{L_f(s)/3}{1 + L_f(s)/3} \right) \psi(s)} \quad (5.1-1)$$

The idea of the SOANL is to keep the existing advantages of the SOAL, i.e., elimination of the factor $\left(\frac{K_{\max}}{K_{\min}} \right)$ in the outer loop, but to eliminate it also from the secondary loop by eliminating K in Equation 5.1-1. This could be achieved by introducing a multiplier in the secondary loop, with multiplication factor inversely proportional to K . But K is not available directly, so B , which is related to K , can be used, since in the steady state case KB is constant (Equation 4.3-5). In the transient situation the information about K existing at the A_{me} block output could also be used to identify K , because if B has not achieved its steady state, then $A_m \neq A_r$ (Figures 4.1-1, 5.1-1). In this study this transient information has not been used, but can be considered in future research.

Figure 5.1-1 represents the SOANL structure which, if compared with the SOAL in Figure 4.1-1, includes a multiplier which multiplies $(A_r - A_m)$ by $\left(\frac{B}{B_{\min}}\right)$.

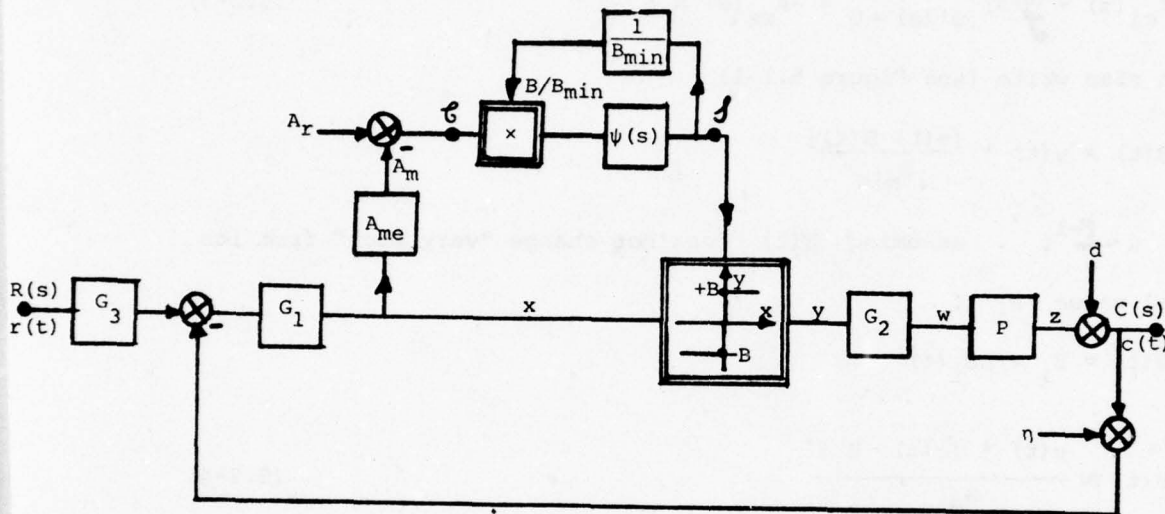


Figure 5.1-1 - SOANL Structure

The multiplier changes the dynamics of the secondary loop, which will be analyzed in Section 5.2. Just as in the SOAL, the main loop is not affected.

5.2 The Stability and Dynamics of the Secondary Loop - SOANL

As in Section 4.2, the fundamental feedback equation will be used, leading to:

$$\frac{0}{J} \triangleq t_{oi}(s) + t_{ci}(s) \cdot t_{os}(s) \cdot \frac{\psi'(s)}{1 - \psi'(s) t_{cs}(s)} \quad (5.2-1)$$

where $\psi'(s)$ is the equivalent relation between $\frac{d}{c}(s) = \psi'(s)$ ($d = \psi' \cdot c$)

All the other terms have the same meanings as in Section 4.2.

In Figure 5.1-1 the independent input is considered as a change in A , and the output as a change in B . The several transmissions are:

$$t_{oi}(s) = \frac{\Delta B}{\Delta A}(s) \Big|_{\psi'(s)=0} = 0 \quad (5.2-2)$$

$$t_{ci}(s) = \frac{t}{f}(s) \Big|_{\psi'(s)=0} = -A_{me}(s) = e^{-.5T_o s} \quad (5.2-3)$$

We can also write (see Figure 5.1-1)

$$B(t) = \mu(t) * \frac{[e(t) B(t)]}{B_{min}}$$

where $\mu = \mathcal{L}^{-1} \psi$. Assuming $B(t)$ does not change "very much" from its initial value B_i ,

$$B(t) = B_i + \Delta B_i(t)$$

so

$$B(t) \approx \frac{\mu(t) * [e(t) \cdot B_i]}{B_{min}} \quad (5.2-4)$$

so

$$B(s) = \psi(s) \times E(s) \left(\frac{B_i}{B_{min}} \right) \quad (5.2-5)$$

Then

$$t_{sc}(s) = \frac{B}{E}(s) = \psi'(s) = \psi(s) \cdot \left(\frac{B_i}{B_{min}} \right) \quad (5.2-6)$$

$t_{cs}(s)$ and $t_{os}(s)$ are identical to the functions found for the SOAL.

$$t_{cs}(s) \approx -\frac{4}{\pi} |G_1 G_2 K P_h(j\omega_o)| \cdot \frac{L_f(s)/3}{1 + L_f(s)/3} \cdot e^{-.5T_o s} \quad (5.2-7)$$

$$t_{os}(s) = 1 \quad (5.2-8)$$

Substituting Equations 5.2-2,3,6,7,8 in 1,

$$\frac{\Delta B}{\Delta A}(s) = \frac{-\left(\frac{B_i}{B_{min}}\right) \cdot \psi(s) e^{-.5T_o s}}{1 + \left|\frac{4}{\pi} G_1 G_2 P_h(j\omega_o)\right| \cdot \frac{KB_i}{B_{min}} \cdot e^{-.5T_o s} \cdot \psi(s) \cdot \frac{L_f(s)/3}{1 + L_f(s)/3}} \quad (5.2-9)$$

In Equation 5.2-9 B_i , the initial value of $B(t)$, is such that if the steady state was achieved (Equation 4.3-5), $B_i K = \text{constant}$, and the denominator is independent of the gain of the plant, so the dynamics of the secondary loop are independent of the plant gain. The assumption that $B(t)$ does not change "very much" once the steady state is achieved, is valid, considering the dynamics of the adjustment loop being faster than the changes in K . More than that, simulations have shown that even considering bigger changes in K and consequently in B , the results are still valid for Equation 5.2-9.

When $K = K_{\max}$ (in Equation 5.2-9), B equals B_{\min} , so Equation 5.2-9 is identical to the equivalent SOAL equation (4.2-9). This means that for $K = K_{\max}$ the SOANL has the same dynamics for the secondary loop as the SOAL. Suppose now $K = K_{\min}$, so

$$B = B_{\max} = B_{\min} \times \frac{K_{\max}}{K_{\min}}, \text{ and again the denominator of Equation 5.2-9 has}$$

the same function as before ($K = K_{\min}$), and the dynamics of the adjustment loop are constant.

SOANL Sensitivity to Dynamic Changes

Section 4.4 for the SOAL is valid for the SOANL.

5.3 Synthesis Procedure and Numerical Example (Smooth Solution) - SOANL

The synthesis procedure, the specifications, data and constraints are the same as for the SOAL, Section 4.5.

For the main loop, the SOANL is identical to the SOAL both for command and disturbance signals. The advantage is in the secondary loop, where the dynamics of adaptation are now almost constant.

The same specifications of the SOAL numerical example are used in the SOANL numerical example. As a consequence, all the SOANL blocks have the same functions as the SOAL blocks, including $\psi(s)$. The only change is the multiplier in the secondary loop.

A set of runs were made at the CDC 6400 system - C.U., using Mimic language. Two types of runs were performed: First, changes in gain of the plant, showing the dynamics of the adjustment loop. Next, the system response to extreme command and disturbance inputs for several plant gains.

The results show that for the same proportional plant gain change, the adjustment loop dynamics are constant and independent of K , which is the SOANL main advantage if compared with the SOAL. The system response for both the extreme command and disturbance inputs is similar to the SOAL response, as expected.

Some details should be considered, to avoid "pitfalls" in the SOANL implementation. Figure 5.4-1 represents the part of the secondary loop involving the multiplier.

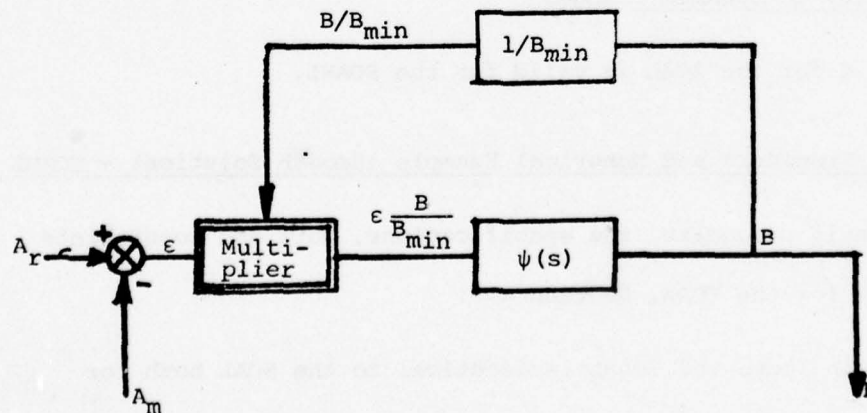


Figure 5.4-1 - Details in the Secondary Loop

First, if for any reason (due to dynamic overshoot), B goes to zero, both loops are open. A minimum expected value for B , based on the maximum of K , should be established, and if necessary, non-linear circuits used to avoid passing this minimum value. Second, it is advisable to have an integrator in $\psi(s)$, so there is no steady error in A , the limit cycle amplitude at x_0 . It is also recommended to avoid pure gains in $\psi(s)$. As an example, suppose we choose

$$\psi(s) = \frac{P_1}{s} + P_2$$

so in Figure 5.4-1

$$\epsilon(t) \times \frac{B(t)}{B_{\min}} \times P_2 + P_1 \int_0^t \frac{B(t)}{B_{\min}} \times \epsilon(t) dt = B(t)$$

If at t_1 , it so happens that $\epsilon(t_1) = \frac{B_{\min}}{P_2}$, then the above equation becomes

$$\int_0^{t_1} \frac{B(t)}{B_{\min}} \times \epsilon(t) dt = 0$$

which may not be true, i.e., there is no solution for $B(t)$.

The simulation results are presented in the next figures. First the plant gain is changed and no input applied. This is shown in Figures 5.4-2 - 10. For the same relative plant gain change the adjustment dynamics are identical. In Figure 5.4-10 when K , the plant gain, changes instantaneously from its maximum value (100) to its minimum value (1), the oscillations are temporarily quenched.

Next, the system response to the extreme command input is shown, for several plant gains (Figures 5.4-11 - 13). Finally, the system response to the extreme disturbance input for several plant gains is represented in Figures 5.4-14 - 16.

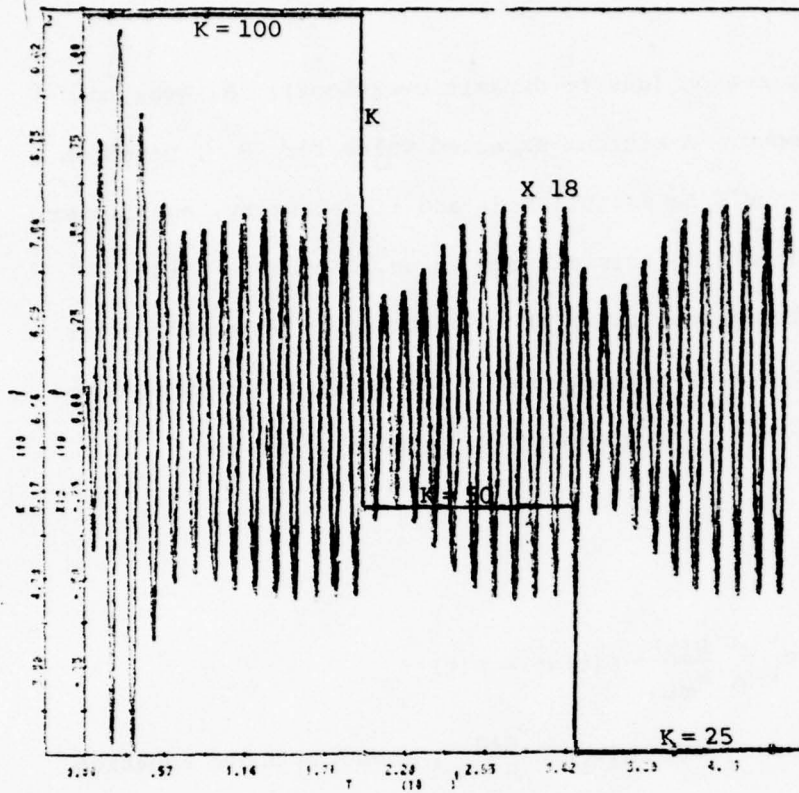


Figure 5.4-2a

X 18 - Non-linearity Input

K - Plant Gain

SOANL System Response
Secondary Loop Dynamics

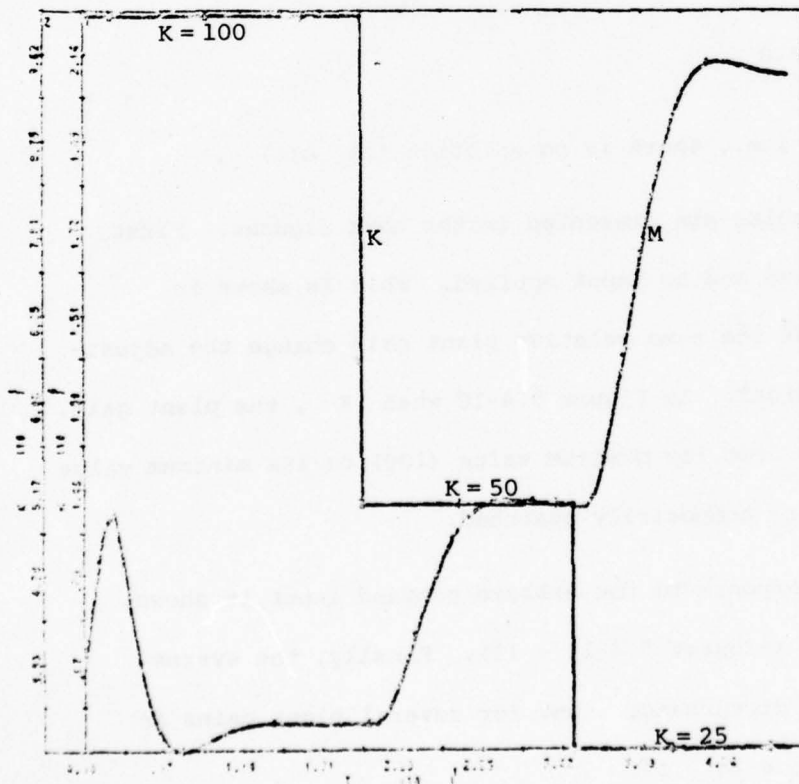


Figure 5.4-2b

M - Relay Saturation Level

K - Plant Gain

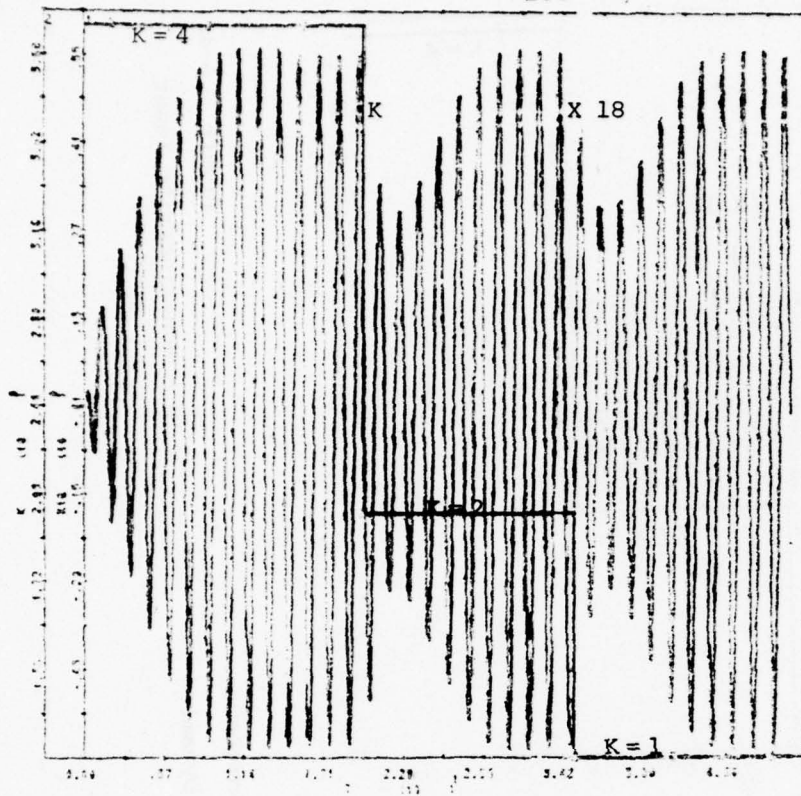


Figure 5.4-3a

X 18 - Non-linearity Input

K - Plant Gain

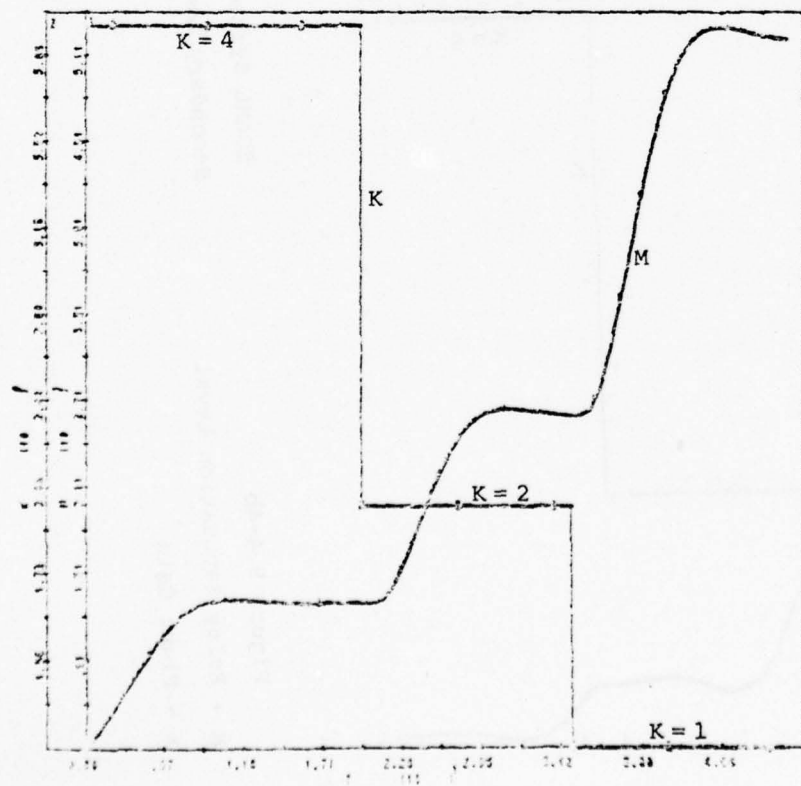


Figure 5.4-3b

M - Relay Saturation Level

K - Plant Gain

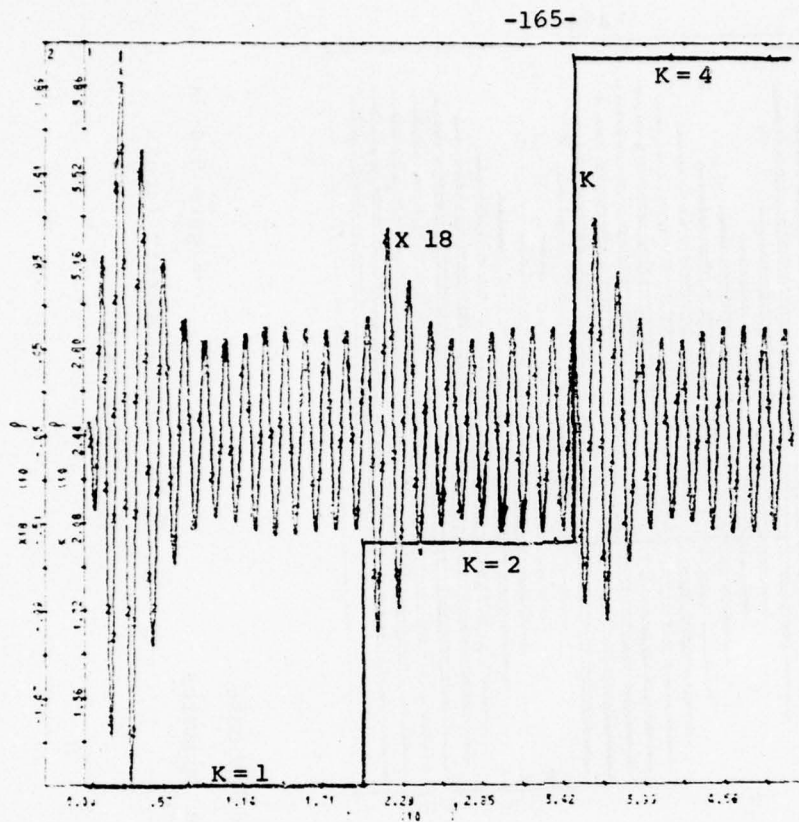
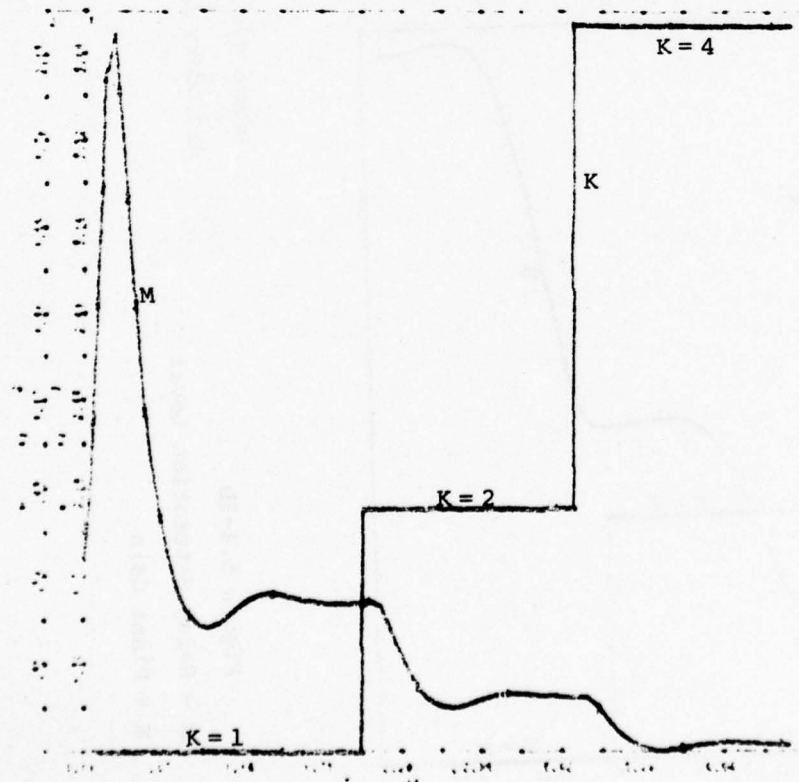


Figure 5.4-4a

X 18 - Non-linearity Input

K - Plant Gain



SOANL System Response

Secondary Loop Dynamics

Figure 5.4-4b

M - Relay Saturation Level

K - Plant Gain

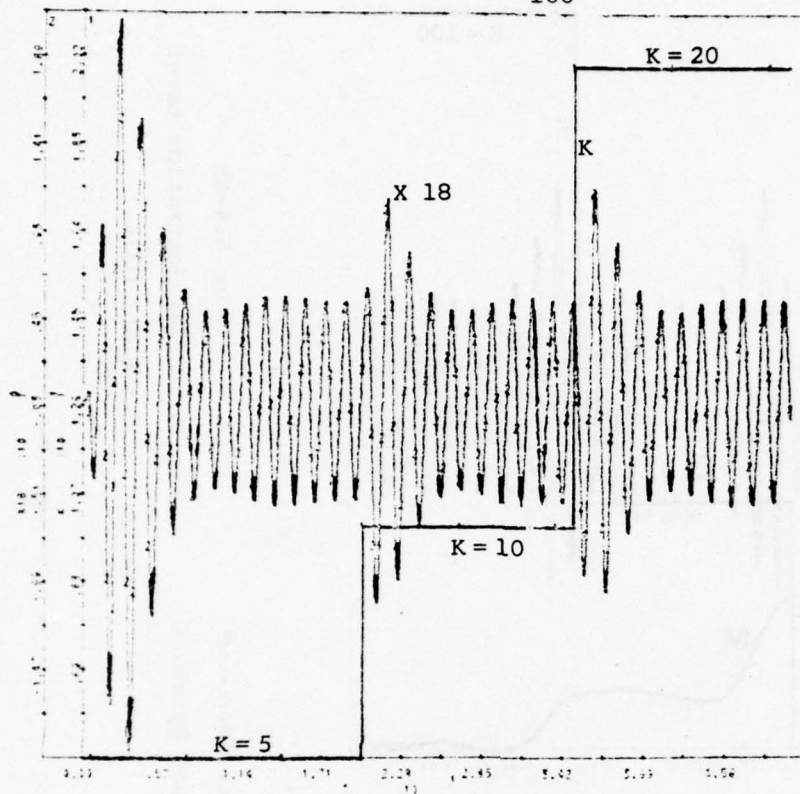
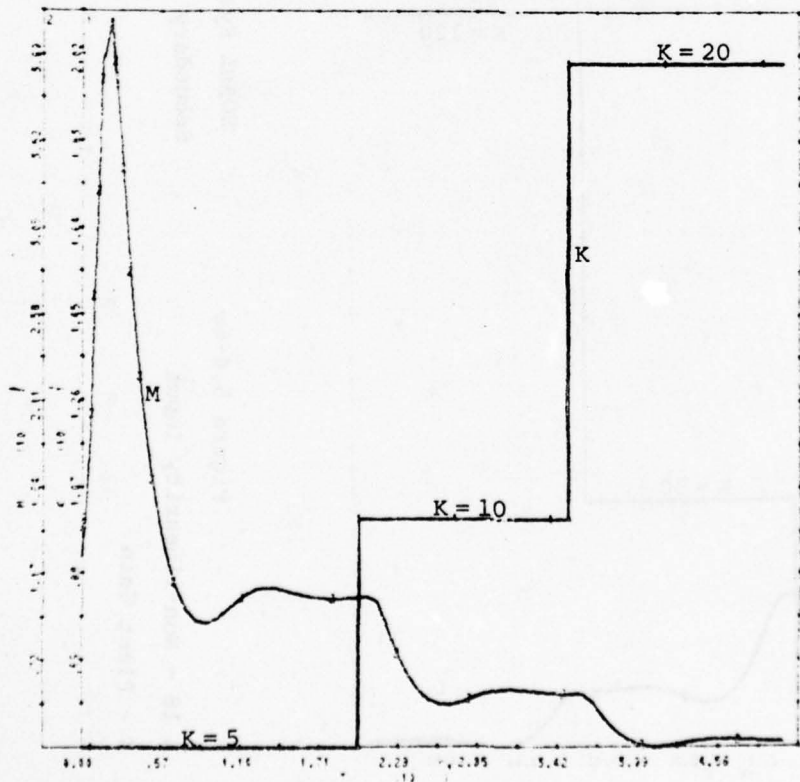


Figure 5.4-5a

X 18 - Non-linearity Input

K - Plant Gain



SOANL System Response

Secondary Loop Dynamics

Figure 5.4-5b

M - Relay Saturation Level

K - Plant Gain

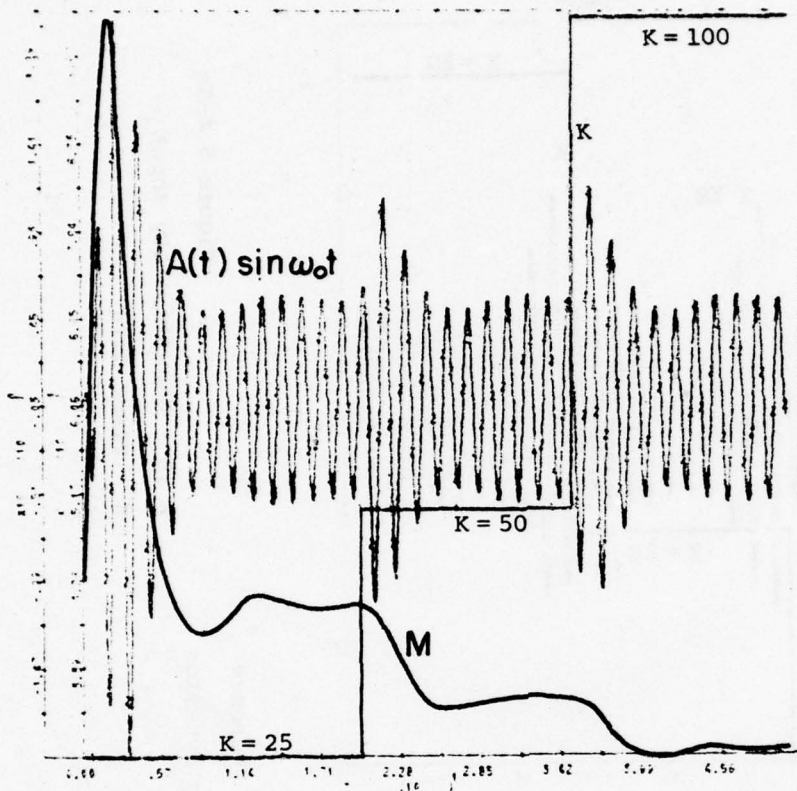
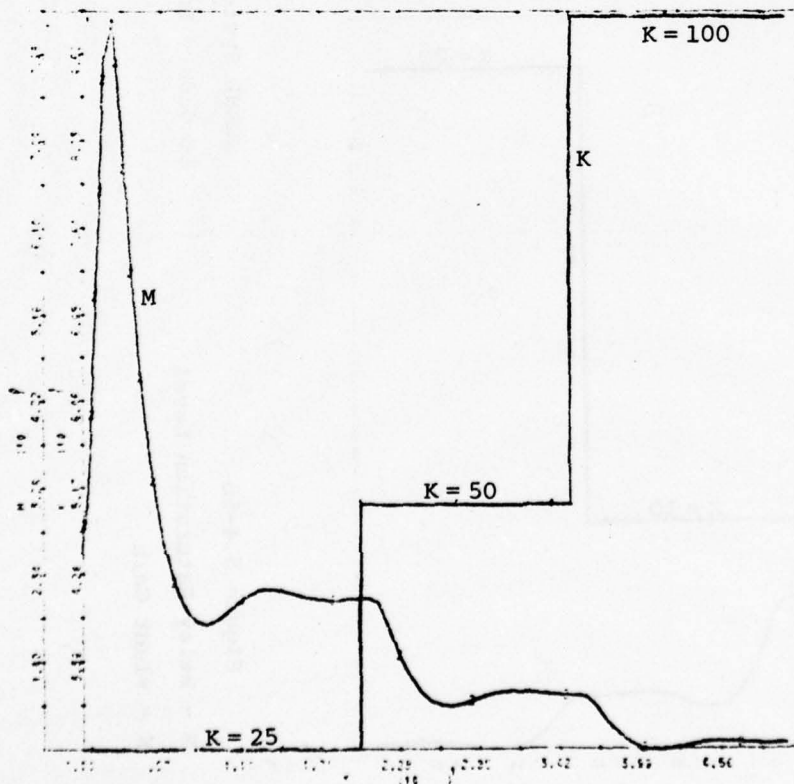


Figure 5.4-6b
M - Relay Saturation Level
K - Plant Gain



SOANL System Response
Secondary Loop Dynamics

Figure 5.4-6a
X 18 - Non-linearity Input
K - Plant Gain

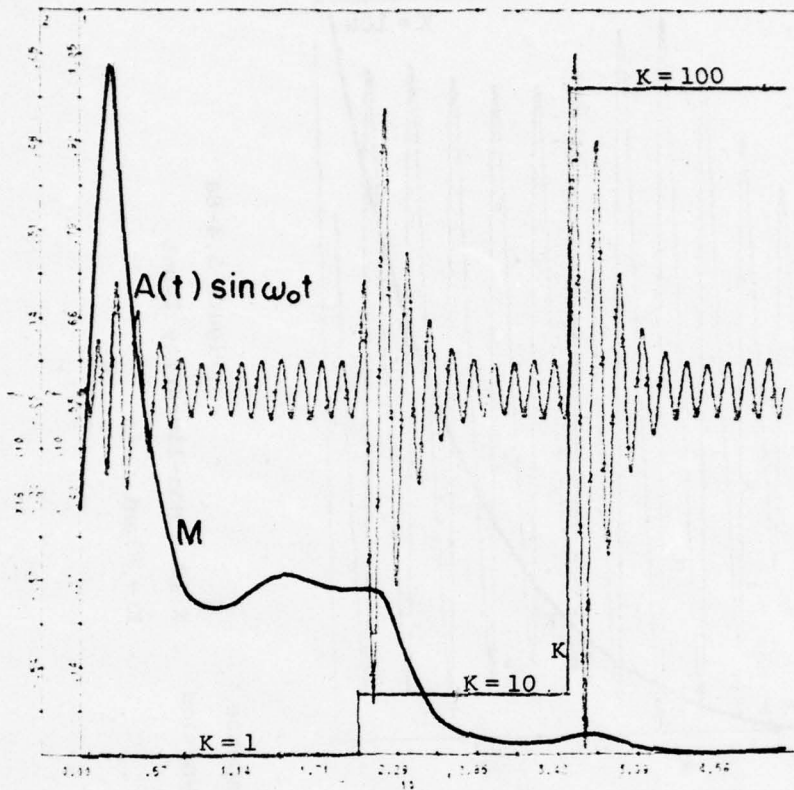
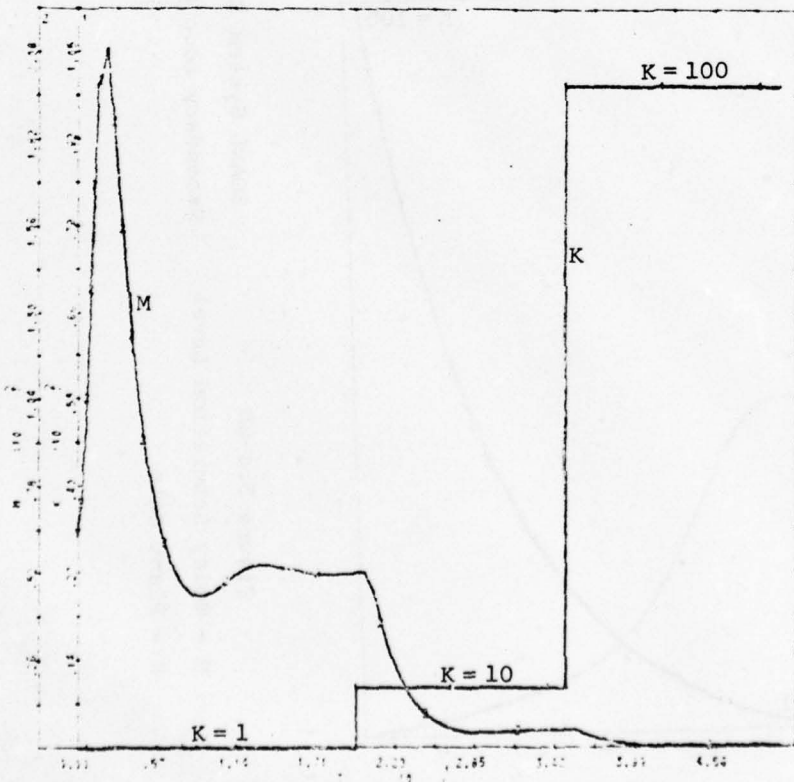


Figure 5.4-7a
X 18 - Non-linearity Input
K - Plant Gain



SOANL System Response
Secondary Loop Dynamics

Figure 5.4-7b
M - Relay Saturation Level
K - Plant Gain

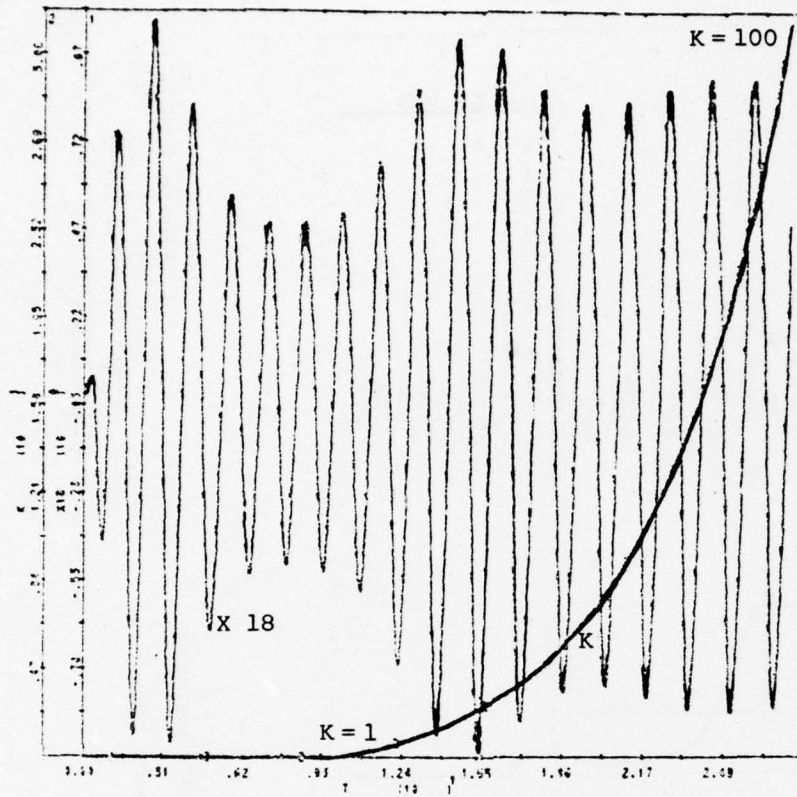


Figure 5.4-8a

X 18 - Non-linearity Input

K - Plant Gain

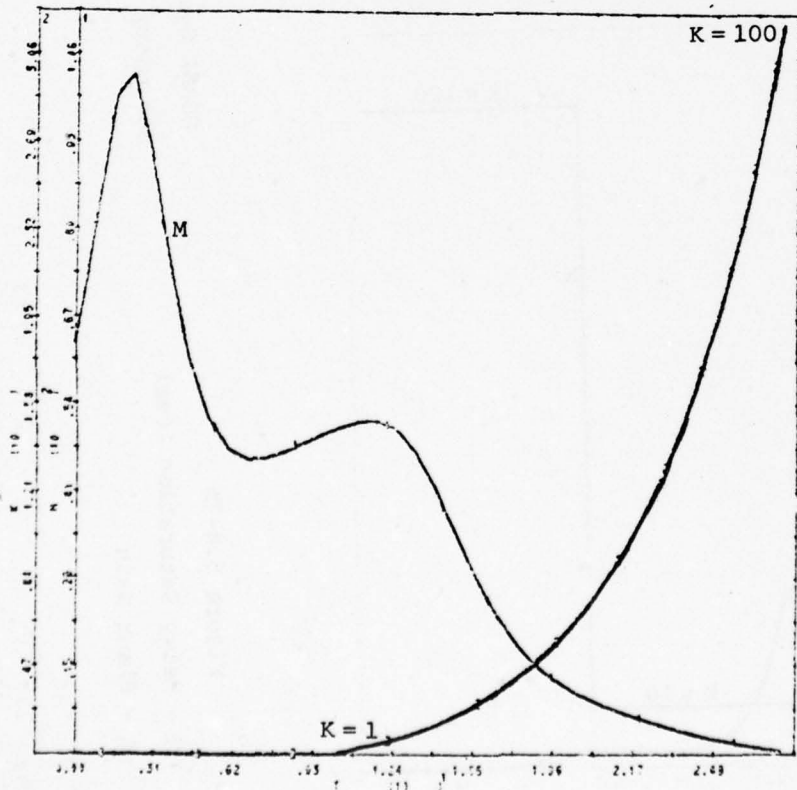


Figure 5.4-8b

M - Relay Saturation Level

K - Plant Gain

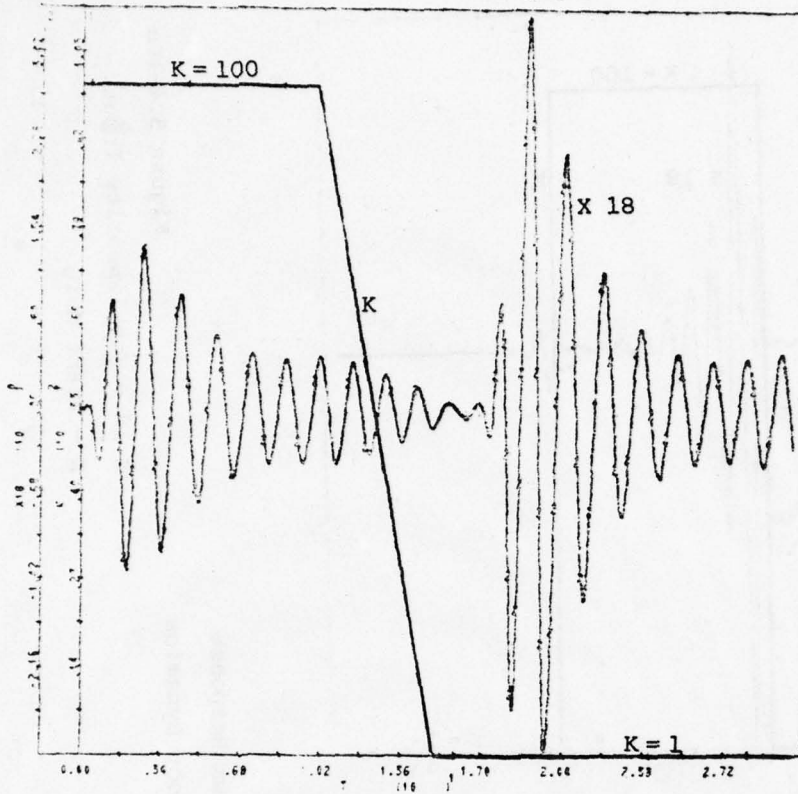


Figure 5.4-9a

X 18 - Non-linearity Input

K - Plant Gain

SOANL System Response
Secondary Loop Dynamics

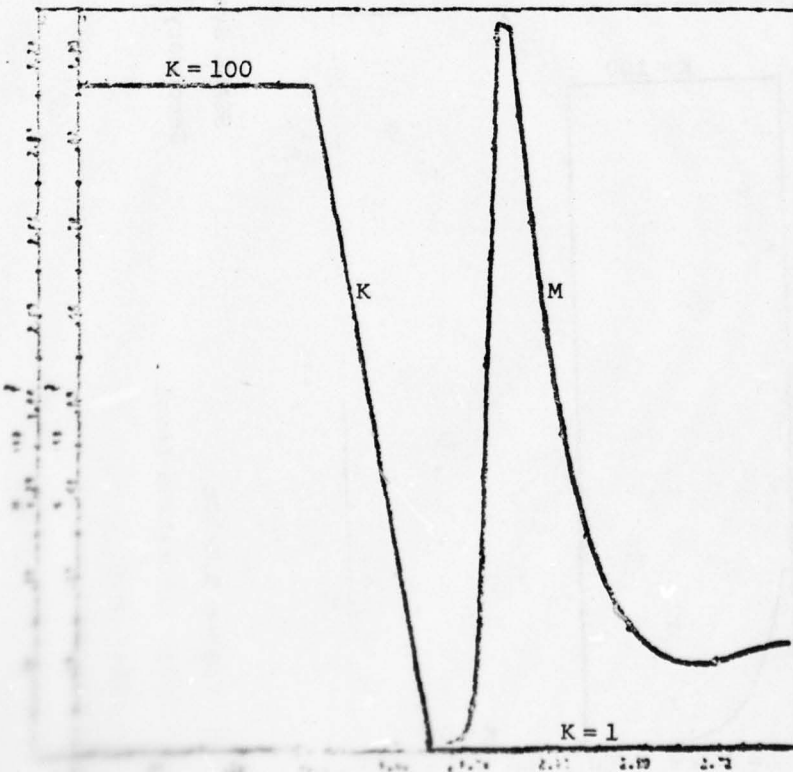


Figure 5.4-9b

M - Relay Saturation Level

K - Plant Gain

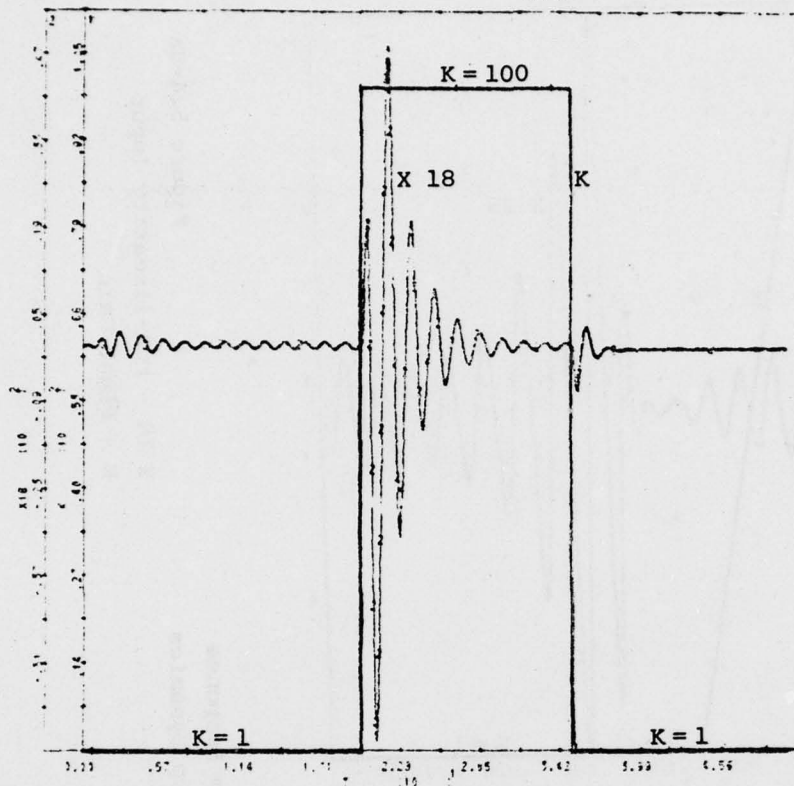
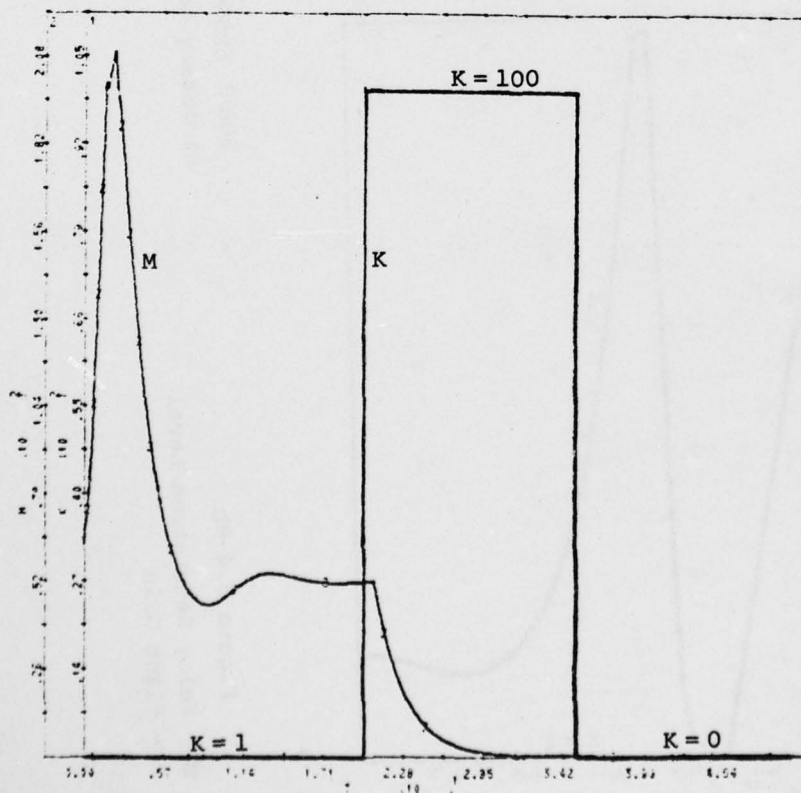


Figure 5.4-10a
X 18 - Non-linearity Input
K - Plant Gain



SOANL System Response
Secondary Loop Dynamics

Figure 5.4-10b
M - Relay Saturation Level
K - Plant Gain

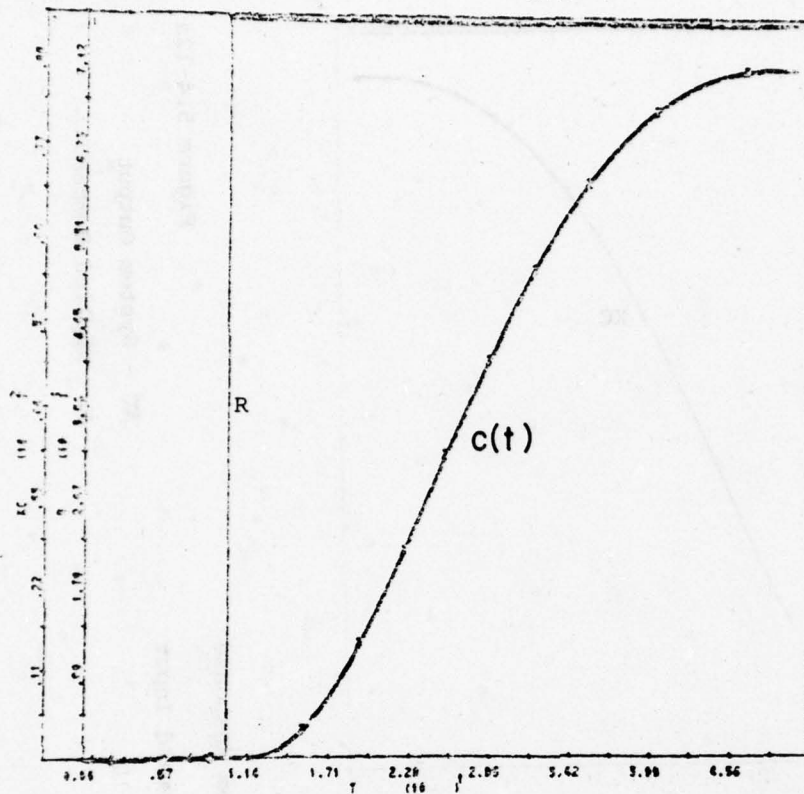


Figure 5.4-11a
XC - System Output
R - Applied Command

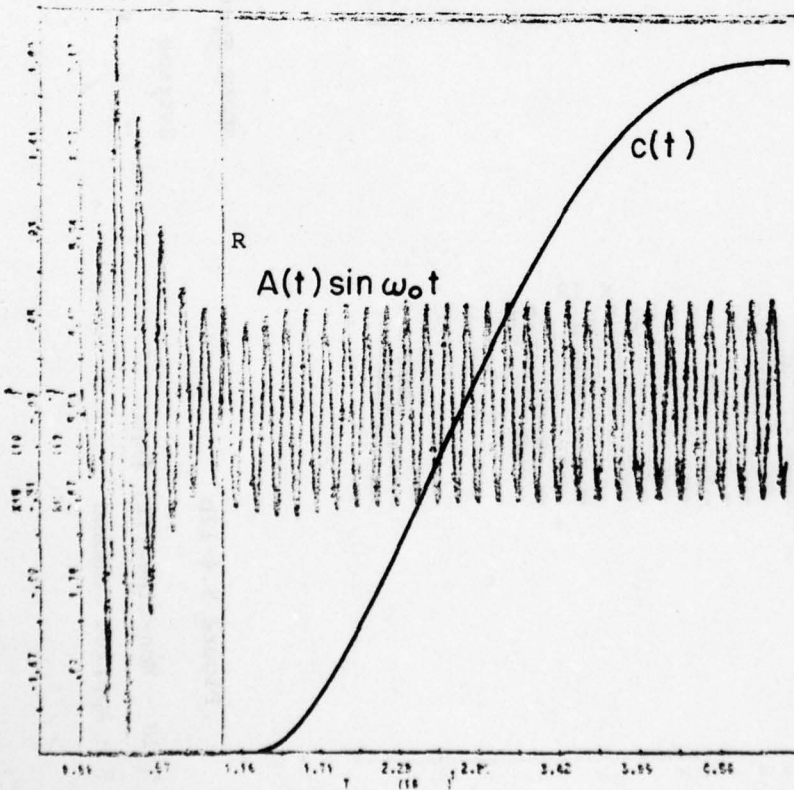


Figure 5.4-11b
X 18 - Non-linearity Input
R - Applied Command

SOANL System Response
Extreme Command Input
K = 100

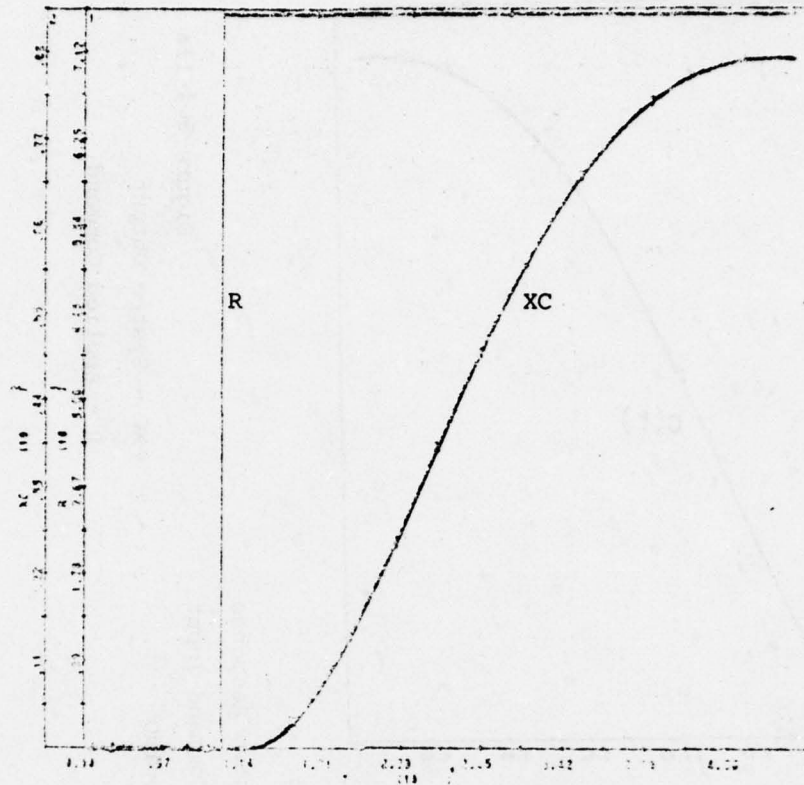
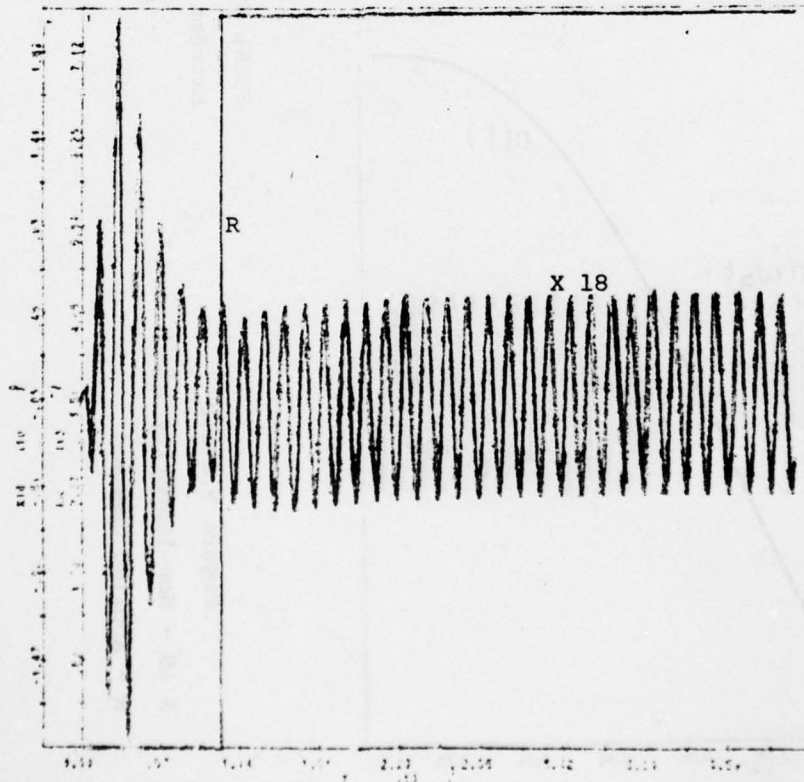


Figure 5.4-12a

XC - System Output
R - Applied Command



SOANL System Response

Extreme Command Input

K = 10

Figure 5.4-12b

X 18 - Non-linearity Input
R - Applied Command

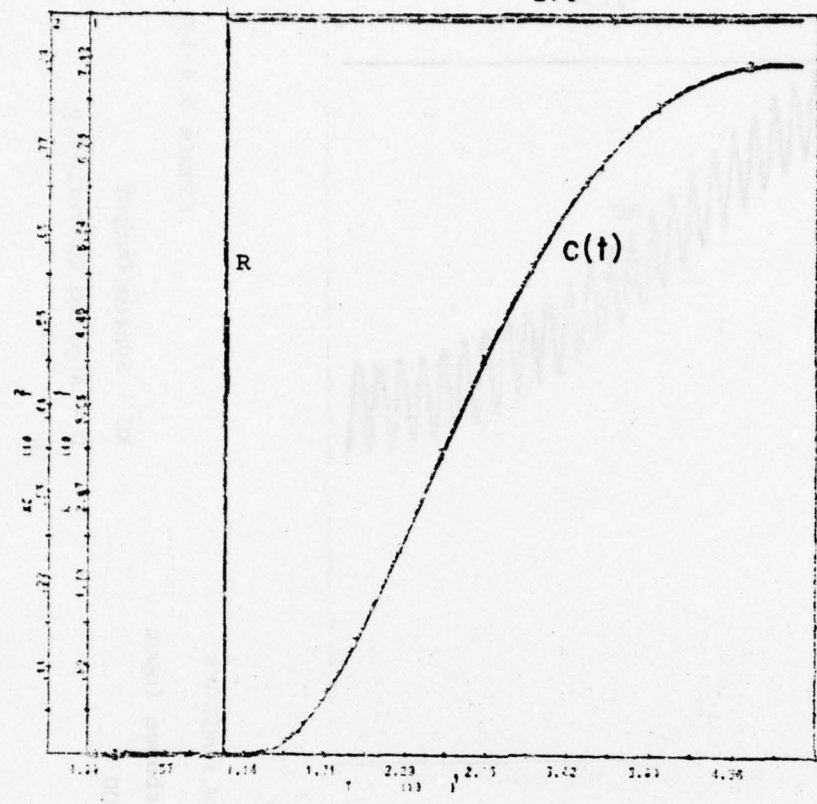


Figure 5.4-13a

XC - System Output
R - Applied Command

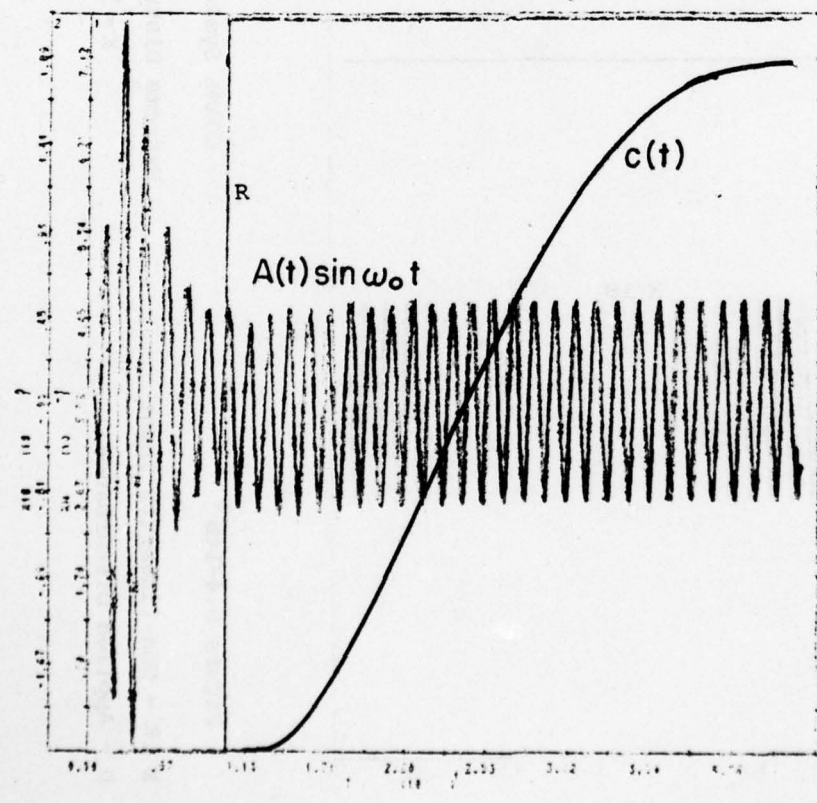


Figure 5.4-13b

X 18 - Non-linearity Input
R - Applied Command

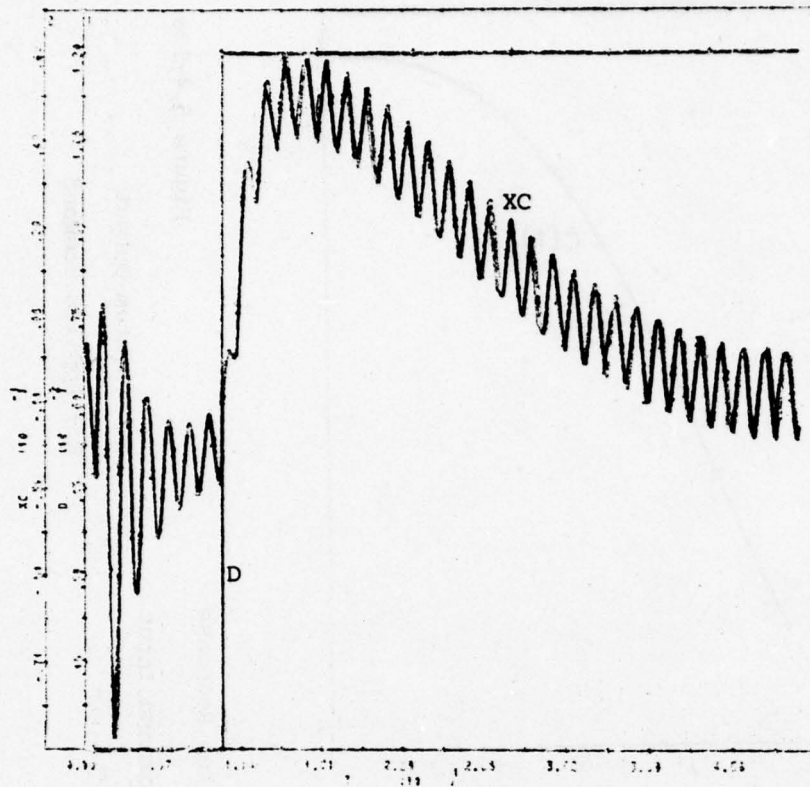


Figure 5.4-14a

XC - System Output
D - Applied Disturbance

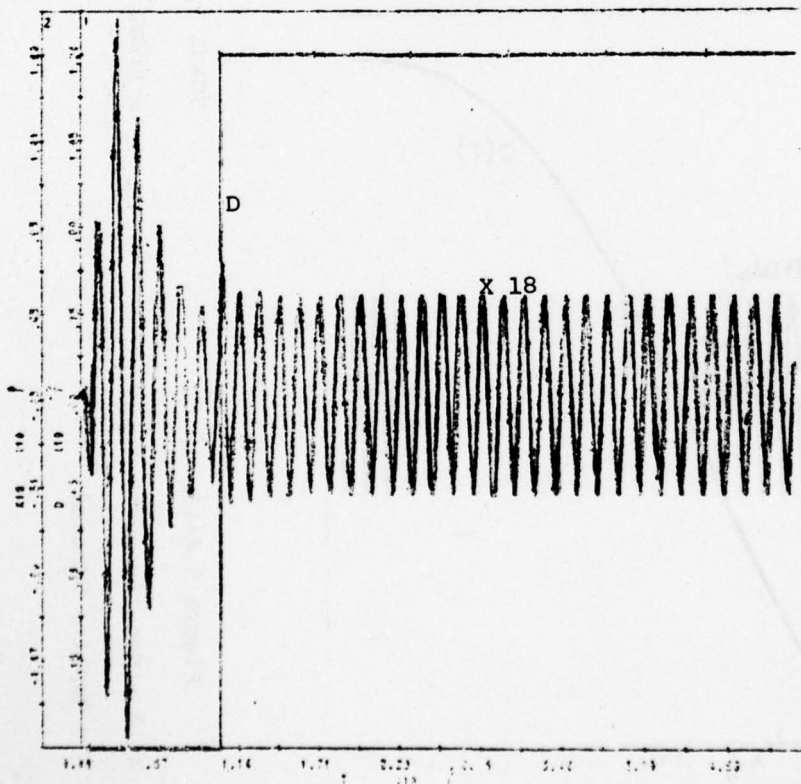


Figure 5.4-14b

X 18 - Non-linearity Input
D - Applied Disturbance

SOANL System Response
Extreme Disturbance Input
K = 100

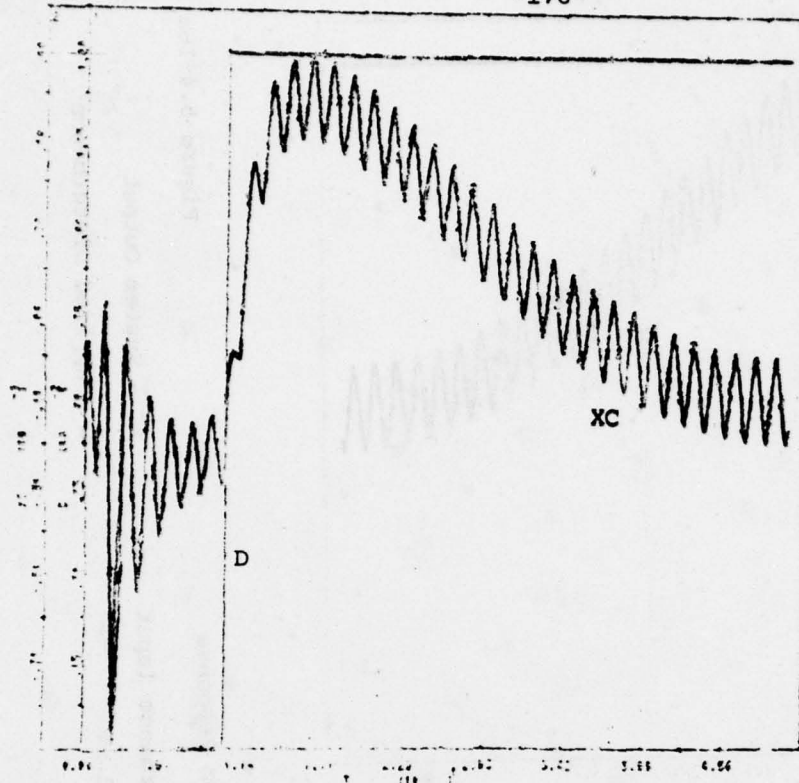
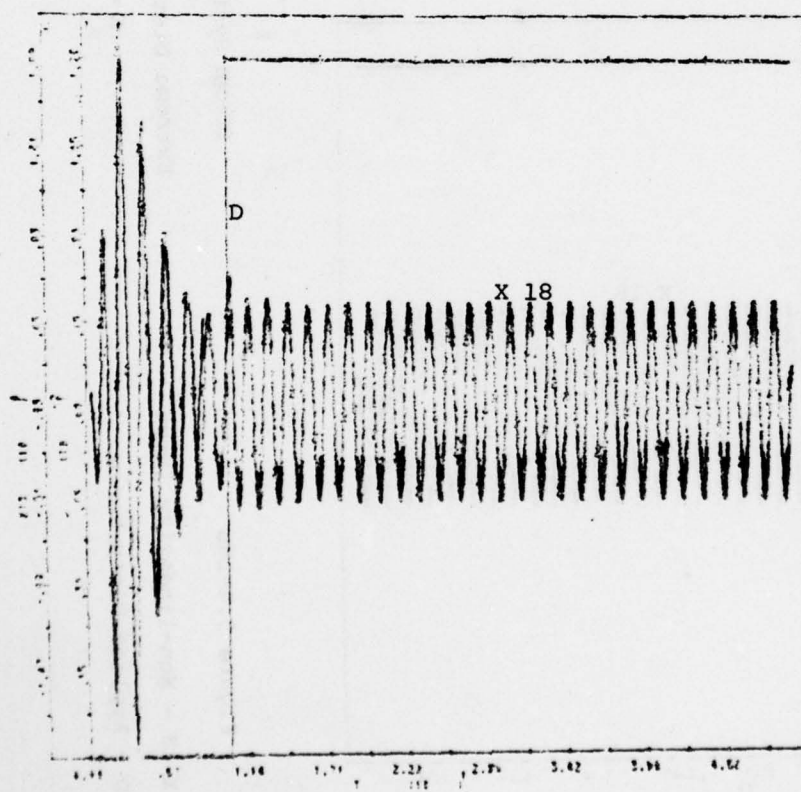


Figure 5.4-15a

XC - System Output
D - Applied Disturbance



SOANL System Response
Extreme Disturbance Input
K = 10

X 18 - Non-linearity Input
D - Applied Disturbance

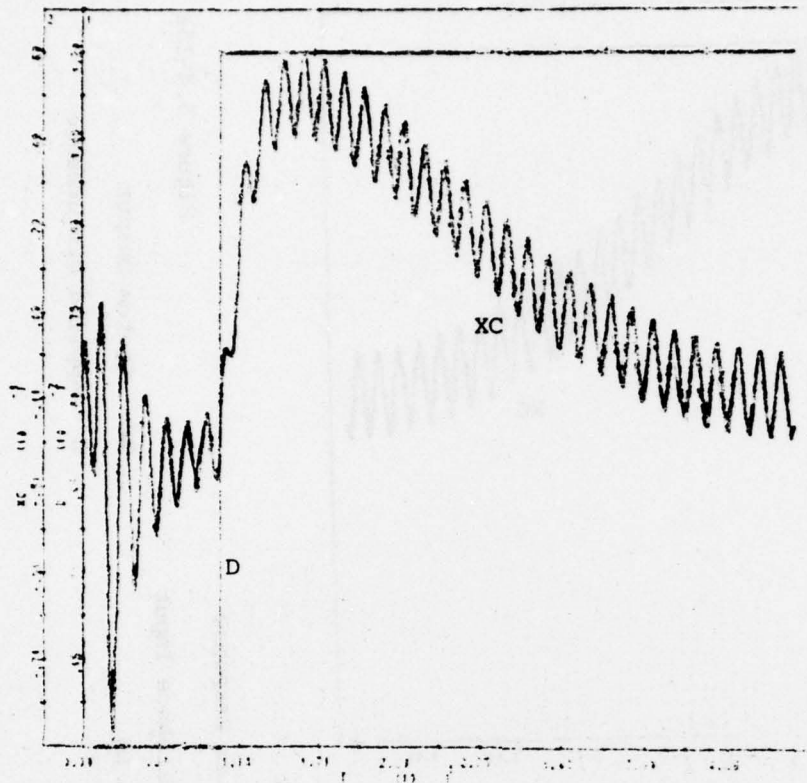


Figure 5.4-16a

XC - System Output
D - Applied Disturbance

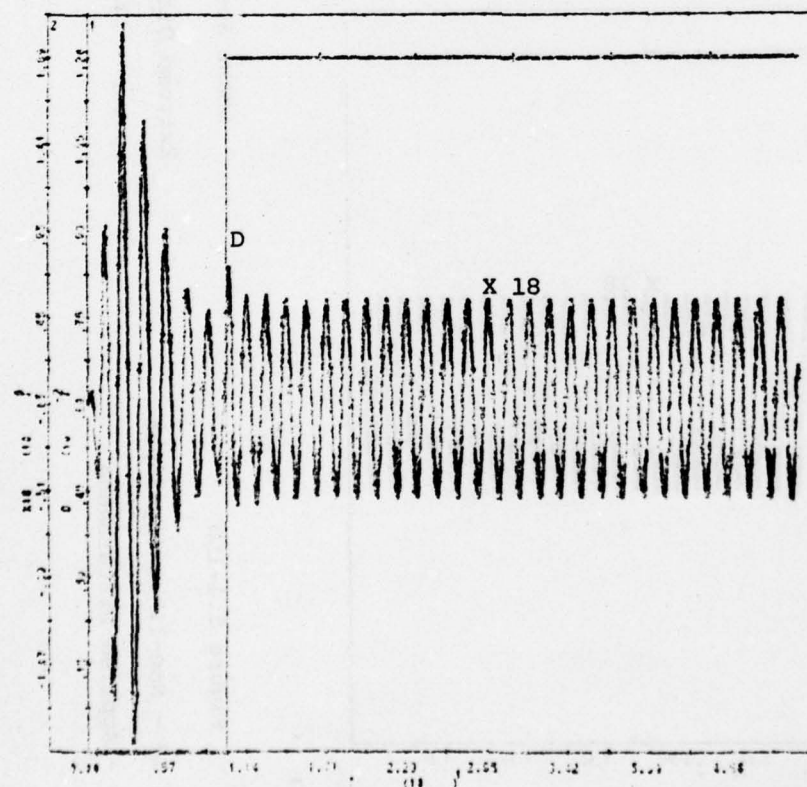


Figure 5.4-16b

X 18 - Non-linearity Input
D - Applied Disturbance

SOANL System Response

Extreme Disturbance Input
K = 1

CHAPTER SIX

E.E.A.L.

(EEAS with a secondary loop

controlling the non-linear adaptive saturating level)

6.1 General

In Chapter 3 it was shown that the EEAS has some advantages and greater flexibility than the SOAS. The advantages due to the fact that $L_o(j\omega_o)$ need not be equal to -1 are in the bandwidth of the loop transmission and on the maximum disturbance signals levels, which do not violate the quasi-linearity constraints. But the factor $\frac{K_{\max}}{K_{\min}}$ still appears in the expression determining these properties (Equations 3.5-30 and 33), and still there exist severe limitations on the possible (less severe than for the SOAS) disturbances, if quasi-linearity conditions are not to be violated (Equation 3.5-33).

In Chapter 4 it was shown that there is no "advantage" in the SOAL flexibility if compared with the SOAS, since $L_o(j\omega_o) = -1$, but there is an advantage in the system loop transmission and/or in the disturbances limitations because $\frac{K_{\max}}{K_{\min}}$ disappears from the expression defining these parameters (Equations 4.5-23,24). The idea of the EEAL is to use the advantages of the SOAL and to widen the EEAS flexibility. Several possible structures are reviewed in Section 6.2, and the specific one shown in Figure 6.2-2 is chosen. This structure seems to be the one which can meet most of the above EEAL requirements.

6.2 Possible EEAL Structures

Several possible structures for the EEAL will be considered. In each structure some costs and benefits will be pointed out.

EEAL - Structure Number 1

Structure number 1 is represented in Figure 6.2-1, and can be seen as an EEAS which received the same "increment" as the one introduced in the SOAS-SOAL transformation.

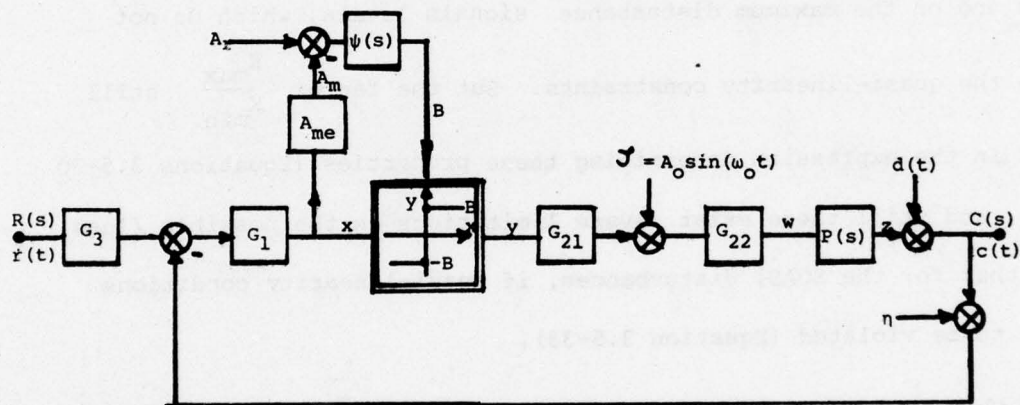


Figure 6.2-1 - Structure Number 1 - EEAS

In this structure, special care should be taken to allow a possible solution (with positive B), for all values of the gain of the plant. Assuming such a solution exists, and by a similar development to the one used in Section 3.5, the following equations are obtained:

$$\left| \frac{X_r}{A}(j\omega_o) \right| \geq \frac{1}{m} \left| \frac{R_e T_r}{L_f}(j\omega_o) \right| \quad (6.2-1)$$

$$\left| \frac{X_d}{A}(j\omega_o) \right| \geq \frac{1}{m} |D_e T_d(j\omega_o)| \quad (6.2-2)$$

$$\left| \frac{x_f}{A}(j\omega_o) \right| \geq \frac{1}{m} \left| \frac{z_e}{L_f}(j\omega_o) \right| \quad (6.2-3)$$

which are similar expressions to Equations 3.5-30,33,36, where the factor $\frac{K_2}{K_1}$ has disappeared. The relative advantages of the SOAL over the SOAS have been achieved in this structure, but no more flexibility than the EEAS is obtained.

EEAL - Structure Number 2

Structure number 2 is represented in Figure 6.2-2, and is the one chosen to be analyzed with more detail.

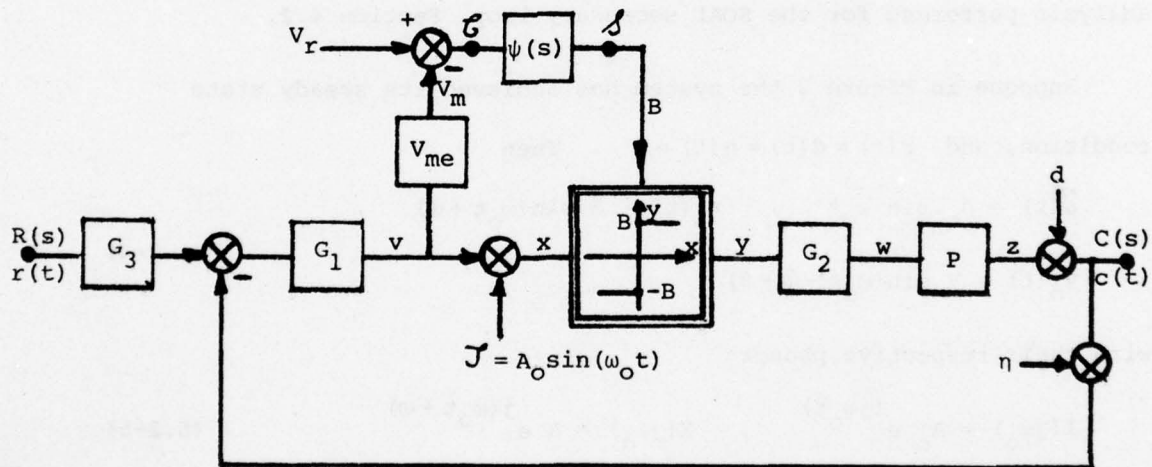


Figure 6.2-2 - Structure Number 2 - EEAL

The main difference between structures number 2 and 1 (or the EEAS), is the place where the external signal is injected. In Figure 2 the output of $G_1(s)$ ($v(t)$) is not the input $x(t)$ to the non-linearity.

Quasi-linearity constraints must be satisfied by $x(t)$ and not necessarily by $v(t)$.

In this structure the amplitude V of the oscillating signal $v_o(t)$ is kept (or at least tried to be kept) constant. This is done by the "secondary" loop of this structure, Figure 6.2-2. V_{me} measures the amplitude of oscillation of $v_o(t)$. The result of this measurement V_m is compared with a reference value V_r . The difference (error) passes through a compensation network $\psi(s)$, whose output controls B , which affects the amplitude V of $v_o(t)$. This "secondary" loop is not an "instantaneous" loop and its dynamics and stability problems must be analyzed. This is done in Section 6.5 in a similar way to the analysis performed for the SOAL secondary loop, Section 4.2.

Suppose in Figure 2 the system has achieved its steady state condition, and $r(t) = d(t) = \eta(t) = 0$. Then

$$\begin{aligned} \mathcal{J}(t) &= A_o \sin \omega_o t, \quad x_o(t) = A \sin(\omega_o t + \varphi), \\ v_o(t) &= V \sin(\omega_o t + \varphi + \theta) \end{aligned} \quad (6.2-4)$$

with their respective phasors

$$I(j\omega_o) = A_o e^{j\omega_o t}, \quad X(j\omega_o) = A e^{j(\omega_o t + \varphi)} \quad (6.2-5)$$

Also:

$$X(j\omega_o) = \frac{I(j\omega_o)}{1 + L_o(j\omega_o)} \quad (6.2-6)$$

$$L_o(j\omega_o) = \frac{M_o}{A} G_1 G_2 K P_h(j\omega_o) \quad (6.2-7)$$

Combining Equations 6.2-5, 6, 7,

$$A e^{j\varphi} + M_o G_1 G_2 K P_h(j\omega_o) e^{j\varphi} = A_o \quad (6.2-8)$$

$$|A + K M_o G_1 G_2 P_h(j\omega_o)| = A_o \quad (6.2-9)$$

Since A_o is constant if KM_o was kept constant, A remains constant (as K varies). As explained before, V is kept constant (in the steady state) by the secondary loop.

$$|V(j\omega_o)| = M_o K |G_1 G_2 P_h(j\omega_o)| = \text{constant} \quad (6.2-10a)$$

So

$$\frac{4}{\pi} BK = 2M_f K = M_o K = \frac{|V(j\omega_o)|}{|G_1 G_2 P_h(j\omega_o)|} = \text{constant} \quad (6.2-10b)$$

The factors BK , $M_f K$, $M_o K$ have constant values. The loop transmission for the forced and disturbance signals has the property of zero sensitivity to pure gain changes, since

$$L_f(j\omega) = \frac{M_o K}{2A} G_1 G_2 P_h(j\omega) = \frac{M_f K}{A} G_1 G_2 P_h(j\omega) \quad (6.2-11)$$

is independent of K .

Structure number 2 seems to be very convenient because one of the links existing in all systems studied (SOAS, EEAS, SOAL, SOANL), given by

$$A = C_o |G_1(j\omega_o)| \quad (6.2-12)$$

is broken. A and C_o are the oscillation components at the non-linearity input and at the system output. In the EEAL the input A to the non-linearity is the sum of \mathcal{J} and of $V_o = C_o |G_1(j\omega_o)|$.

The "real" information about the plant gain is in V ; that is the reason why v was the chosen variable from which the amplitude of oscillation is measured (x had the advantage that the sinusoid was easily the biggest part of the signal and peak to peak measurement wiped out x_f).

These facts are also part of the EEAL problems and limitations. If the injected signal $\mathcal{J} = A_o \sin(\omega_o t)$ has a much larger amplitude than $v = V \sin(\omega_o t + \phi + \theta)$, $|A_o| \gg |V|$, which is a common case for

the EEAL (see numerical example, Section 6.7), then

$v(t) = v_r(t) + v_d(t) + v_o(t)$, does not satisfy quasi-linearity constraints and $|v_r(t)|$ or $|v_d(t)|$ could be larger than $|v_o(t)|_{\max} = V$, making the oscillation amplitude measurement a difficult process, probably with added dynamic lags. This structure, due to the non-existing link expressed by Equation 6.2-12, gives the expected flexibility for the EEAL.

EEAL - Structure Number 3

Structure number 3 is similar to structure number 2, in almost all aspects. The only difference is in the variable chosen to measure the oscillation component. Figure 6.2-3 represents structure number 3.

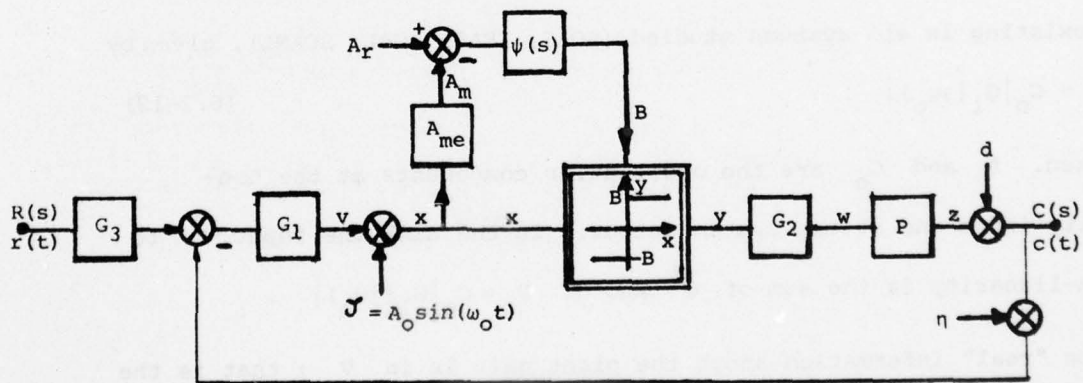


Figure 6.2-3 - Structure Number 3 - EEAS

At x quasi-linearity conditions are satisfied, so the same peak to peak measurement system used for the SOAL can be also used. The problem in this structure is the high sensitivity of the plant identification due to errors in the oscillation measurement. Suppose

AD-A046 011

COLORADO UNIV BOULDER SYSTEMS ENGINEERING LAB
SYNTHESIS OF OSCILLATING ADAPTIVE SYSTEMS.(U)
JUL 77 A SHAPIRO, I HOROWITZ

F/G 9/4

UNCLASSIFIED

3 OF 4

AD
A046011

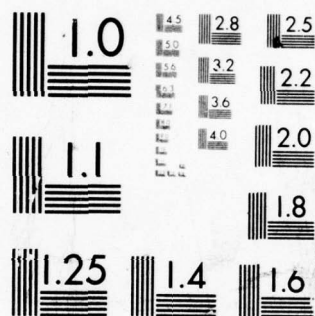


AFOSR-76-2946

AFOSR-TR-77-1223

NL





MICROCOPY RESOLUTION TEST CHART
NATIONAL BUREAU OF STANDARDS-1963-A

$|A_o| \approx 60 \text{ V}$, as in the EEAL numerical example. If there exists an error of 1.6 % in the measurement of A from $x(t)$, the secondary loop will force V to have an error of at least 100 % , by an improper B adjustment. The plant gain identification is incorrect. In case $x_o(t)$ and $v_o(t)$ are not in phase (0° or 180°) the sensitivity can be even larger, as depicted in Figure 6.2-4 (V is the amplitude of $v_o(t)$, and A the amplitude of $x_o(t)$). For this reason structure number 3 is not chosen.

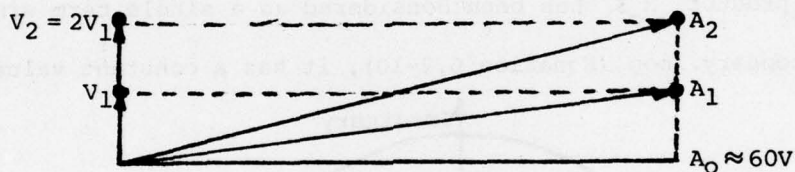


Figure 6.2-3 - Small Influence of V in Plant Identification
($V_2 \approx 2V_1$, $A_2 \approx A_1$)

6.3 Mathematical Relations

Suppose in Figure 6.2-2, the chosen structure, $r(t) = d(t) = \eta(t) = 0$, the system is in its steady state, the linear functions and the injected signal defined and known.

First the oscillating input to the non-linearity is calculated.

Based on Equation 6.2-6,

$$X(j\omega_o) = \frac{I(j\omega_o)}{1 + L_o(j\omega_o)} \quad (6.3-1a)$$

or

$$\frac{A}{A_o} = \left| \frac{1}{1 + L_o(j\omega_o)} \right| \quad (6.3-1b)$$

where

$$L_o(j\omega_o) = \frac{M_o}{A} \cdot G_1 G_2 K P_h(j\omega_o) \quad (6.3-2)$$

We repeat here Equation 6.2-8

$$A e^{j\varphi} + M_o G_1 G_2 K P_h(j\omega_o) e^{j\varphi} = A_o \quad (6.3-3)$$

$$\frac{A}{A_o} + \frac{M_o K}{A_o} \cdot |G_1 G_2 P_h(j\omega_o)| = e^{-j\varphi} \quad (6.3-4)$$

A graphical solution for Equation 6.3-4 is provided in Figure 6.3-1, giving the values of A and φ once A_o , $M_o K$ and $G_1 G_2 P_h(j\omega_o)$ are defined. The product $M_o K$ has been considered as a single term since, due to the secondary loop (Equation 6.2-10), it has a constant value.

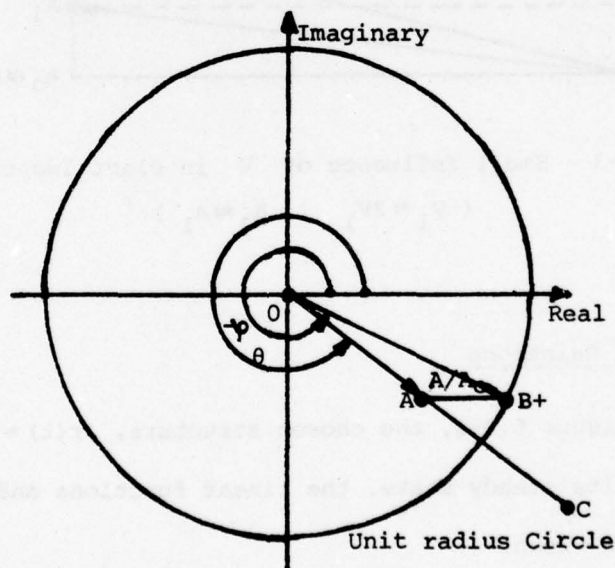


Figure 6.3-1 - Graphical Solution - Equation 6.3-4

In Figure 6.3-1, the vector \vec{OA} represents

$$\vec{OA} = \frac{M_o K}{A_o} |G_1 G_2 P_h(j\omega_o)| \quad (6.3-5)$$

where

$$\angle G_1 G_2 P_h(j\omega_o) = \theta \quad (6.3-6)$$

$\frac{A}{A_0}$, which gives the solution for A , is a real positive number and is obtained by tracing a parallel line to the real axis, with origin in A until B , intersection of this line with the unit radius circle.

$$|\vec{AB}| = \frac{A}{A_0} \quad (6.3-7)$$

\vec{OB} represents $e^{-j\varphi}$, which gives the solution for the phase angle φ .

$$\vec{OB} = e^{-j\varphi} \quad (6.3-8)$$

As in Section 3.3 for the EEAS, sometimes there are "two" solutions, and sometimes there is "no" solution for Equation 6.3-4. The discussion of the possible solutions as well as its physical interpretation are similar to the results obtained in Section 3.3, and are not going to be reviewed here. As an example if $\frac{M_0}{A_0} |G_1 G_2 K P_h(j\omega_0)|$, and $\frac{3\pi}{2} \leq \theta \leq 2\pi$, as represented by the vector \vec{OC} in Figure 6.3-1, there is no possible real positive solution for A (and φ), so the system self-oscillates at ω_π .

6.4 EEAL Sensitivity to Change in Plant Dynamics

It was shown that the EEAL (the chosen structure) has zero sensitivity to pure gain changes of the plant (Equation 6.2-11). It was also shown that for the SOAS, SOAL and SOANL, the oscillation frequency changes if the plant changes its dynamic characteristics. For the EEAS (Section 3.4-3), since the oscillation frequency is defined by the injected signal, there is no change in the oscillation frequency, but there is a change in the $L_0(j\omega_0)$ position in the Nichol's chart, as per Section 3.4-3. In this research the only case studied is the one where the plant changes its overall gain, but it is interesting to see

what happens to $L_o(j\omega_o)$ position when there are changes in the poles and zeros of the plant. In Figure 6.2-2,

$$\left| \frac{V(j\omega_o)}{I(j\omega_o)} \right| = \left| \frac{L_o(j\omega_o)}{1 + L_o(j\omega_o)} \right| \quad (6.4-1)$$

If there is a change in the dynamics of the plant and the system is oscillating only at ω_o , the secondary loop, after the transient period, assures that $|V(j\omega_o)|$ returns to its pervious constant amplitude, so in Equation 6.4-1, $\left| \frac{L_o(j\omega_o)}{1 + L_o(j\omega_o)} \right| = \text{constant}$, is defined in the Nichol's chart as one of the constant closed loop contours. Thus as the plant changes its phase angle $\angle P(j\omega_o)$, $L_o(j\omega_o)$ follows this change in open loop, along the constant closed loop contour defined previously for the EEAS, in Section 3.4-3.

The idea suggested in that section, for "zero sensitivity" to changes in plant dynamics, is valid for the EEAL, by using a dynamic non-linearity instead of a static one.

6.5 Dynamics and Stability of the Secondary Loop - EEAL

In Figure 6.2-2 the function of the secondary loop containing $\psi(s)$ is to adjust the saturation level B , so that the amplitude of v_o is kept constant (in the steady state). The dynamics of this secondary loop are studied here, using the same technique as for the SOAL, Section 4.2, based on the Fundamental Feedback Equation [2].

$$\frac{O}{J}(s) \triangleq t_{oi}(s) + t_{ci}(s) \cdot t_{os}(s) \cdot \frac{\psi(s)}{1 - \psi t_{cs}(s)} \quad (6.5-1)$$

In Figure 6.2-2 consider the independent input as a change in V , and the output as a change in B . \mathcal{C} and \mathcal{A} are marked in this

figure. The transmissions are:

$$t_{oi}(s) = \left. \frac{\Delta B}{\Delta V} \right|_{\psi(s)=0} = 0 \quad (6.5-2)$$

There is no "leakage" transmission in the loop.

$$t_{ci}(s) = \left. \frac{G}{J} \right|_{\psi(s)=0} = \left. \frac{G}{\Delta V} \right|_{\psi(s)=0} = V_{me}(s) \quad (6.5-3)$$

$V_{me}(s)$ is the block representing the measurement characteristics of the amplitude of oscillation $v_o(t)$ from $v(t)$. The technique used for the EEAL is more complicated than the "peak to peak" technique used in the SOAL, since quasi-linearity conditions are not satisfied at $v(t)$. The technique used assumes that $v_f(t)$ ($v(t) = v_o(t) + v_f(t)$), is linear in t for each cycle; (in Figure 6.5-1, $x_f(t)$ is considered as a straight line in the interval of time $t_1 - t_3$).

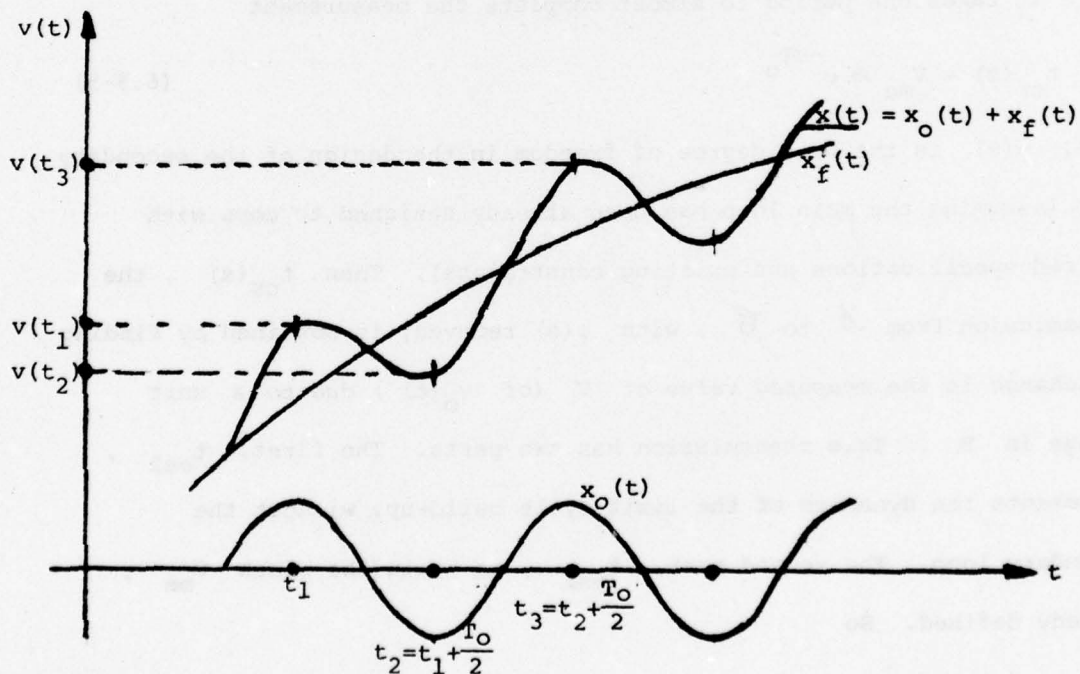


Figure 6.5-1 - Oscillation-Amplitude Measurement - Linear Approximation

This $x_f(t)$ "linear approximation" for each cycle seems to satisfy most of the cases (see numerical example simulations). A "parabolic approximation" can be also used with added time delay in the measurement characteristics and with better static accuracy.

We can write (Figure 6.5-1):

$$v(t_1) = a + bt_1 + V$$

$$v(t_2) = a + bt_2 - V$$

$$v(t_3) = a + bt_3 + V$$

But $t_2 - t_1 = t_3 - t_2 = T_0/2$, where T_0 is the oscillation period. So

$$v(t_1) - 2v(t_2) + v(t_3) = 4V$$

or

$$V = \frac{1}{4} [v(t_1) - 2v(t_2) + v(t_3)] \quad (6.5-4)$$

since it takes one period to almost complete the measurement

$$t_{ci}(s) = V_{me} \approx e^{-sT_0} \quad (6.5-5)$$

Next, $\psi(s)$ is the only degree of freedom in the design of the secondary loop (assuming the main loop has been already designed to cope with desired specifications and existing constraints). Then $t_{cs}(s)$, the transmission from A to C , with $\psi(s)$ removed, is obtained by finding the change in the measured value of V (of $v_o(t)$) due to a unit change in B . This transmission has two parts. The first, t_{cs1} , represents the dynamics of the limit cycle build-up, without the secondary loop. The second part, t_{cs2} , is again the block V_{me} , already defined. So

$$t_{cs}(s) = t_{cs1} \times t_{cs2}(s) \quad (6.5-6)$$

and

$$t_{cs2}(s) \approx e^{-T_0 s} \quad (6.5-7)$$

In this case $t_{csl}(s)$ is easier to calculate than in the SOAL, since the input to the non-linearity is "almost" defined by the injected signal. This is due to the tendency in the EEAL optimization design to have $|\mathcal{J}_O(t)|_{\max} \gg |V_O(t)|_{\max}$, as explained in the synthesis procedure (Section 6.6). In this case

$$V_O(s) = I_O(s) \cdot \frac{4B}{A_O \pi} \cdot G_1 G_2 K P_h(s)$$

But $|I_O(s)| \approx A_O$ (as mentioned above), so

$$t_{csl}(s) \approx \frac{4}{\pi} G_1 G_2 K P_h(s) \quad (6.5-8)$$

The last transmission $t_{os}(s)$, from δ to the output $\Delta B \triangleq 1$.

Substituting the above in Equation 6.5-1,

$$\frac{\Delta B}{\Delta V}(s) = \frac{-\psi(s) e^{-T_O s}}{1 + \frac{4}{\pi} G_1 G_2 P_h \psi(s) K e^{-T_O s}} \quad (6.5-9)$$

In Equation 6.5-9 the maximum possible loop transmission is about $\frac{\omega_O}{5}$, because of the inherent delay of $\frac{2\pi}{\omega_O} = T_O$, in the measurement process.

Again it is interesting to see how "mother nature" reintroduces the plant gain uncertainty into the secondary loop, by the presence of K in the denominator of Equation 6.5-9. Hence, as in the SOAL, the secondary loop must be designed to be stable over the entire region of variation of K . At large K the dynamics of the adjustment loop will be relatively fast, and at $K = K_{\min}$, the dynamics of this adjustment loop will be relatively slow. A comment regarding the "stability" of the main loop. It has been noticed that for the EEAS (and EEAL) it is necessary to have a minimum gain margin to avoid self-oscillation. The gain margin is defined by $L_f(j\omega_\pi) = \frac{2B}{\pi A} |G_1 G_2 K P_h(j\omega_\pi)|$. But A is the amplitude of $x_O(t)$, the sum of the constant injected signal $\mathcal{J}(t)$

and $v_o(t)$. If there occurs an abrupt change in the gain of the plant (K increases its value), $v_o(t)$ changes its amplitude but $x_o(t)$ (and A) does not follow the same proportional change. While the secondary loop has not achieved the steady state condition, the loop $L_f(s)$ increases (or decreases) its gain, not being zero sensitive in the transient period. It is therefore recommended that an extra gain margin to the existing specification for the EEAS - 2.56 dB (Equations 3.2-8, 3.5-21), should be considered.

6.6 Synthesis Procedure for the EEAL

A synthesis procedure is developed for the EEAL. Assumptions are the same as in Section 3.5 for the EEAS.

6.6-1 Specifications and Data

It is assumed that the set of specifications and data listed below are known or can be estimated.

- Desired Command Input Response
- Disturbance Attenuation
- The Plant
- Extreme Command Input
- Extreme Disturbance Input

The meanings and comments given in Sections 2.5-1 and 3.5-1 are valid here.

If there are "abrupt" changes of gain (expected), this should also be specified. The reason for this new specification, explained in Section 6.5, is related to the minimum gain margin condition, which guarantees no self-oscillation in the loop.

While in all the structures studied until now, the loop transmission adjusts itself automatically, the EEAL adaptive properties are only effective when the secondary loop achieved its steady state. Note the difference between the SOAL and the EEAL. The SOAL has inherent adaptive properties, even when the secondary loop has not achieved its steady state. In the transient situation quasi-linearity constraints can be violated, if oscillations are smaller than the steady state oscillation and an extreme input or disturbance is applied, or plant output oscillation level might exceed the specified level.

In the EEAL, since the input in the non-linearity is predominantly defined by the injected signal, if there is a change in the plant gain and the secondary loop is not able to "follow" this change, adaptive properties are not kept during this dynamic process, and the minimum gain margin of the main loop should be kept, to avoid self-oscillation, taking into account the possible "transient" changes of $L_f(j\omega)$. So, "abrupt" $\frac{\Delta K}{K}$ changes should be specified.

Note - There is a possibility to inject a signal $J(t)$ with a variable amplitude based on V_m (see Figure 6.2-2), which would partly avoid this problem, but no studies or simulations were performed.

Dynamics of the Adjustment Loop

As in the SOAL, Section 4.5, it is desirable to obtain the largest possible crossover frequency for the secondary loop.

6.6-2 The Constraints

The EEAL has to satisfy the same constraints defined for the EEAS, Section 3.5-2, with the difference that self-oscillation "quenching" is

more complex.

Quasi-linearity Constraints

$$\max_t |x_i(t)| \leq \frac{A}{\alpha} \quad ; \quad i=r,d \quad (6.6-1a)$$

$$\omega_{bi} \leq \frac{\omega_o}{\beta} \quad ; \quad i=r,d \quad (6.6-1b)$$

$$\alpha = 3 \quad (6.6-1c)$$

$$\beta = 3 \quad (6.6-1d)$$

These conditions, if satisfied, permit us to write:

$$v = v_o + v_r + v_d \quad (6.6-2a)$$

$$x = x_o + x_r + x_d \quad (6.6-2b)$$

$$y = y_o + y_r + y_d \quad (6.6-2c)$$

$$y_i = N_i x_i \quad (6.6-2d)$$

$$N_r = N_d = \frac{M_f}{A} \quad (= \frac{2B}{A} \text{ for ideal relay}) \quad (6.6-2e)$$

$$N_o = \frac{M_o}{A} = \frac{2M_f}{A} \quad (= \frac{4B}{A} \text{ for ideal relay}) \quad (6.6-2f)$$

B is the output of $\psi(s)$, defining the saturating level of the ideal relay (Figure 6.2-2).

Self-oscillation "Quenching"

It has been shown (Section 3.5-2) and explained the problems involved if a self-oscillation exists in the loop. For the EEAL the problem is more serious since the system is not "dynamically adaptive", so one should take the loop transmission gain margin constraint, to cope with transient changes of L_f or errors in the measurement processes during the transient period, due to the command input or to disturbances. A gain margin of 12 dB seems to be reasonable to cope with "errors" in the measurement processes. If there are expected abrupt gain changes

of more than 6 dB, an equivalent increase in the gain margin specifications should be considered.

$$L_f(j\omega_\pi) \leq \rho' \quad (6.6-3)$$

$$\rho' = f\left(\frac{\Delta K}{K}\right), \quad \omega_\pi \ni \angle L_f(j\omega_\pi) = -180^\circ$$

Maximum Plant Output Oscillation

As in the EEAS, Section 3.5-2,

$$[C_o(t)]_{\max} \leq m \quad (6.6-4)$$

Based on Figure 6.6-1,

$$|C_o(j\omega_o)| = |M_o G_2 K P_h(j\omega_o)| = |2M_f G_2 K P_h(j\omega_o)| \leq m \quad (6.6-5)$$

6.6-3 The Synthesis Procedure - EEAL - Smooth Solution

The basic EEAL structure is repeated in Figure 6.6-1.

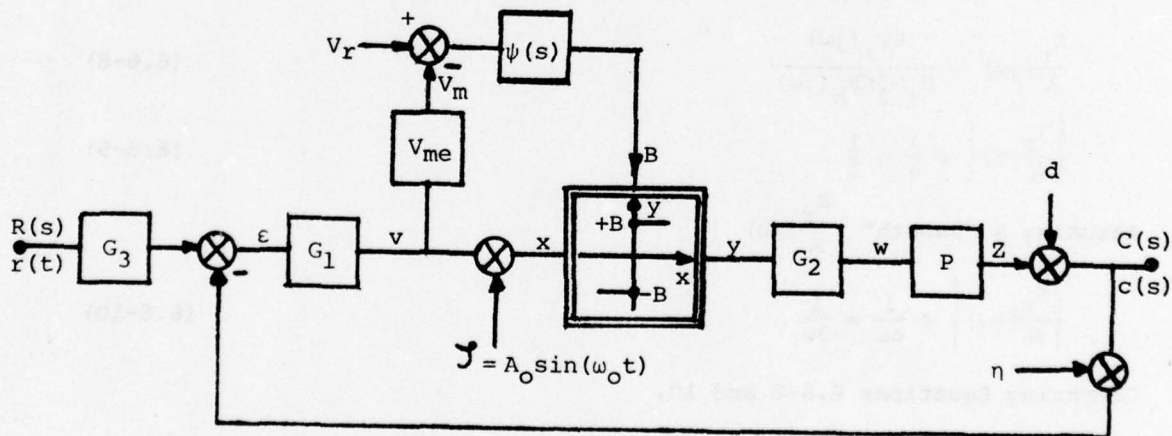


Figure 6.6-1 - Basic EEAL Structure

As in the SOAL, there exist two types of loops. One, the main loop, valid for the forced and disturbance signals, is directly related to $L_o(j\omega_o)$ and valid only for these. The second, called the secondary loop, is responsible for the adjustment of the relay saturation level B, assuring to $v_o(t)$ a constant amplitude V.

The equations below follow the same development reasoning and have the same constraints as in the EEAS, Equations 3.5-5 - 9.

$$L_f(j\omega) = N_f G_1 G_2 K P_h(j\omega) \quad (6.6-5a)$$

$$N_f = \frac{2B}{\pi A} \quad (\text{for the ideal relay}) \quad (6.6-5b)$$

$$L_o(j\omega_o) = N_o G_1 G_2 K P_h(j\omega) \quad (6.6-5c)$$

$$N_o = \frac{4B}{\pi A} \quad (\text{for the ideal relay}) \quad (6.6-5d)$$

$$T_r(j\omega) = \frac{C_r}{R}(j\omega) = G_3(j\omega) \cdot \frac{L_f(j\omega)}{1 + L_f(j\omega)} \quad (6.6-6)$$

$$X_r(j\omega) = \frac{C_r(j\omega)}{N_f G_2 K P_h(j\omega)} \quad (6.6-7)$$

$$\frac{X_r}{A}(j\omega) = \frac{RT_r(j\omega)}{M_f G_2 K P_h(j\omega)} \quad (6.6-8)$$

$$\left| \frac{x_r}{A}(t) \right| \leq \frac{1}{\alpha} = \frac{1}{3} \quad (6.6-9)$$

Assuming a "smooth" $\frac{X_r}{A}(j\omega)$

$$\left| \frac{X_r}{A}(j\omega) \right| \leq \frac{1}{\alpha\omega} = \frac{1}{3\omega} \quad (6.6-10)$$

Comparing Equations 6.6-8 and 10,

$$\left| \frac{X_r}{A}(j\omega) \right| = \frac{RT_r(j\omega)}{M_f G_2 K P_h(j\omega)} \leq \frac{1}{\alpha\omega} \quad (6.6-11)$$

There is now a difference between the EEAS and the EEAL, since there is no "most difficult" situation for Equation 6.6-11 to be satisfied,

as regards the plant gain and amplitude of oscillation, since $M_f K$ and A are constant values in the steady state (Equations 6.2-9,10). The only variable affecting $\frac{x_r}{A}(j\omega)$ in Equation 6.2-11 is the input $R(j\omega)$. It is most difficult to satisfy this equation when the command input has its extreme value $r_e(t)$, with Laplace transform $(s=j\omega)$, $R_e(j\omega)$. Substituting in Equation 6.2-11,

$$|M_f G_2 K P_h(j\omega)| \geq \alpha \cdot \omega \cdot |R_e T_r(j\omega)| \quad (6.6-12)$$

A similar expression to Equation 6.6-12 is obtained concerning the extreme disturbance input.

$$Z_d(j\omega) = -D(j\omega) \cdot \frac{L_f(j\omega)}{1 + L_f(j\omega)} \quad (6.6-13)$$

$$X_d(j\omega) = \frac{Z_d(j\omega)}{N_f G_2 K P_h(j\omega)} \quad (6.6-14)$$

But

$$Z_d(j\omega) = -D(j\omega) \cdot \frac{L_f(j\omega)}{1 + L_f(j\omega)}, \quad N_f = \frac{M_f}{A}$$

Substituting these two equations in 6.6-14,

$$\frac{X_d}{A}(j\omega) = \frac{-D(j\omega)}{M_f G_2 K P_h(j\omega)} \cdot \frac{L_f(j\omega)}{1 + L_f(j\omega)} \quad (6.6-15)$$

Considering a "smooth" $\frac{X_d}{A}(j\omega)$

$$\frac{X_d}{A}(j\omega) \leq \frac{1}{\alpha\omega} = \frac{1}{3\omega} \quad (6.6-16)$$

Combining Equations 6.6-15 and 16,

$$\left| \frac{X_d}{A}(j\omega) \right| = \left| \frac{D(j\omega)}{M_f G_2 K P_h(j\omega)} \right| \cdot \left| \frac{L_f(j\omega)}{1 + L_f(j\omega)} \right| \leq \left| \frac{1}{\alpha\omega} \right| \quad (6.6-17)$$

In this last inequality the "most difficult" condition to be satisfied is when the extreme disturbance $d_e(t)$ is applied. So:

$$|M_f G_2 K P_h(j\omega)| \geq \alpha \cdot \omega \cdot |D_e(j\omega)| \left| \frac{L_f(j\omega)}{1 + L_f(j\omega)} \right| \quad (6.6-18)$$

Conditions 6.6-12 and 18 being satisfied, assure amplitude quasi-linearity constraints are not violated if $r(t) \leq r_e(t)$, $d \leq d_e(t)$.

There is less explicitness in Equation 6.6-18 if compared with 12, since $T_r(j\omega)$ is "almost" determined and $L_f(j\omega)$ is unknown, being the main purpose of the synthesis procedure.

Next, using Equation 6.6-5,

$$|M_f G_2 K P_h(j\omega_o)| \leq \frac{m}{2} \quad (6.6-19)$$

Since $M_f K$ remains constant (Equation 6.2-10), there is no "most difficult" case to satisfy. Recalling Equations 6.6-11 and 17, and replacing $\omega = \omega_o$, by extrapolation (Appendix III)

$$\left| \frac{X_r}{A}(j\omega_o) \right| \approx \left| \frac{R_e T_r(j\omega_o)}{M_f G_2 K P_h(j\omega_o)} \right| \quad (6.6-20)$$

$$\left| \frac{X_d}{A}(j\omega_o) \right| \approx \left| \frac{D_e(j\omega_o)}{M_f G_2 K P_h(j\omega_o)} \right| \times \left| \frac{L_f(j\omega_o)}{1 + L_f(j\omega_o)} \right| \quad (6.6-21)$$

Substituting Equation 6.6-19 in 20 and 21,

$$\left| \frac{X_r}{A}(j\omega_o) \right| \geq \frac{2}{m} |T_r R_e(j\omega_o)| \quad (6.6-22)$$

$$\left| \frac{X_d}{A}(j\omega_o) \right| \geq \frac{2}{m} |D_e(j\omega_o)| \cdot \left| \frac{L_f(j\omega_o)}{1 + L_f(j\omega_o)} \right| \quad (6.6-23)$$

Equations 6.6-22 and 23 give non-linear functions which define the oscillating frequency for a "smooth" $X_r(j\omega)$ and $X_d(j\omega)$. These two results give a big advantage compared with those obtained for the EEAS or SOAL.

Comparing the first EEAL result, Equation 6.6-22, with the equivalent EEAS one, Equation 3.5-30, the factor $\frac{K_2}{K_1}$ has disappeared

in Equation 6.6-22, which is already an advantage for the EEAL, and $|L_f(j\omega_o)|$ has also disappeared from the denominator, which could also be an advantage for the EEAL if $|L_f(j\omega_o)| \ll 1$. There is no difference when comparing Equation 6.6-22 with the equivalent SOAL result, Equation 4.5-23.

Next, comparing the second EEAL result, Equation 6.6-23, with the EEAS one, Equation 3.5-31, the factor $\frac{K_2}{K_1}$ has disappeared and $D_e(j\omega_o)$ is multiplied by $\left| \frac{L_f(j\omega_o)}{1 + L_f(j\omega_o)} \right|$ in Equation 6.6-23, instead of being multiplied by $\left| \frac{1}{1 + L_f(j\omega_o)} \right|$ in Equation 3.5-31, and this gives the flexibility the EEAL was looking for. In the EEAS the tendency was to have $|L_f(j\omega_o)| \gg 1$, to cope with the disturbance input. Since $\omega_o > \omega_\pi$, and $|L_f(j\omega_\pi)| < 1$, the EEAS loop transmission asked for a relative "peaking" at ω_o , with all the problems involved in it, as demonstrated in the EEAS numerical example, Section 3.6.

In the EEAL, $D_e(j\omega_o)$ being multiplied by $\left| \frac{L_f(j\omega_o)}{1 + L_f(j\omega_o)} \right|$ leads to $|L_f(j\omega_o)| \ll 1$, so $\omega_o > \omega_\pi$ and $|L_f(j\omega_o)| < |L_f(j\omega_\pi)| < \frac{1}{2}$ is obtained in a more "natural" loop shaping manner, as shown in Figure 6.6-2.

Comparing this same EEAL result, Equation 6.6-23, with the SOAL equivalent one, Equation 4.5-23, the same relative advantages exist as above, due to $\left| \frac{L_f(j\omega_o)}{1 + L_f(j\omega_o)} \right| = 1$ for the SOAL, so Equation 4.5-24 is a special case for Equation 6.6-23.

In all structures seen before, the disturbance has been the main problem to handle, especially when the equivalent applied disturbance signal at the plant output was a step function. It seems there is

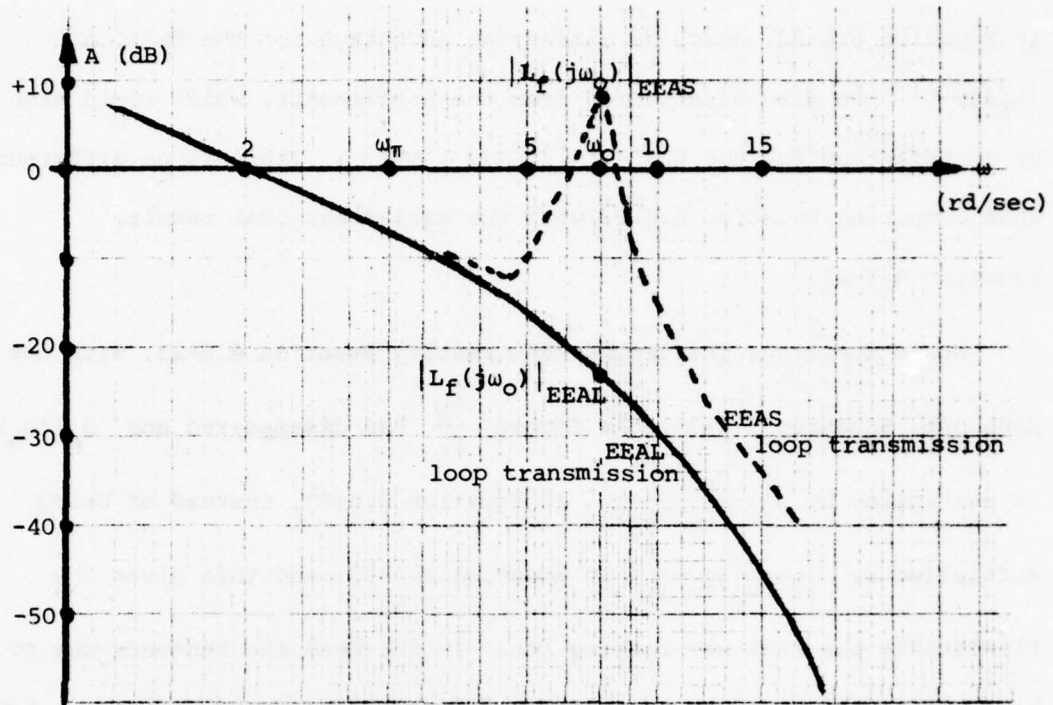


Figure 6.6-2 - Comparison of EEAS and EEAL Loop Shaping
Same Oscillation Frequency

"no limitation" in the EEAL regarding this aspect, since there is no limit on how small $\left| \frac{L_f(j\omega_o)}{1 + L_f(j\omega_o)} \right|$ can be in Equation 6.6-23. The "physical" explanation for this fact is due to the breaking of the linkage between $c_o(t)$, the plant output oscillation signal, and $x_o(t)$, the non-linearity input oscillation signal. This has already been discussed in Equation 6.2-12.

But there is a limitation on how small $\left| \frac{L_f(j\omega_o)}{1 + L_f(j\omega_o)} \right|$ can be since, as per Equation 6.4-1,

$$\left| \frac{V(j\omega_o)}{I(j\omega_o)} \right| = \left| \frac{L_o(j\omega_o)}{1 + L_o(j\omega_o)} \right| \quad (6.6-24)$$

$$\text{If } \left| \frac{L_f(j\omega_o)}{1 + L_f(j\omega_o)} \right| \ll 1, \text{ then } \left| \frac{L_f(j\omega_o)}{1 + L_f(j\omega_o)} \right| \approx |L_f(j\omega_o)| = \left| \frac{L_o(j\omega_o)}{2} \right| \approx$$

$$\approx \frac{1}{2} \left| \frac{L_o(j\omega_o)}{1 + L_o(j\omega_o)} \right| \ll 1, \text{ and } \left| \frac{L_o(j\omega_o)}{1 + L_o(j\omega_o)} \right| \ll 1.$$

This last conclusion means in Equation 6.6-24 that $|V(j\omega_o)| \ll I(j\omega_o)$, so V , the amplitude of oscillation at $v(t)$, is also very small compared to the injected signal.

$$x_o(t) = v_o(t) + \mathcal{J}(t) \approx \mathcal{J}(t) = A_o \sin(\omega_o t) \quad (6.6-25)$$

The quasi-linearity condition being satisfied at x means $\left| \frac{x_f}{A_o}(t) \right| \leq \frac{1}{3}$,

so $\left| \frac{x_f}{V}(t) \right|$ could achieve large values, since $\frac{V}{A_o} \ll 1$, as per

Equations 6.6-24 and 25, with quasi-linear conditions probably not satisfied, making it difficult to measure the amplitude of oscillation of $v_o(t)$, and "obtain" the real information. This fact gives the limit on how small $\frac{L_f(j\omega_o)}{1 + L_f(j\omega_o)}$ may become.

The measurement of this oscillation is more difficult to obtain than in the SOAL, where a "peak to peak" detector was used. The used technique and approximations have already been described in Section 6.5 (in this technique the information of the phase $\angle L_o(j\omega_o)$ is used).

Finally, if $Z_{er}(j\omega)$ and $Z_{ed}(j\omega)$ are the extreme plant output due to the forced signal and disturbance.

$$Z_{er}(j\omega) = R_e T_r(j\omega) \quad (6.6-26)$$

$$Z_{ed}(j\omega) = \frac{D_e L_f(j\omega)}{1 + L_f(j\omega)} \quad (6.6-27)$$

In Equations 6.6-26 and 27 $\omega = \omega_o$, and substituting in 22 and 23,

$$\left| \frac{x_r}{A}(j\omega_o) \right| \geq \frac{2}{m} |z_{er}(j\omega_o)| \quad (6.6-28)$$

$$\left| \frac{x_d}{A}(j\omega_o) \right| \geq \frac{2}{m} |z_{ed}(j\omega_o)| \quad (6.6-29)$$

which can be combined in a single expression:

$$\frac{1}{3\omega_o} \geq \left| \frac{x_f}{A}(j\omega_o) \right| \geq \frac{2}{m} |z_e(j\omega_o)| \quad (6.6-30)$$

which is plotted in Figure 6.6-3.

In Equation 6.6-30, z_e represents the extreme plant output, and x_f the input to the non-linearity, both due to the forced command or disturbance.

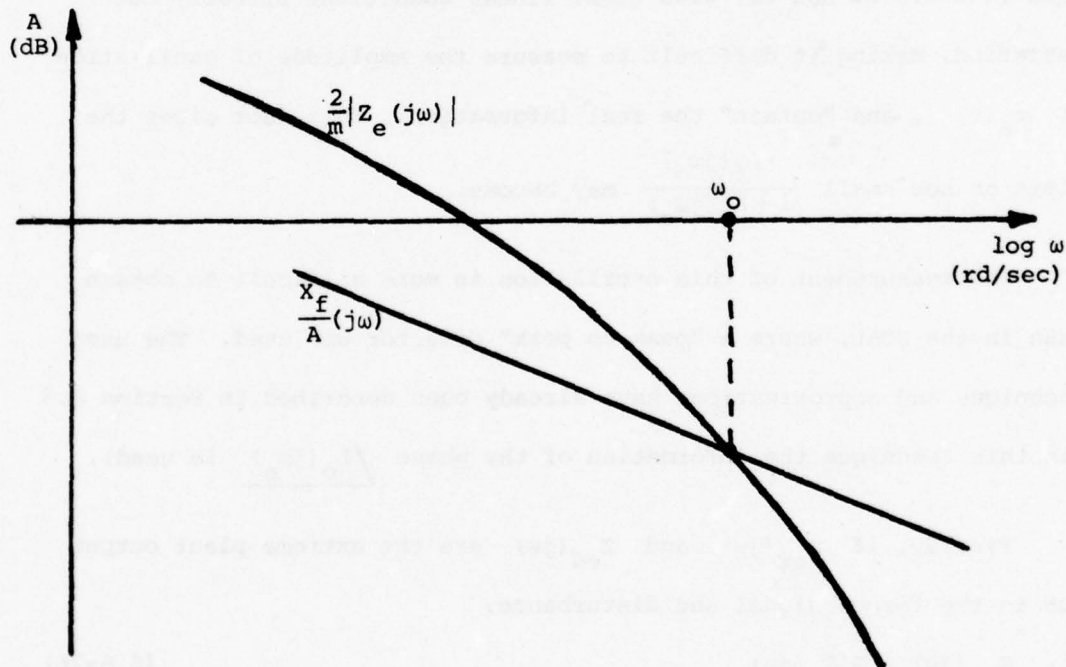


Figure 6.6-3 - EEAL Oscillation Frequency Determination

A final expression is derived. Combining Equations 6.6-17 and 19,

$$\frac{1}{3\omega_o} \geq \left| \frac{x_d}{A}(j\omega_o) \right| \geq \frac{2}{m} |D_e(j\omega_o)| \left| \frac{L_f(j\omega_o)}{1+L_f(j\omega_o)} \right| \quad (6.6-31)$$

Considering the two extreme factors in this inequality:

$$\left| \frac{L_f(j\omega_o)}{1+L_f(j\omega_o)} \right| \leq \frac{1}{6\omega_o |D_e(j\omega_o)|} \quad (6.6-32)$$

Then the Nichol's chart is used as in the EEAS. Disturbance attenuation constraints and self-oscillation "quenching" are translated as bounds for the different frequencies, as per Section 3.5-3, Figure 3.5-4.

The bound due to constraint 6.6-32 is also plotted in the same Nichol's chart for several values of ω_o , which is still unknown. The technique used to define $L_f(j\omega)$ is very similar to the one used in the EEAS, Section 3.5-3.

In the numerical example, Section 6.7, the synthesis procedure is followed step by step.

6.7 Numerical Example - EEAL - Smooth Solution

The chosen EEAL structure is repeated in Figure 6.7-1.

The defined set of specifications and constraints in this numerical example is:

Desired Command Input Response

$$T_r(s) = \frac{1}{1 + \frac{2 \times .5}{.1} s + \frac{s^2}{.1^2}} \times \phi(s)$$

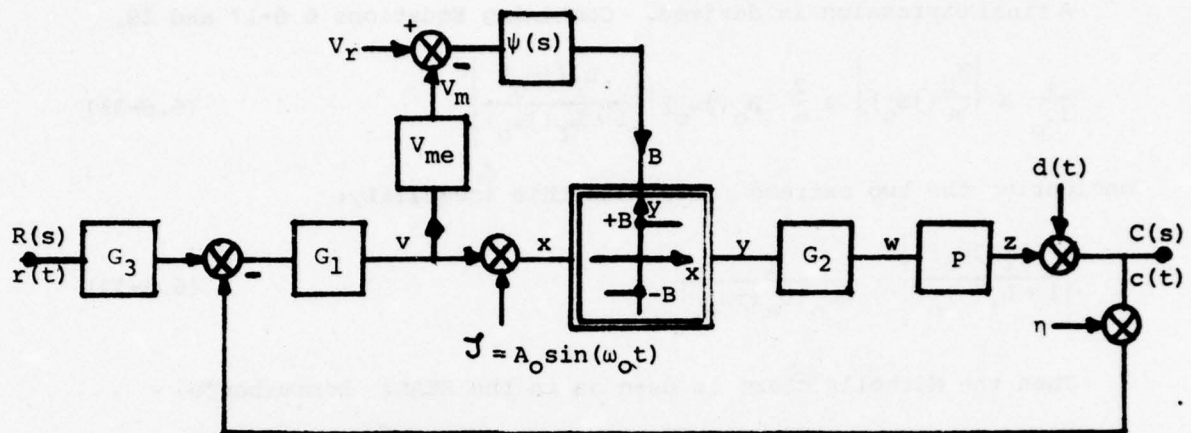


Figure 6.7-1 - EEAL Structure

where $\phi(s)$ includes far-off poles and zeros that can be added to the "nominal" desired transmission.

Minimum Disturbance Attenuation

The minimum disturbance attenuation required is plotted in Figure 6.6-2. Note there are no specifications for $\omega \geq \omega_H = .1 \text{ rd/sec}$.

The Plant

$$P(s) = \frac{K}{s} \quad 1 \leq K_1 \leq K \leq K_2 = 100$$

"Abrupt" changes of 6 dB in the plant gain are possible.

Extreme Command Input

$$r_e(t) = 75 \mu(t) \rightarrow R_e(s) = \frac{75}{s}$$

Extreme Disturbance Input

$$d_e(t) = 20 \mu(t) \rightarrow D_e(s) = \frac{20}{s}$$

The disturbance response should not be oscillatory.

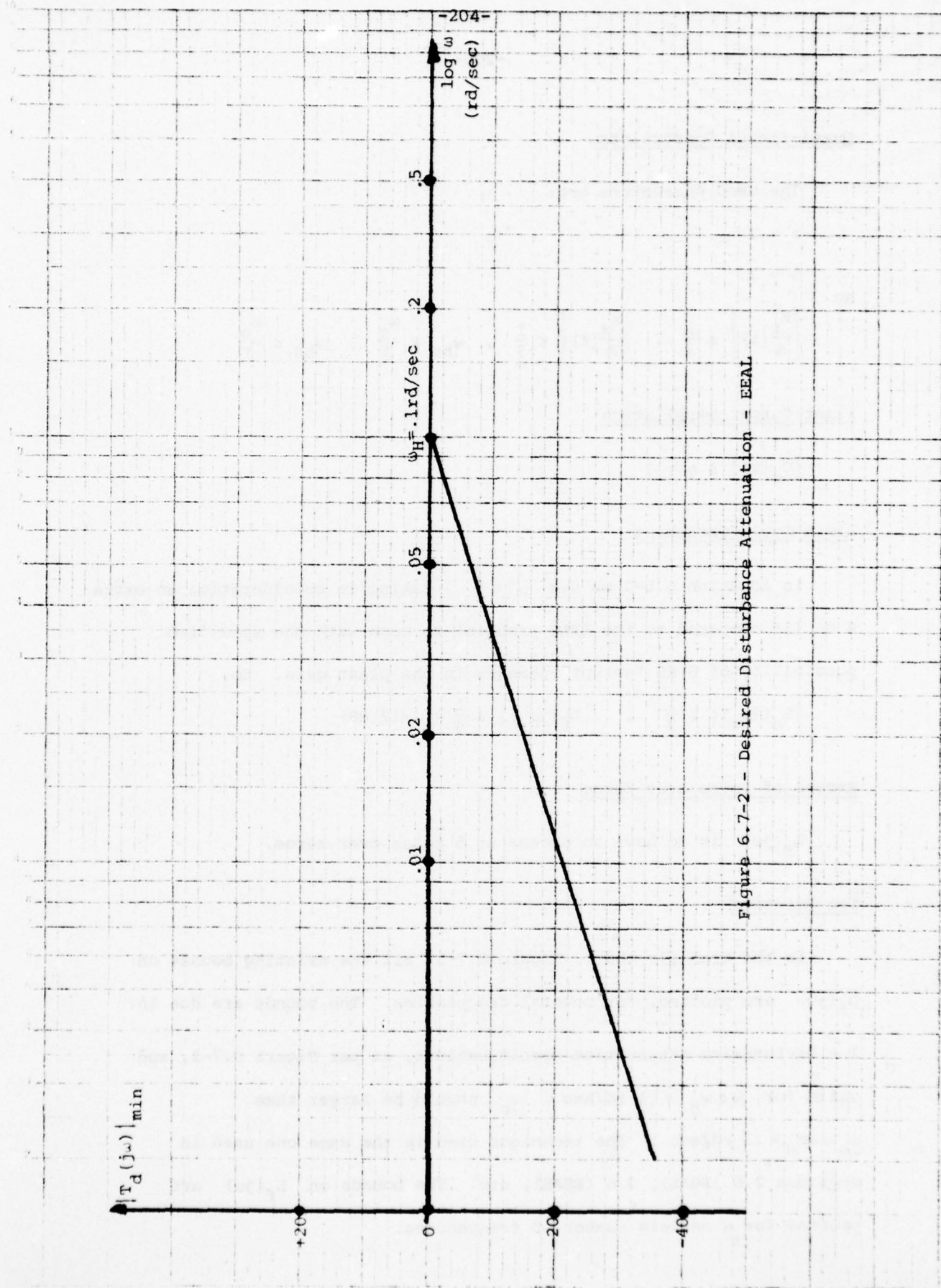


Figure 6.7-2 - Desired Disturbance Attenuation - EEAL

Quasi-linear Constraints

The used parameters are:

$$\alpha = 3$$

$$\beta = 3$$

so

$$\left| \frac{x_r}{A}(t) \right| \leq \frac{1}{3}, \quad \left| \frac{x_d}{A}(t) \right| \leq \frac{1}{3}, \quad \omega_{br} \leq \frac{\omega_o}{3}, \quad \omega_{bd} \leq \frac{\omega_o}{3}$$

Plant Output Oscillation

$$|C_o(t)| \leq m = 1$$

Limit Cycle Quenching

In Equation 6.6-3 we use $\rho' = \frac{1}{4}$, taking in consideration an extra 6 dB (if compared to the EEAS problem) to cope with the specified possibility of 6 dB "abrupt" changes in the plant gain. So,

$$|L_o(j\omega_\pi)| \leq \frac{1}{2}, \quad |L_f(j\omega_\pi)| \leq \frac{1}{4} = (-12 \text{ dB})$$

Excess of Poles over Zeros

$L_f(j\omega)$ is to have an excess of 5 poles over zeros.

The Solution

In the Nichol's chart (Figure 6.7-3) all the existing bounds on $L_f(j\omega)$ are plotted, for several frequencies. The bounds are due to:

- 1 - Disturbance attenuation specifications, as per Figure 6.7-2, and valid for $\omega \leq \omega_H = .1 \text{ rd/sec}$. ω_o should be larger than $\omega_o \geq \omega_{\beta_H} = .3 \text{ rd/sec}$. The technique used is the same one used in Sections 2.6 (SOAS), 3.6 (EEAS), etc. The bounds on $L_f(j\omega)$ are plotted for a certain number of frequencies.

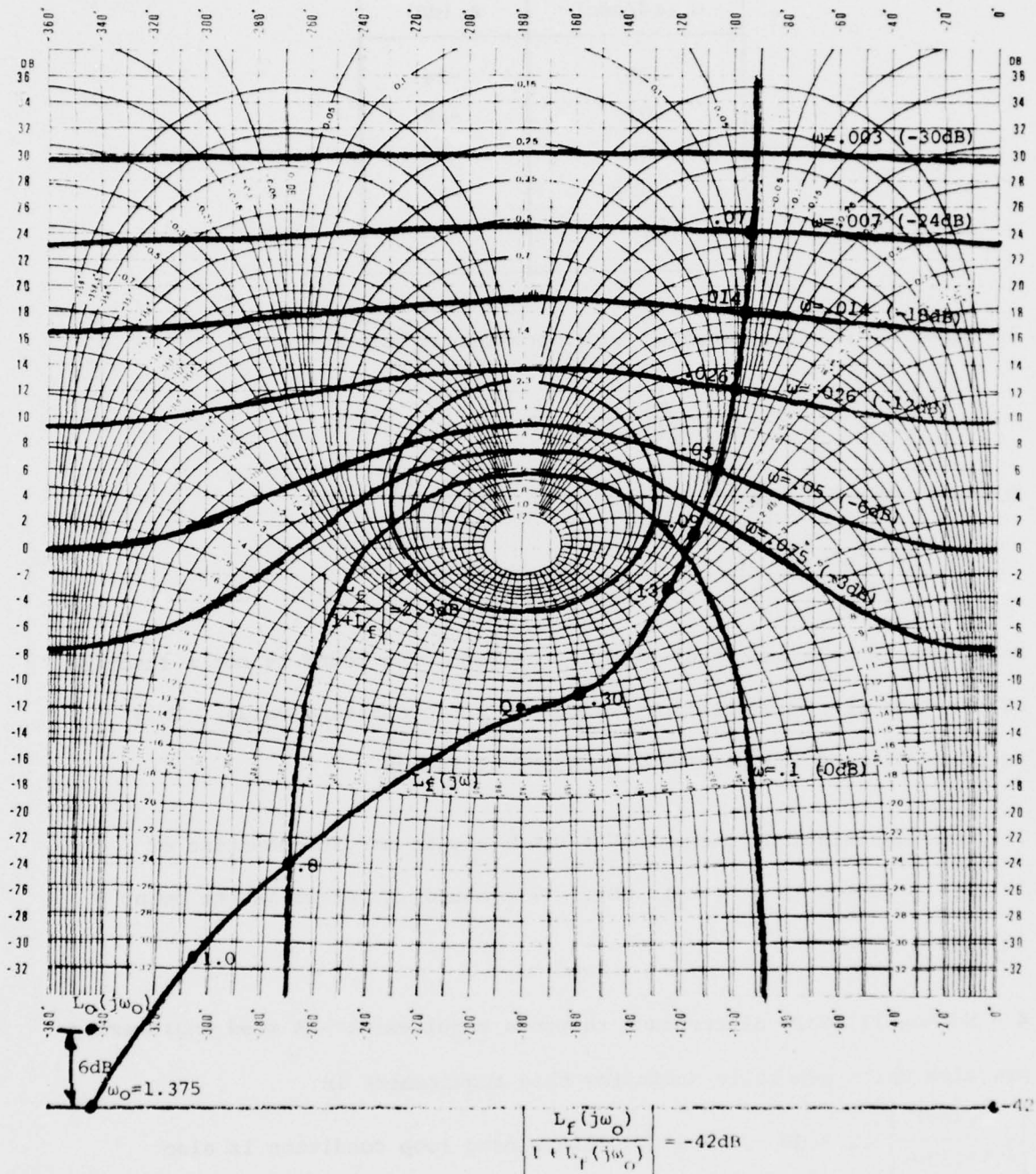


Figure 6.7-1 - EEAL - Numerical Example - Bounds on L_f and Solution

ω (rd/sec)	A (dB)
.007	-24
.013	-18
.05	-6
.075	-3
.1	0

2 - Equation 6.6-32, repeated here, provides a bound

$$\left| \frac{L_f(j\omega_o)}{1 + L_f(j\omega_o)} \right| \leq \frac{m}{6\omega_o |D_e(j\omega_o)|}$$

In this numerical example, $m=1$, $D_e(j\omega_o) = \frac{20}{\omega_o}$, so

$$\left| \frac{L_f(j\omega_o)}{1 + L_f(j\omega_o)} \right| \leq \frac{1}{120} \quad (= -41.56 \text{ dB})$$

Note that in this numerical example the resulting bound is not a function of the "possible" oscillation frequency, but a constant value. This bound is plotted in the Nichol's chart, at -42 dB.

3 - Self-oscillation "quenching" - Gives a gain margin condition of 12 dB, so $L_f(j\omega_\pi) < \frac{1}{4}$ ($= -12 \text{ dB}$). This bound is marked as the point Q in Figure 6.7-3.

4 - Non-oscillatory disturbance response requirement - A good engineering practice which generally satisfies this requirement is

$$\left| \frac{L_f(j\omega)}{1 + L_f(j\omega)} \right| < 2.3 \text{ dB} , \quad \forall \omega .$$

This closed loop condition is also plotted as a bound in the Nichol's chart, Figure 6.7-3.

5 - $L_f(j\omega)$ has to satisfy all these bounds and ω_o is the minimum frequency allowing $L_f(j\omega)$ to satisfy these bounds. It has been

shown [5] that the optimum loop transmission, in the sense defined in that reference ([5]), is the one that "stays" in its respective bound for each frequency.

The chosen L_f is

$$L_f(s) = \frac{.1}{s \left(1 + \frac{2 \times .7}{.8} s + \frac{s^2}{.8^2} \right)^2}$$

which has an excess of 5 poles over zeros as specified.

The oscillation frequency ω_o is the one corresponding to the intersection of $L_f(j\omega)$ with the bound $\left| \frac{L_f(j\omega_o)}{1 + L_f(j\omega_o)} \right| = -42 \text{ dB}$. So

$$\omega_o = 1.375 \text{ rd/sec}$$

$L_f(j\omega)$ is plotted in Figure 6.7-3.

Once L_f is known, it is possible to define the various parts of the loop. The limits of $|M_f G_2 K P_h(j\omega)|$, due to Equations 6.6-18,12, are repeated here,

$$|M_f G_2 K P_h(j\omega)| \geq \alpha \cdot \omega \cdot |D_e(j\omega)| \left| \frac{L_f(j\omega)}{1 + L_f(j\omega)} \right|$$

as curve number one in Figure 6.7-4.

$$|M_f G_2 K P_h(j\omega)| \geq \alpha \cdot \omega \cdot |R_e T_r(j\omega)|$$

as curve number two in Figure 6.7-4. In the first expression, $\alpha = 3$,

$$|D_e(j\omega)| = \frac{20}{\omega}, \text{ and } L_f(j\omega) = \frac{.1}{s \left(1 + \frac{2 \times .7}{.8} s + \frac{s^2}{.8^2} \right)} \bigg|_{s=j\omega}, \text{ and this}$$

limit is completely defined.

In the second expression, $\alpha = 3$, $|R_e(j\omega)| = \frac{75}{\omega}$ and

$$T_r(j\omega) = \frac{1}{1 + \frac{2 \times .5}{.1} s + \frac{s^2}{.1^2}} \bigg|_{s=j\omega} \times \phi(j\omega). \quad \phi(j\omega) \text{ represents the far off}$$

poles and zeros which have not been yet defined, and leaves some freedom to the designer to decide what can be added to the nominal $T_r(j\omega)$, "without affecting" the system response. In our case, we choose

$$\Phi(j\omega) = \frac{L_f(j\omega)}{1 + L_f(j\omega)} \quad (\text{this makes the } G_3 \text{ calculation and implementation very easy}).$$

The transmission T_r is

$$T_r(j\omega) = \frac{1}{1 + \frac{2 \times .5}{.1} s + \frac{2}{.1} s^2} \bigg|_{s=j\omega} \times \frac{L_f(j\omega)}{1 + L_f(j\omega)}$$

As noted earlier, it is up to the designer to choose the far-off poles and zeros to be added to the transmission. $\Phi(s)$ was chosen in this case for reasons of easy implementation of G_3 .

Since $\left| \frac{L_f(j\omega_o)}{1 + L_f(j\omega_o)} \right|$ satisfies Equation 6.6-32, and $|M_f G_2 K P_h(j\omega)|$ satisfies 6.6-18, Equation 6.6-19 repeated here is automatically satisfied.

$$|M_f G_2 K P_h(j\omega_o)| \leq \frac{m}{2} = \frac{1}{2} \quad (= -6 \text{ dB})$$

One can see in Figure 6.7-4 that at $\omega = \omega_o = 1.375 \text{ rd/sec}$, if $|M_f G_2 K P_h(j\omega_o)|$ in curve ① is equaled, it has the above value $= \frac{1}{2} = -6 \text{ dB}$. In this numerical example the limit of $|M_f G_2 K P_h(j\omega)|$ due to the extreme command input, curve ②, at ω_o , is lower than that due to extreme disturbance input, curve ①, at ω_o , so the last limit prevails and there is no problem with the maximum plant oscillation constraint. In case this is not so, more far-off poles could be added to T_r , until

$$|M_f G_2 K P_h(j\omega_o)|_{\text{due to } R_e} \leq |M_f G_2 K P_h(j\omega_o)|_{\text{due to } D_e}$$

In case more far-off poles significantly affect the desired response, then ω_o has to be increased until the above inequality can be satisfied.

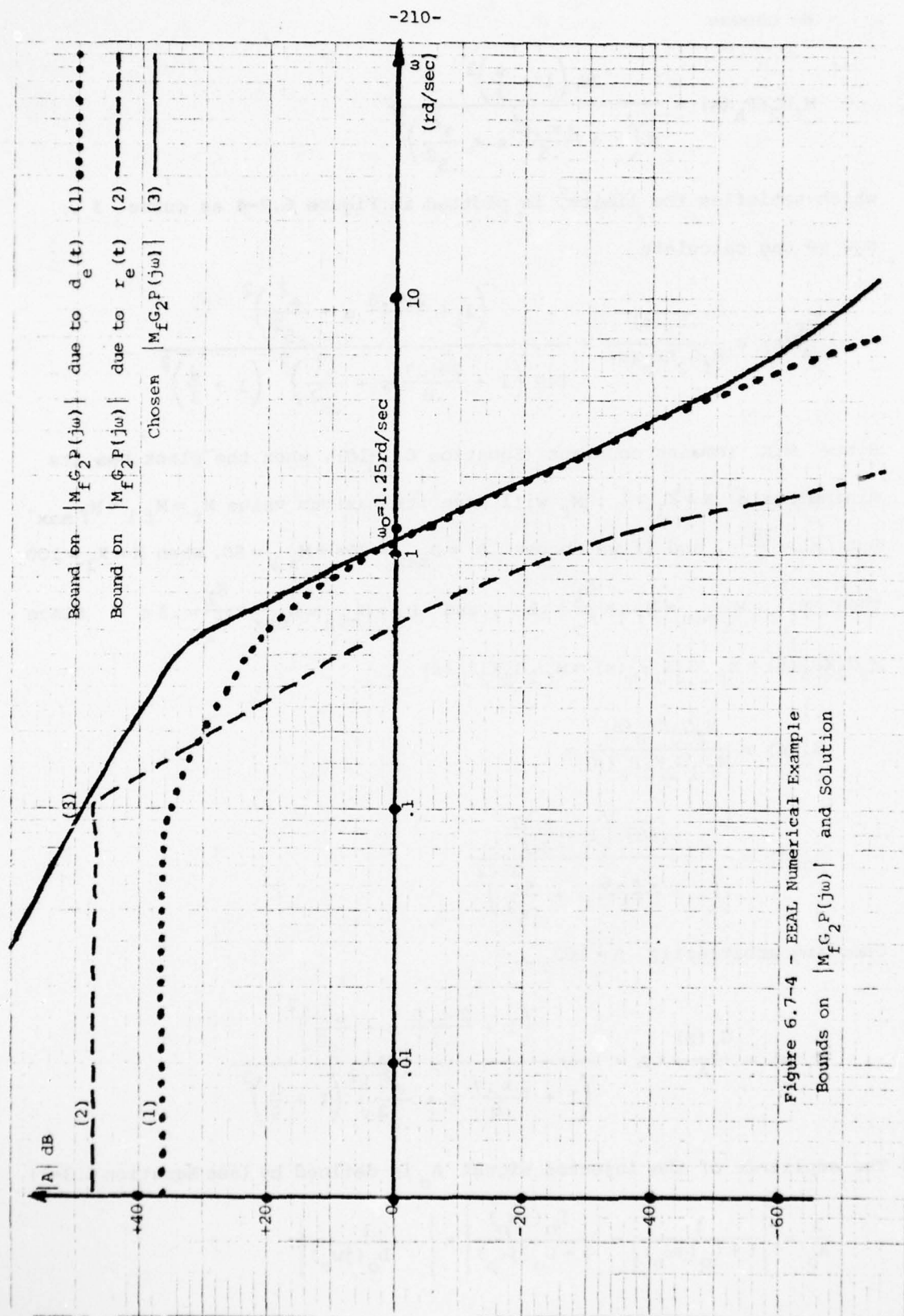


Figure 6.7-4 - EEAL Numerical Example
Bounds on $|M_f G_2 P(j\omega)|$ and Solution

We choose

$$M_f G_2^{KP_h}(s) = \frac{28 \left(1 + \frac{s}{3}\right)^2}{s \left(1 + \frac{2 \times .6}{.5} s + \frac{s^2}{.5^2}\right)^2}$$

which satisfies the limits, is plotted in Figure 6.7-4 as curve 3.

Now we can calculate

$$\frac{G_1}{A}(s) = \frac{L_f(s)}{M_f G_2^{KP_h}(s)} = \frac{\left(1 + \frac{2 \times .6}{.5} s + \frac{s^2}{.5^2}\right)^2}{140 \left(1 + \frac{2 \times .7}{.8} s + \frac{s^2}{.8^2}\right)^2 \left(1 + \frac{s}{3}\right)^2}$$

Since $M_f K$ remains constant (Equation 6.2-10), when the plant has its

minimum gain $K = K_1 = 1$, M_f will have its maximum value $M_f = M_{f1} = M_{f \max}$.

But $M_f = \frac{2B}{\pi}$, and if we choose $B_1 = B_{\max} = 30\pi \rightarrow M_{f1} = 60$. When $K = K_2 = 100$,

then $M_{f2} = M_{f \min} = M_{f1} \times \frac{K_1}{K_2} = .6$, and $B_2 = B_{\min} = B_{\max} \times \frac{K_1}{K_2} = .3\pi$. Since

$$M_f G_2^{KP_h}(s) = M_{f1} G_2^{K_1 P_h}(s) = M_{f2} G_2^{K_2 P_h}(s),$$

$$G_2(s) = \frac{M_f G_2^{KP_h}(s)}{M_{f1} G_2^{K_1 P_h}(s)} =$$

$$G_2(s) = \frac{.467 \left(1 + \frac{s}{3}\right)^2}{\left(1 + \frac{2 \times .6}{.5} s + \frac{s^2}{.5^2}\right)^2}$$

Choosing arbitrarily $A = 140$,

$$G_1(s) = \frac{G_1(s)}{A} \times A = \frac{\left(1 + \frac{2 \times .6}{.5} s + \frac{s^2}{.5^2}\right)^2}{\left(1 + \frac{2 \times .7}{.8} s + \frac{s^2}{.8^2}\right)^2 \left(1 + \frac{s}{3}\right)^2}$$

The amplitude of the injected signal A_o is defined by (see Equation 6.3-1)

$$\frac{A}{A_o} = \left| \frac{1}{1 + L_o(j\omega_o)} \right| = \left| \frac{L_o(j\omega_o)}{1 + L_o(j\omega_o)} \right| \times \left| \frac{1}{L_o(j\omega_o)} \right|$$

In the Nichol's chart, Figure 6.7-3, $L_o(j\omega_o) = 2L_f(j\omega_o)$, and the following values are read:

$$\left| \frac{L_o(j\omega_o)}{1 + L_o(j\omega_o)} \right| \approx -36 \text{ dB} \quad , \quad L_o(j\omega_o) \approx -36 \text{ dB}$$

so

$$\frac{A}{A_o} \approx 1 \quad , \quad A \approx A_o = 140$$

Since $\omega_o = 1.375 \text{ rd/sec}$, the injected signal is

$$J = 140 \sin(1.375 t)$$

The amplitude V of $v_o(t)$ can be calculated.

$$\frac{V}{A_o} = \left| \frac{L_o}{1 + L_o(j\omega_o)} \right| = -36 \text{ dB} \quad \left(\approx \frac{1}{60} \right)$$

so

$$V = \frac{140}{60} \approx 2.33$$

In the extreme case, when quasi-linearity conditions are most likely to be violated,

$$\left| \frac{x_f}{A}(t) \right| \approx \frac{1}{3} \quad , \quad \text{so} \quad |x_f(t)| \approx \frac{A}{3} \approx 46$$

The forced signal (v_r or v_d) can be 20 times larger than the amplitude of oscillation V of v_o .

Due to the far-off poles and zeros definition in $T_r(j\omega)$,

$$G_3(s) = \frac{1}{1 + \frac{2 \times .5}{.1} s + \frac{s^2}{.1^2}}$$

Finally the function $\psi(s)$ is defined based on the maximum possible secondary loop bandwidth, when the plant has its maximum gain (Equation 6.5-9).

$$\psi(s) = \frac{.02}{s}$$

6.8 EEAL Numerical Example - Simulation Results

A digital simulation of the complete system was performed on the CDC system. First the system "response" is shown when the secondary loop is open ($\psi(s) = 0$). The results show mainly the oscillation amplitude measurement dynamic properties when there is an abrupt change in the gain, and the oscillation amplitude measurement error when an extreme input or disturbance is applied. As a reference, the system response for these signals is also shown (Figures 6.8-1 - 4).

One can see that for abrupt changes in the gain of the plant, after one cycle, the measurement has "almost" been completed. When the extreme command and disturbance are applied, the change in the measurement is an error, since the plant keeps its gain value, and there is no change in the oscillation amplitude, and this error is equivalent to a "disturbance" in the EEAL secondary loop.

Next, the secondary loop is closed, and (Figures 6.8-5 - 7) the extreme command input and (Figures 6.8-6 - 8) the extreme disturbance are applied for several values of the gain of the plant. The results are close to the previous (secondary loop open) ones obtained.

Finally, the change in the dynamics of the secondary loop is depicted in Figures 6.8-9 - 14. The results show: First, the lower the gain of the plant, the lower the dynamics of the adjustment, as per Equation 6.5-9; Second, the system response is not the same when the plant gain changes upwards or downwards. This is due to the reasons explained at the end of Section 6.5. The results show the capability of the system to cope with relatively large step disturbances.

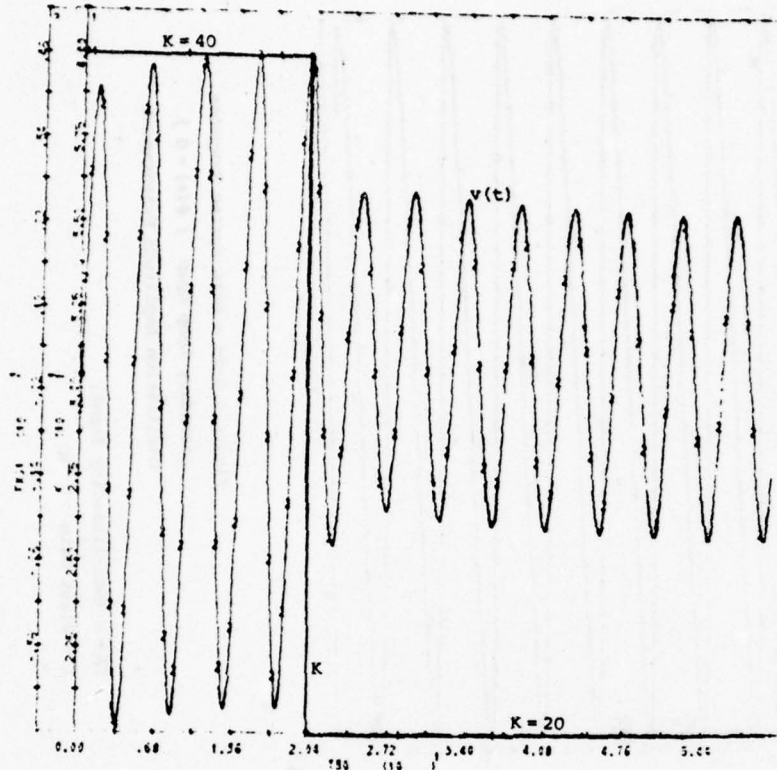


Figure 6.8-1a - EEAL System Response
Secondary Loop Open ($\psi(s) = 0$)
Oscillation Amplitude Measurement

$PX61 = v(t)$ (output of G_1)
 K - Plant Gain

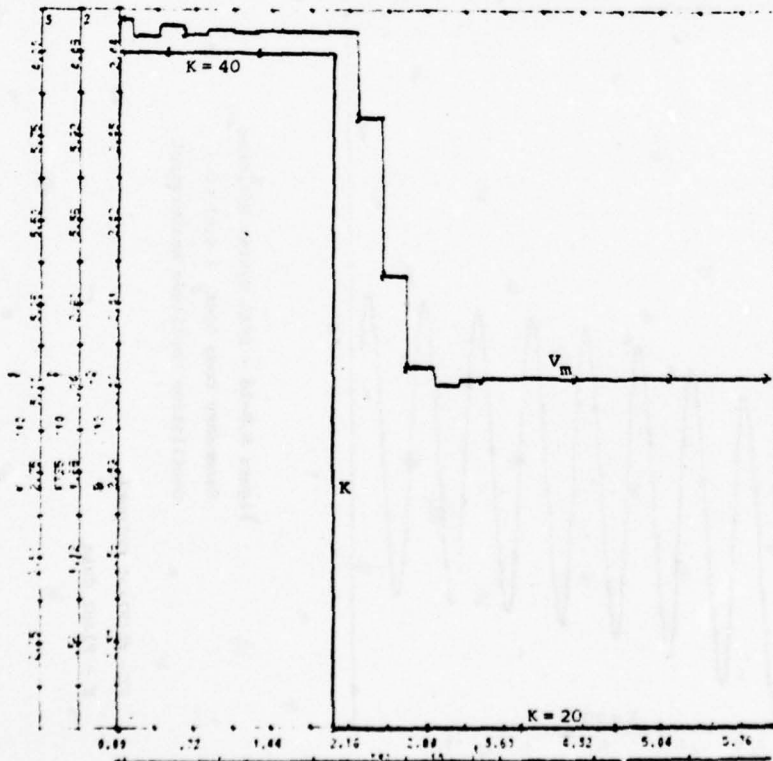


Figure 6.8-1b - EEAL System Response
Secondary Loop Open ($\psi(s) = 0$)
Oscillation Amplitude Measurement

$FTS-5 = v_m$ - Measured Amplitude
 K - Plant Gain

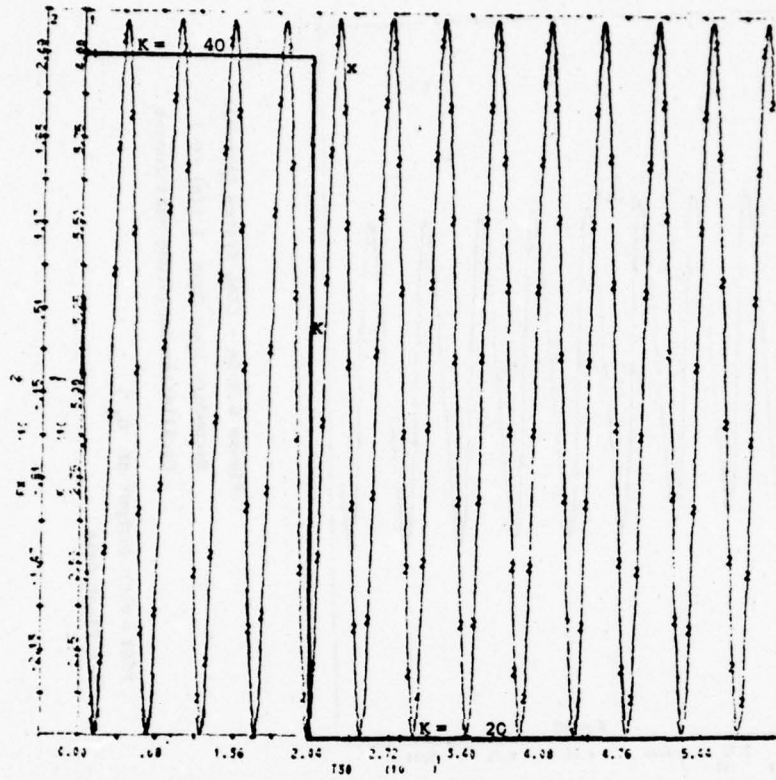


Figure 6.8-1c - EEAL System Response
Secondary Loop Open ($\psi(s) = 0$)
Oscillation Amplitude Measurement

$FX = x$ (Non-linearity Input)
 K - Plant Gain

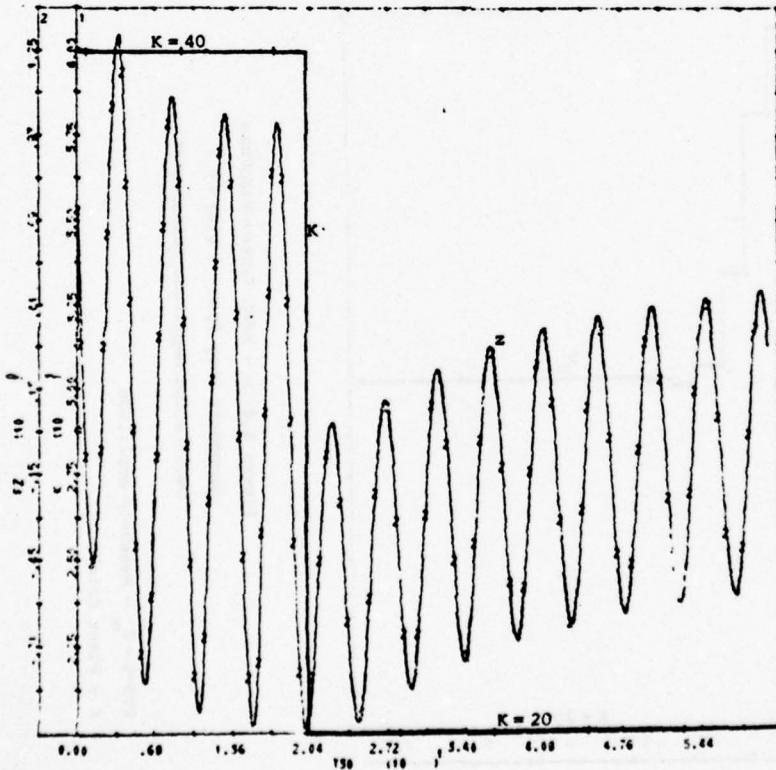


Figure 6.8-1d - EEAL System Response
Secondary Loop Open ($\psi(s) = 0$)
Oscillation Amplitude Measurement

$FZ = z$ (Plant Output)
 K - Plant Gain

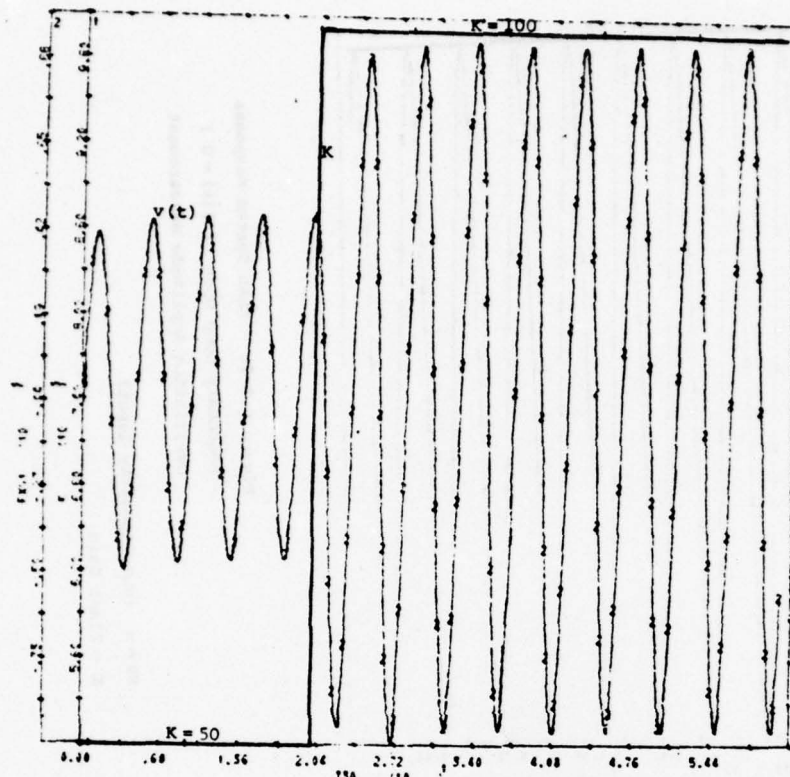


Figure 6.8-2a - EEAL System Response
Secondary Loop Open ($\psi(s) = 0$)
Oscillation Amplitude Measurement

$FX61 = v(t)$ (Output of G_1)
 K - Plant Gain

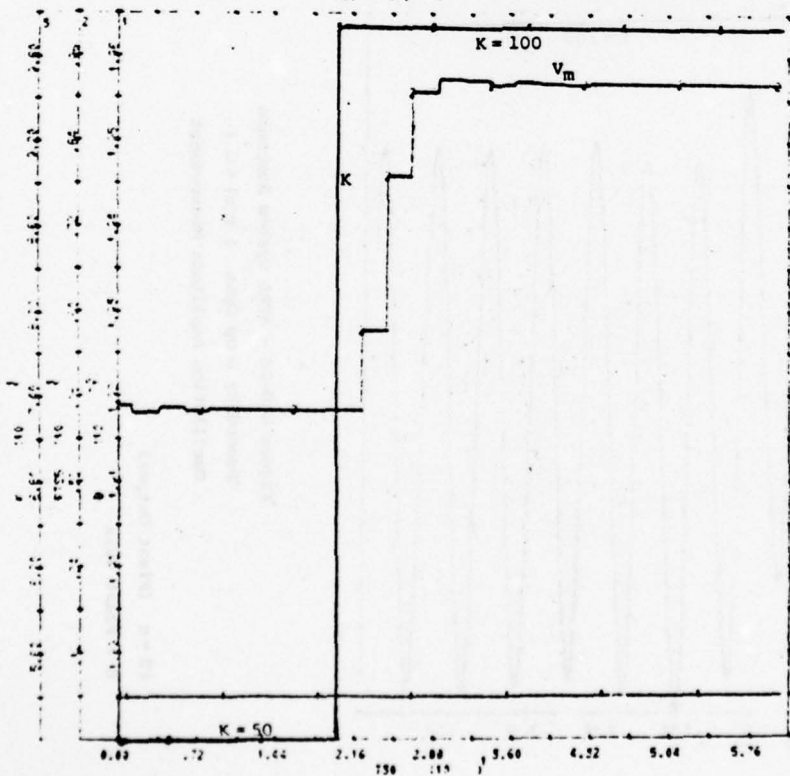


Figure 6.8-2b - EEAL System Response
Secondary Loop Open ($\psi(s) = 0$)
Oscillation Amplitude Measurement

$FTS-5 = v_m$ - Measured Amplitude
 K - Plant Gain

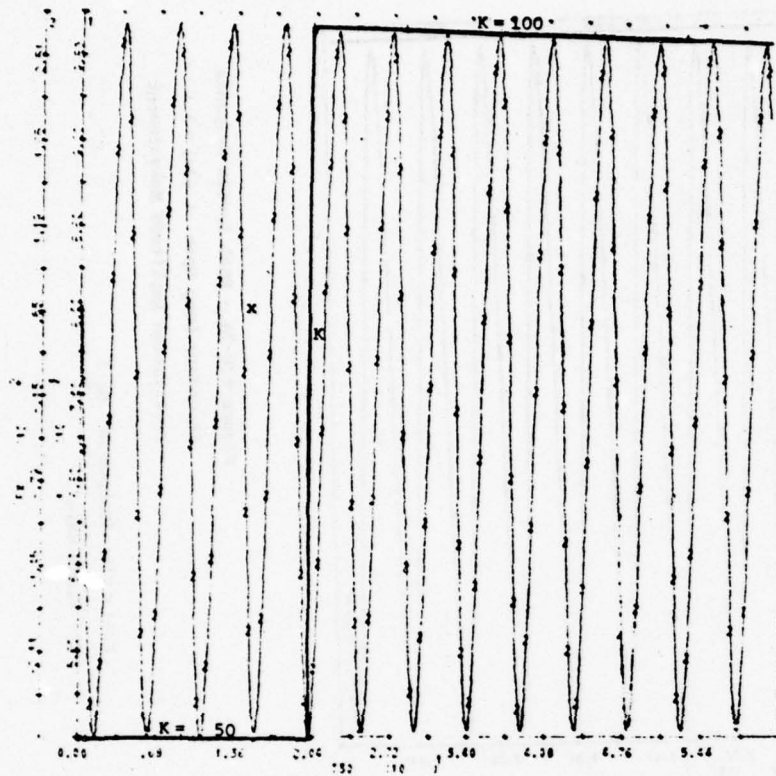


Figure 6.8-2c - EEAL System Response
Secondary Loop Open ($\psi(s) = 0$)
Oscillation Amplitude Measurement

$FX = x$ (Non-linearity Input)
 K - Plant Gain

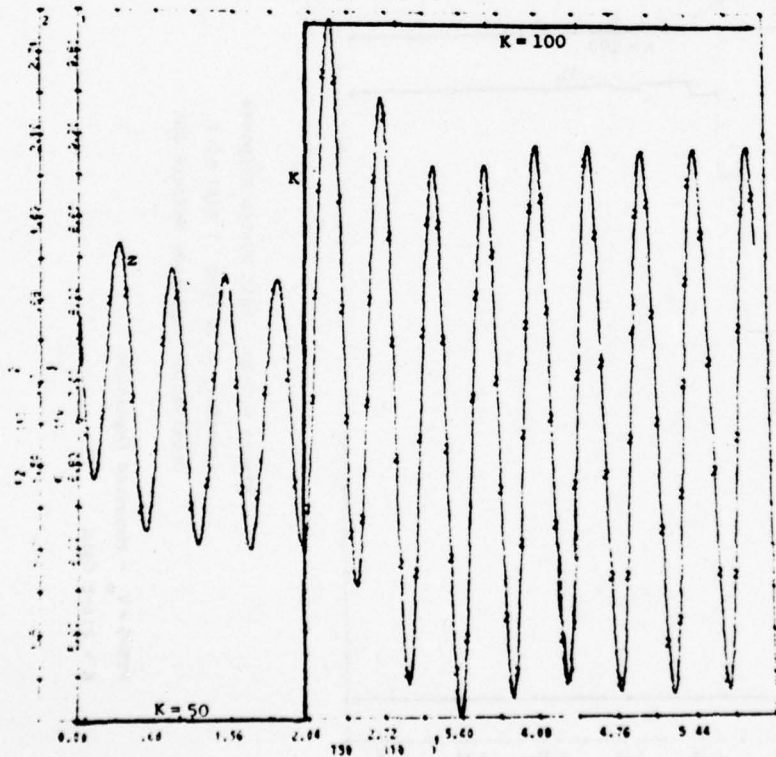


Figure 6.8-2d - EEAL System Response
Secondary Loop Open ($\psi(s) = 0$)
Oscillation Amplitude Measurement

$FZ = z$ (Plant Output)
 K - Plant Gain

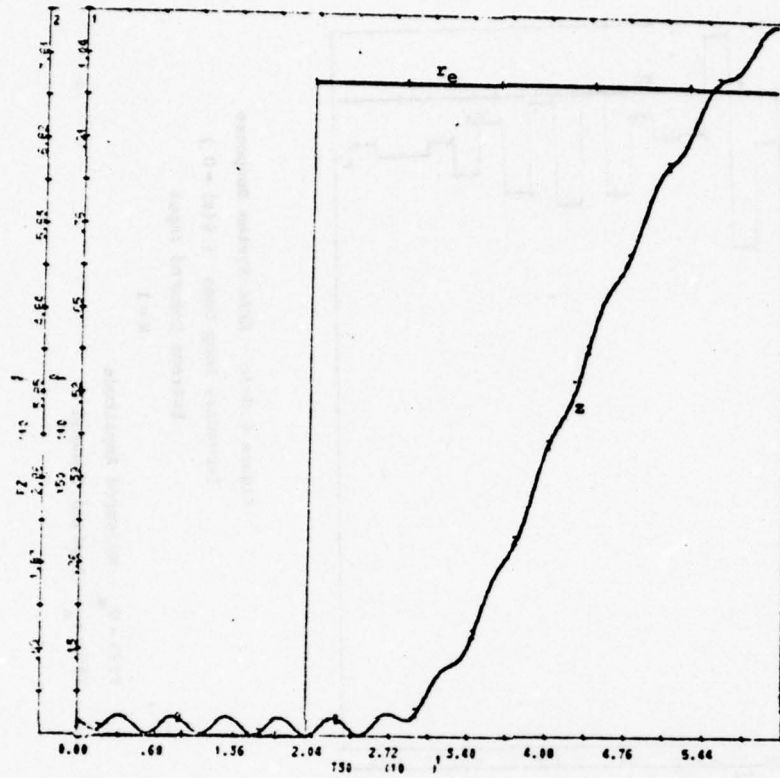


Figure 6.8-3a - EEAL System Response

Secondary Loop Open ($\psi(s) = 0$)

Extreme Command Input

$K = 1$

FZ = z - Plant Output

Y50 = r_e - Applied Command

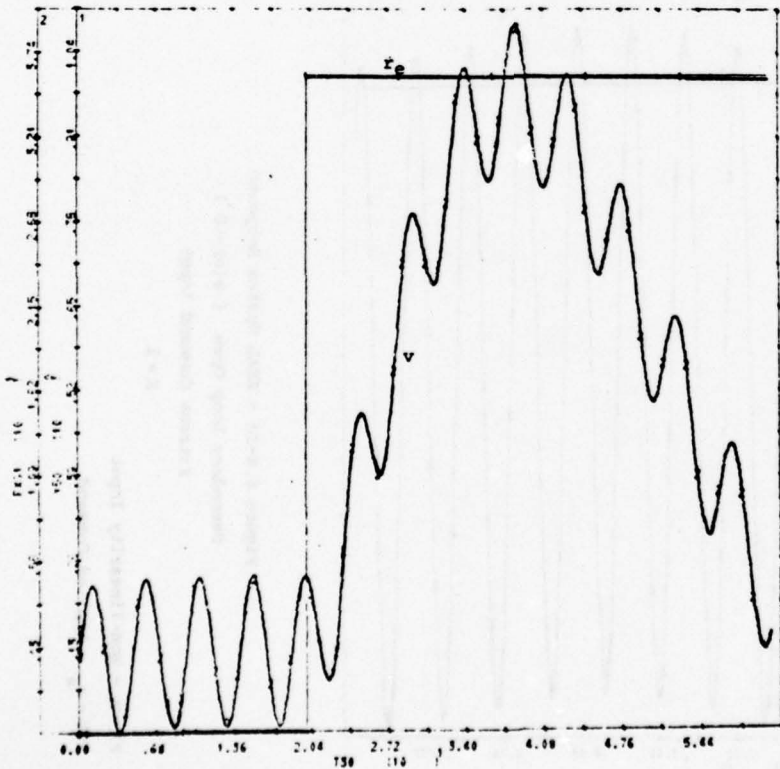


Figure 6.8-3b - EEAL System Response

Secondary Loop Open ($\psi(s) = 0$)

Extreme Command Input

$K = 1$

FXG1 = v (Output of G_1)

Y50 = r_e - Applied Command)

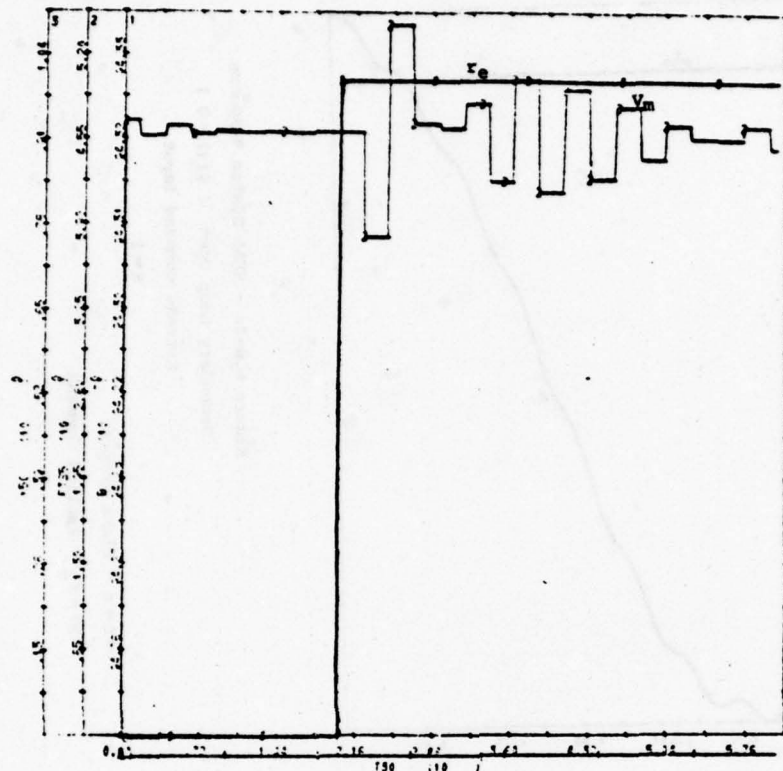


Figure 6.8-3c - EEAL System Response

Secondary Loop Open ($\psi(s) = 0$)

Extreme Command Input

$K = 1$

$FTS = V_m$ - Measured Amplitude

$Y50 = r_e$ - Applied Command

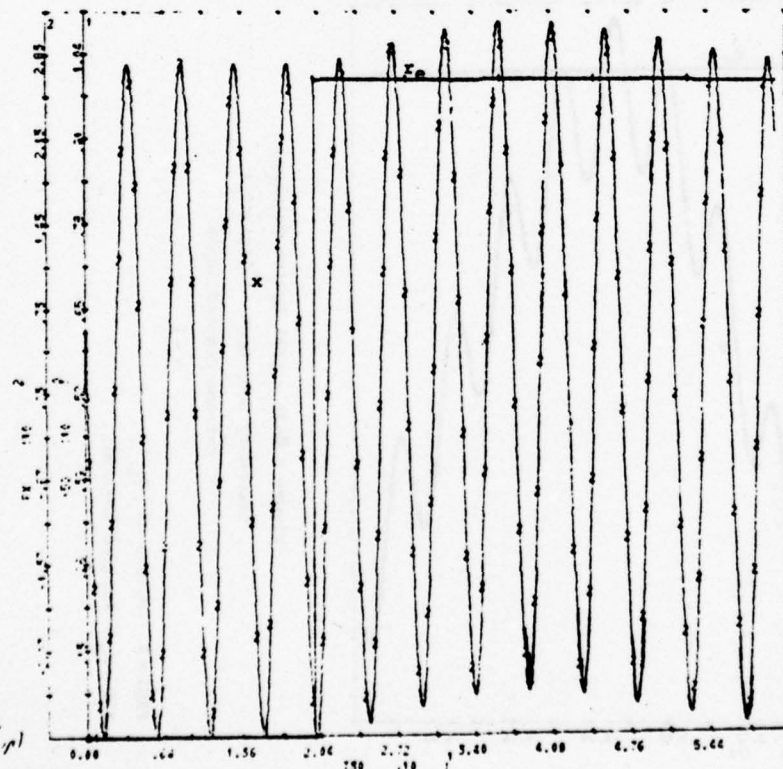


Figure 6.8-3d - EEAL System Response

Secondary Loop Open ($\psi(s) = 0$)

Extreme Command Input

$K = 1$

$FX = x$ - Non-linearity Input

$Y50 = r_e$ - Applied Command

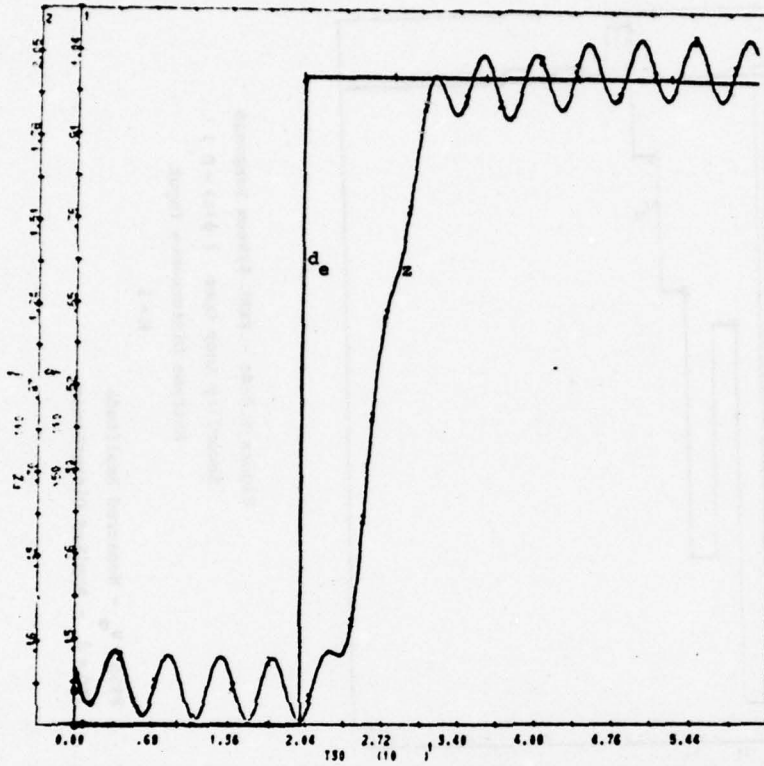


Figure 6.8-4a - EEAL System Response
Secondary Loop Open ($\psi(s) = 0$)
Extreme Disturbance Input
 $K = 1$

FZ = z - Plant Output
Y50 = d_e - Applied Disturbance

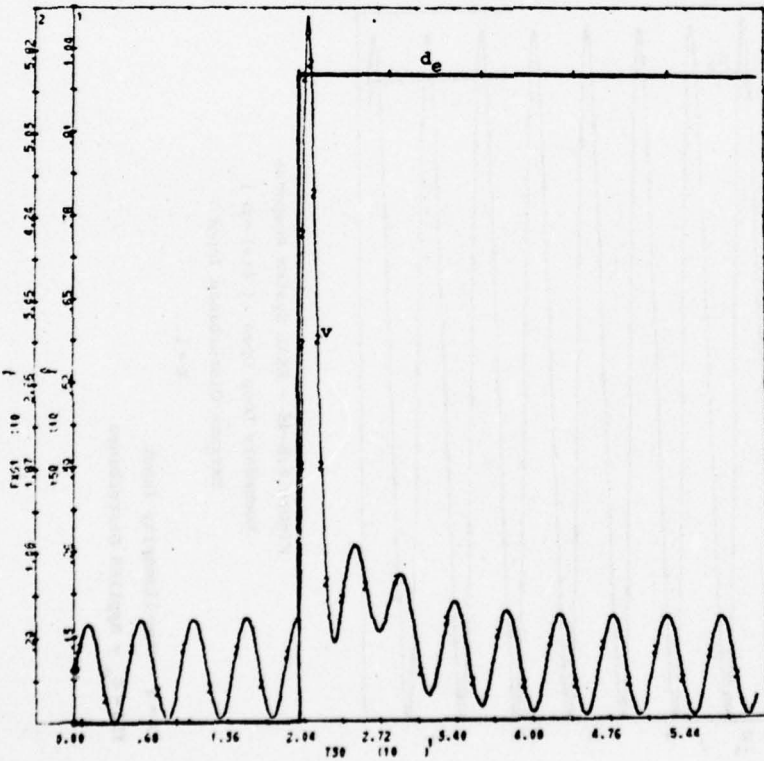


Figure 6.8-4b - EEAL System Response
Secondary Loop Open ($\psi(s) = 0$)
Extreme Disturbance Input
 $K = 1$

FXG1 = v - Output of G_1
Y50 - Applied Disturbance

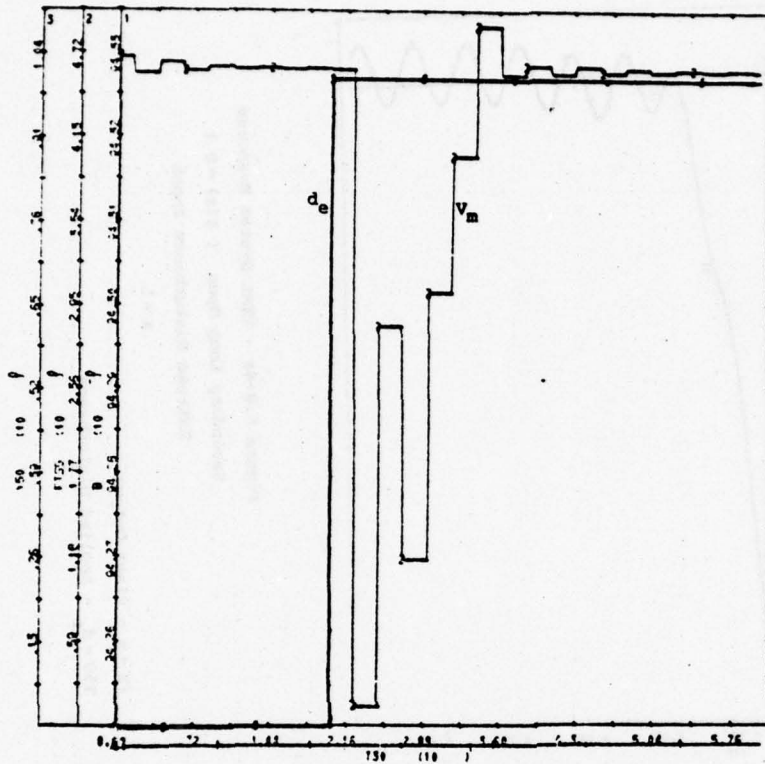


Figure 6.8-4c - EEAL System Response

Secondary Loop Open ($\psi(s) = 0$)

Extreme Disturbance Input

$K = 1$

$FTS5 = V_m$ - Measured Amplitude

$Y50 = d_e$ - Applied Disturbance

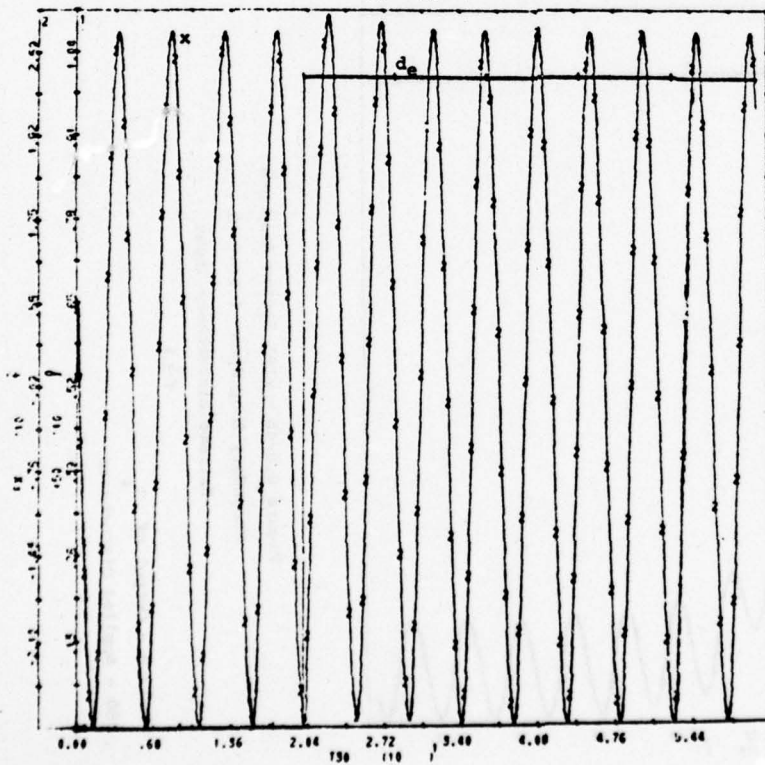


Figure 6.8-4d - EEAL System Response

Secondary Loop Open ($\psi(s) = 0$)

Extreme Disturbance Input

$K = 1$

$FX = x$ - Non-linearity Input

$Y50 = d_e$ - Applied Disturbance

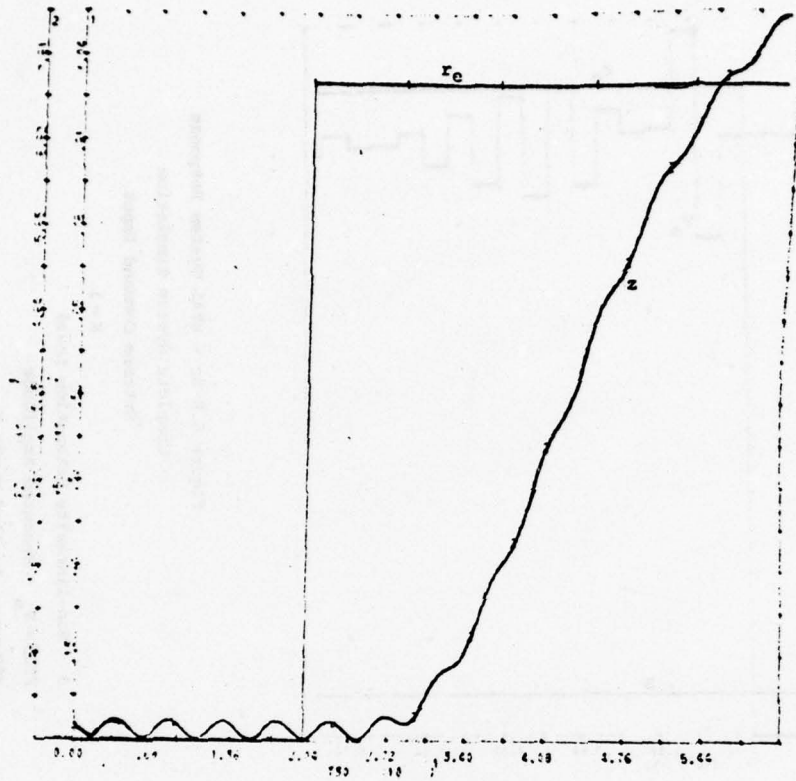


Figure 6.8-5a - EEAL System Response
Complete System Simulation
Extreme Command Input
 $K = 1$

FZ = z - Plant Output
Y50 = r_e - Applied Command

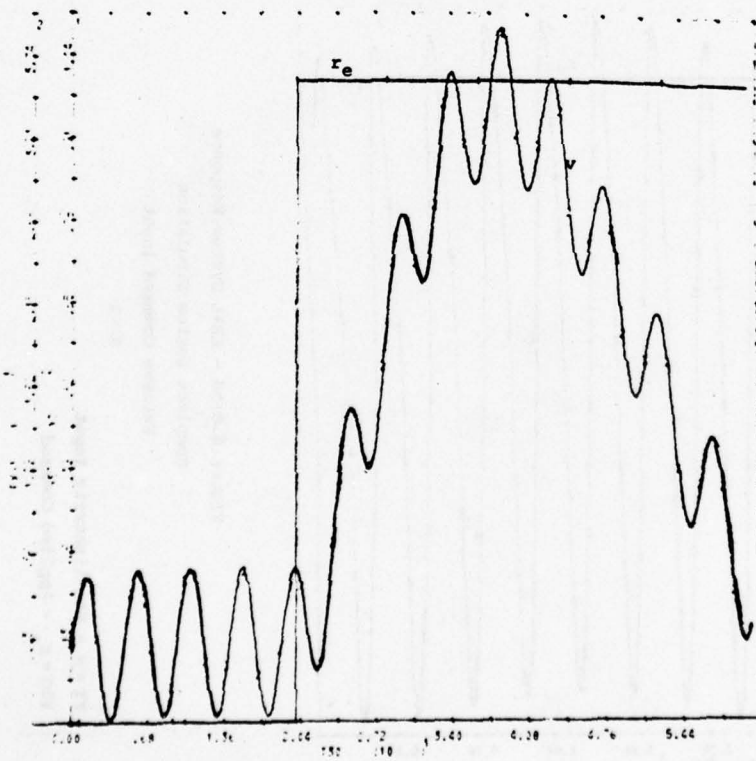


Figure 6.8-5b - EEAL System Response
Complete System Simulation
Extreme Command Input
 $K = 1$

FXG1 = v - Output of G_1
Y50 - Applied Command

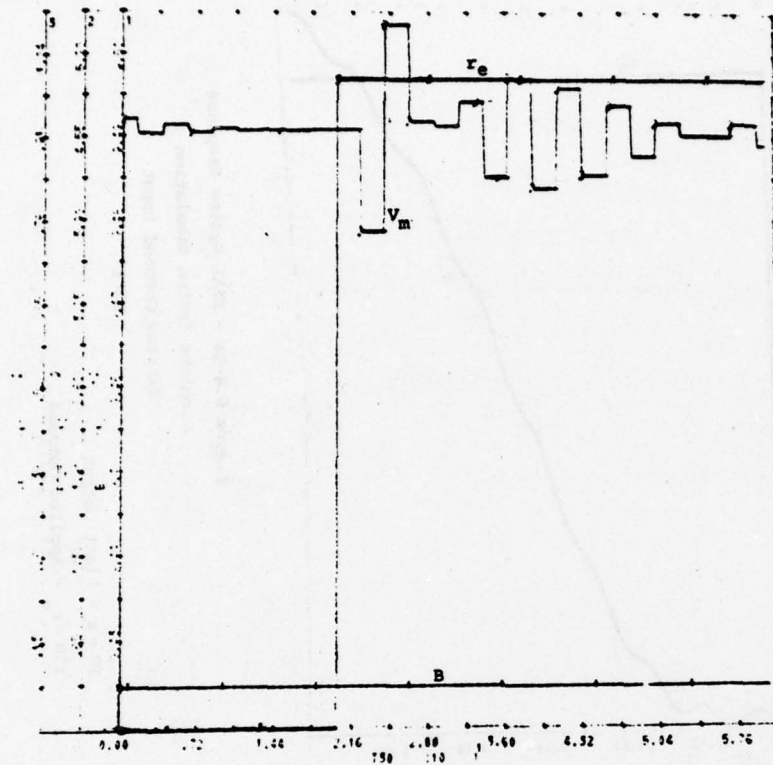


Figure 6.8-5c - EEAL System Response

Complete System Simulation

Extreme Command Input

$K = 1$

B - Non-linearity Saturation Level

FTS5 = V_m - Measured Amplitude

Y50 = r_e - Applied Command

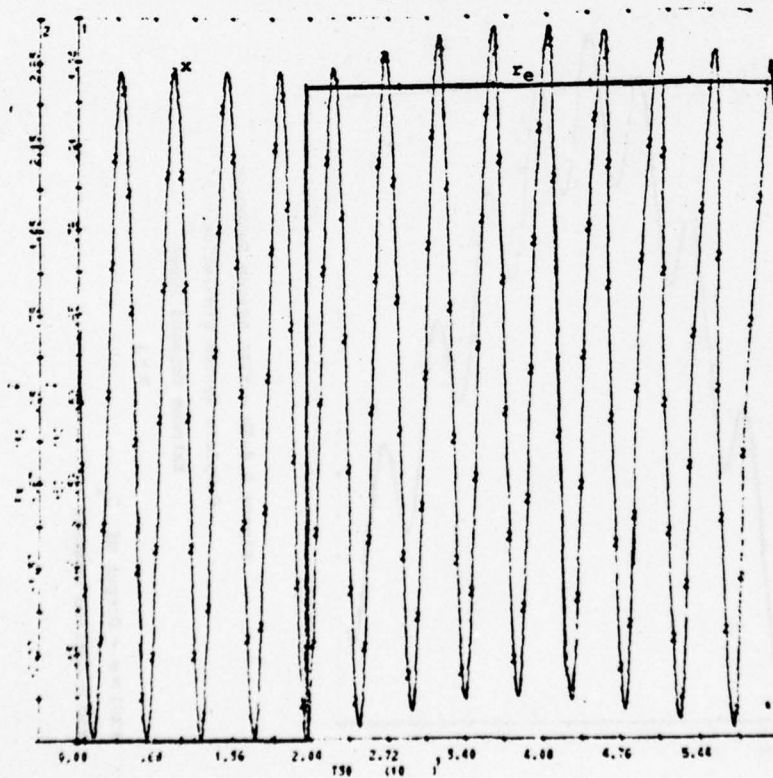


Figure 6.8-5d - EEAL System Response

Complete System Simulation

Extreme Command Input

$K = 1$

FX = x - Non-linearity Input

Y50 = r_e - Applied Command

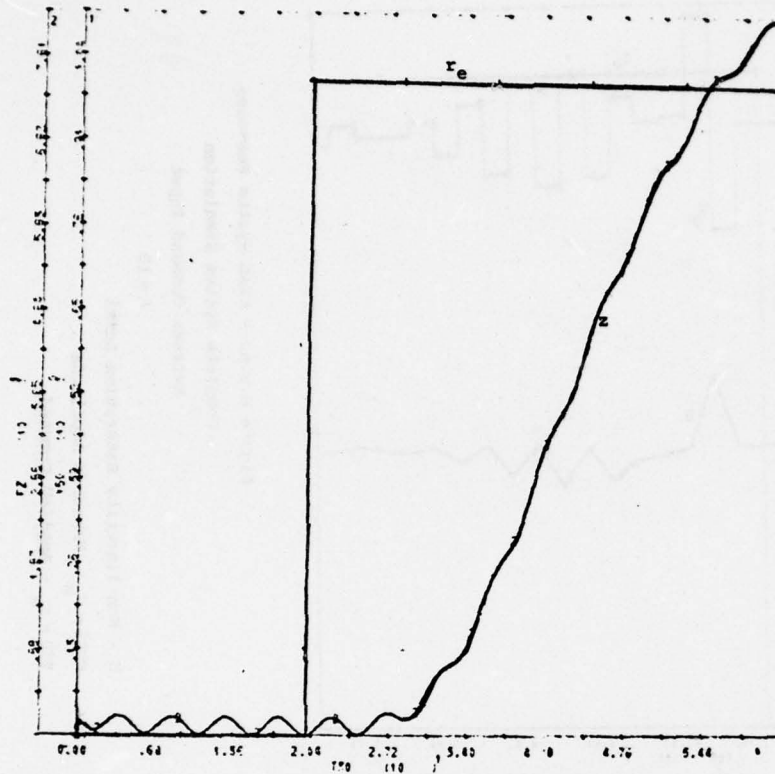


Figure 6.8-6a - EEAL System Response
Complete System Simulation
Extreme Command Input
 $K = 10$

$FZ = z$ - Plant Output
 $Y50 = r_e$ - Applied Command

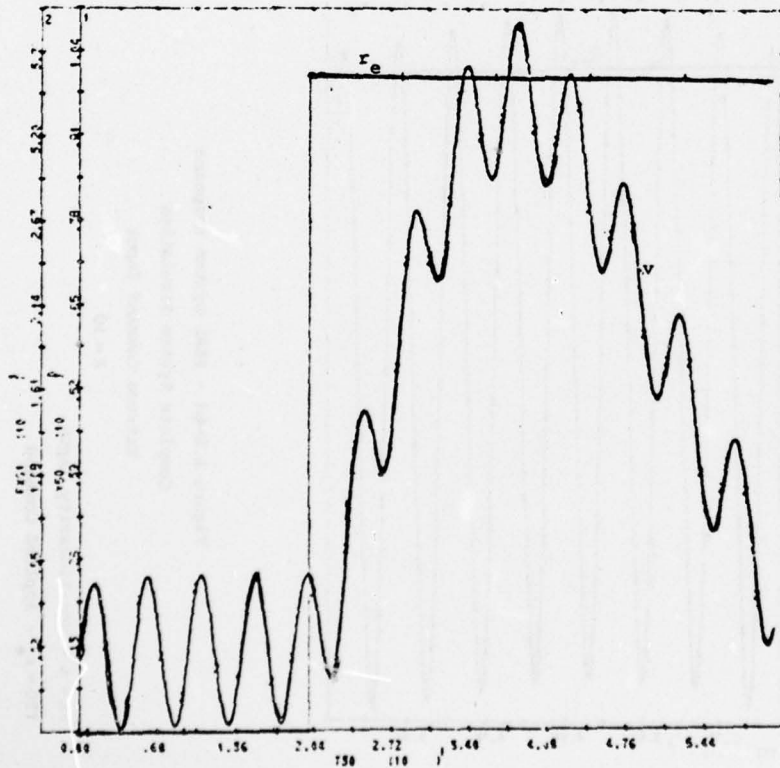


Figure 6.8-6b - EEAL System Response
Complete System Simulation
Extreme Command Input
 $K = 10$

$FXG1 = v$ - Output of G_1
 $Y50 = r_e$ - Applied Command

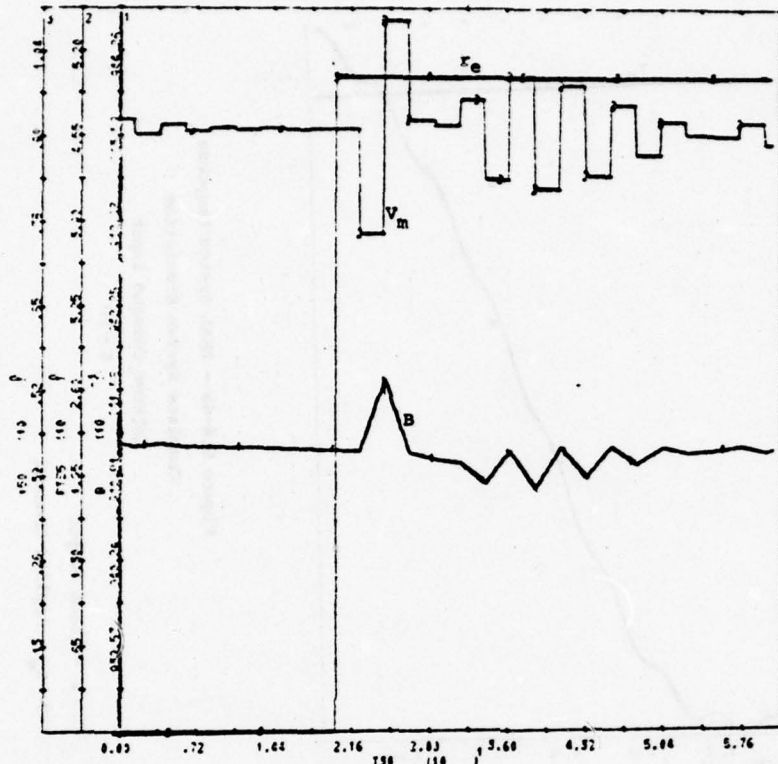


Figure 6.8-6c - EEAL System Response

Complete System Simulation

Extreme Command Input

$K = 10$

B - Non-linearity Saturation Level

$PTS5 = V_m$ - Measured Amplitude

$Y50 = r_e$ - Applied Command

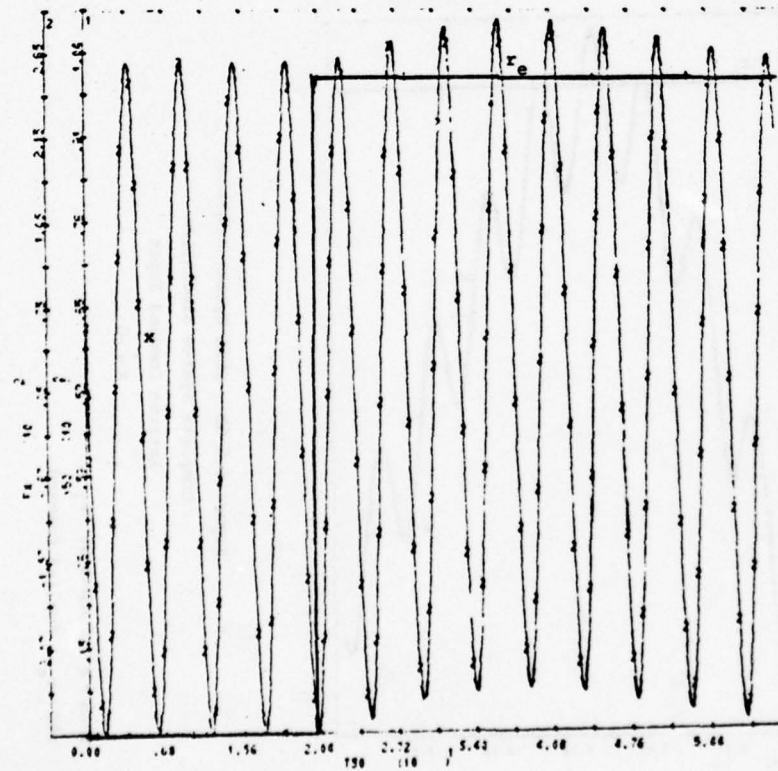


Figure 6.8-6d - EEAL System Response

Complete System Simulation

Extreme Command Input

$K = 10$

$PX = x$ - Non-linearity Input

$Y50 = r_e$ - Applied Command

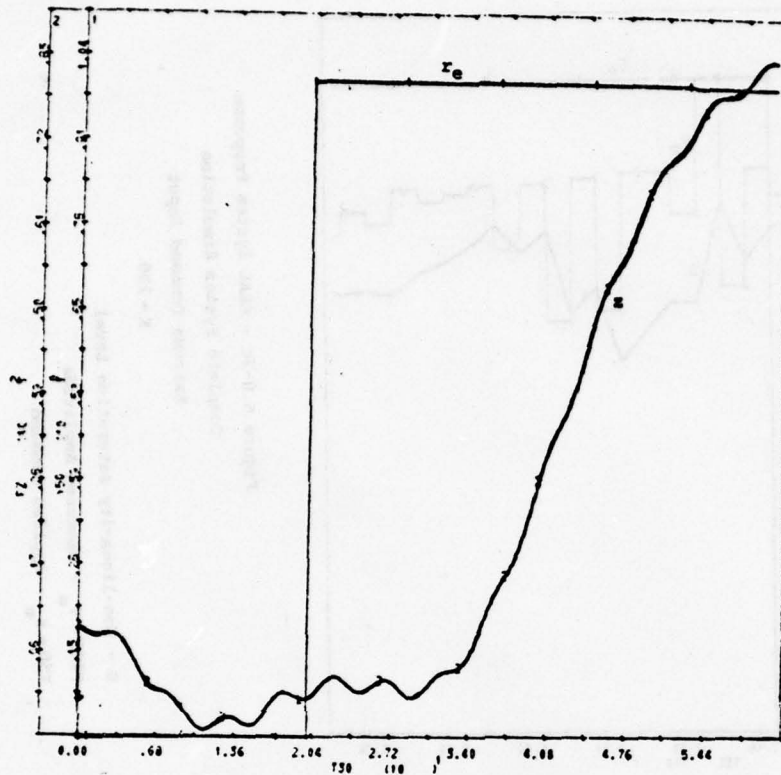


Figure 6.8-7a - EEAL System Response
Complete System Simulation
Extreme Command Input
 $K = 100$

$r_e = z$ - Plant Output
 $y_{50} = r_e$ - Applied Command

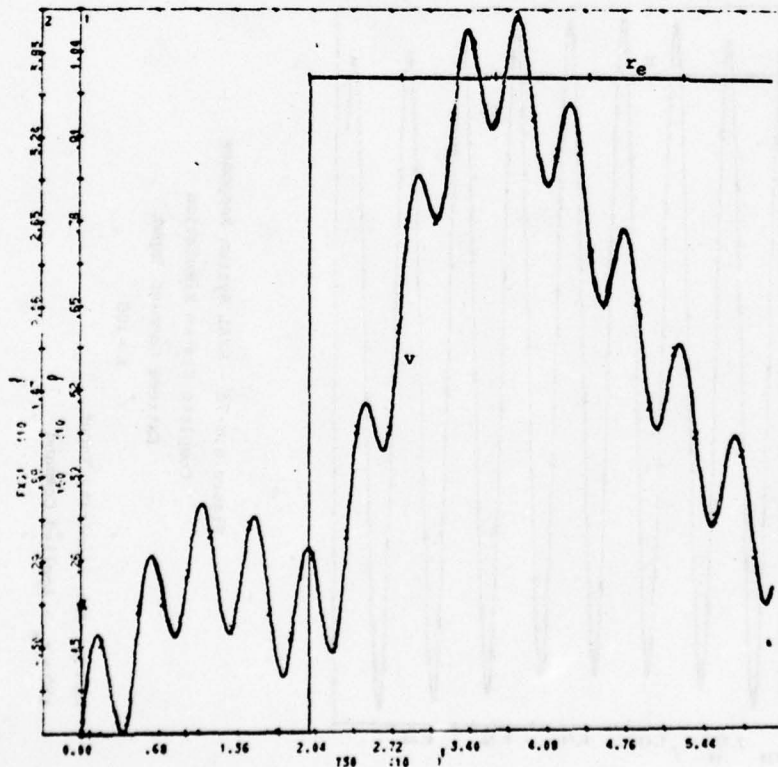


Figure 6.8-7b - EEAL System Response
Complete System Simulation
Extreme Command Input
 $K = 100$

$FXG1 = v$ - Output of G_1
 $y_{50} = r_e$ - Applied Command

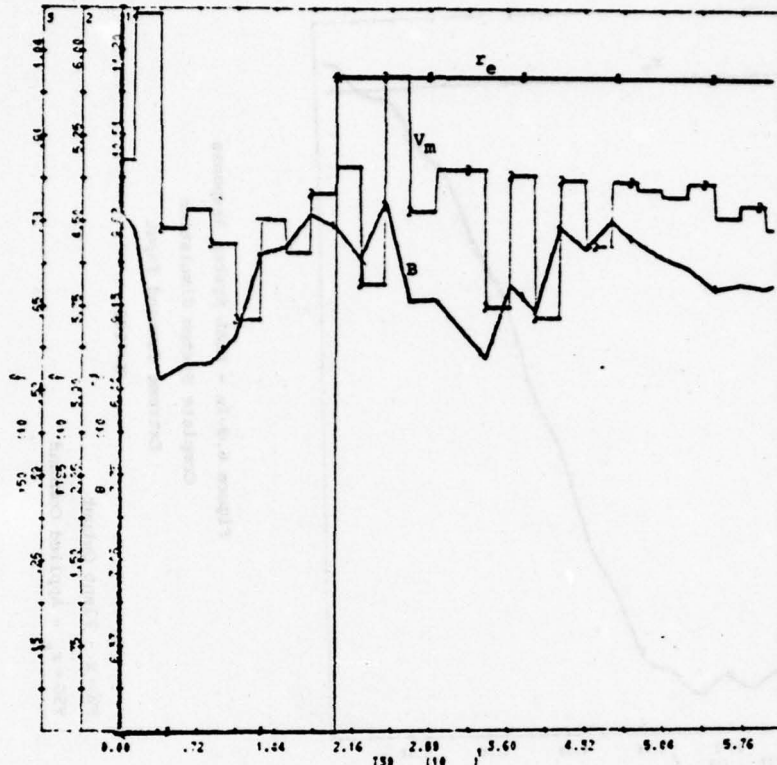


Figure 6.8-7c - EEAL System Response
Complete System Simulation
Extreme Command Input
K = 100

B - Non-linearity Saturation Level
FTS5 = v_m - Measured Amplitude
Y50 = r_e - Applied Command

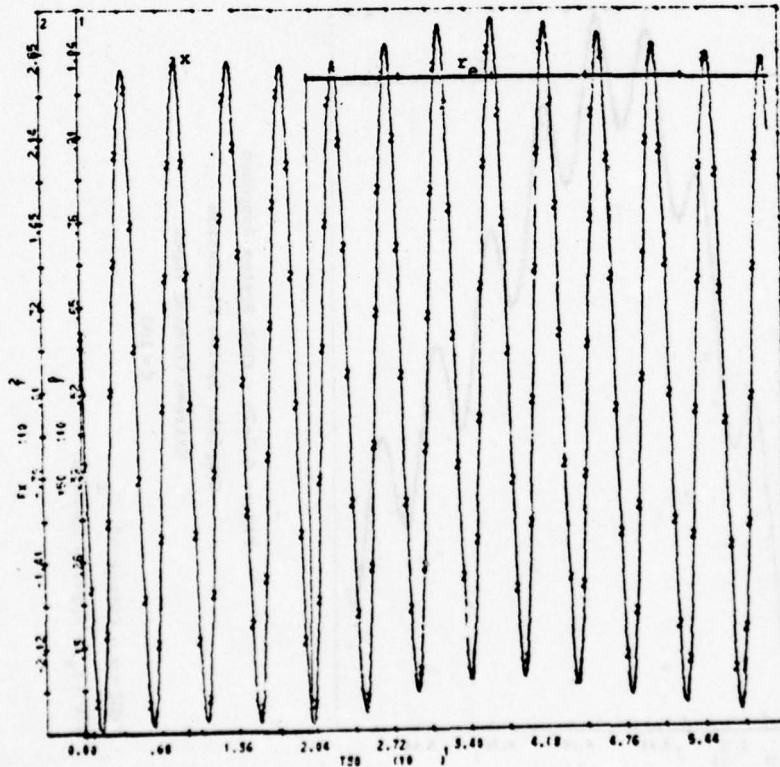


Figure 6.8-7d - EEAL System Response
Complete System Simulation
Extreme Command Input
K = 100

FX = x - Non-linearity Input
Y50 = r_e - Applied Command

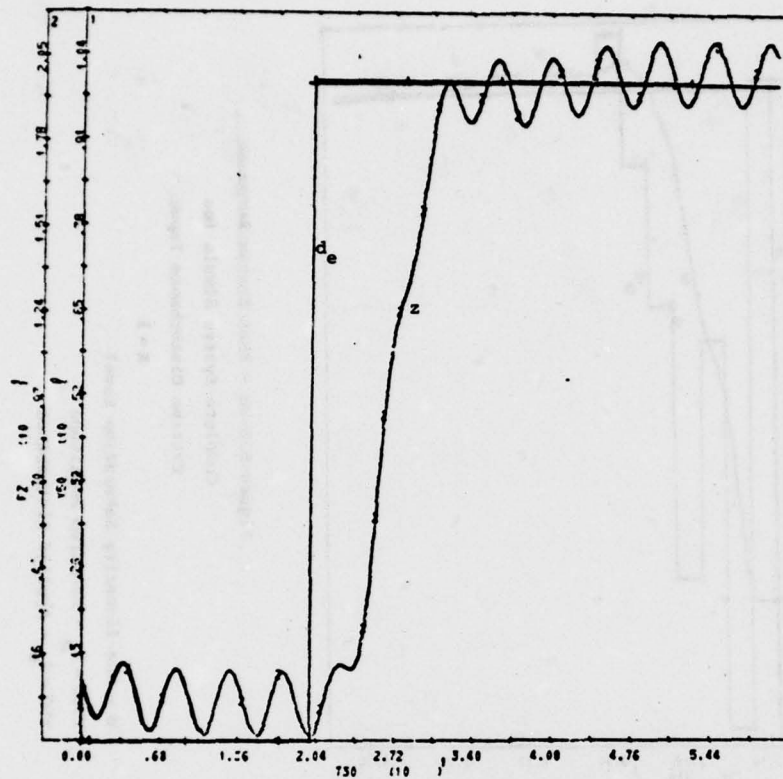


Figure 6.8-8a - EEAL System Response
Complete System Simulation
Extreme Disturbance Input
 $K = 1$

FZ = z - Plant Output
YSO = d_e - Applied Disturbance

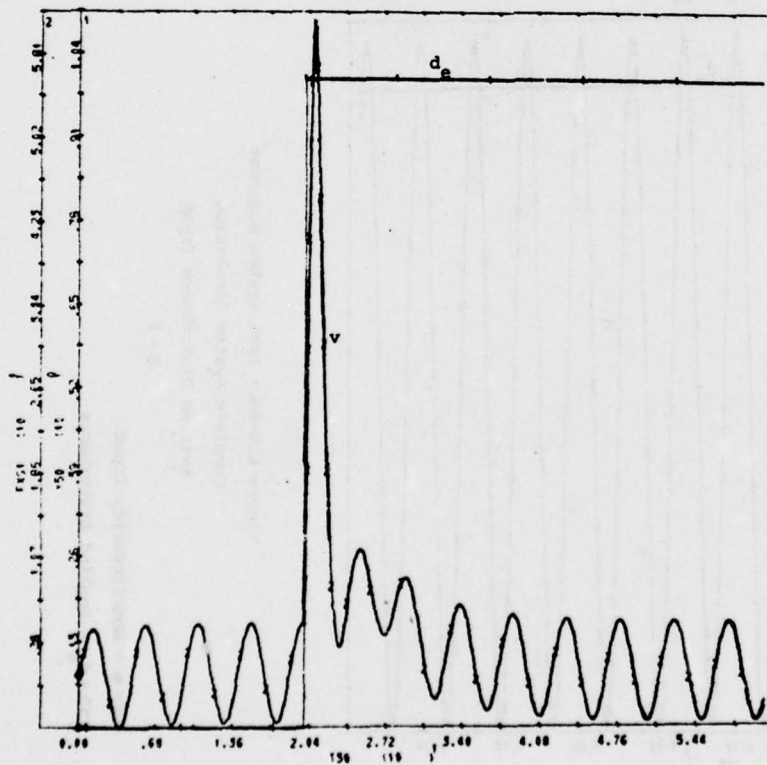
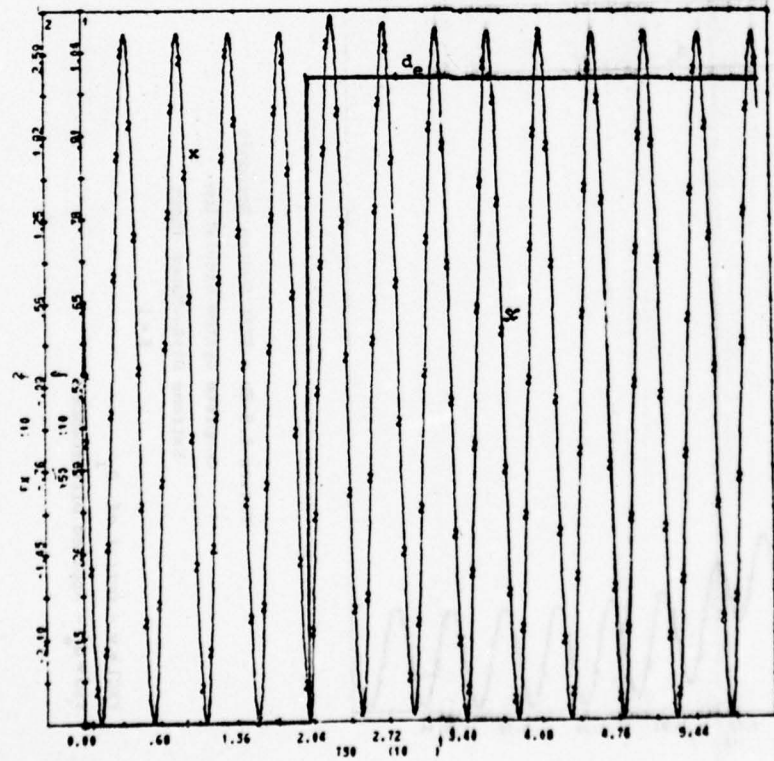
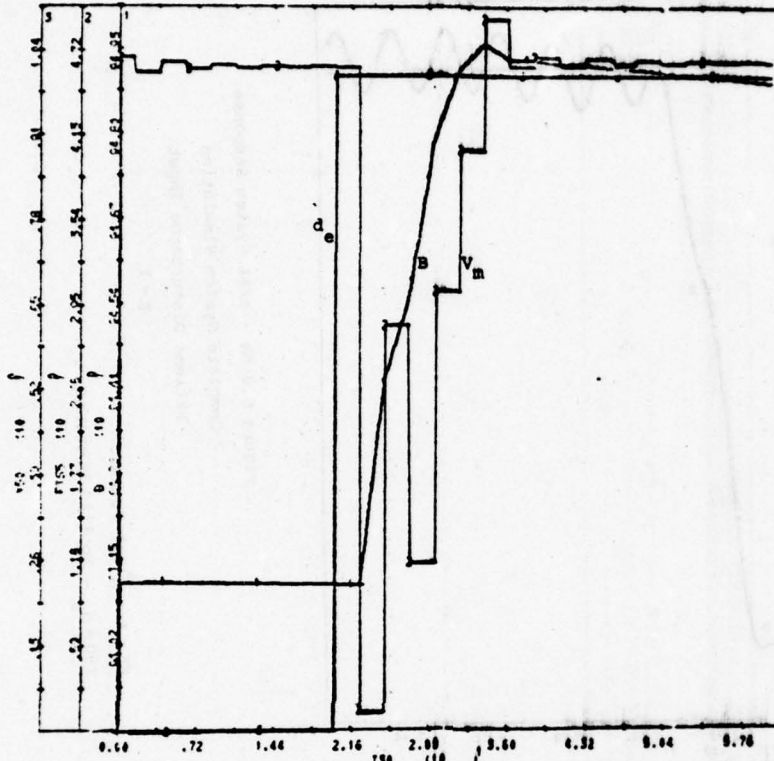


Figure 6.8-8b - EEAL System Response
Complete System Simulation
Extreme Disturbance Input
 $K = 1$

FXG1 = v - Output of G_1
YSO = d_e - Applied Disturbance



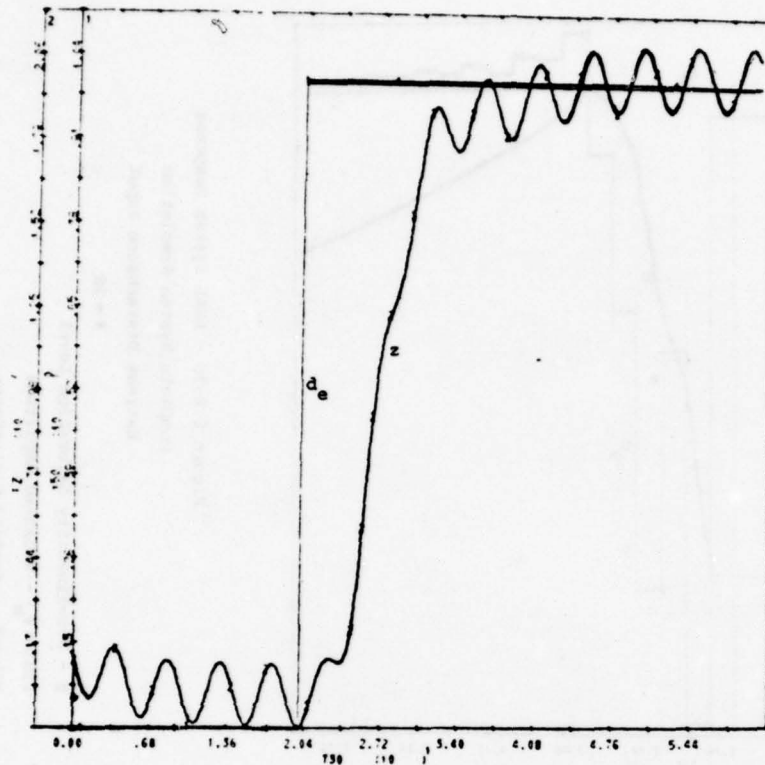


Figure 6.8-9a - EEAL System Response
Complete System Simulation
Extreme Disturbance Input
 $K=10$

$FZ = z$ - Plant Output
 $Y50 = d_e$ - Applied Disturbance

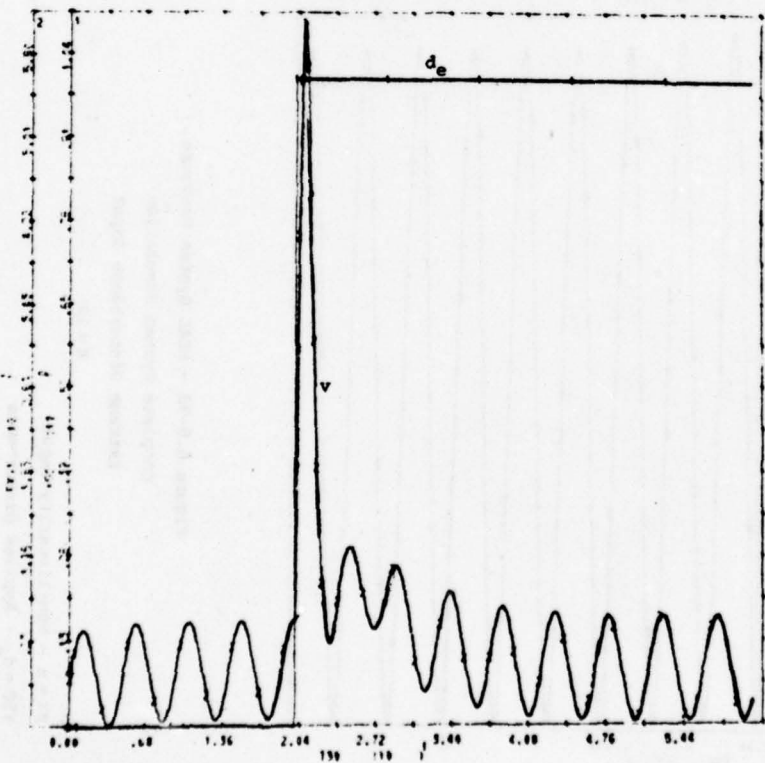


Figure 6.8-9b - EEAL System Response
Complete System Simulation
Extreme Disturbance Input
 $K=10$

$FXG1 = v$ - Output of G_1
 $Y50 = d_e$ - Applied Disturbance

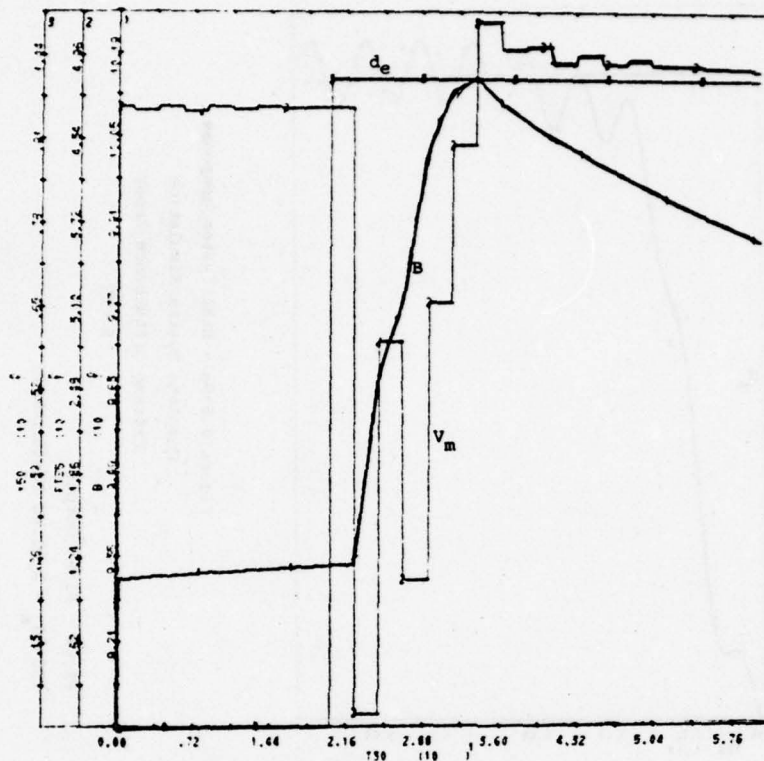


Figure 6.8-9c - EEAL System Response

Complete System Simulation

Extreme Disturbance Input

$K = 10$

B - Non-linearity Saturation Level

$FTS5 = V_m$ - Measured Amplitude

$Y50 = d_e$ - Applied Disturbance

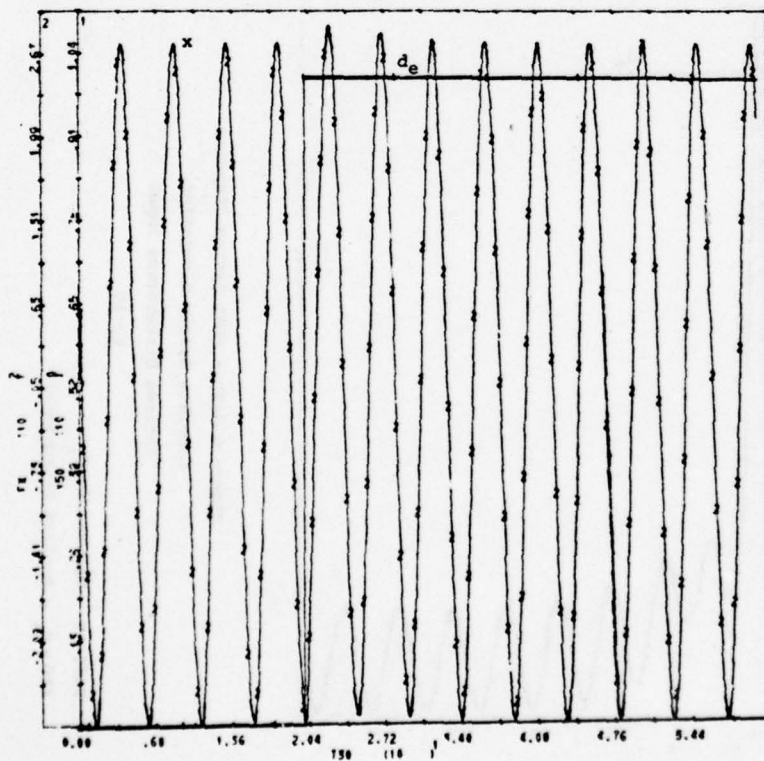


Figure 6.8-9d - EEAL System Response

Complete System Simulation

Extreme Disturbance Input

$K = 10$

$FX = x$ - Non-linearity Input

$Y50 = d_e$ - Applied Disturbance

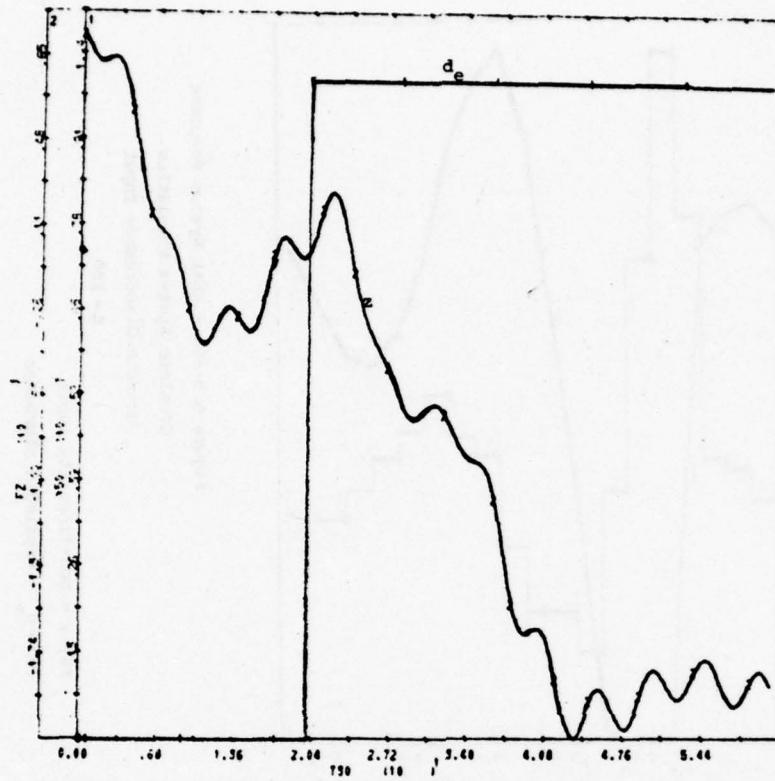


Figure 6.8-10a - EEAL System Response
Complete System Simulation
Extreme Disturbance Input
 $K = 100$

FZ = z - Plant Output

Y50 = d_e - Applied Disturbance

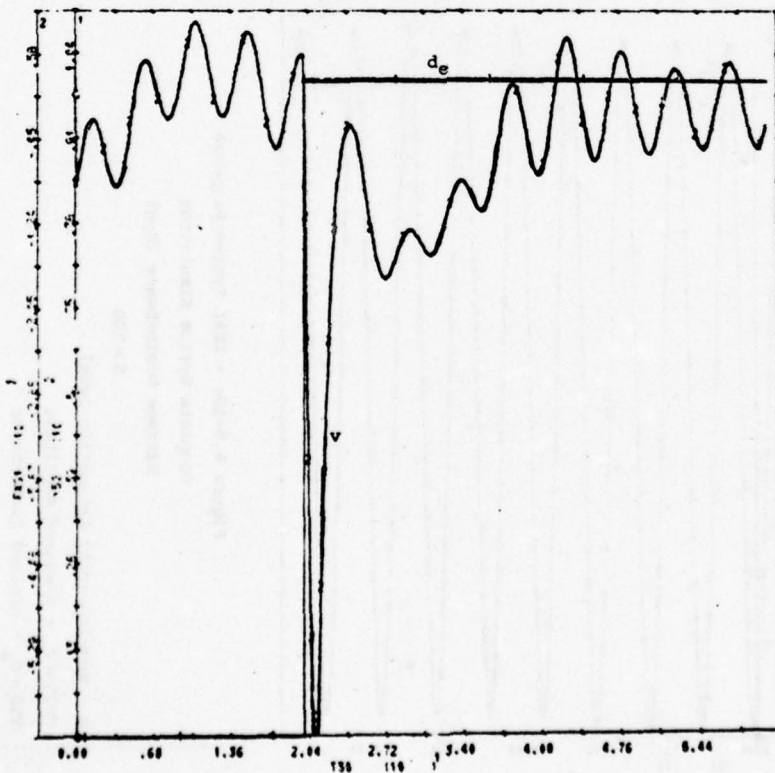


Figure 6.8-10b - EEAL System Response
Complete System Simulation
Extreme Disturbance Input
 $K = 100$

FXG1 = v - Output of G_1

Y50 = d_e - Applied Disturbance

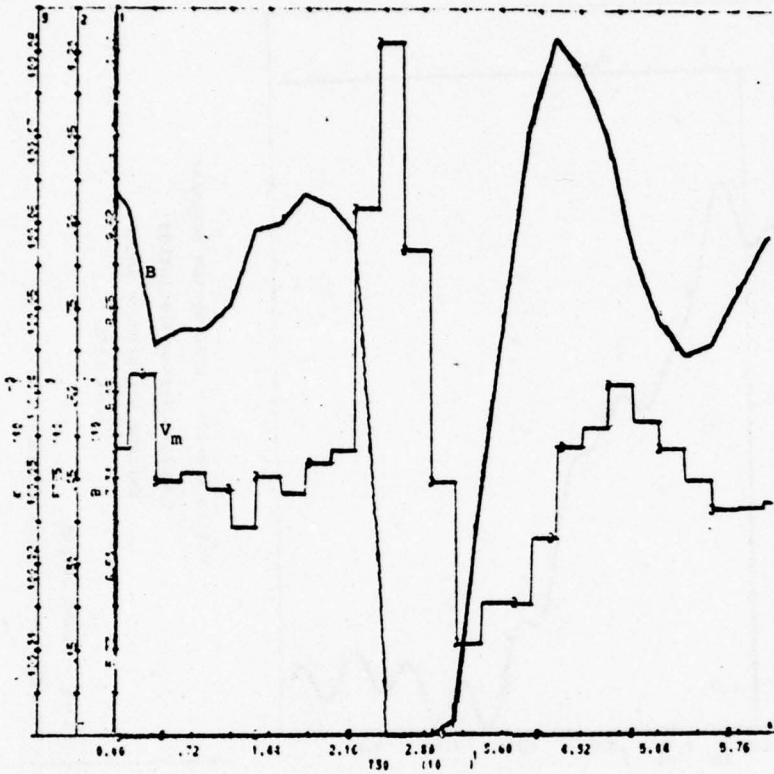


Figure 6.8-10c - EEAL System Response

Complete System Simulation
Extreme Disturbance Input

K = 100

B - Non-linearity Saturation Level

FTS5 = V_m - Measured Amplitude

Y50 = d_e - Applied Disturbance

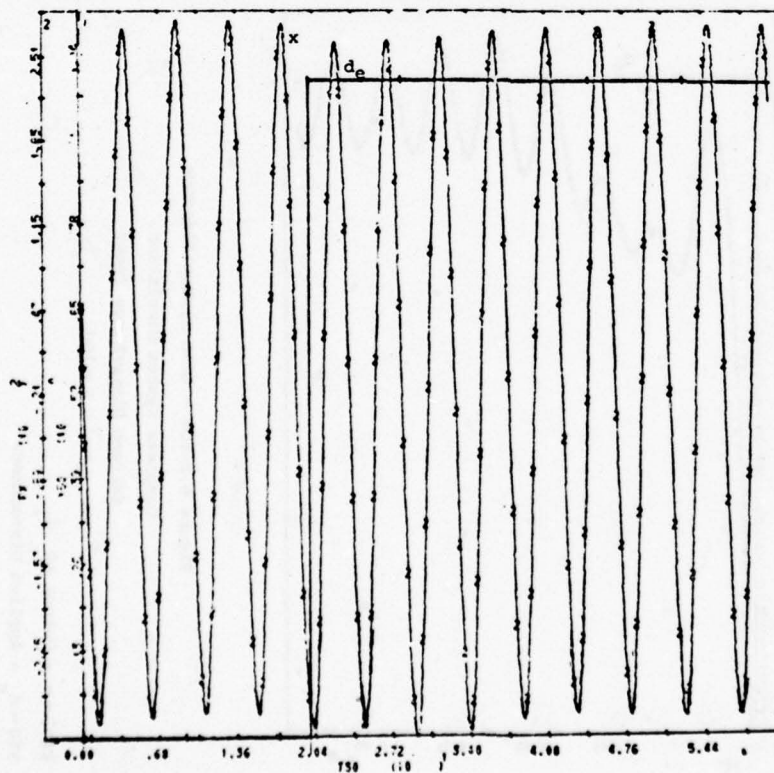


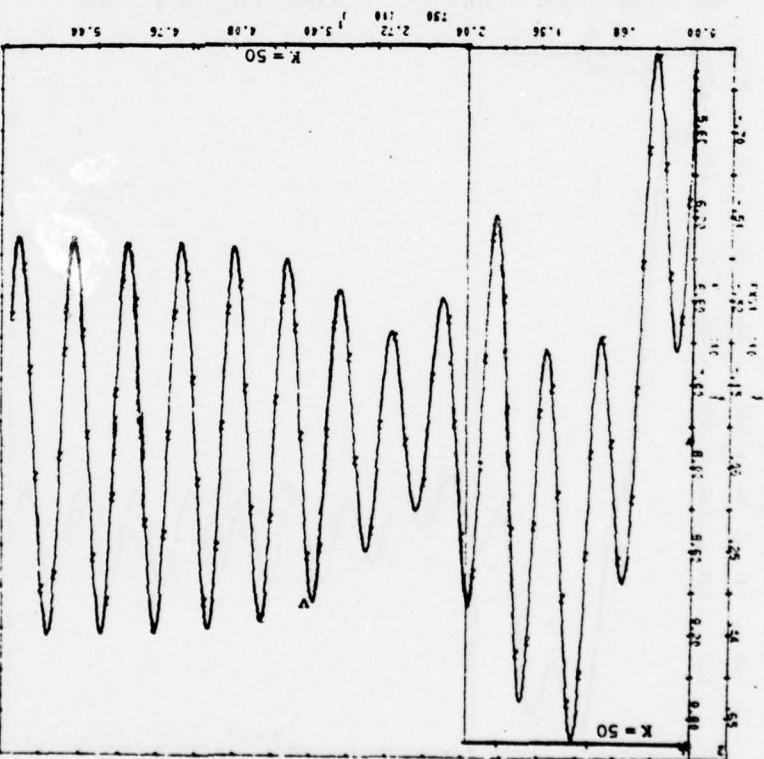
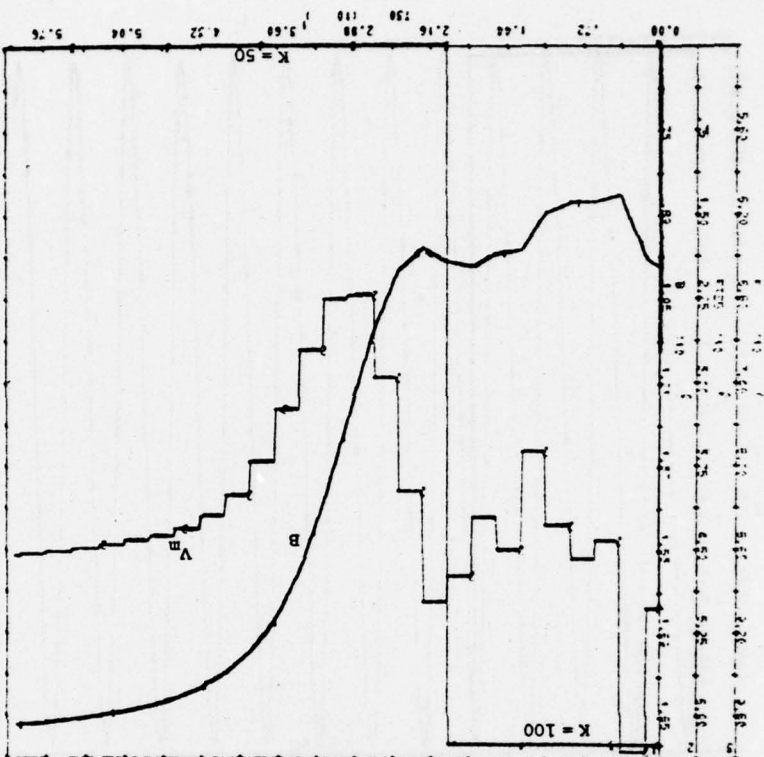
Figure 6.8-10d - EEAL System Response

Complete System Simulation
Extreme Disturbance Input

K = 100

FX = x - Non-linearity Input

Y50 = d_e - Applied Disturbance



B - Non-linearity Saturation Level
FTSS = V_m - Measured Amplitude
K - Plant Gain

FSG1 = v - Output of G_1
K - Plant Gain

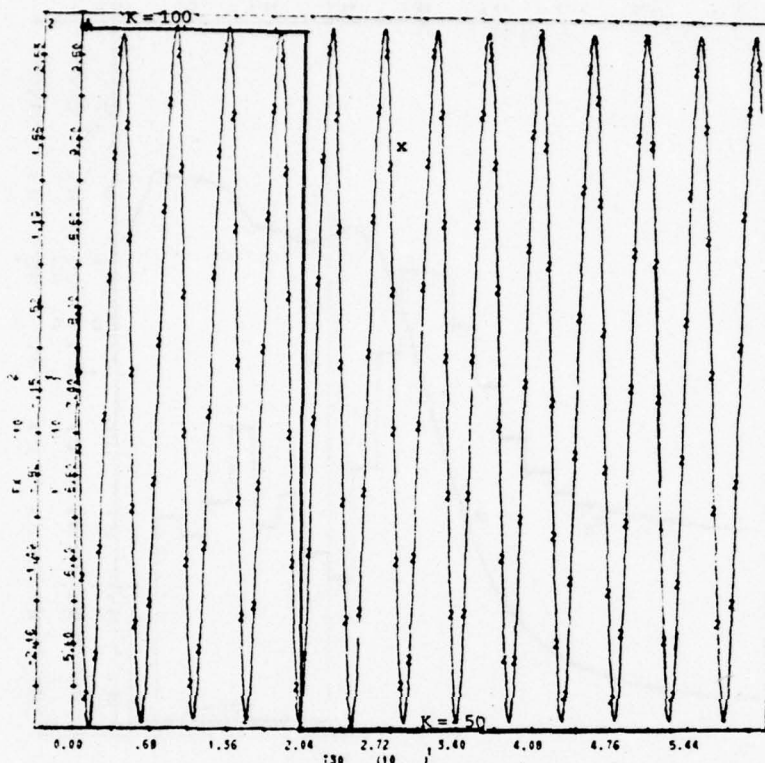


Figure 6.8-11c - EEAL System Response

Complete System Simulation
Dynamics of the Adjustment Loop

$$K_1 = 100, K_{f1} = 50$$

FX = x - Non-linearity Input

K - Plant Gain

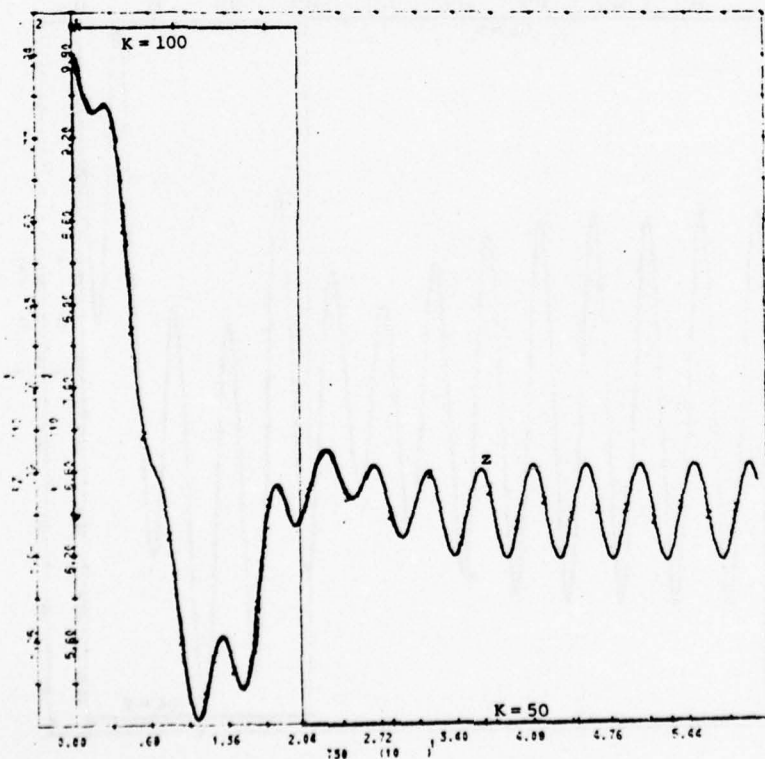


Figure 6.8-11d - EEAL System Response

Complete System Simulation
Dynamics of the Adjustment Loop

$$K_1 = 100, K_{f1} = 50$$

FZ = z - Plant Output

K - Plant Gain

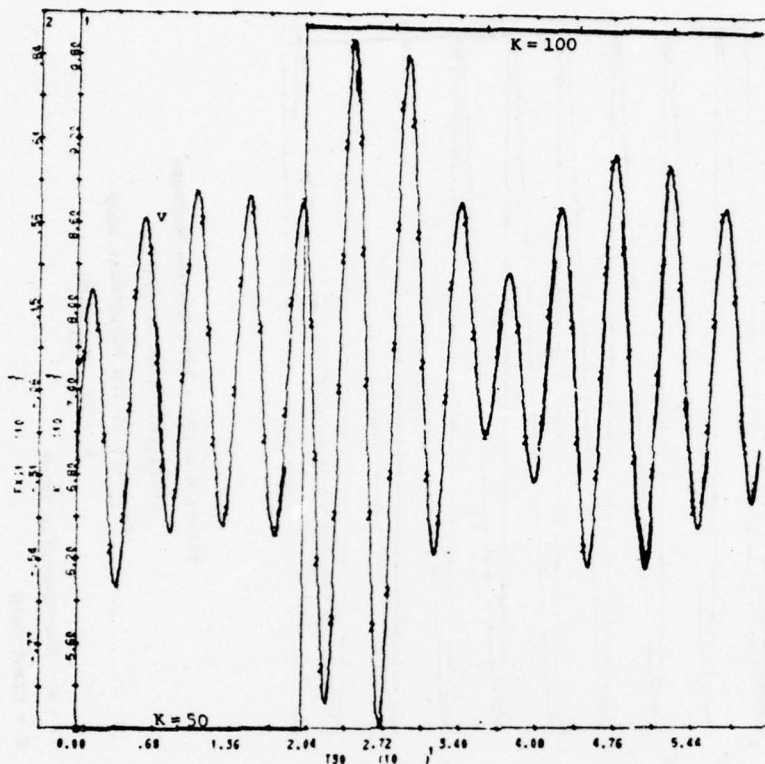


Figure 6.8-12a - EEAL System Response

Complete System Simulation

Dynamics of the Adjustment Loop

$K_i = 50$, $K_{f1} = 100$

FSGL = v - Output of G_1

K - Plant Gain

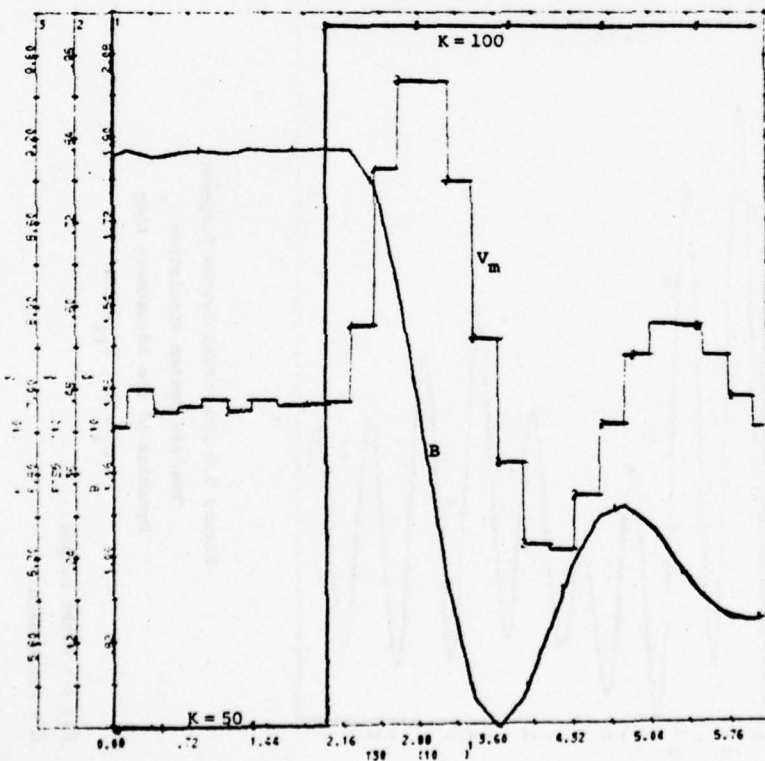


Figure 6.8-12b - EEAL System Response

Complete System Simulation

Dynamics of the Adjustment Loop

$K_i = 50$, $K_{f1} = 100$

B - Non-linearity Saturation Level

FTSS = V_m - Measured Amplitude

K - Plant Gain

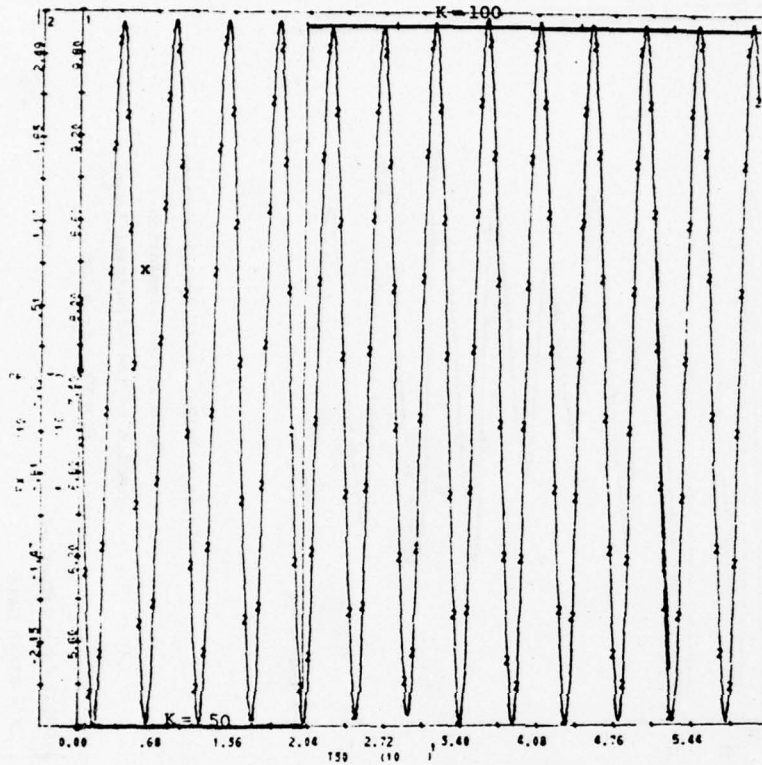


Figure 6.8-12c - EEAL System Response
Complete System Simulation
Dynamics of the Adjustment Loop
 $K_1 = 50$, $K_{fi} = 100$

FX = x - Non-linearity Input
K - Plant Gain

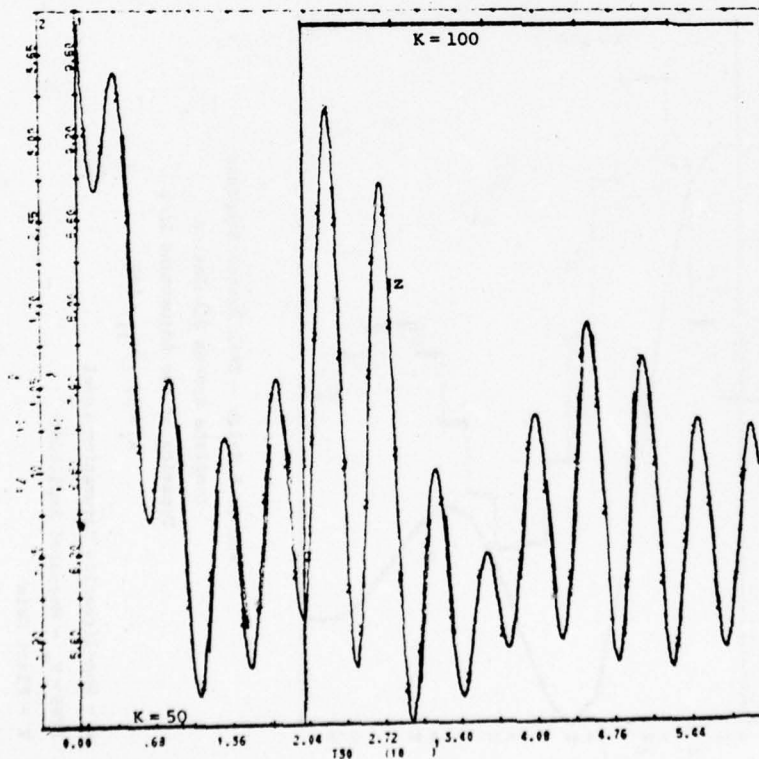


Figure 6.8-12d - EEAL System Response
Complete System Simulation
Dynamics of the Adjustment Loop
 $K_1 = 50$, $K_{fi} = 100$

FZ = z - Plant Output
K - Plant Gain

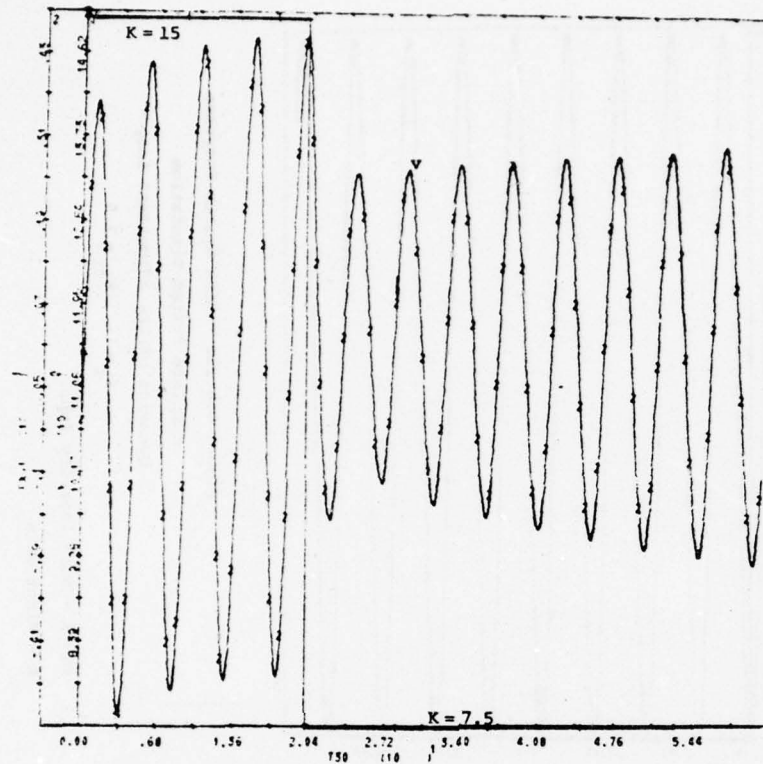


Figure 6.8-13a - EEAL System Response

Complete System Simulation

Dynamics of the Adjustment Loop

$K_i = 15$, $K_{fi} = 7.5$

FSGL = v - Output of G_1

K - Plant Gain

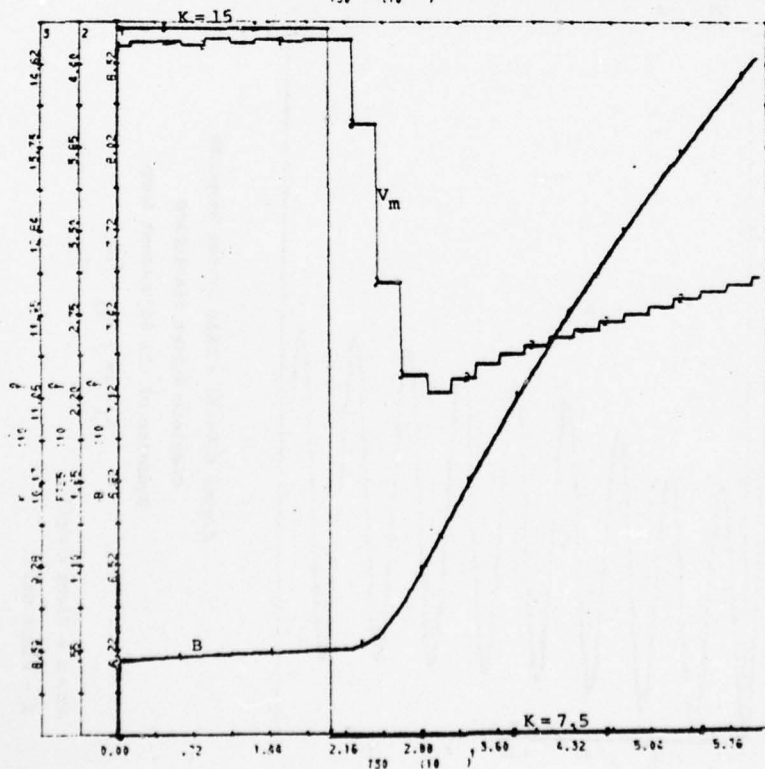


Figure 6.8-13b - EEAL System Response

Complete System Simulation

Dynamics of the Adjustment Loop

$K_i = 15$, $K_{fi} = 7.5$

B - Non-linearity Saturation Level

FTS5 = V_m - Measured Amplitude

K - Plant Gain

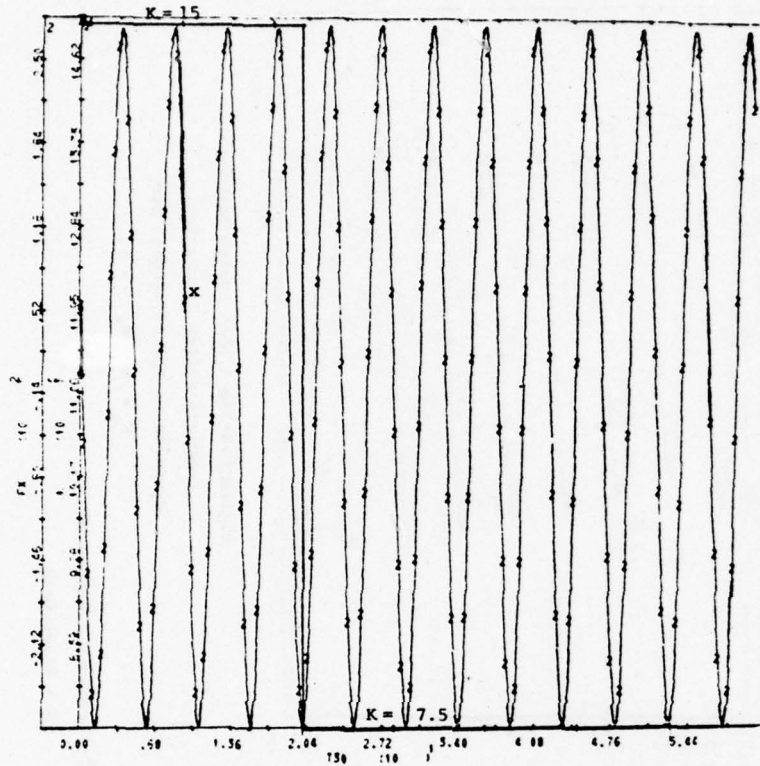


Figure 6.8-13c - EEAL System Response
Complete System Simulation
Dynamics of the Adjustment Loop

$K_1 = 15, K_{f1} = 7.5$

FX = x - Non-linearity Input

K - Plant Gain

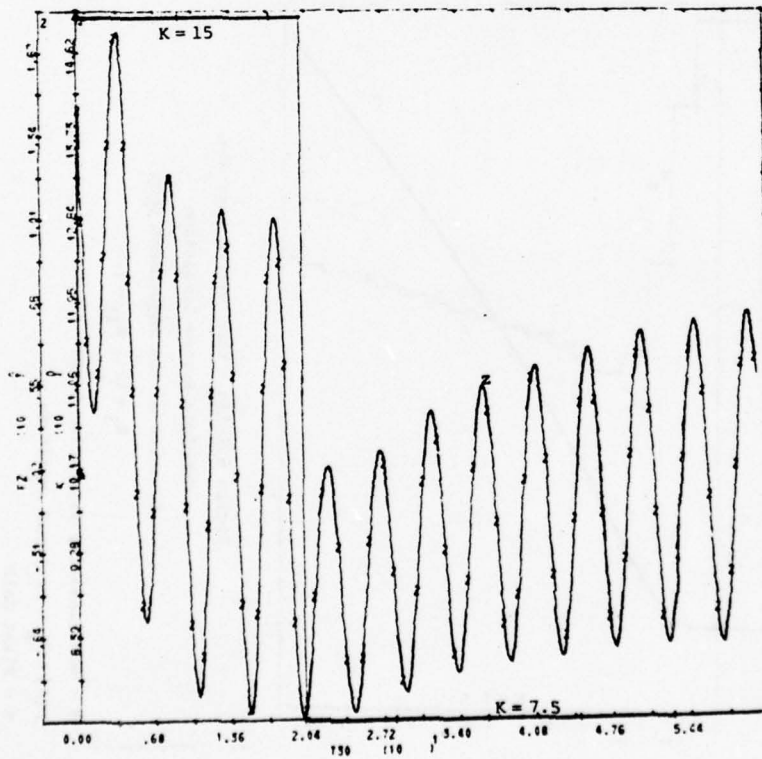


Figure 6.8-13d - EEAL System Response
Complete System Simulation
Dynamics of the Adjustment Loop

$K_1 = 15, K_{f1} = 7.5$

FZ = z - Plant Output

K - Plant Gain

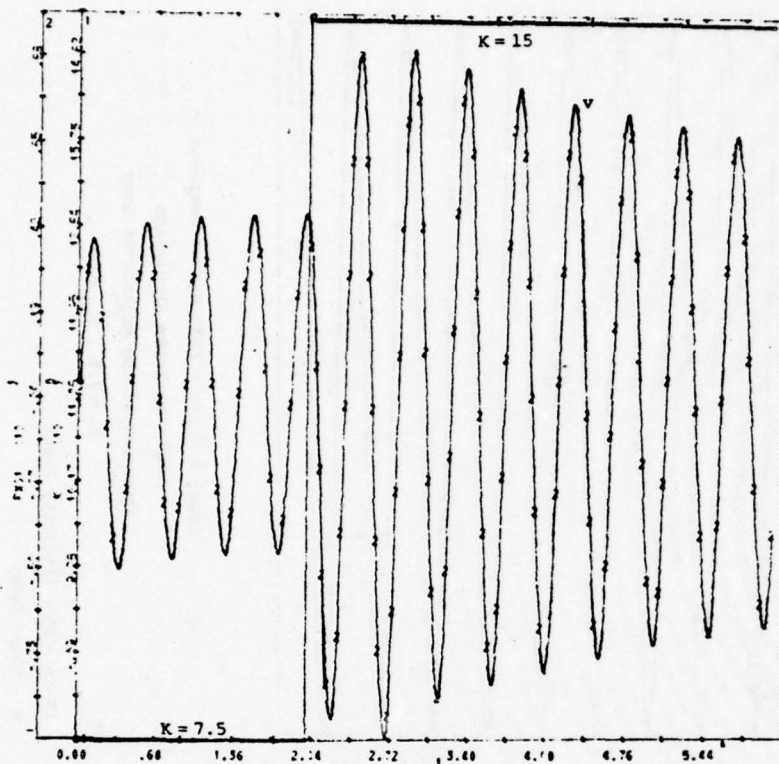


Figure 6.8-14a - EEAL System Response
Complete System Simulation
Dynamics of the Adjustment Loop
 $K_i = 7.5$, $K_{fi} = 15$

FSG1 = v - Output of G_1
K - Plant Gain

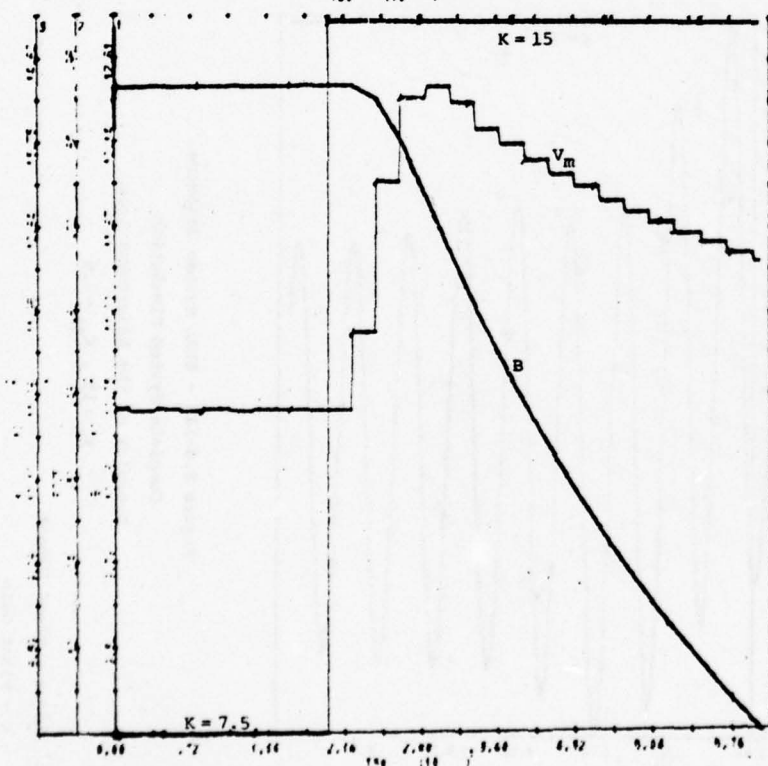


Figure 6.8-14b - EEAL System Response
Complete System Simulation
Dynamics of the Adjustment Loop
 $K_i = 7.5$, $K_{fi} = 15$

B - Non-linearity Saturation Level
FTS5 = v_m - Measured Amplitude
K - Plant Gain

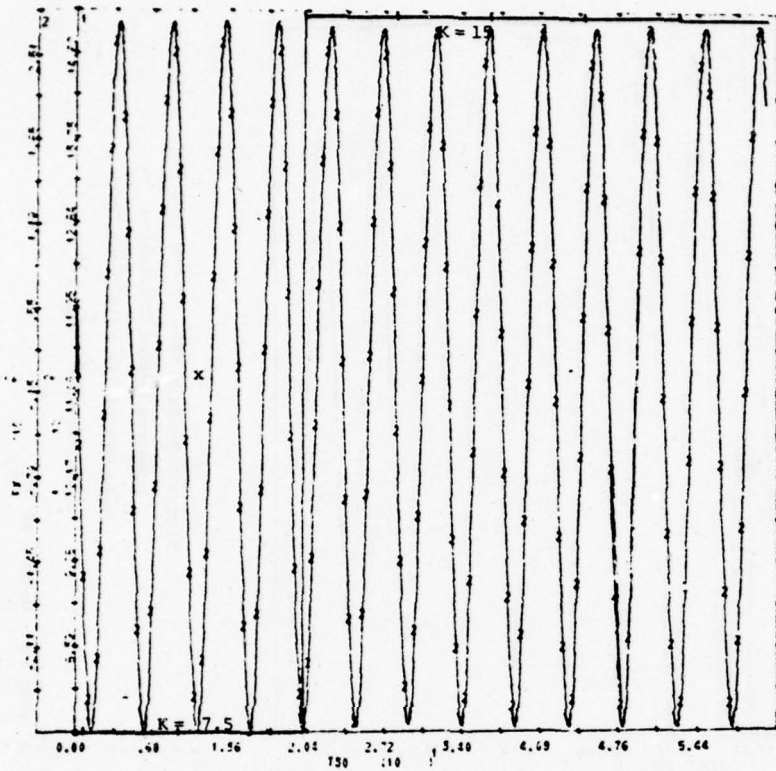


Figure 6.8-14c - EEAL System Response
Complete System Simulation
Dynamics of the Adjustment Loop

$K_1 = 7.5$, $K_{f1} = 15$

PX = x - Non-linearity Input

K - Plant Gain

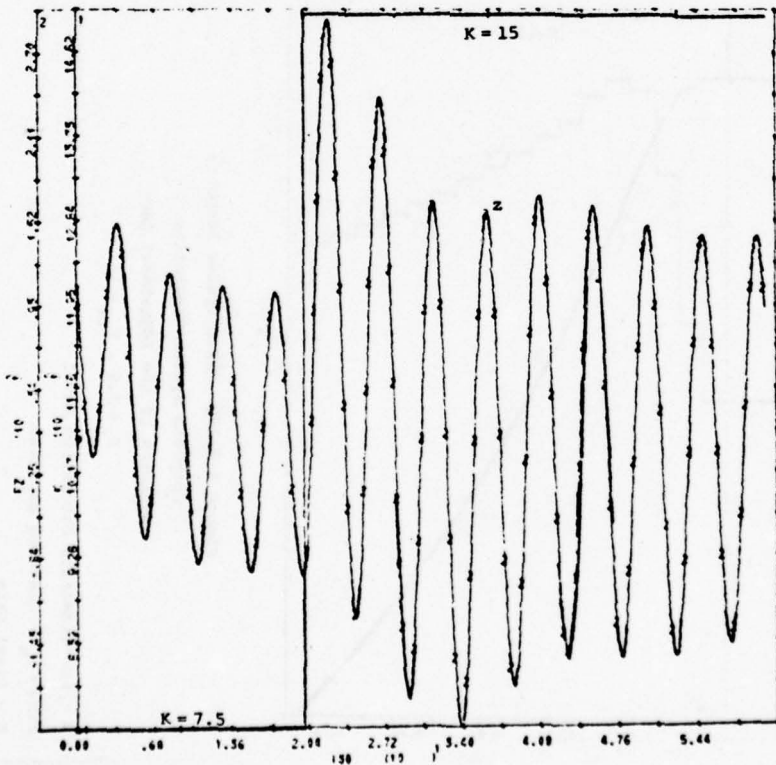


Figure 6.8-14d - EEAL System Response
Complete System Simulation
Dynamics of the Adjustment Loop

$K_1 = 15$, $K_{f1} = 7.5$

PZ = z - Plant Output

K - Plant Gain

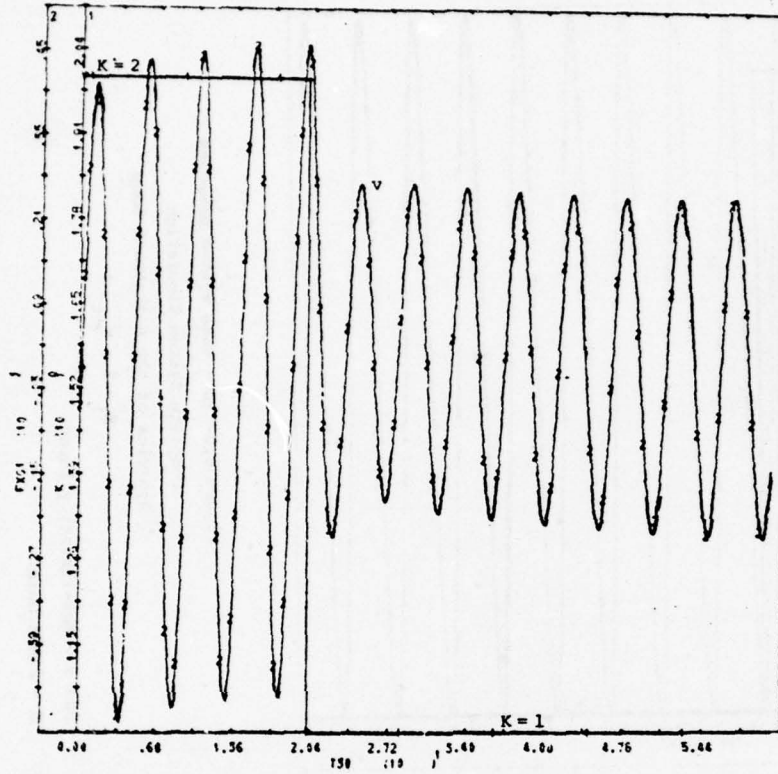


Figure 6.8-15a - EAL System Response
Complete System Simulation
Dynamics of the Adjustment Loop
 $K_1 = 2, K_{f1} = 1$

FSG1 = v - Output of G_1
 K - Plant Gain

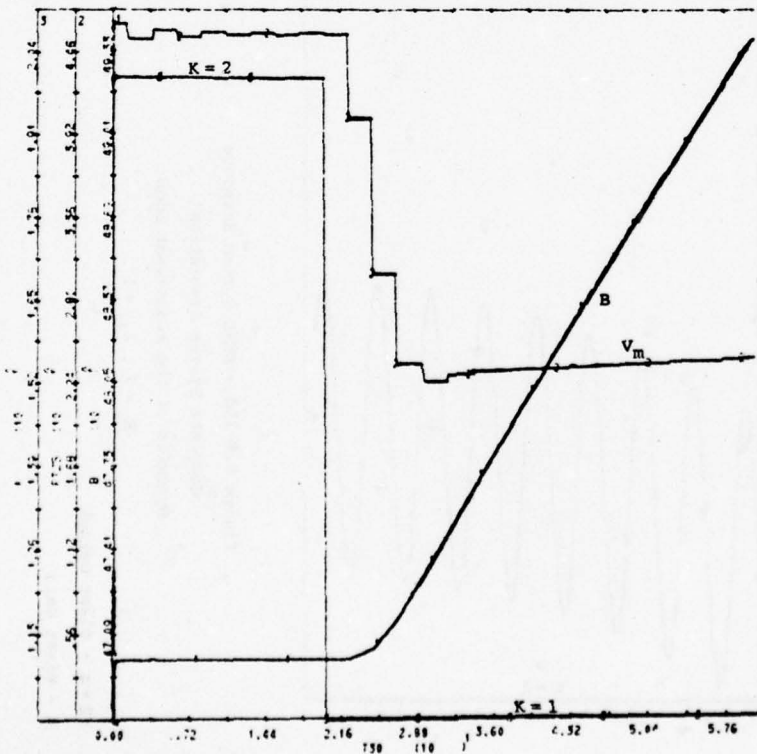


Figure 6.8-15b - EAL System Response
Complete System Simulation
Dynamics of the Adjustment Loop
 $K_1 = 2, K_{f1} = 1$

B - Non-linearity Saturation Level
 $FTS3 = v_m$ - Measured Amplitude
 K - Plant Gain

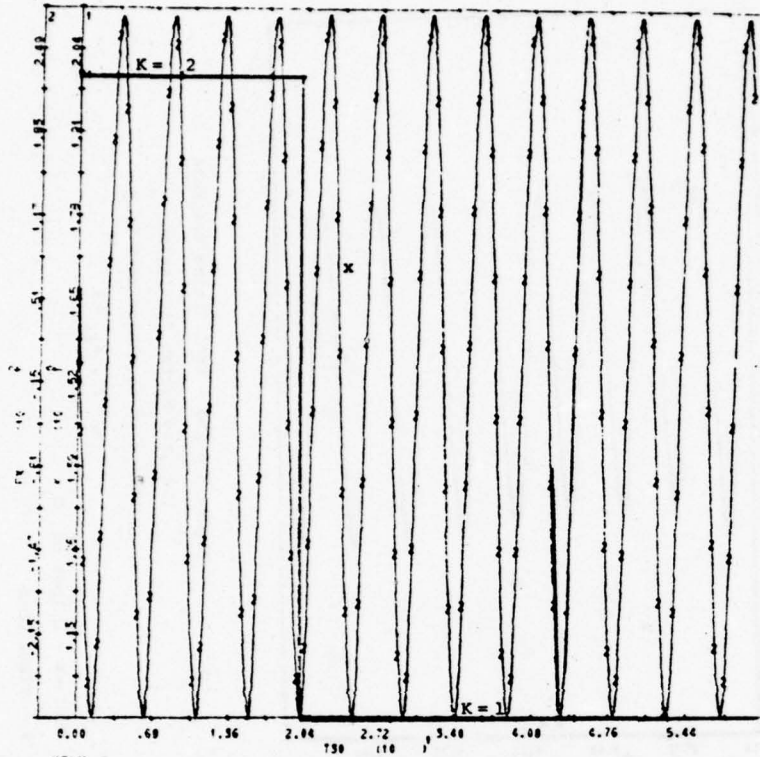


Figure 6.8-15c - EEAL System Response

Complete System Simulation

Dynamics of the Adjustment Loop

$$K_1 = 2, K_{f1} = 1$$

FX = x - Non-linearity Input

K - Plant Gain

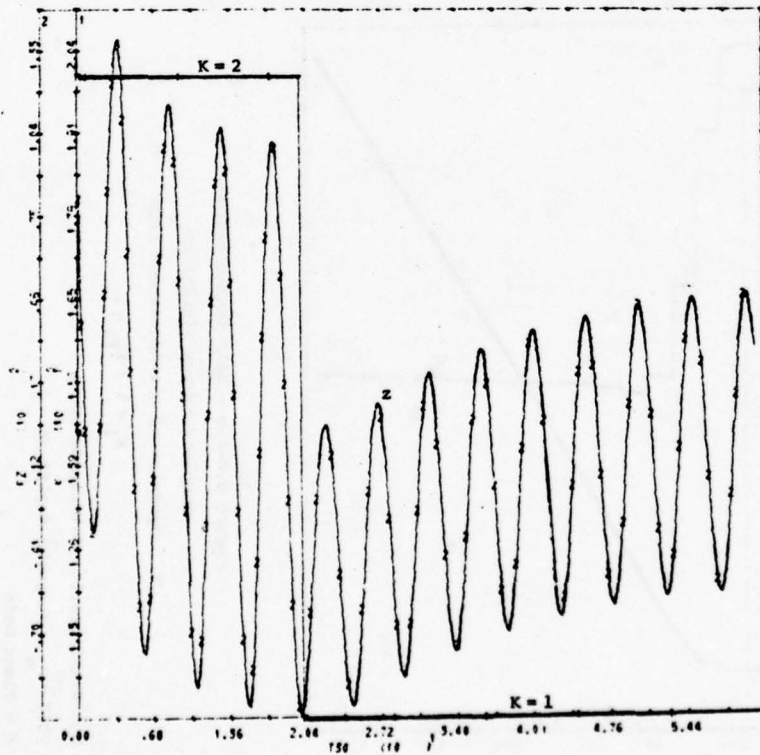


Figure 6.8-15d - EEAL System Response

Complete System Simulation

Dynamics of the Adjustment Loop

$$K_1 = 2, K_{f1} = 1$$

FZ = z - Plant Output

K - Plant Gain

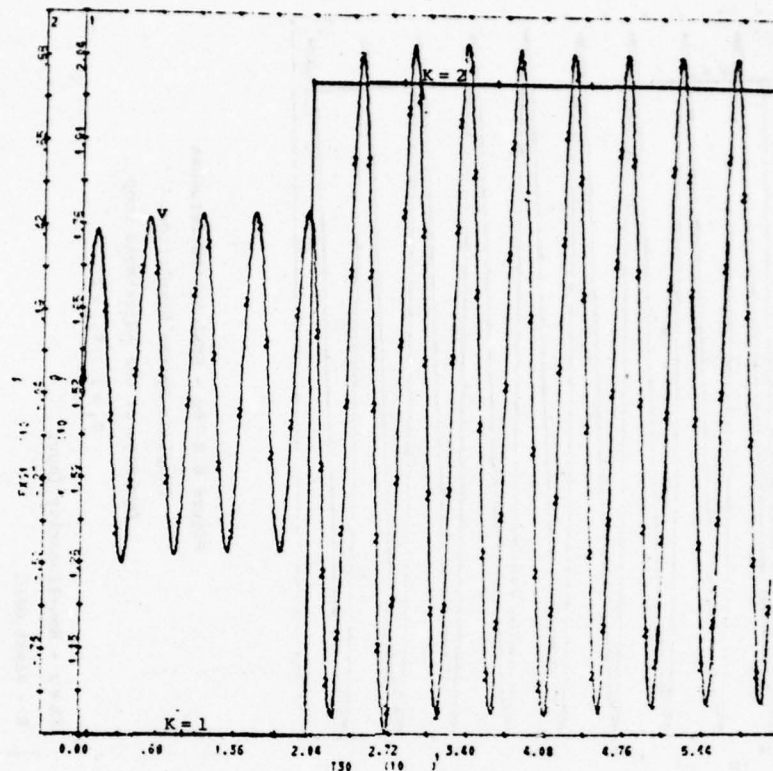


Figure 6.8-16a - EEAL System Response
Complete System Simulation
Dynamics of the Adjustment Loop

$$K_i = 1, K_{ff} = 2$$

FSGL = v - Output of G_1
K - Plant Gain

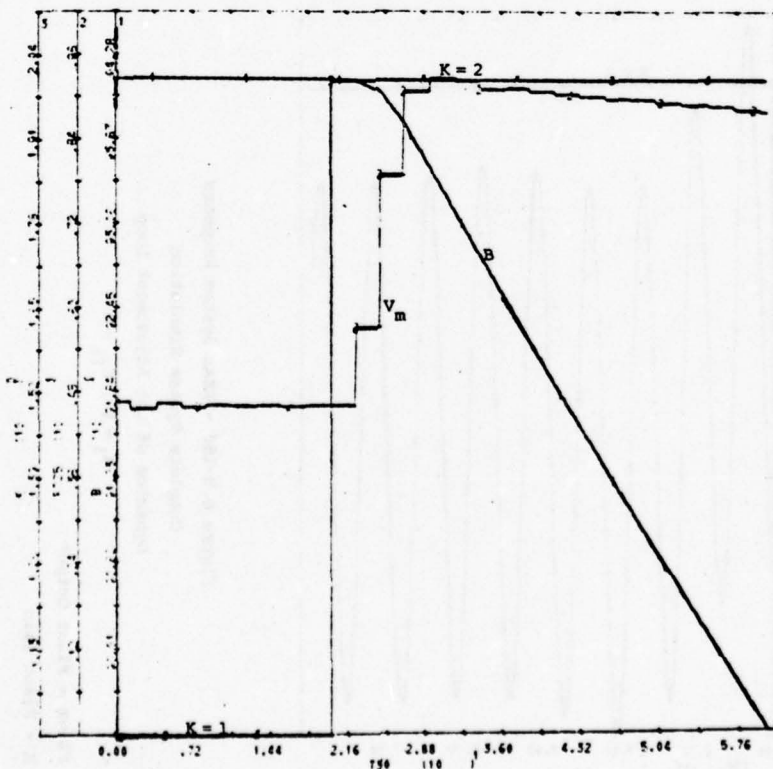


Figure 6.8-16b - EEAL System Response
Complete System Simulation
Dynamics of the Adjustment Loop

$$K_i = 1, K_{ff} = 2$$

B - Non-linearity Saturation Level
FTSS = v_m - Measured Amplitude
K - Plant Gain

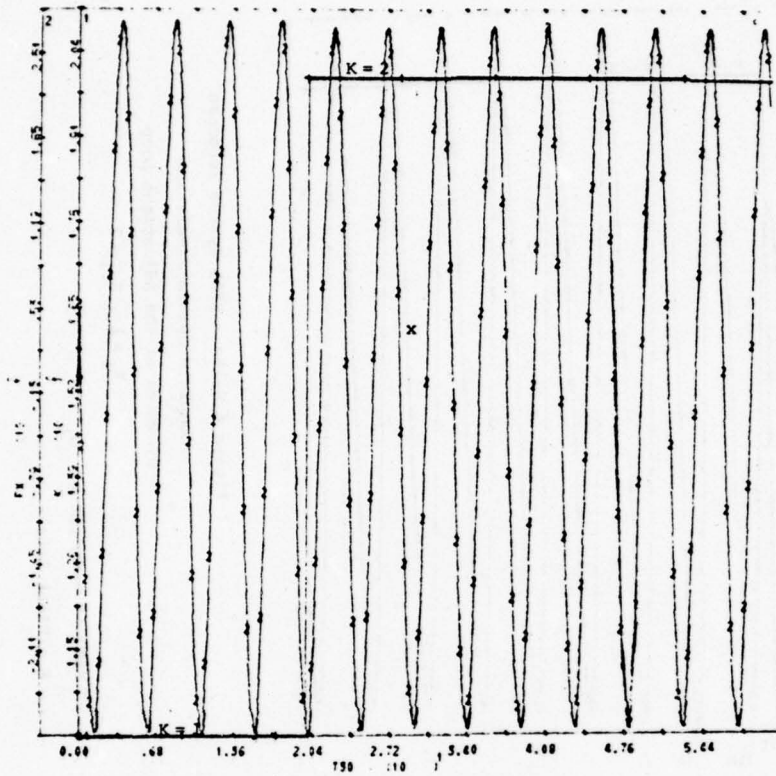


Figure 6.8-16c - EEAL System Response
Complete System Simulation
Dynamics of the Adjustment Loop
 $K_1 = 1, K_{fi} = 2$

FX = x - Non-linearity Input
K - Plant Gain

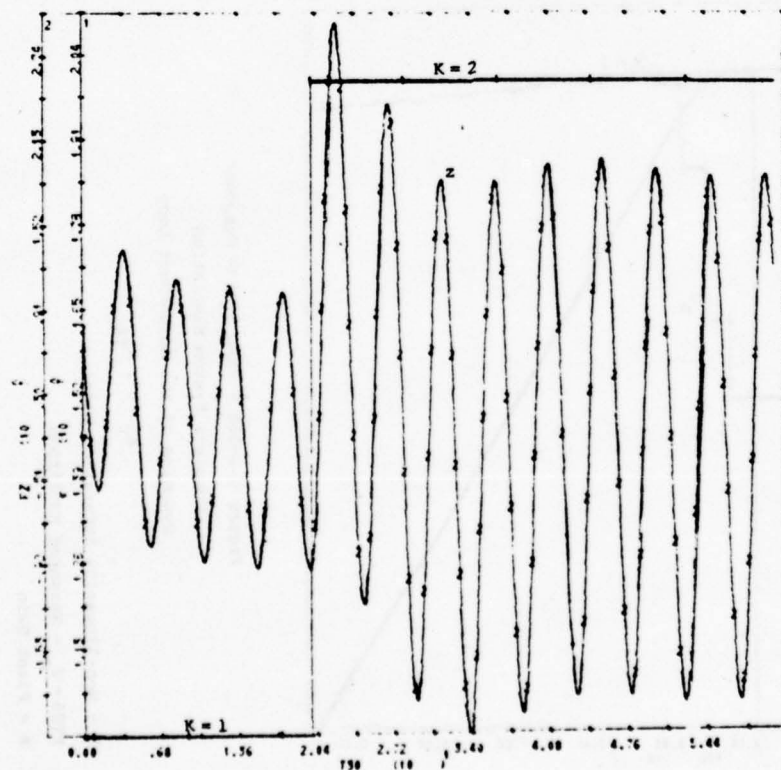


Figure 6.8-16d - EEAL System Response
Complete System Simulation
Dynamics of the Adjustment Loop
 $K_1 = 1, K_{fi} = 2$

FZ = z - Plant Output
K - Plant Gain

CHAPTER SEVEN

E.E.A.N.L.

(EEAL with a Non-linearity in the Secondary Loop)

7.1 General

Chapter 6 dealt with the EEAL structure, which presented significant advantages over all the other structures. The EEAL was able to cope with almost any problem, with respect to the extreme command and (mainly) disturbance response. The limitation is due to the capability of measuring the amplitude V of an oscillating signal $v_o(t)$, combined with an aperiodic signal $v_f(t)$, which can be much larger than the oscillation amplitude. The main disadvantage of the EEAL is the "reappearance" of the factor K , gain of the plant, in the secondary loop, which determines the rate of adaptation of the system. The later is given by Equation 6.5-9, repeated here.

$$\frac{\Delta B}{\Delta V}(s) \approx \frac{-\psi(s) e^{-T_o s}}{1 + \frac{4}{\pi} G_1 G_2 P_h \psi(s) K e^{-T_o s}} \quad (7.1-1)$$

The idea of the EEANL is to keep the advantages of the EEAL, and "eliminate" the factor K from the secondary loop, in Equation 7.1-1 denominator. The increment $EEAL \rightarrow EEANL$, is basically the same as the $SOAL \rightarrow SOANL$ one.

The "elimination" of K in Equation 7.1-1 could be achieved by introducing a multiplier in the secondary loop, with multiplication factor inversely proportional to K . But K is not available directly, so B , which is related to K , can be used, since in the steady state KB is constant, as per Equation 6.2-10.

Figure 7.1-1 represents the EEANL structure which, if compared with the EEAL in Figure 6.2-2, includes a multiplier in the secondary loop.

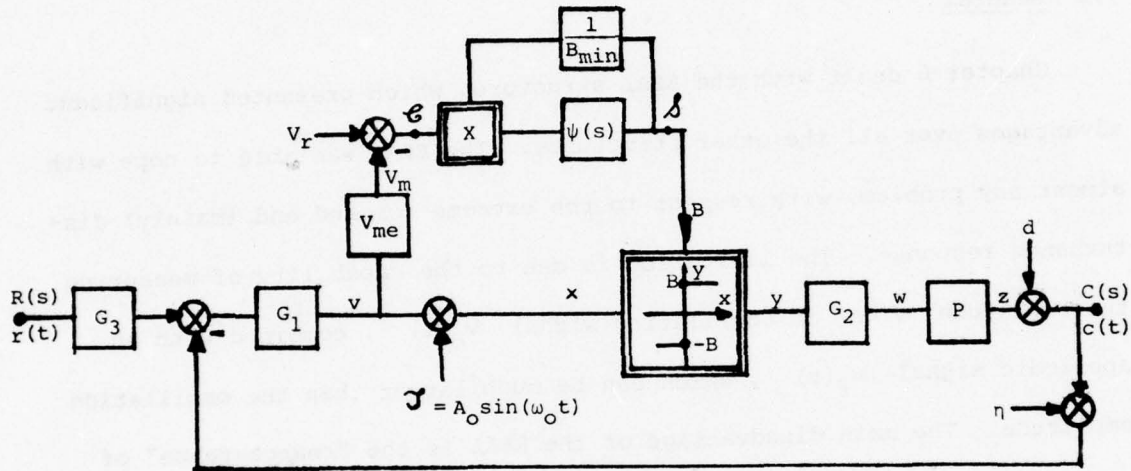


Figure 7.1-1 - EEANL Structure

The multiplier changes the dynamics of the secondary loop, as analyzed in Section 7.2.

7.2 The Stability and Dynamics of the Secondary Loop - EEANL

As in Section 6.5, the fundamental feedback equation is used,

$$\frac{O}{J}(s) \triangleq t_{oi}(s) + t_{ci}(s) t_{os}(s) \cdot \frac{\psi'(s)}{1 - \psi'(s) t_{cs}(s)} \quad (7.2-1)$$

where, in Figure 7.1-1, $\psi'(s)$ is the equivalent relation

$$\psi'(s) = \frac{f}{e}(s) \quad (f = \psi' e) \quad (7.2-2)$$

Most of the transmissions are the same as in the EEAL, Section 6.5, and repeated here.

$$t_{oi}(s) = 0 \quad (7.2-3)$$

$$t_{ci}(s) \approx e^{-T_o s} \quad (7.2-4)$$

$$t_{cs}(s) \approx \frac{4}{\pi} G_1 G_2 K P_h(s) e^{-T_o s} \quad (7.2-4)$$

$$t_{os}(s) = 1 \quad (7.2-4)$$

The only function to be defined is $\psi'(s)$. We can write (Figure 7.1-1)

$$B(t) = \mu(t) * \frac{[(v_r - v_m) \cdot B(t)]}{B_{min}} \quad (7.2-5)$$

where $\mu = \mathcal{L}^{-1}(\psi)$. Assuming $B(t)$ does not change "very much" from its initial value B_i ,

$$B(t) = B_i + \Delta B_i(t)$$

so

$$B(t) \approx \mu(t) * \frac{[(v_r - v_m) \cdot B_i(t)]}{B_{min}} \quad (7.2-6)$$

$$B(s) \approx \psi(s) [V_R(s) - V_m(s)] \cdot \left(\frac{B_i}{B_{min}} \right) \quad (7.2-7)$$

Then

$$\psi'(s) \approx \psi(s) \cdot \left(\frac{B_i}{B_{min}} \right) \quad (7.2-8)$$

Substituting the above in Equation 7.2-1,

$$\frac{\Delta B}{\Delta V} \approx \frac{-\left(\frac{B_i}{B_{min}} \right) \psi(s) e^{-T_o s}}{1 + \frac{4}{\pi} G_1 G_2 P_h \psi(s) \cdot \frac{K B_i}{B_{min}} e^{-T_o s}} \quad (7.2-9)$$

In Equation 7.2-9's denominator, B_i is the initial value of $B(t)$, and assuming the steady state was achieved, $B_i K = \text{constant}$ (Equation 6.2-10), and this expression is independent of K . The dynamic of the secondary loop is independent of the plant gain. The

assumption that $B(t)$ does not change "very much", once the secondary loop steady state is achieved, is valid, considering the dynamics of the adjustment loop being faster than the changes in K . Simulations have shown (Section 7.3) than even considering bigger changes in K and consequently in B , the results are still valid for Equation 7.2-9.

When $K = K_{\max}$, then $B = B_{\min}$, and Equation 7.2-9 is identical to the EEAL equivalent equation (6.5-9), if all the other functions are the same. This means that when $K = K_{\max}$, the EEANL secondary loop dynamics is identical to the EEAL one. Suppose now $K = K_{\min}$, then $B = B_{\max} = B_{\min} \times \frac{K_{\max}}{K_{\min}}$, and the denominator of Equation 7.2-9 has the same function as before (when $K = K_{\min}$), and the dynamics of the adjustment loop is kept constant.

EEANL Sensitivity to Dynamic Changes

Section 6.4, EEAL is valid for the EEANL.

7.3 Synthesis Procedure and Numerical Example - EEANL

The synthesis procedure, the specifications, data and constraints are the same as for the EEAL, Section 6.6.

The EEAL main loop synthesis procedure and results are also valid for the EEANL. The advantage is in the secondary loop, where the EEANL synthesis procedure is the same as the EEAL one, but the results provide the dynamics of adaptation be almost constant.

The same specifications of the EEAL numerical example are taken in the EEANL numerical example. As a result, all the EEANL blocks have the same functions as the EEAL blocks, including $\psi(s)$. The only difference is the added multiplier in the secondary loop.

Some implementation details mentioned in Section 5.3 for the SOANL are also valid for the EEANL.

EEANL simulations were performed on the CDC 6400 system. Results are presented in the next figures, and show that the EEANL structure, which is the most complex of the studied structures, can cope with very large inputs (command or disturbance) and severe plant gain changes.

Figures 7.3-1 to 7.3-6 show the system response when abrupt changes of gain (± 6 dB) are applied. The dynamics of adjustment is the same when an equivalent gain change is applied independently of the initial plant gain value.

Figures 7.3-7 to 7.3-9 show the system response when the extreme command input is applied.

Figures 7.3-10 to 7.3-12 show the system response when the extreme disturbance input is applied. Notice that quasi-linearity constraints are satisfied at x and not at v , and that some errors are introduced in the measurement process of the amplitude V (obtained from v) during the transient state due to the applied command or disturbance input.

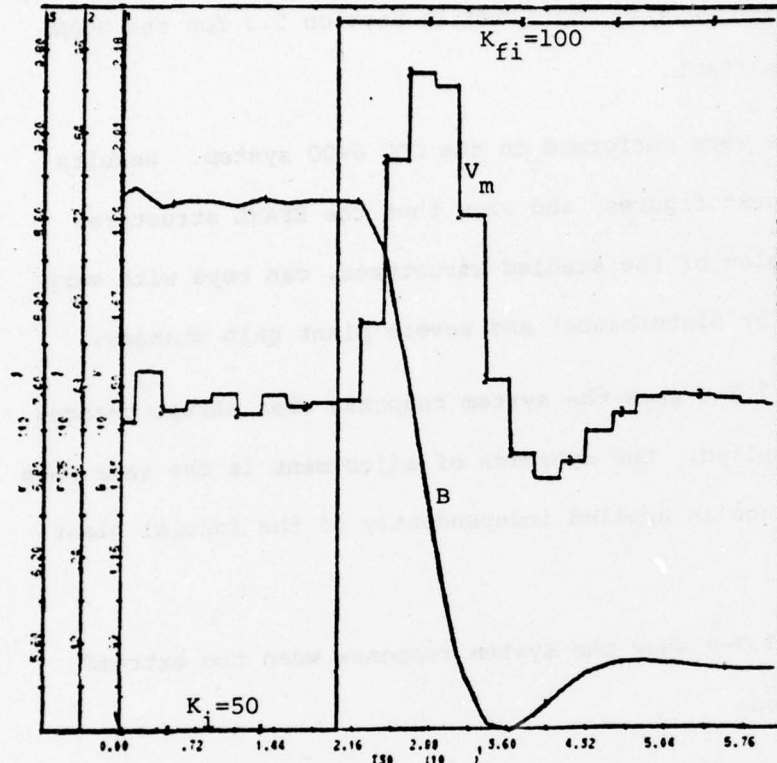


Figure 7.3-1a

EEANL - System Response
Dynamics of the Secondary Loop

r - Plant Gain
 V_m - Measured Amplitude of Oscillation
 B - Non-linearity Saturation Level

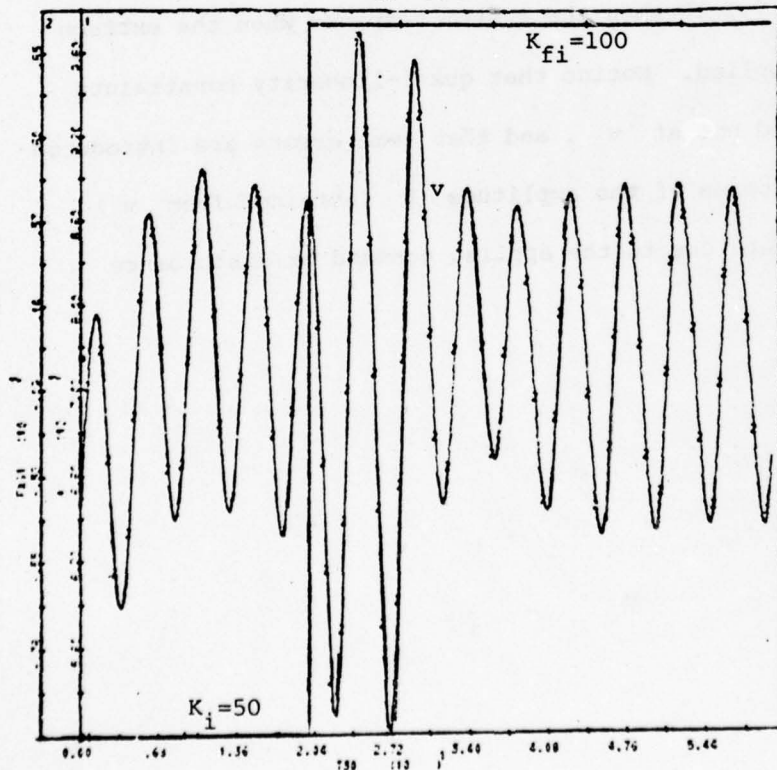


Figure 7.3-1b

K - Plant Gain
 v - Output of G_1

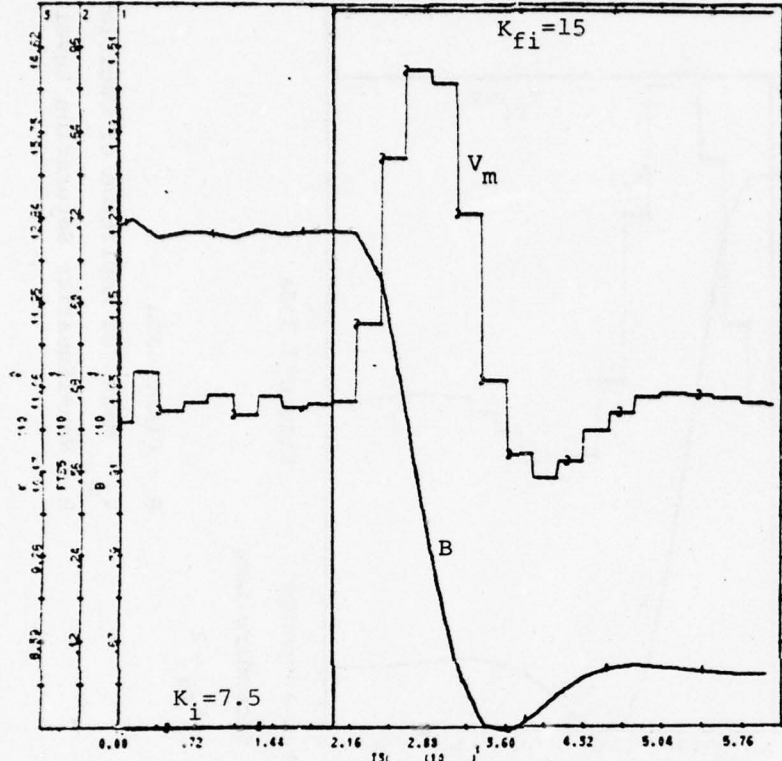


Figure 7.3-2a

EEANL - System Response
Dynamics of the Secondary Loop

$K_i = 7.5$ $K_{fi} = 15$

K - Plant Gain

V_m - Measured Amplitude of Oscillation

B - Non-linearity Saturation Level

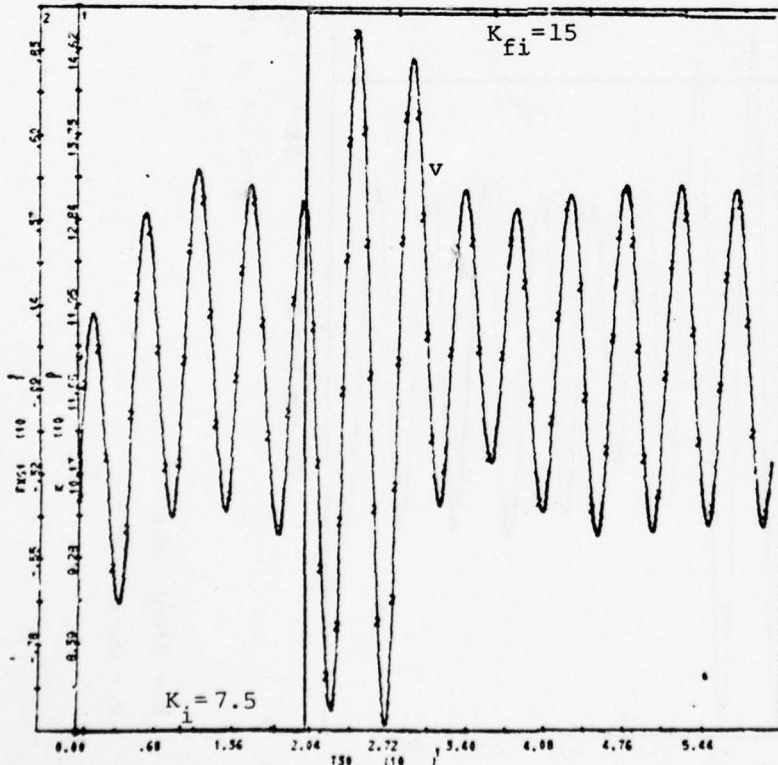


Figure 7.3-2b

K - Plant Gain

v - Output of G_L

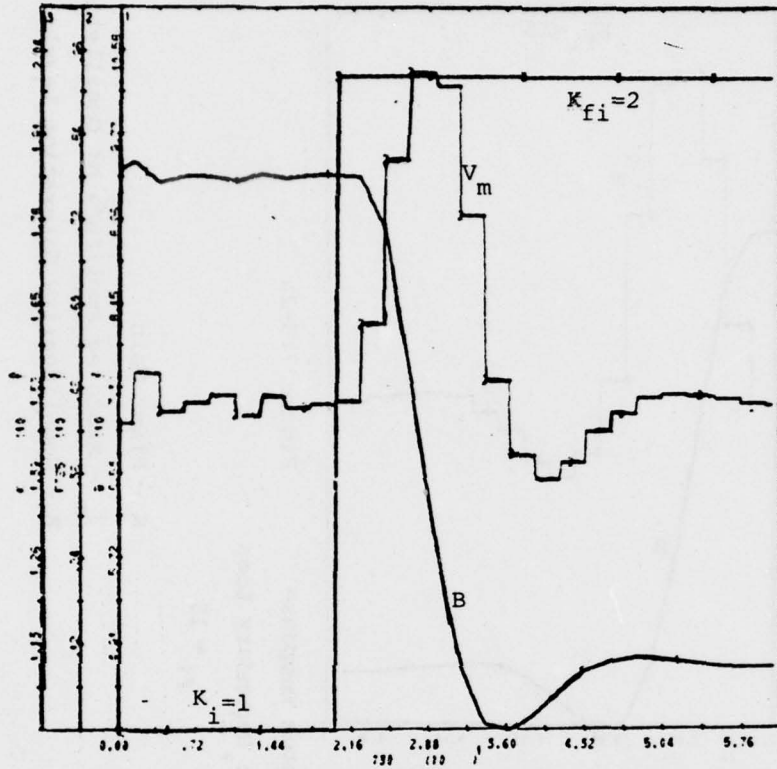


Figure 7.3-3a

EEANL - System Response
Dynamics of the Secondary Loop

$K_i = 1$ $K_{fi} = 2$

K - Plant Gain

V_m - Measured Amplitude of Oscillation

B - Non-linearity Saturation Level

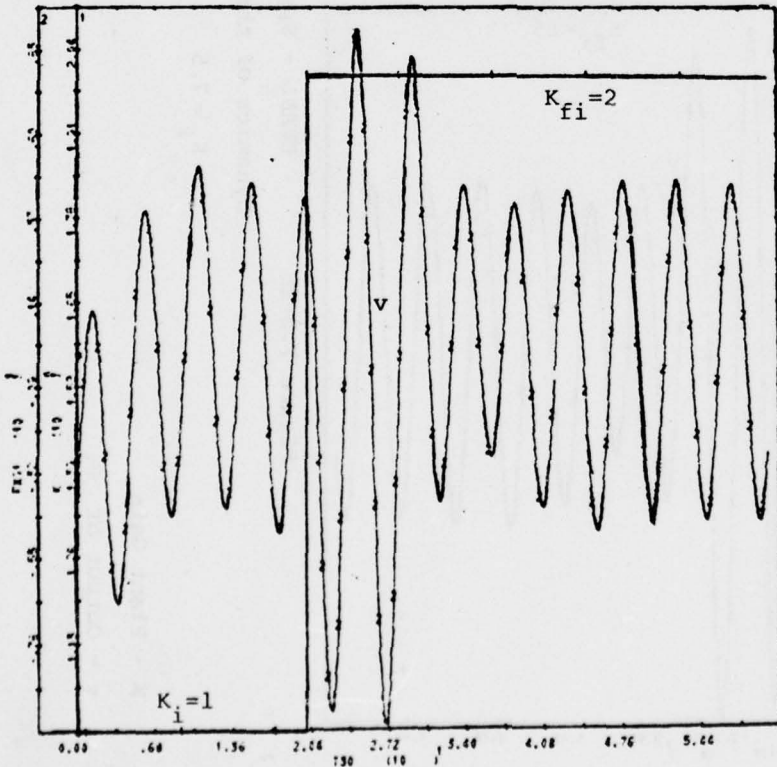


Figure 7.3-3b

K - Plant Gain

v - Output of G_1

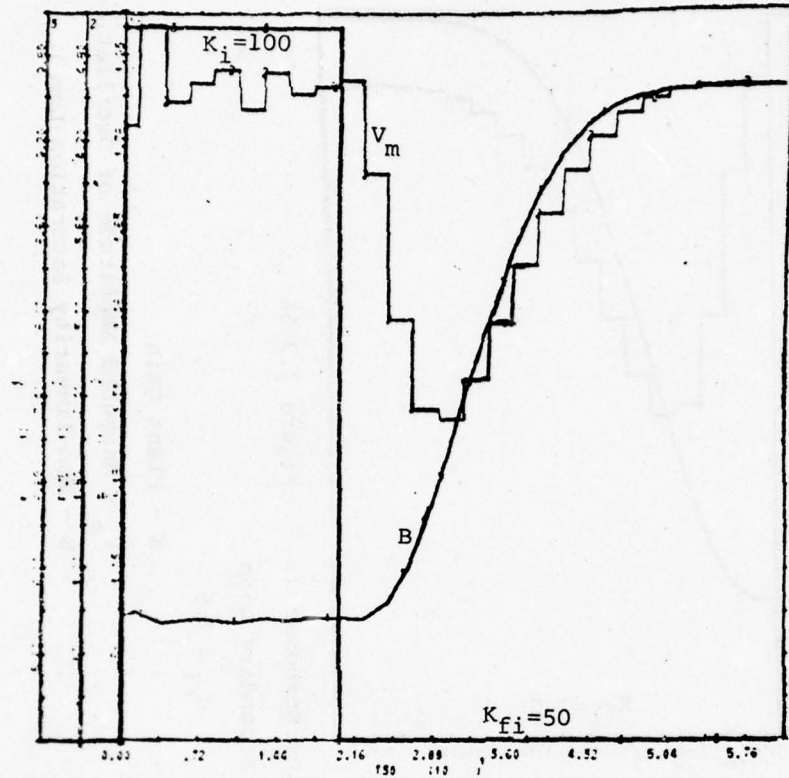


Figure 7.3-4a

K - Plant Gain
 V_m - Measured Amplitude of Oscillation
 B - Non-linearity Saturation Level

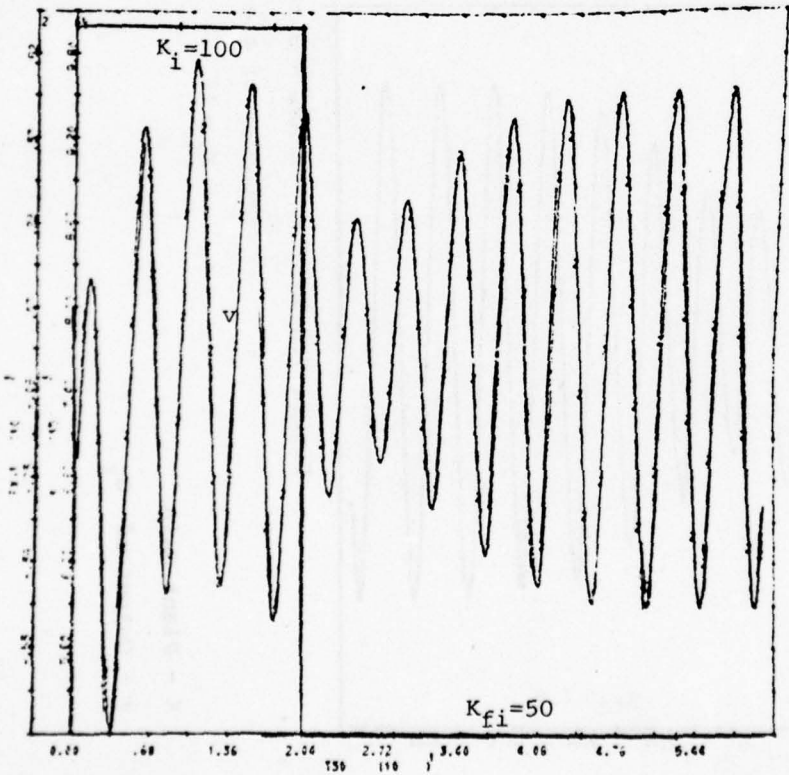


Figure 7.3-4b

K - Plant Gain
 v - Output of G_1

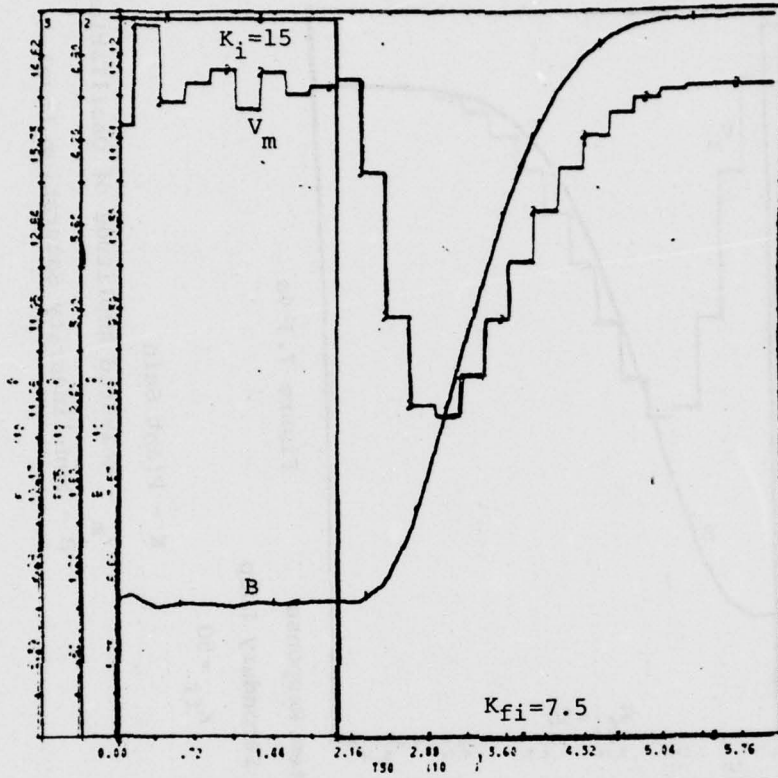


Figure 7.3-5a

EEANL - System Response
Dynamics of the Secondary Loop

$K_{fi} = 7.5$

K - Plant Gain

V_m - Measured Amplitude of Oscillation

B - Non-linearity Saturation Level

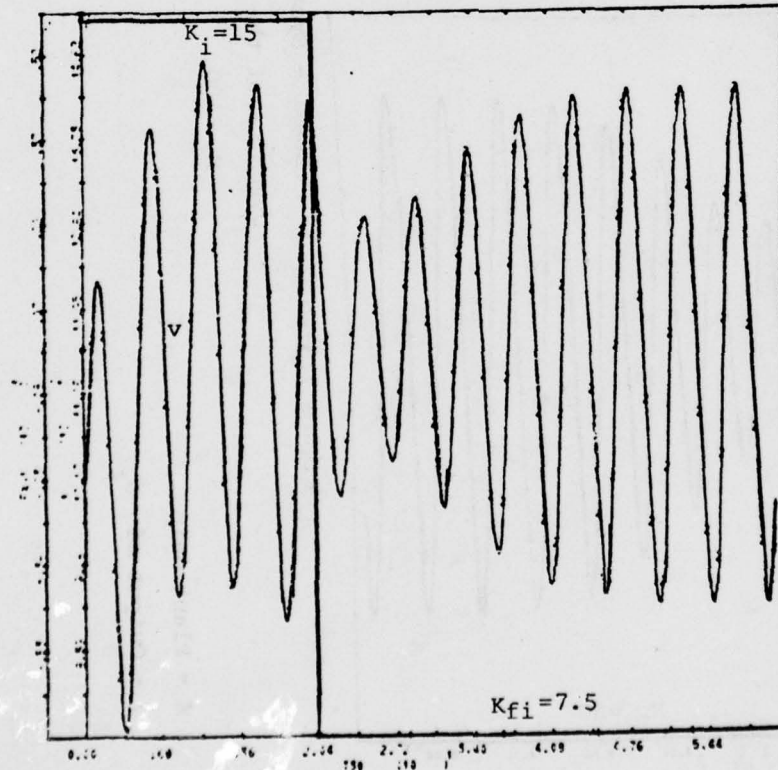


Figure 7.3-5b

$K_i = 15$

K - Plant Gain

v - Output of G_1

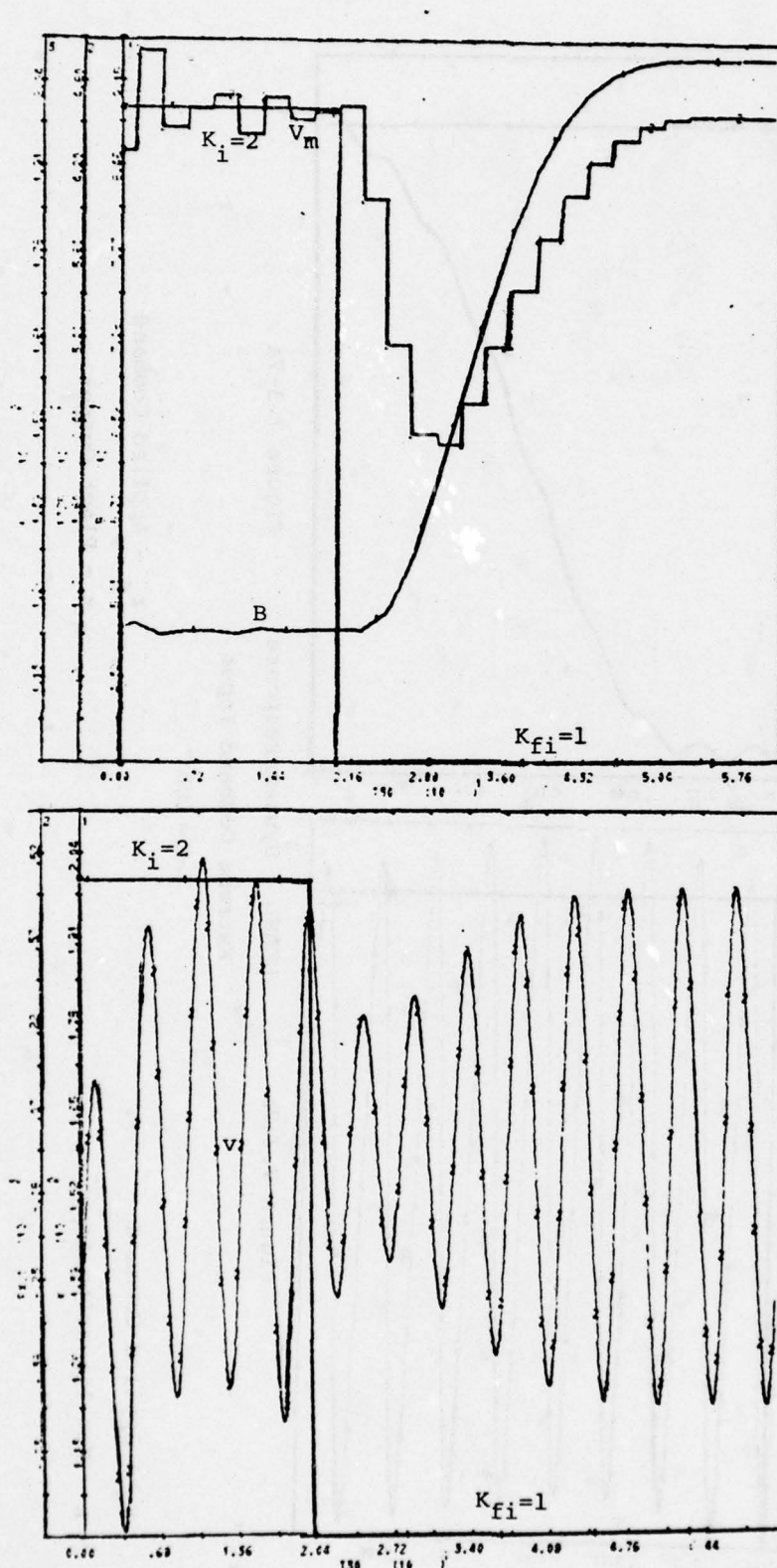


Figure 7.3-6a

EEANL - System Response
Dynamics of the Secondary Loop

Figure 7.3-6b

$K_{fi} = 1$

$K_1 = 2$

K - Plant Gain

V_m - Measured Amplitude of Oscillation

B - Non-linearity Saturation Level

K - Plant Gain

V_1 - Output of G_1

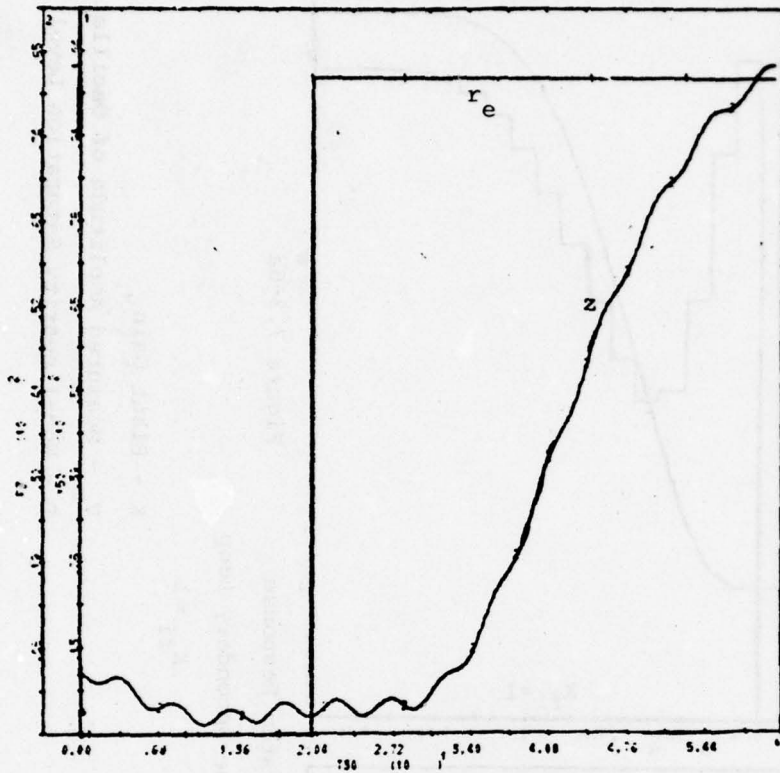


Figure 7.3-7a

r_e - Applied Command
 z - Plant Output

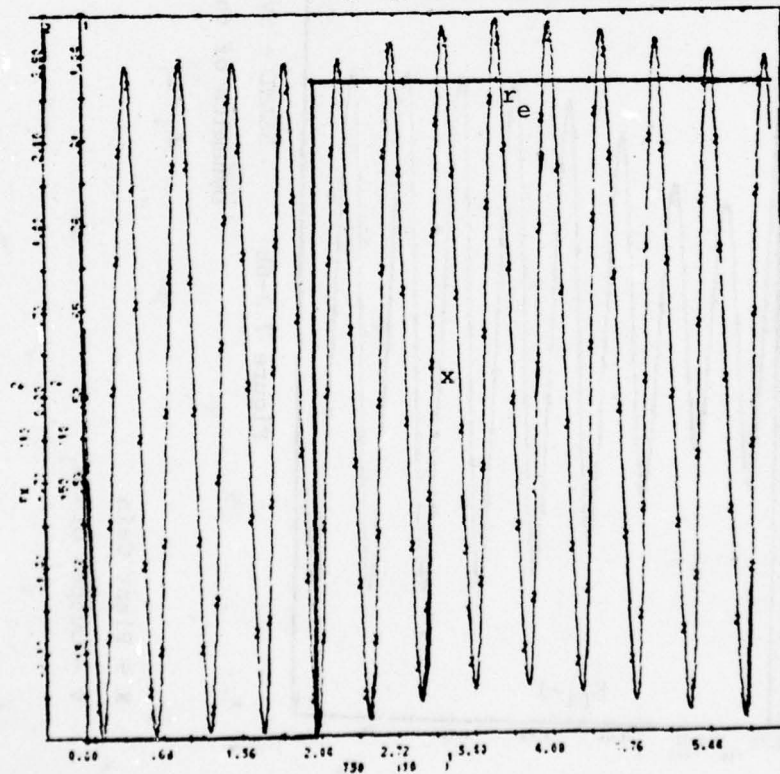


Figure 7.3-7b

r_e - Applied Command
 x - Non-linearity Input

EEANL - System Response
 Extreme Command Input

$K = 100$

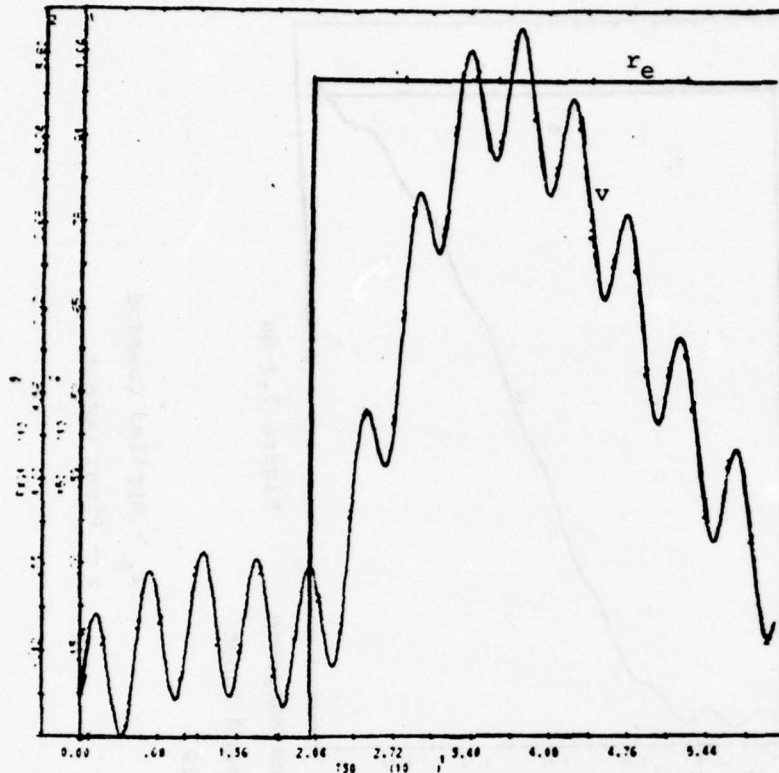


Figure 7.3-7c

r_e - Applied Command
 v - Output of G_1

$K = 100$

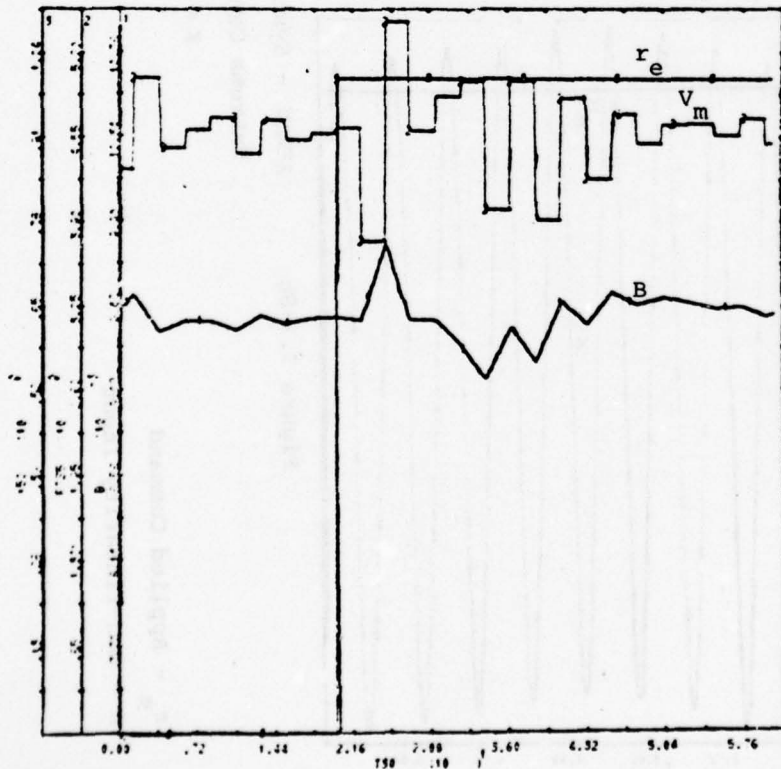


Figure 7.3-7d

r_e - Applied Command
 v_m - Measured Oscillation Amplitude
 B - Non-linearity Saturation Level

5 2 1

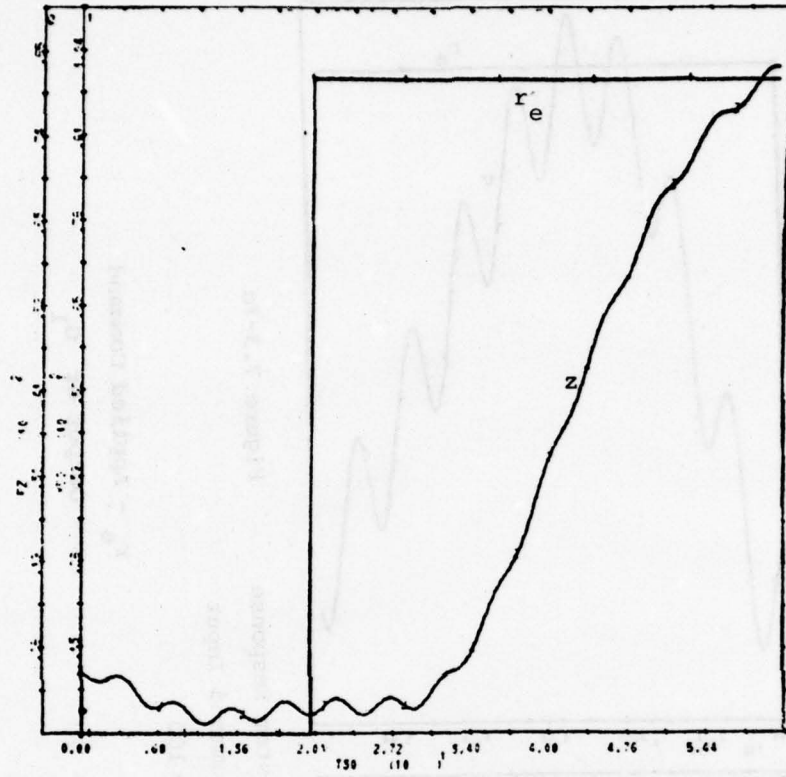


Figure 7.3-8a

EEANL - System Response
Extreme Command Input

$K = 10$

r_e - Applied Command
 z - Plant Output

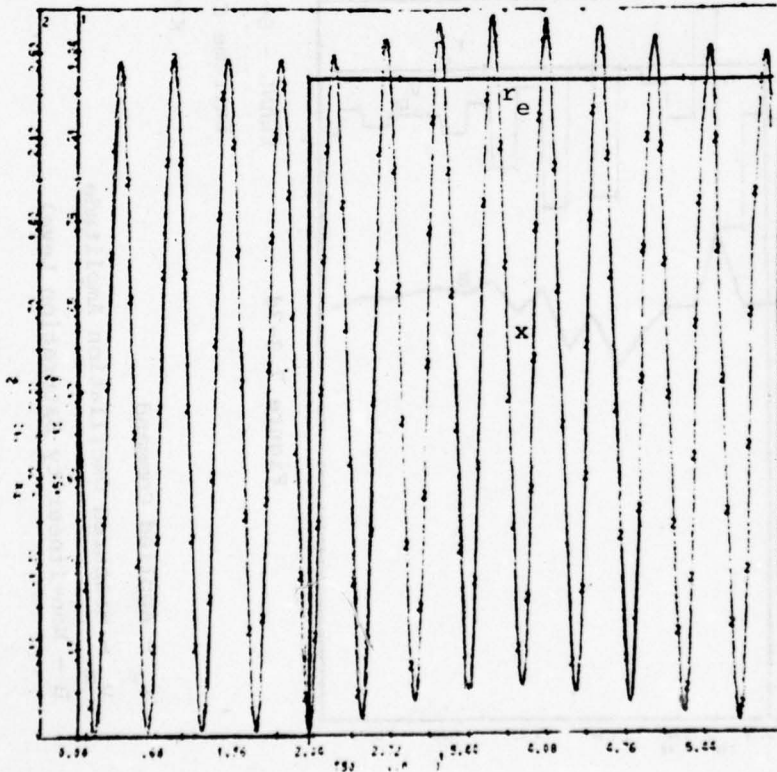


Figure 7.3-8b

r_e - Applied Command
 x - Non-linearity Input

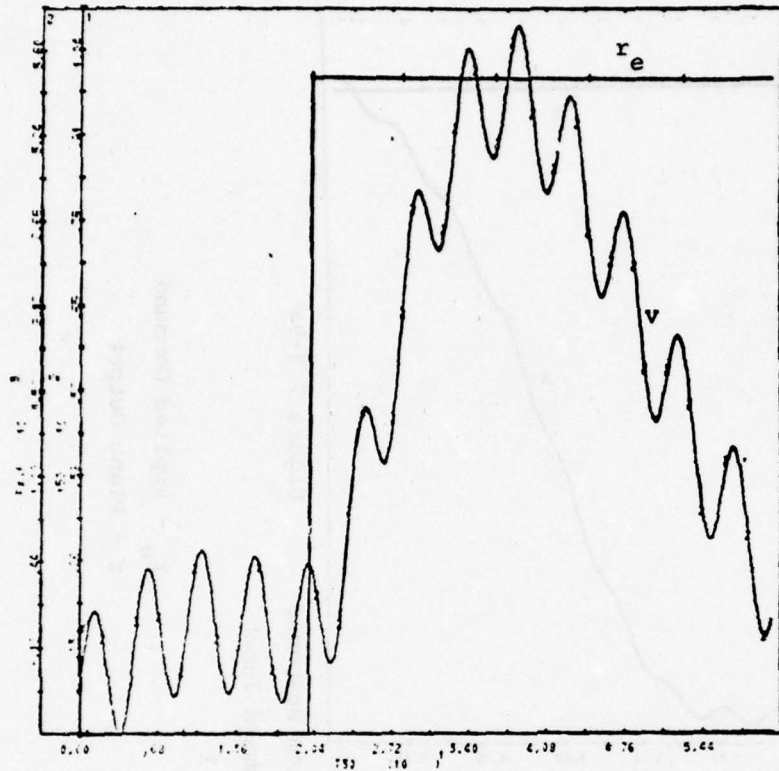


Figure 7.3-8c

r_e - Applied Command
 v - Output of G_1

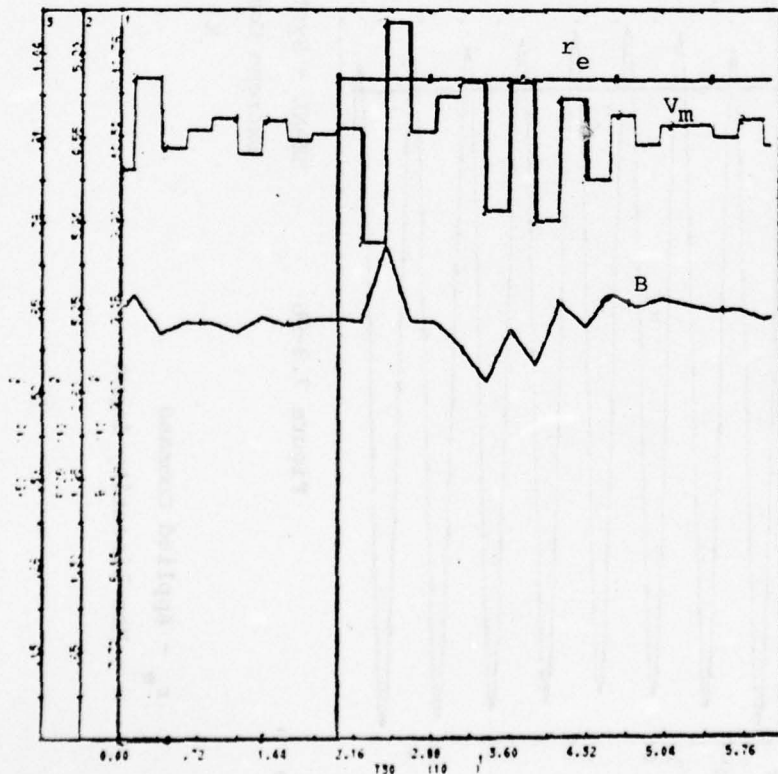


Figure 7.3-8d

r_e - Applied Command
 v_m - Measured Oscillation Amplitude
 B - Non-linearity Saturation Level

EEANL - System Response
 Extreme Command Input

$K = 10$

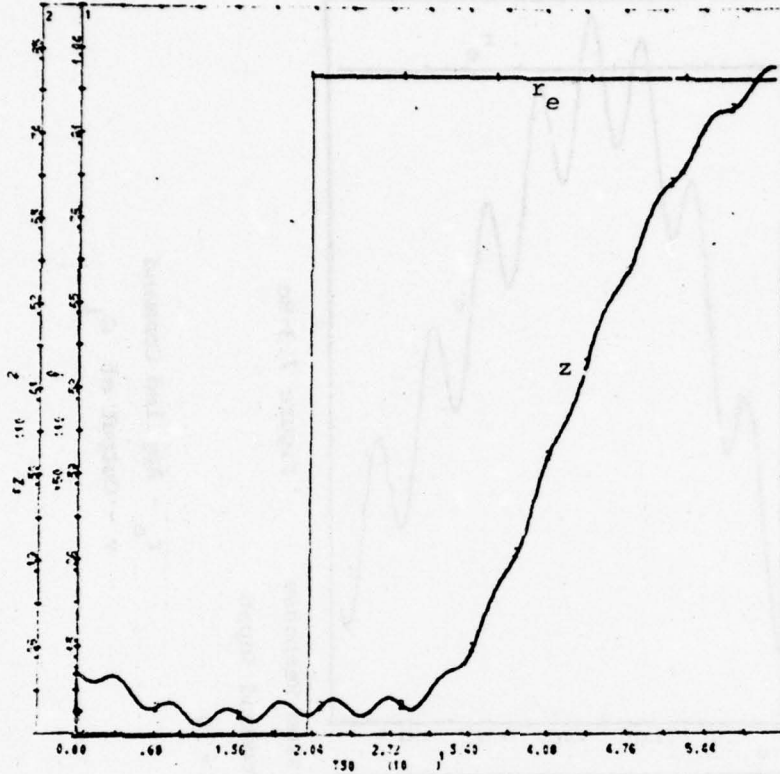


Figure 7.3-9a

EEANL - System Response
Extreme Command Input

$K = 1$

r_e - Applied Command
 z - Plant Output

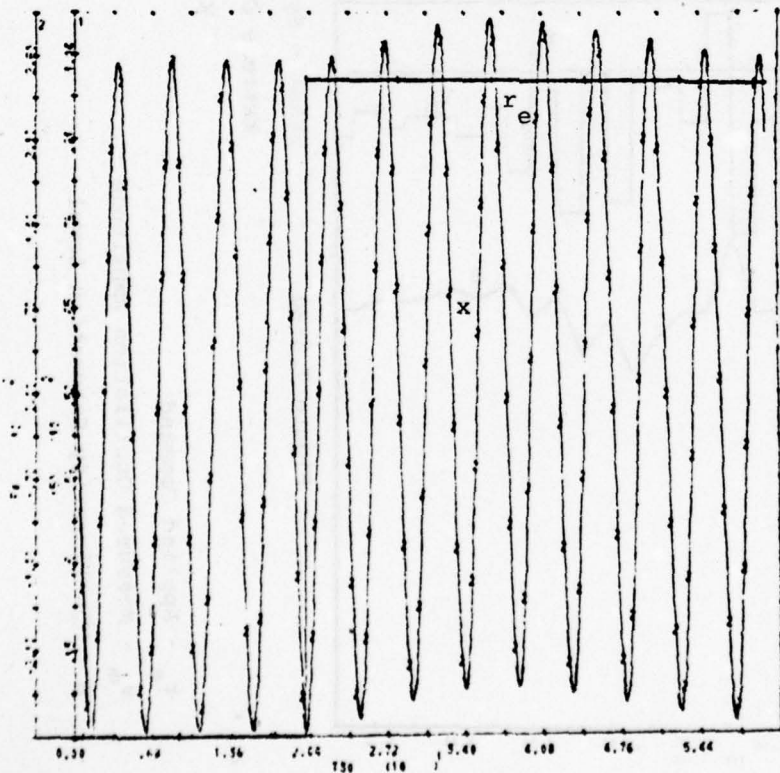


Figure 7.3-9b

r_e - Applied Command
 x - Non-linearity Input

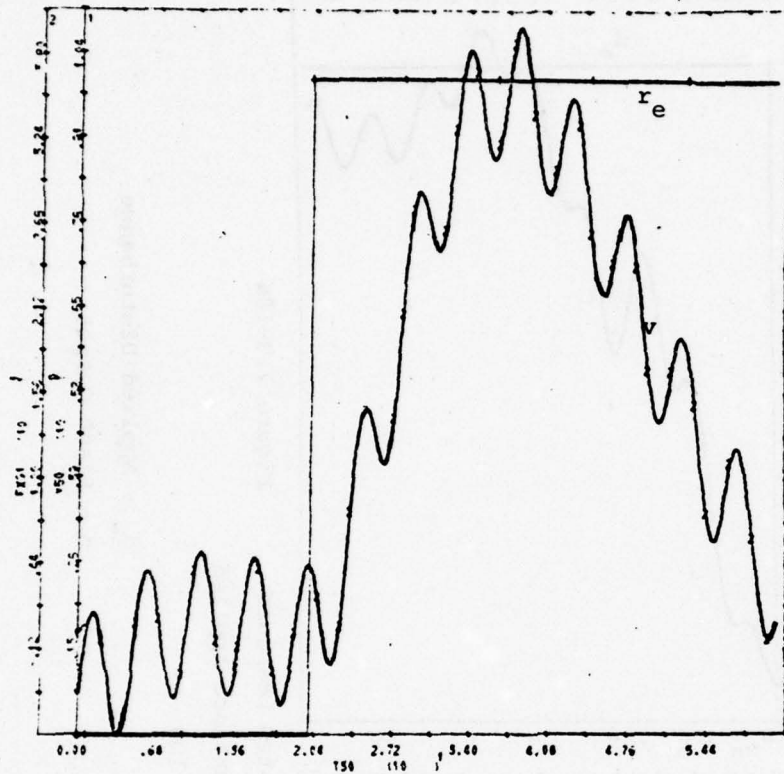


Figure 7.3-9c

r_e - Applied Command
 v - Output of G_1

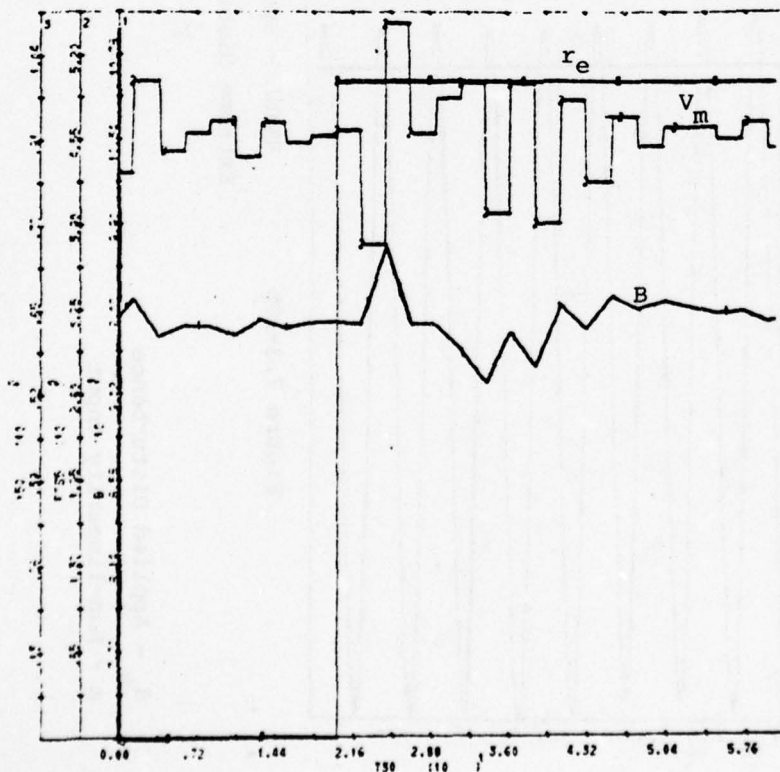


Figure 7.3-9d

r_e - Applied Command
 v_m - Measured Oscillation Amplitude
 B - Non-linearity Saturation Level

EEANL - System Response
 Extreme Command Input

$K=1$

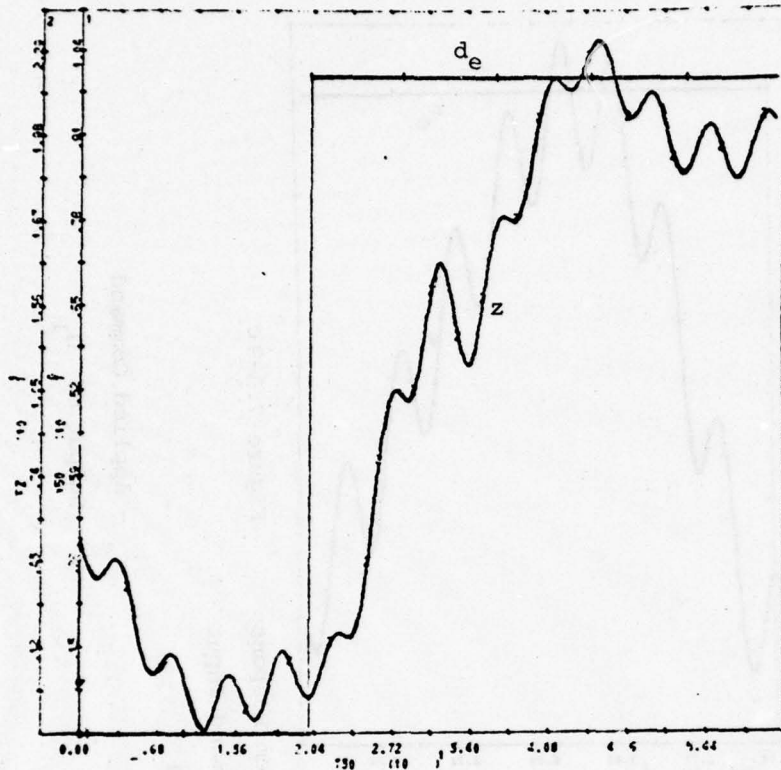


Figure 7.3-10a

EEANL - System Response
Extreme Disturbance Applied

$K = 100$

d_e - Applied Disturbance
 z - Plant Output

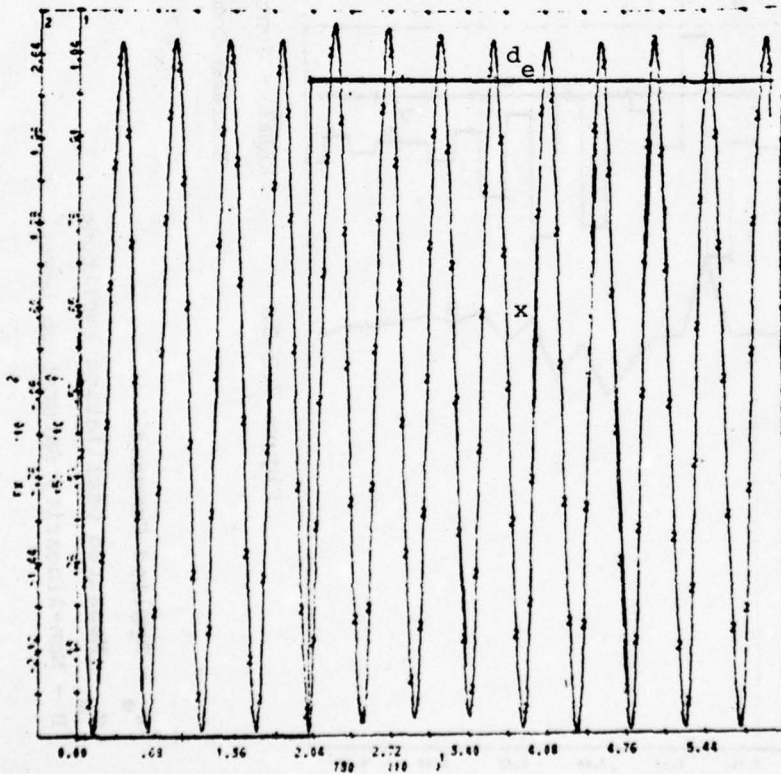


Figure 7.3-10b

d_e - Applied Disturbance
 x - Non-linearity Input

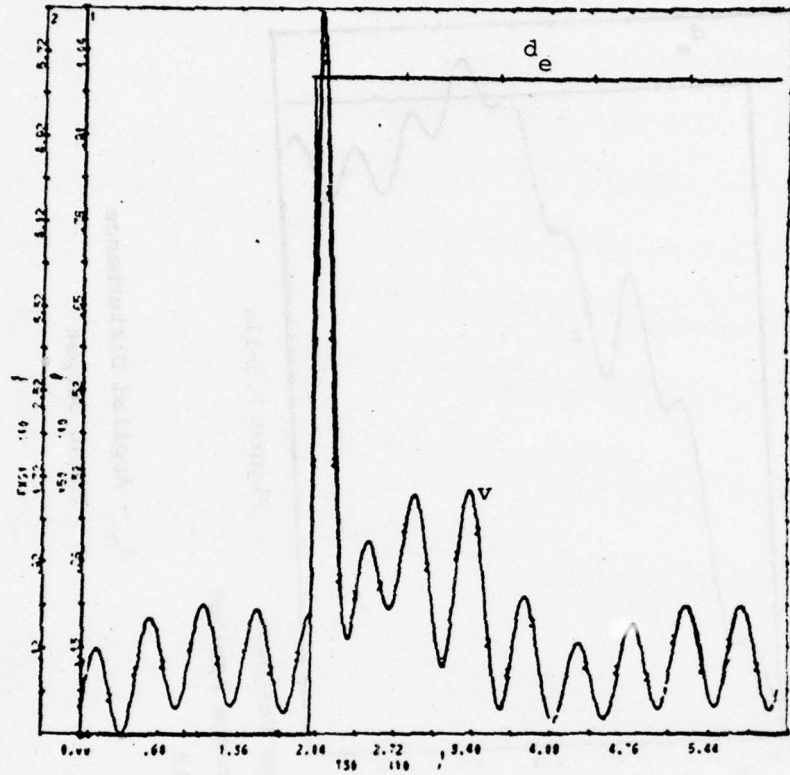


Figure 7.3-10c

d_e - Applied Disturbance
 v - Output of G_1

$K = 100$

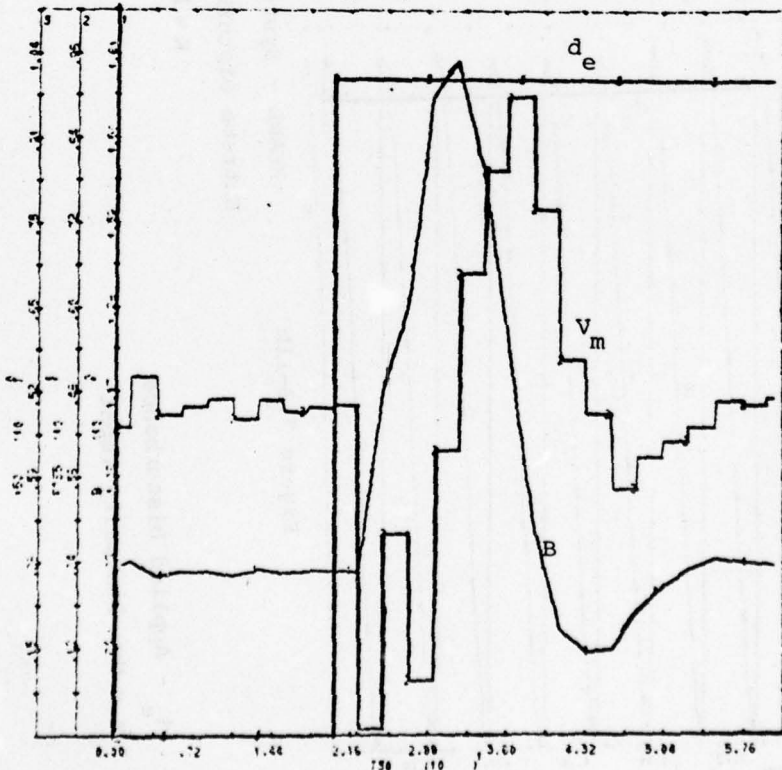


Figure 7.3-10d

d_e - Applied Disturbance
 v_m - Oscillation Amplitude Measurement
 B - Non-linearity Saturation Level

EEANL - System Response
 Extreme Disturbance Applied

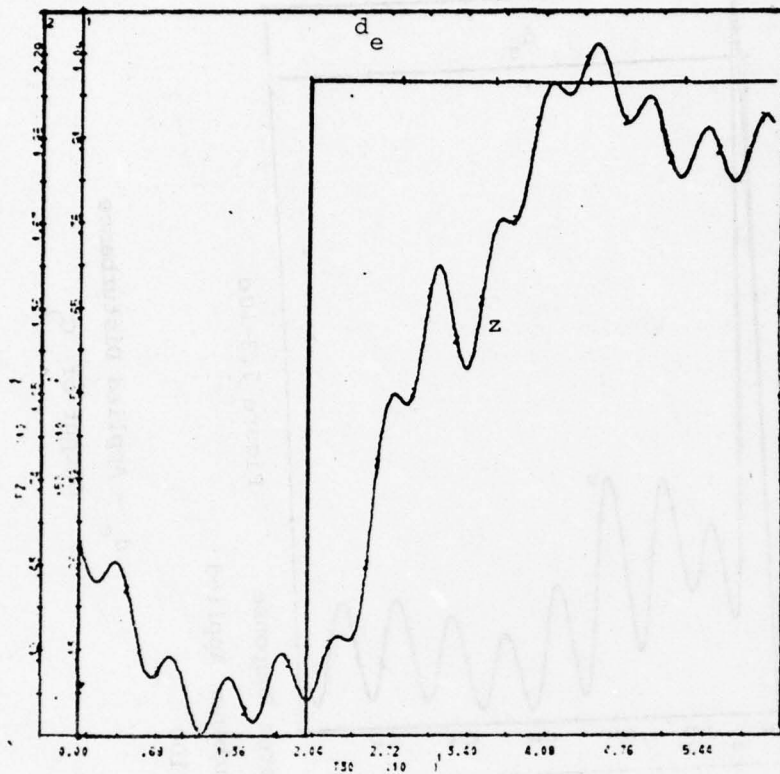


Figure 7.3-11a

d_e - Applied Disturbance
 z - Plant Output

EEANL - System Response
 Extreme Disturbance Applied

$K = 10$

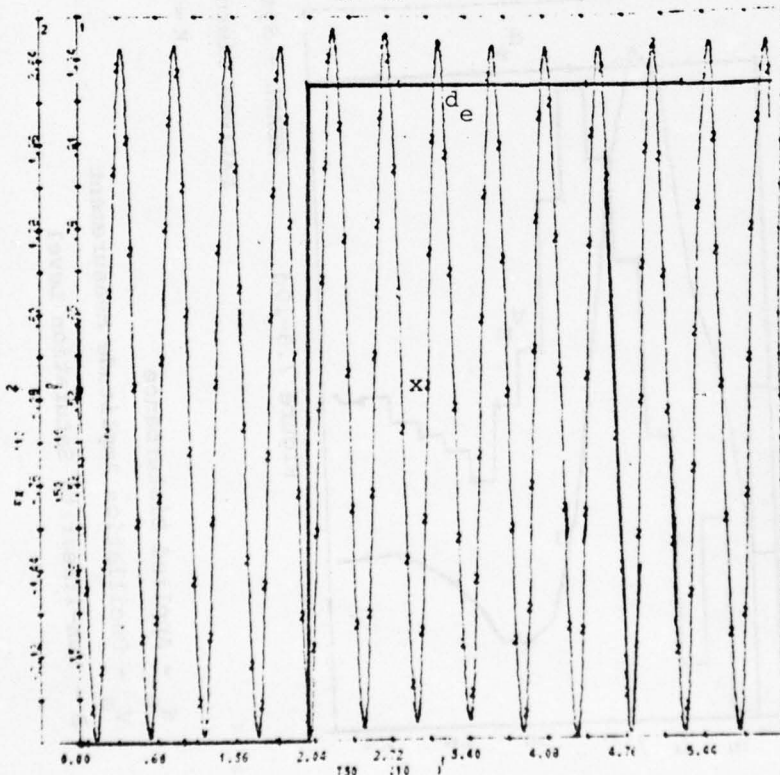


Figure 7.3-11b

d_e - Applied Disturbance
 x - Non-linearity Input

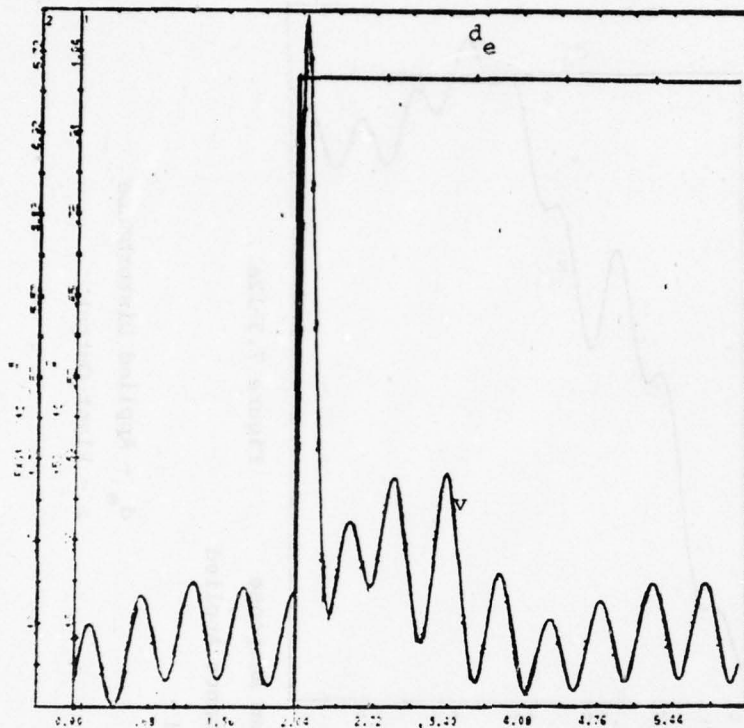


Figure 7.3-11c

EEANL - System Response
Extreme Disturbance Applied

K = 10

d_e - Applied Disturbance
 v - Output of G_1

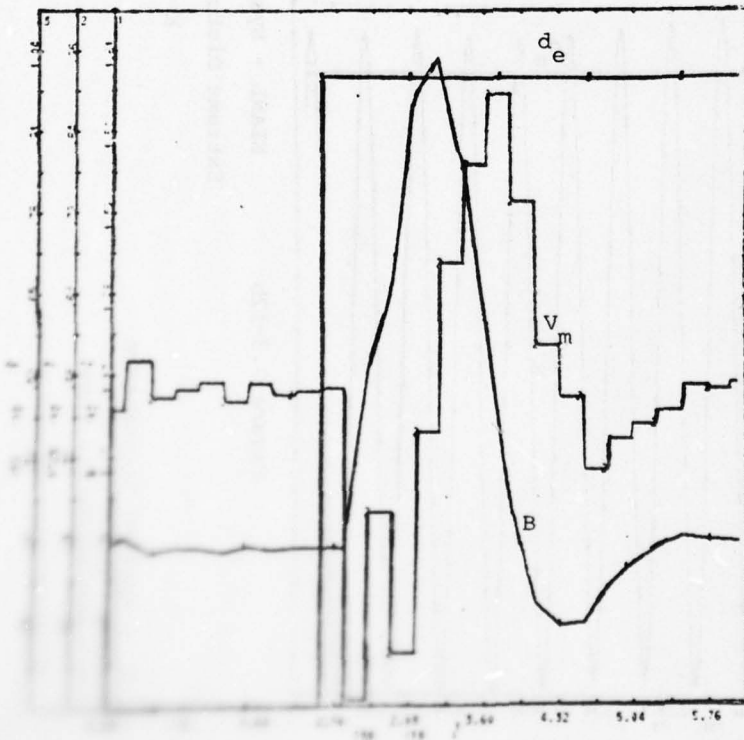


Figure 7.3-11d

d_e - Applied Disturbance
 v_m - Oscillation Amplitude Measurement
B - Non-linearity Saturation Level

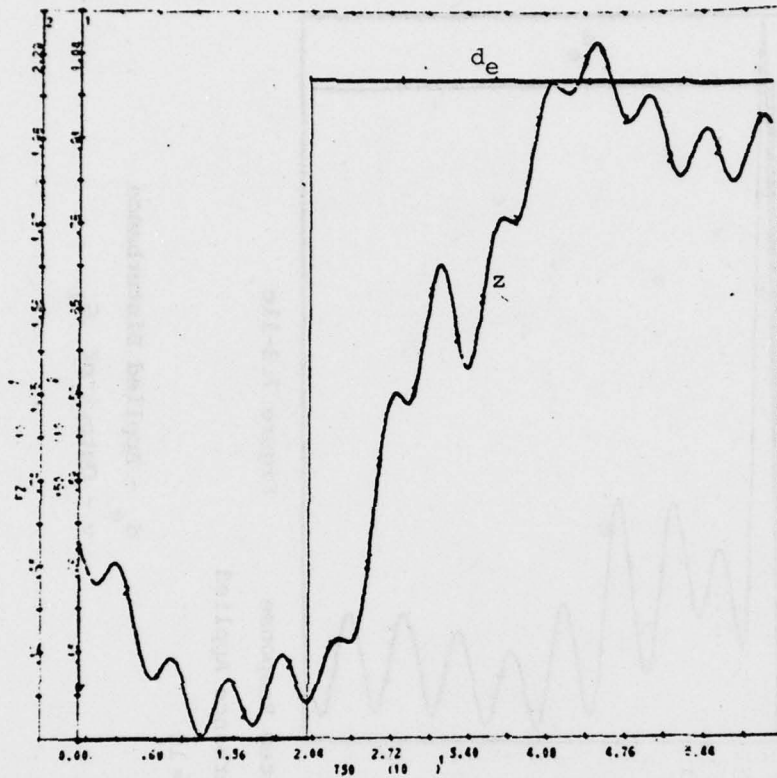


Figure 7.3-12a

EEANL - System Response
Extreme Disturbance Applied

$K = 1$

d_e - Applied Disturbance
 z - Plant Output

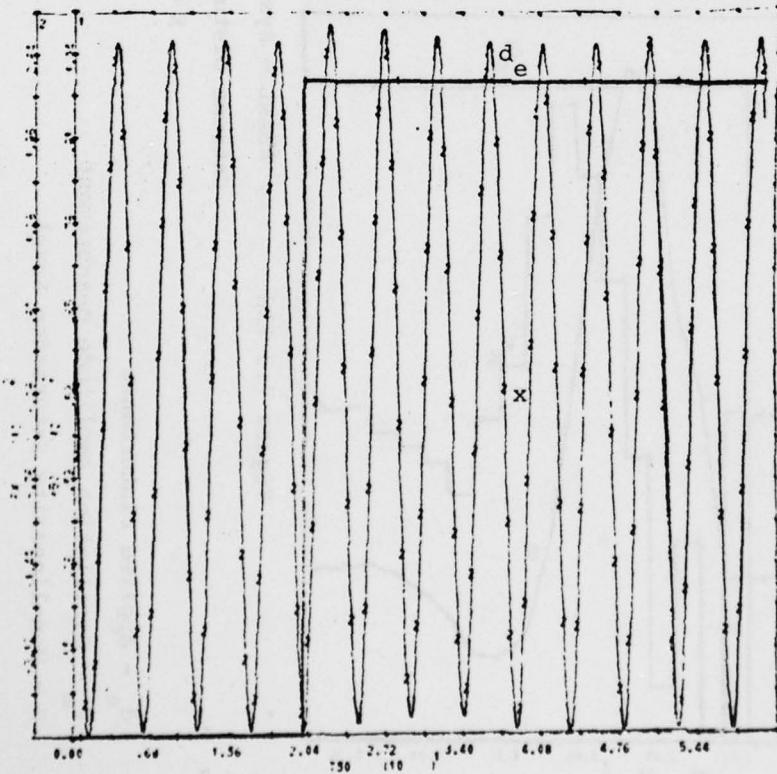


Figure 7.3-12b

d_e - Applied Disturbance
 x - Non-linearity Input

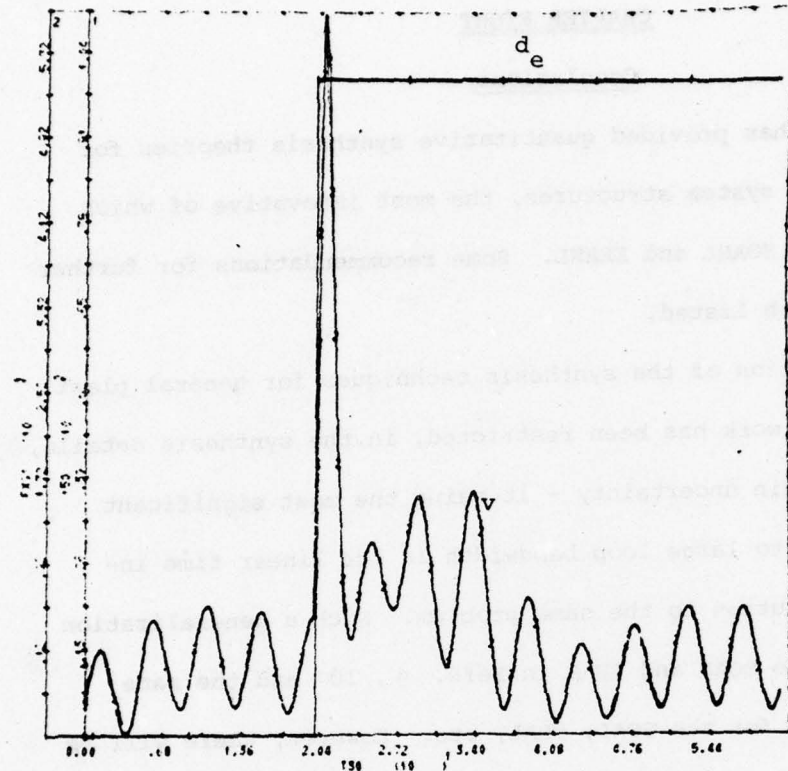


Figure 7.3-12c

d_e - Applied Disturbance
 v - Output of G_1

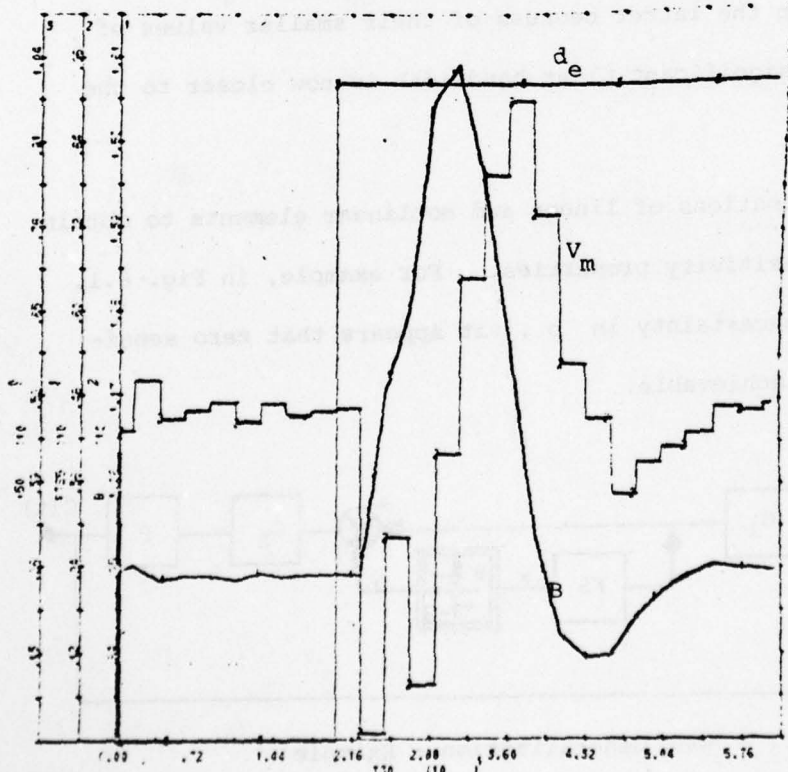


Figure 7.3-12d

d_e - Applied Disturbance
 v_m - Oscillation Amplitude Measurement
 B - Non-linearity Saturation Level

EEANL - System Response
 Extreme Disturbance Applied

$K=1$

5 2 1

CHAPTER EIGHT

Conclusions

This research has provided quantitative synthesis theories for several oscillating system structures, the most innovative of which are the SOAL, EEAL, SOANL and EEANL. Some recommendations for further research are herewith listed.

1. Generalization of the synthesis techniques for general plant uncertainty. This work has been restricted, in the synthesis details, to high frequency gain uncertainty - it being the most significant factor contributing to large loop bandwidth in the linear time invariant feedback solution to the same problem. Such a generalization was performed for the SOAS and EEAS in Refs. 9, 10 and the same approach can be used for the SOAL, EEAL, etc. However, there will be more complications in the latter because of their smaller values of ω_o , such that the significant plant bandwidth is now closer to the value of ω_o .

2. Use of combinations of linear and nonlinear elements to obtain more complex zero sensitivity properties. For example, in Fig. 8.1, with $P = \frac{p}{s+p}$ with uncertainty in p , it appears that zero sensitivity to p may be achievable.

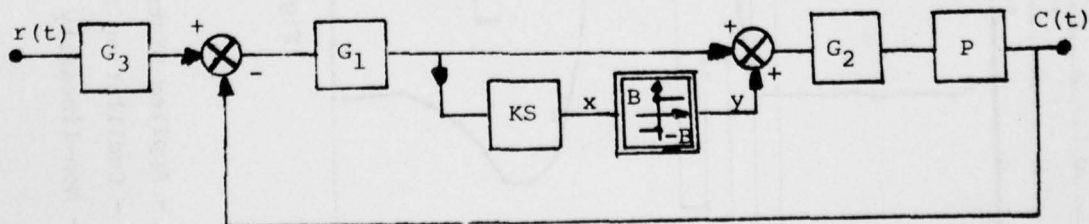


Figure 8.1 - SOAS Generalization - Example

3. More general relationship between L_f and L_o . If N is a static nonlinear element, then $L_f = L_o/2$. It is possible to achieve more complex relations, by using dynamic nonlinear elements. This might permit, for example, the bandwidth of L_f to be considerably smaller than that of L_o and thus enable one to tailor L_f to the actual feedback needs. Ideally, one could then tailor the nonlinearity to the specific design problem. The cascading of nonlinear elements separated by dynamic linear elements, is a possible approach.

4. In the present structures, the nonlinearity appears both in the feedback loop and in the direct transmission from input to output (when the return path in the feedback loop is open). One could modify the latter, as in Fig. 8.2, to have a parallel path bypassing the nonlinear element.

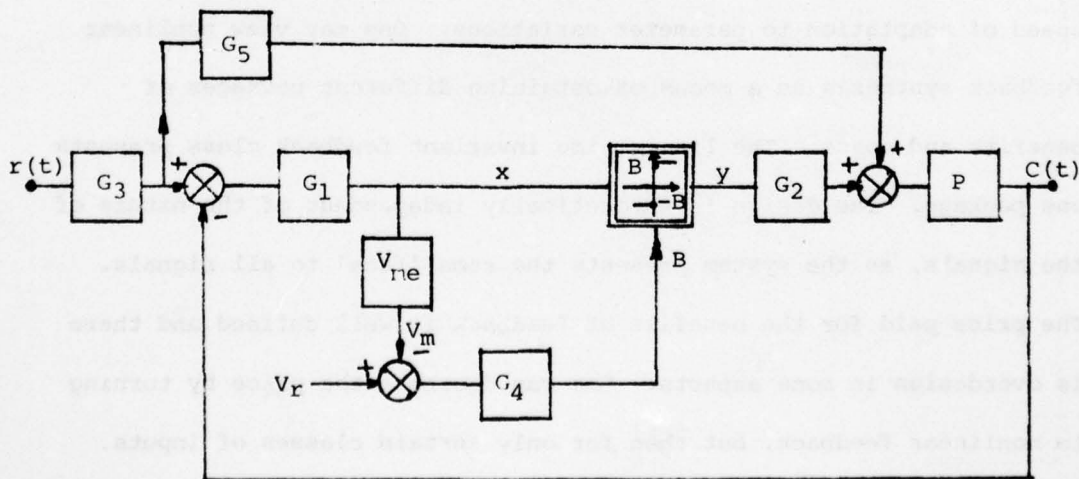


Figure 8.2 - SOAL with Parallel Path

Knowledge of K in $P = K P_h$ is available from the value of B , the saturation level of the nonlinearity, which can be used to modify G_5 . The latter could be used to speed up, if necessary, the system transfer function, without increasing ω_0 . This might be appropriate in the SOAL, SOANL, EEAL, EEANL in those cases where the ratio of desired system response bandwidth to ω_0 , becomes a significant design factor.

5. Finally, it would obviously be very desirable to have a mathematical theory for the dynamics of limit cycle build-up, and of limit cycle quenching by 'large' amplitude external signals.

6. It is interesting how the factor K_{\max}/K_{\min} reappears in various guises in the various dithered structures. It is banished completely as an adaptive problem in all of them. But in the SOAS and EEAS it appears as a very important factor in the quasilinearity problem. In the other structures (SOAL, etc.), it is banished as a quasilinearity problem but reappears as an important factor in the speed of adaptation to parameter variations. One may view nonlinear feedback synthesis as a means of obtaining different packages of benefits and costs. The linear time invariant feedback class presents one package. The design is theoretically independent of the nature of the signals, as the system presents the same 'face' to all signals. The price paid for the benefits of feedback is well defined and there is overdesign in some aspects. One can decrease the price by turning to nonlinear feedback, but then for only certain classes of inputs. One gets a different 'package deal'. Ideally, a nonlinear feedback synthesis theory would provide one with the means of choosing the

specific nonlinear structure needed to obtain the 'package deal'
suitable for his specific quantitative design problem.

APPENDIX I

REVIEW OF OPTIMUM SINGLE-LOOP SYNTHESIS^[1,5]

Figure I-1 presents a canonic single-loop structure wherein there is ignorance of P_1 parameters only. Hence, due to such ignorance,

$$\Delta \ln |T(j\omega)| = \Delta \ln \left| \frac{L}{1+L} \right|, \quad T = \frac{FGP}{1+GP}, \quad L = GP$$

$$\Delta \ln L = \Delta \ln P \quad (1a-d)$$

A specific value of frequency is chosen; say ω_1 rps. The values of $P(j\omega_1)$ over the range of plant parameters are calculated and the bounds obtained. The procedure is illustrated for the case

$$P(s) = \frac{ka}{s(s+a)} \quad ; \quad 1 \leq k \leq 10 \quad ; \quad 1 \leq a \leq 10$$

This is conveniently done in the plane of $\ln L(j\omega) = \ln |L| + j \text{Arg } L$, the abscissa in degrees and the ordinate in decibels, the Nichols chart. Thus, at $\omega = 2$ rps, $P(2j)$ lies within the boundaries given by ABCD in Figure I-2. Since $\ln L = \ln G + \ln P$, the pattern outlined by ABCD may be translated, but not rotated, on the Nichols chart, the amount of translation being given by the value of $\ln G(2j)$. For example, if a trial design of $L(2j)$ corresponds to the template of $P(2j)$ at A'B'C'D' in Figure I-2, then

$$\begin{aligned} |G(2j)|_{\text{db}} &= |L(2j)|_{\text{db}} - |P(2j)|_{\text{db}} \\ &= (-2.0) - (-13.0) = 11.0 \text{ DB} \\ \text{Arg } G(2j) &= \text{Arg } L(2j) - \text{Arg } P(2j) \\ &= (-60^\circ) - (-153.4^\circ) = 93.4^\circ \end{aligned}$$

Bounds on $L(j\omega)$ in the Nichols chart

The templates of $P_1(j\omega)$ are manipulated to find the position of $L(j\omega)$ which satisfies the specifications on $\ln |T(j\omega)|$. It is

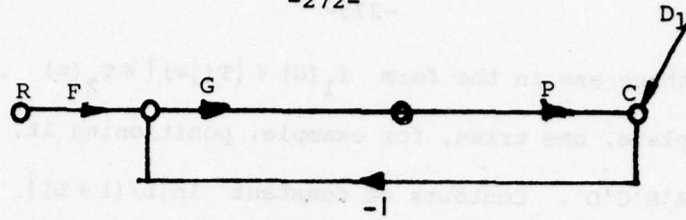


Figure I-1 - Canonic Single-loop Structure

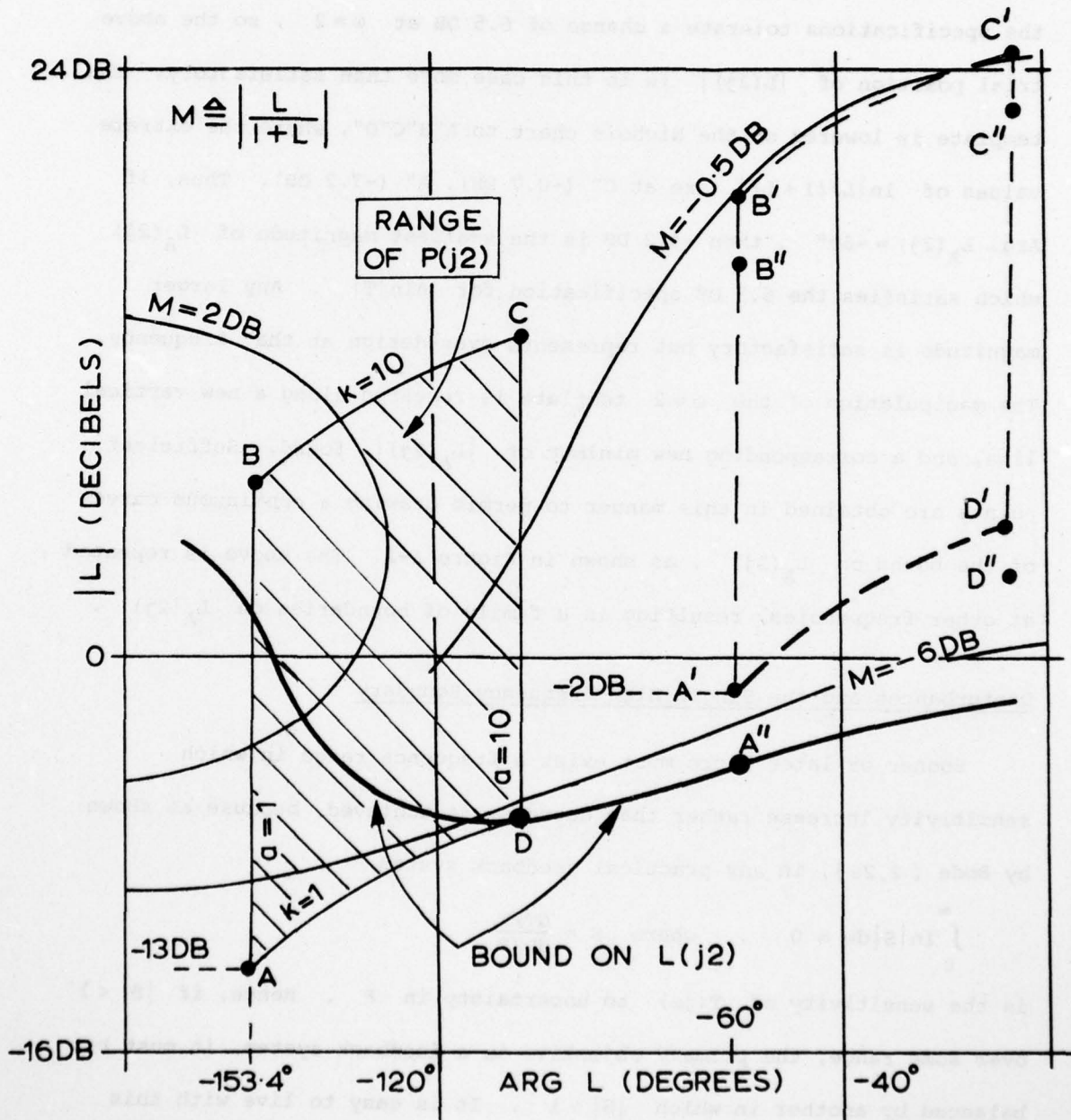


Figure I-2 - Derivation of Bounds on $L_f(j\omega)$ on Nichols Chart

recalled that these are in the form $T_1(\omega) \leq |T(j\omega)| \leq T_2(\omega)$. Taking the $\omega=2$ template, one tries, for example, positioning it, as shown in Figure I-2 at A'B'C'D'. Contours of constant $\ln|L/(1+L)|$ are available on the Nichols chart. Using these contours, it is seen that the maximum change in $\ln|T|$ is closely $(-0.49) - (-5.7) = 5.2$ DB, the maximum being at the point C', the minimum at the point A'. Suppose that the specifications tolerate a change of 6.5 DB at $\omega=2$, so the above trial position of $|L(2j)|$ is in this case more than satisfactory. The template is lowered on the Nichols chart to A"B"C"D", where the extreme values of $\ln|L/(1+L)|$ are at C" (-0.7 DB), A" (-7.2 DB). Thus, if $\text{Arg. } L_A(2j) = -60^\circ$, then -4.2 DB is the smallest magnitude of $L_A(2j)$ which satisfies the 6.5 DB specification for $\Delta \ln|T|$. Any larger magnitude is satisfactory but represents over-design at that frequency. The manipulation of the $\omega=2$ template is repeated along a new vertical line, and a corresponding new minimum of $|L_A(2j)|$ found. Sufficient points are obtained in this manner to permit drawing a continuous curve of the bound on $L_A(2j)$, as shown in Figure I-2. The above is repeated at other frequencies, resulting in a family of boundaries on $L_A(2j)$.

Disturbances and the Single High-frequency Boundary

Sooner or later there must exist a frequency range in which sensitivity increase rather than decrease is achieved, because as shown by Bode [2,26], in any practical feedback system

$$\int_0^{\infty} \ln|S| d\omega = 0, \quad \text{where } S = \frac{dT/T}{dP/P}$$

is the sensitivity of $T(j\omega)$ to uncertainty in P . Hence, if $|S| < 1$ over some range, the primary objective in a feedback system, it must be balanced by another in which $|S| > 1$. It is easy to live with this

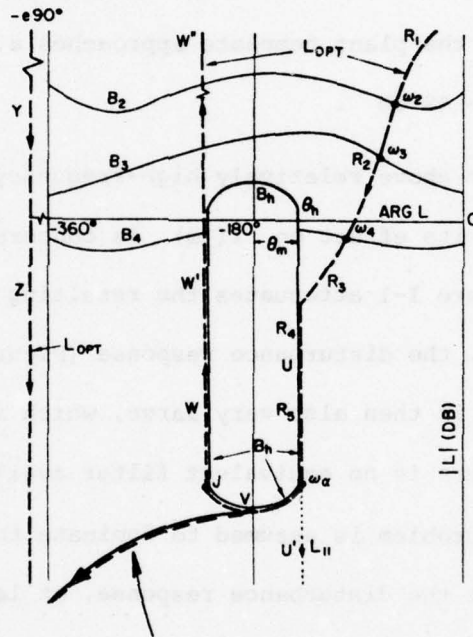
constraint in the two-degree-of-freedom system, because at sufficiently large ω , $|T|$ is negligibly small, so that large relative changes in $|T|$ are inconsequential. It should be noted, however, that in any practical one-degree-of-freedom system, this range where $|S| > 1$, must lie within the important frequency range of $T(j\omega)$. In this higher range or sooner, the plant template approaches a vertical line, because at large ω any realistic minimum-phase $P(j\omega) \rightarrow K(j\omega)^{-p}$, p being its excess of poles over zeros. Thus in the previous example $P(j\omega) \rightarrow ka(j\omega)^{-2}$ and the plant template approaches a vertical line of length $|\Delta \ln(ka)|_{\max} = 40 \text{ db}$.

As noted, in the above relatively high-frequency range $|S| \gg 1$ is tolerable, as far as its effect on $T(j\omega)$ is concerned, because the prefilter F in Figure I-1 attenuates the resulting high peaking in $L/(1+L)$. However, the disturbance response (Figure I-1) $C/D_1 = (1+L)^{-1} = S$, is then also very large, which is generally not tolerable because there is no equivalent filter available. Even if the parameter ignorance problem is assumed to dominate the design, it is necessary to consider the disturbance response, at least to the extent of adding the constraint

$$\exists \gamma > 0, \exists |T_{D1}| \triangleq \left| \frac{C}{D_1} \right| = |(1+L_1)^{-1}| \leq \gamma, \forall \omega \quad (1)$$

This constraint leads to the boundary B_h of Figure I-3 effective for all ω , with $\theta_h = 180 - \theta_m$ a function of γ , e.g. $\theta_m = 50^\circ$ if $\gamma = 2.3 \text{ db}$. At low frequencies the parameter ignorance factor dominates, e.g. B_2, B_3 in Figure I-3, so these boundaries contain no part of B_h . There is an intermediate frequency region in which part of the boundary contains a portion of B_h , e.g. B_4 in Figure I-3.

At sufficiently large ω there exists a frequency ω_h such that B_h becomes the complete boundary for all $\omega \geq \omega_h$.



Practical Suboptimum L

Figure I-3 - Bounds on L and Optimum L on Nichols Chart

The Optimum $L(j\omega)$

It has been shown [1,5] that a realistic definition of optimum in single-loop design is the minimization of K , defined by

$\lim_{s \rightarrow \infty} L(s) = Ks^{-e}$, where e is the excess of poles over zeros assigned to $L(s)$.

It has been proven [5] that the optimum L lies on its boundary B_i at each ω_i and that such an optimum exists and is unique. Most important for the present purpose, is that in significant plant ignorance problems the ideal optimum L has the properties shown in Figure I-3, i.e. over a significant range it follows B_h along UV up to the point J at which it abruptly jumps to infinity along WW'W" and returns on the vertical line YZ, whose phase is -90° . Such an ideal $L(j\omega)$ is, of course, impractical. A practical suboptimum L is shown in Figure I-3.

APPENDIX II

Derivation of Frequency Response Bound from Time Domain Bound

The problem of finding the precise bounds on $\left| \frac{X_f(j\omega)}{A} \right|$ due to that on $\max_t \left| \frac{x_f(t)}{A} \right|$, is a very difficult one in general, because of the integral relation between $x_f(t)$ and its frequency response $X_f(j\omega)$. It is done here approximately, and the results confirmed by numerous experiments and actual system design based on use of the approximate relations.

The basic point is that the search need not be over the set over all possible transforms, but only over the much smaller subset of those which are realistic for the problem under consideration. It has been shown [9] that realistically, the search need be only over the subset of "dominantly first-order" transfer functions, i.e. those which over the significant frequency range are effectively first-order (excess of only one pole over zeros). This means that $\text{Re } X_f(j\omega) > 0$ over the frequency range of importance. In that study [9], the simplest first-order system was then used $\frac{X_f}{A} = \frac{q}{s + \omega_b}$, giving $\max_t \left| \frac{x_f(t)}{A} \right| = q$. In order that the latter be $\leq \frac{1}{\alpha}$, it follows that $\left| \frac{X_f}{A}(j\omega) \right| = \frac{1}{\alpha\omega}$. This was justified by demonstrating that attempted more complex forms for $X_f(j\omega)$ resulted in basically the same result. Other good reasons were given there, why such a simple form for $X_f(s)$ was desirable.

Here, we accept the constraint $\text{Re } X_f(j\omega) > 0$ and use a result by Papoulis [27] that if $R(\omega) = \text{Re } F(j\omega) \geq 0$, $R'(\omega) \leq 0 \quad \forall \omega$, then $\max_t |s(t)| \leq 1.18 R(\omega)_{\max}$, where $s(t)$ is the resulting step response. Since $|R(\omega)| < |F(j\omega)|$, we are conservative in using $|F(j\omega)|_{\max}$,

AD-A046 011

COLORADO UNIV BOULDER SYSTEMS ENGINEERING LAB
SYNTHESIS OF OSCILLATING ADAPTIVE SYSTEMS.(U)
JUL 77 A SHAPIRO, I HOROWITZ

F/G 9/4

UNCLASSIFIED

4 OF 4

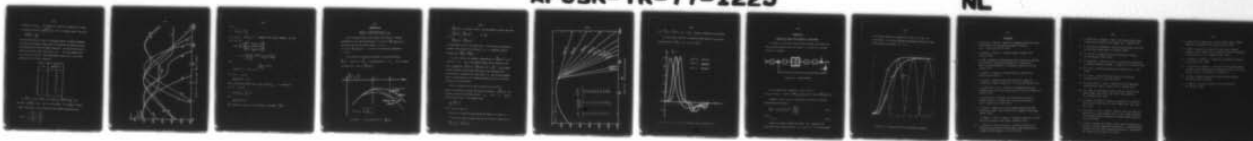
AD
A046011



AFOSR-TR-77-1223

AFOSR-76-2946

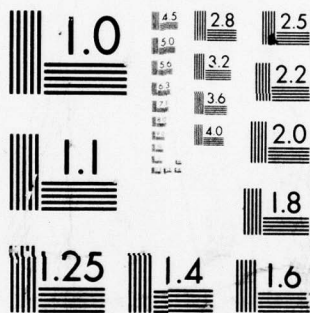
NL



END
DATE
FILMED

11-77

DDC



MICROCOPY RESOLUTION TEST CHART
NATIONAL BUREAU OF STANDARDS-1963-A

in place of $R(\omega)_{\max}$. We simply try to use this inequality as a means of relating the bound $\max_t \left| \frac{x_f(t)}{A} \right| \leq \frac{1}{\alpha}$ into an ω -domain bound. This gives

$$\left| \frac{X_f(j\omega)}{A} \right| \leq \frac{1.18}{\alpha\omega}$$

We confine ourselves in fact to "reasonably smooth" frequency responses, which are here defined as those with only negative-real poles and zeros, and experimentally check the above inequality. The results are given in Figure II-1 and the table below, with $\alpha = 3$. The most complex case has 4 zeros and 9 poles. These experimental results are in very good agreement with the above inequality.

Case	$\max_t \left \frac{x_f(t)}{A} \right $
1	.29
2	.30
3	.28
4	.33
5	.30
6	.33
7	.33
8	.33

If $\frac{X_f(s)}{A}$ is not "smooth", the condition $\left| \frac{X_f(j\omega)}{A} \right| \leq \frac{1}{\alpha\omega}$ still satisfies $\max_t \left| \frac{x_f(t)}{A} \right| \leq \frac{1}{\alpha}$, but it is too severe. For example, consider a simple "band-pass" filter (twin-tee), with complex zero-pole pairs.

$$TT(s) = \frac{1 + \frac{2z_1}{\omega_0} s + \frac{s^2}{\omega_0^2}}{1 + \frac{2z_2}{\omega_0} s + \frac{s^2}{\omega_0^2}}$$

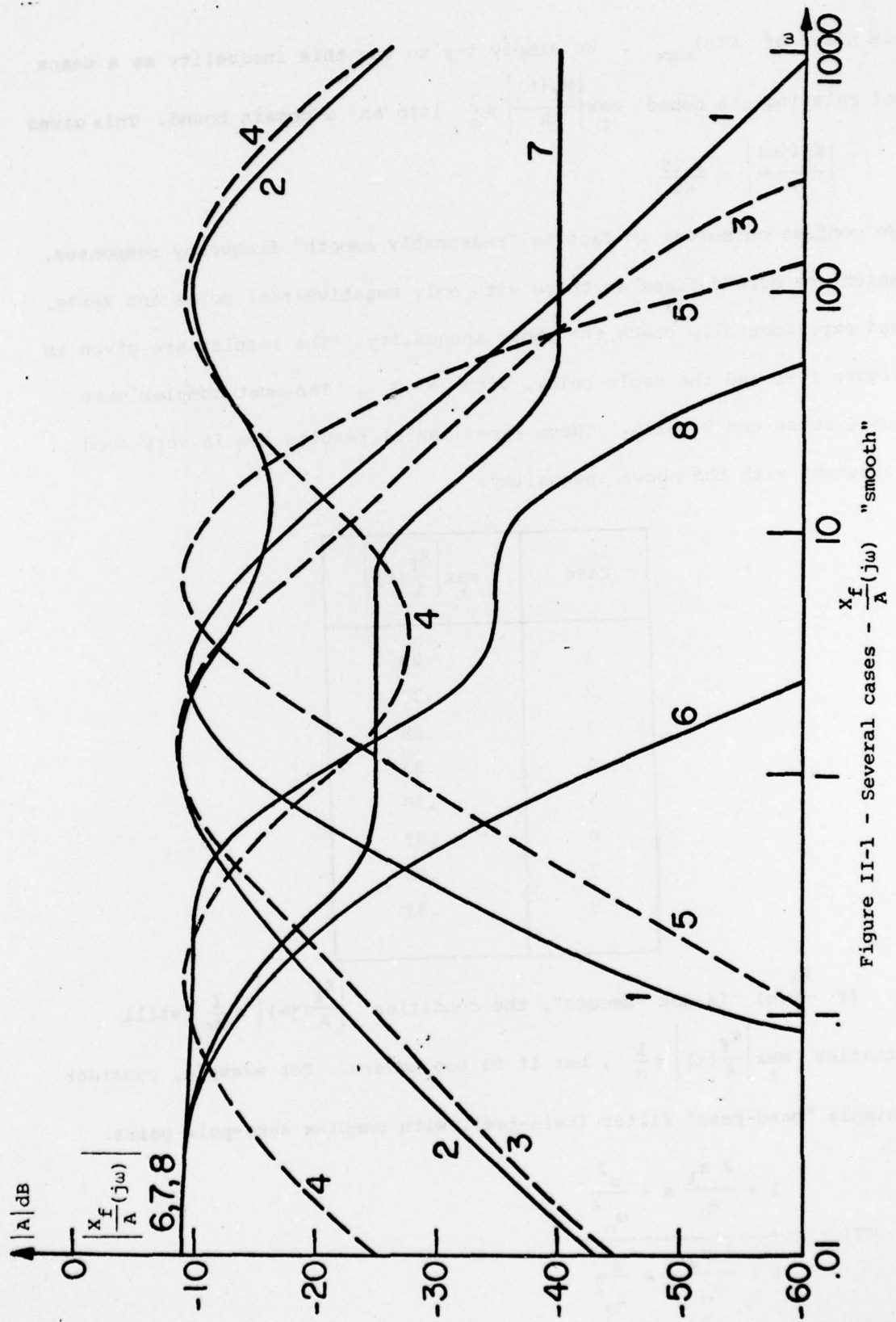


Figure II-1 - Several cases - $x_f(j\omega) / A$ "smooth"

At ω_0 ,

$$|TT(j\omega_0)| = \frac{z_1}{z_2}$$

If $z_1 > z_2$, $|TT(j\omega_0)| > 1$. Suppose a unit step is applied. The output $a(t)$ is

$$a(t) = \mathcal{L}^{-1} \frac{1}{s} \left[\frac{(s^2 + 2z_1\omega_0 s + \omega_0^2)}{(s^2 + 2z_2\omega_0 s + \omega_0^2)} \right]$$

$$= 1 + 2 \frac{(z_1 - z_2)}{\sqrt{1 - z_2^2}} e^{-z_2\omega_0 t} \sin(\omega_0 \sqrt{1 - z_2^2} t)$$

with

$$\max_t |a(t)| = 1 + 2(z_1 - z_2) e^{\frac{z_2}{\sqrt{1 - z_2^2}} \cdot \cos^{-1} z_2}$$

If $z_2 \ll 1$, $z_1 \ll z_2$,

$$\max_t |a(t)| \approx 1 + 2z_1$$

which can be much smaller than $z_1/z_2 = |TT(j\omega)|_{\max}$. For example at

$$z_1 = .5, \quad z_2 = .05,$$

$$|TT(j\omega)|_{\max} = \frac{z_1}{z_2} = 10$$

and

$$\max_t |a(t)| \approx 1.1$$

This property is noted in the discussion on non-smooth $\frac{x_f}{A}(j\omega)$.

APPENDIX III

RESULTS - EXTRAPOLATION FOR $\omega = \omega_0$

In all structures seen in this study, there exists a "strange" combination of two loop transmissions: 1) $L_0(j\omega_0) = \frac{4B}{\pi A} G_1 G_2 K P_h(j\omega_0)$, valid only for the oscillating signal ($\omega = \omega_0$) ,
2) $L_f(j\omega) = \frac{2B}{\pi A} G_1 G_2 K P_h(j\omega)$, valid for the slow signal components ($\omega \leq \omega_0/3$) .

In the synthesis procedures developed, the function defining $\frac{x_f}{A}(j\omega)$, valid for $\omega \leq \frac{\omega_0}{3}$, is extrapolated to $\omega = \omega_0$. This is shown in Figure III-1, case 1 $\left(\frac{x_{f1}}{A}(j\omega) \right)$.

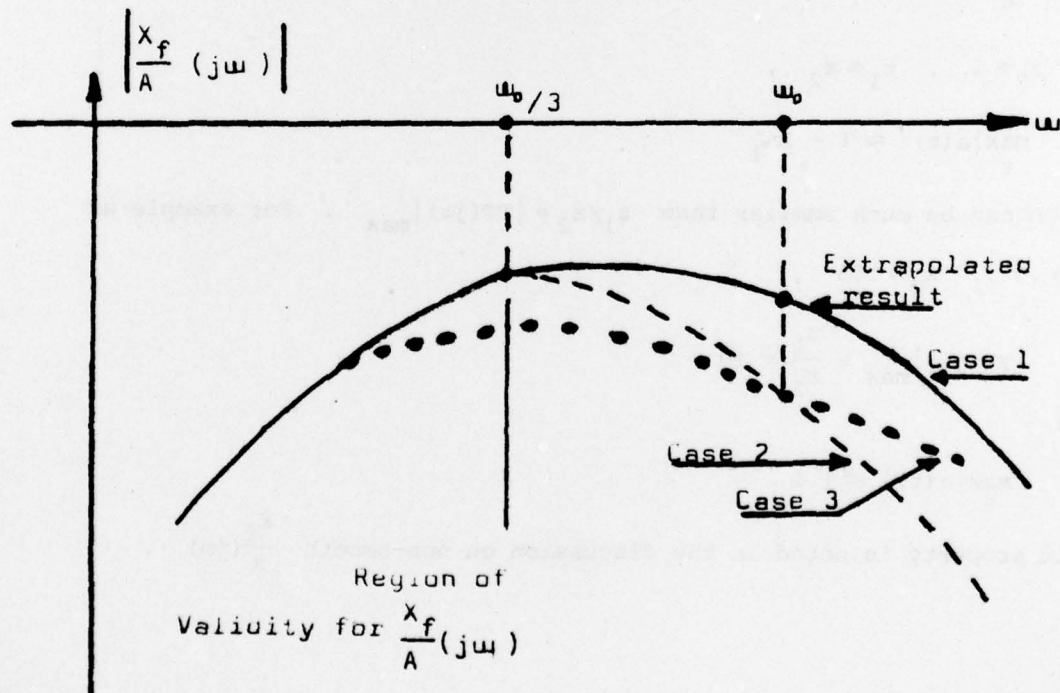


Fig III - 1 - Extrapolation of $\frac{x_f}{A}(j\omega)$

$\left| \frac{x_{f1}}{A}(j\omega) \right|$ as plotted in Case 1, can be modified in such a way that

$$\left| \frac{x_{f2}}{A}(j\omega) \right| = \left| \frac{x_{f1}}{A}(j\omega) \right| \quad \forall \omega \leq \frac{\omega_0}{3}$$
 and

$$\left| \frac{x_{f2}}{A}(j\omega_0) \right| < \left| \frac{x_{f1}}{A}(j\omega_0) \right|$$

as represented as Case 2 in Figure III-1. In this case the system performance, with respect to the value of ω_0 , is improved, and the maximum value $\frac{x_{f2}}{A}(t) \approx \frac{x_{f1}}{A}(t)$.

If such a solution is adopted, extrapolation of $\left| \frac{x_f}{A}(j\omega) \right|$ is not valid for $\omega = \omega_0$, but a very complex system will be achieved, such that the amplitude $\left| \frac{x_{f2}}{A}(j\omega) \right| = \left| \frac{x_{f1}}{A}(j\omega) \right|$ for $\omega \leq \frac{\omega_0}{3}$. This complex system introduces extra delays that could not be tolerated, and oscillations at frequencies not necessarily ω_0 that are not allowed, since it would mask the real information about the gain of the plant, existing in the oscillation.

These conclusions can be seen in Figures III-2 and III-3.

Figure III-2 depicts a typical case where 10 different $\omega_0 \left| \frac{x_f}{A}(j\omega) \right|$ are plotted, having the same amplitude for $\omega < \omega_1$. For $\omega > \omega_1$, several final slopes are used. The maximum value

$$\max_{|t|} \left| \frac{x_{fi}}{A}(t) \right|$$

in all cases is about .27.

Figure III-3 shows the step response for Cases 1a, 1c and 1i.

If relatively simple systems are used, as in Case 3, Figure III-1,

$$\left| \frac{x_{f3}}{A}(j\omega_0) \right| < \left| \frac{x_{f1}}{A}(j\omega_0) \right|,$$

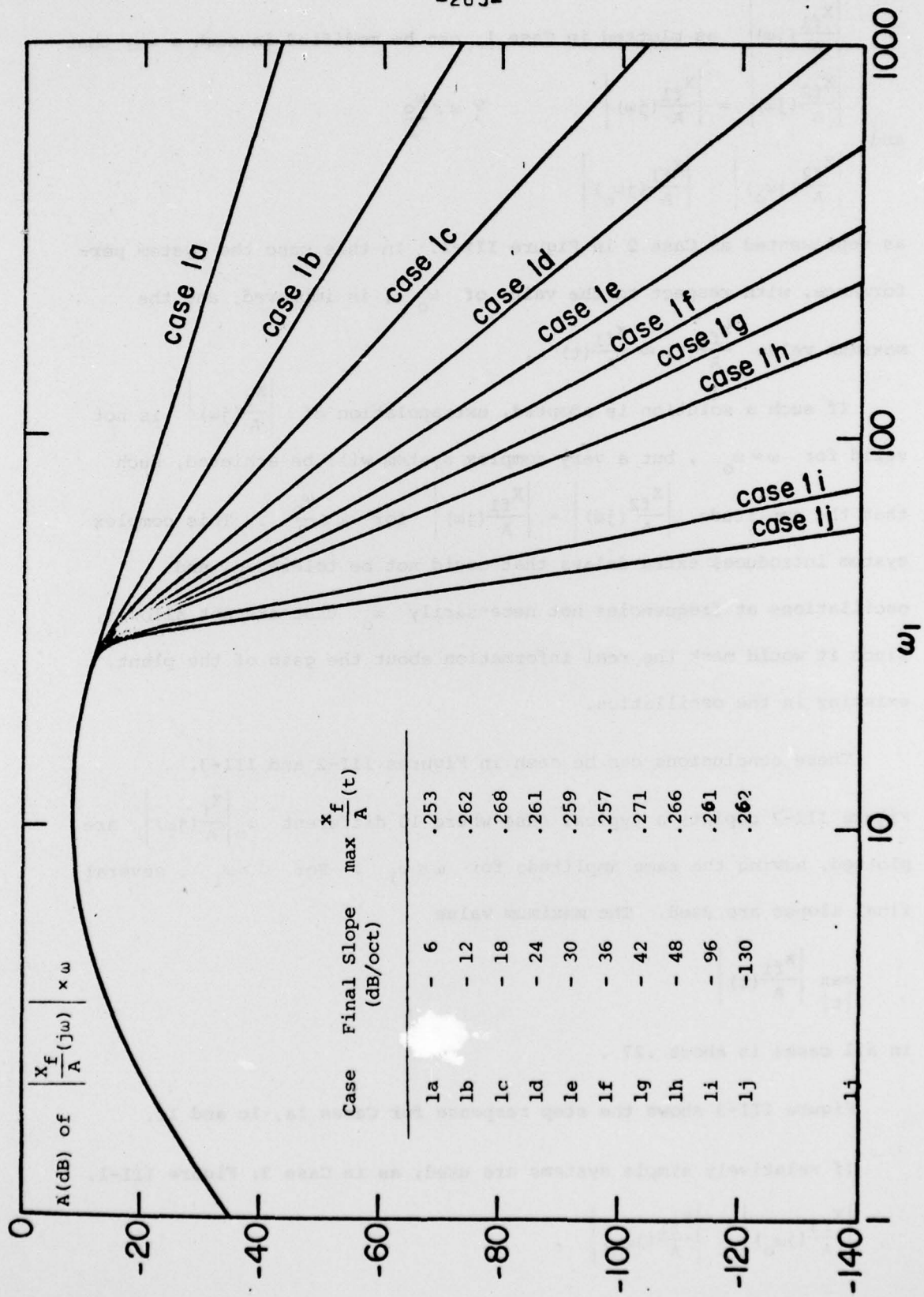


Figure III-2 - Calculated Time Responses.

then $\frac{x_{f3}}{A}(j\omega) \neq \frac{x_{f1}}{A}(j\omega)$ for $\omega \leq \frac{\omega_0}{3}$, causing a different time response.

The conclusion is that if a relatively simple system is to be used, extrapolation of $\frac{x_f}{A}(j\omega)$ for $\omega = \omega_0$ is valid.

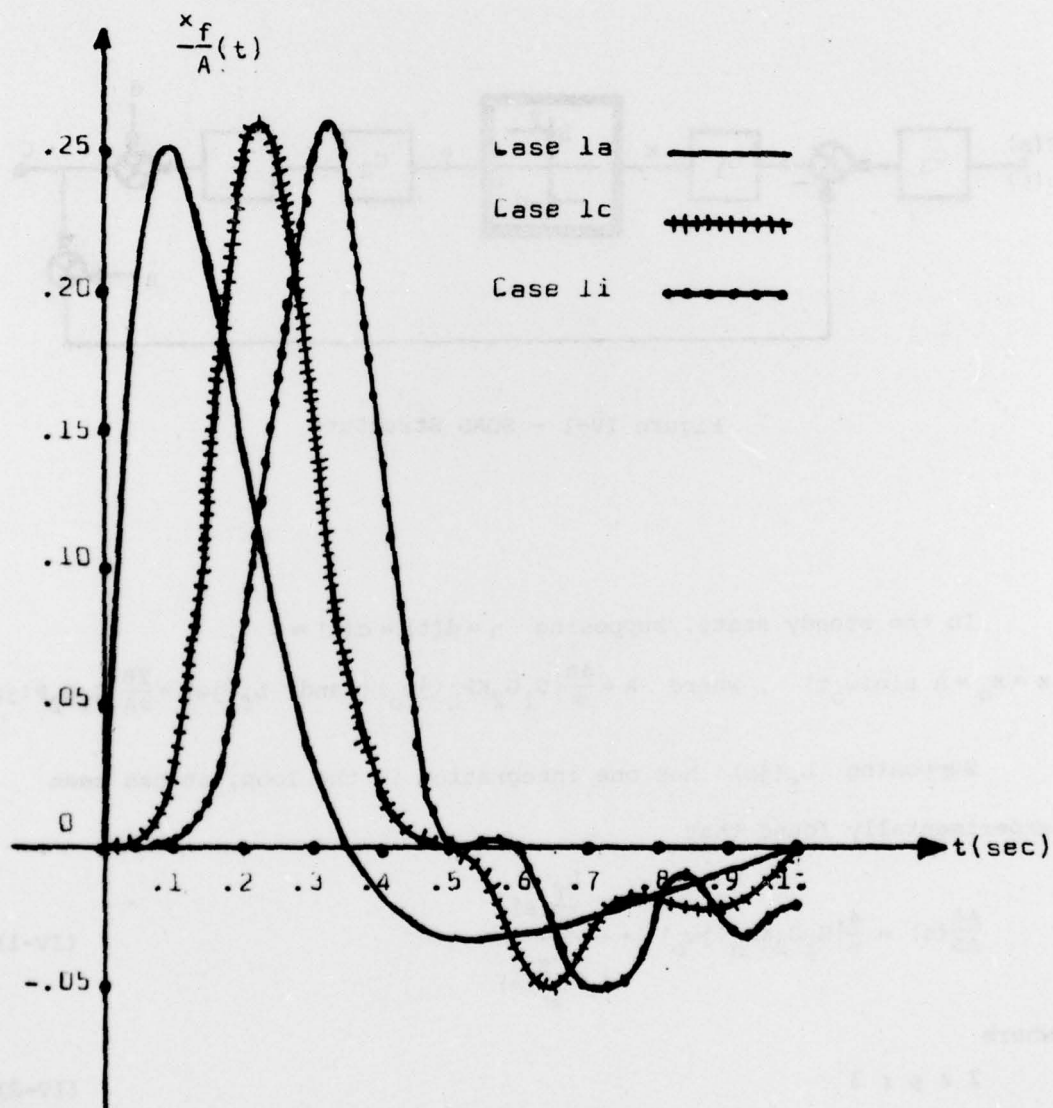


Fig III-3 - Maximum step response value calculations

APPENDIX IV

DYNAMICS OF LIMIT CYCLE BUILD-UP - SOAS SYSTEM

In Chapter 4, which deals with the SOAL structure, the SOAS limit cycle build-up dynamics had to be defined. In Figure IV-1, the SOAS structure is repeated.

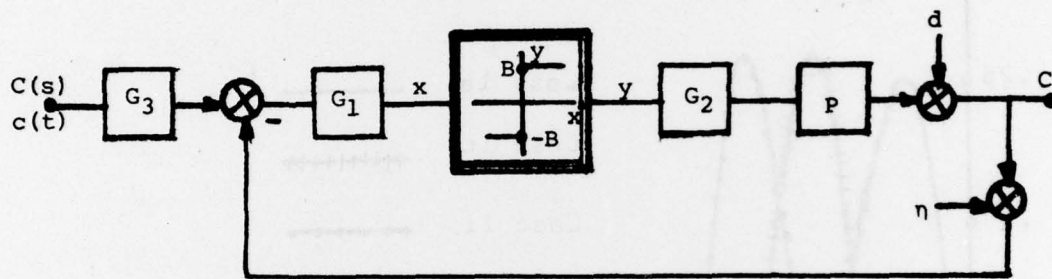


Figure IV-1 - SOAS Structure

In the steady state, supposing $\eta = d(t) = c(t) = 0$,
 $x = x_o = A \sin(\omega_o t)$, where $A = \frac{4B}{\pi} |G_1 G_2 K P_h(j\omega_o)|$ and $L_f(j\omega) = \frac{2B}{\pi A} G_1 G_2 P(j\omega)$.

Supposing $L_f(j\omega)$ has one integration in the loop, it has been experimentally found that

$$\frac{\Delta A}{\Delta B}(s) = \frac{4}{\pi} |G_1 G_2 K P_h(j\omega_o)| \cdot \frac{\frac{L_f(s)}{P}}{1 + \frac{L_f(s)}{P}} \quad (IV-1)$$

where

$$2 \leq p \leq 3 \quad (IV-2)$$

Figure IV-2 shows a typical case where $|x_o|$ represents the oscillation signal absolute value, $p=2$ and $p=3$, the step response

of the model expressed in Equation IV-1, when $p=2$ and $p=3$ respectively. In the SOAL secondary loop dynamics definition, worst conditions were considered, i.e. $p=3$.

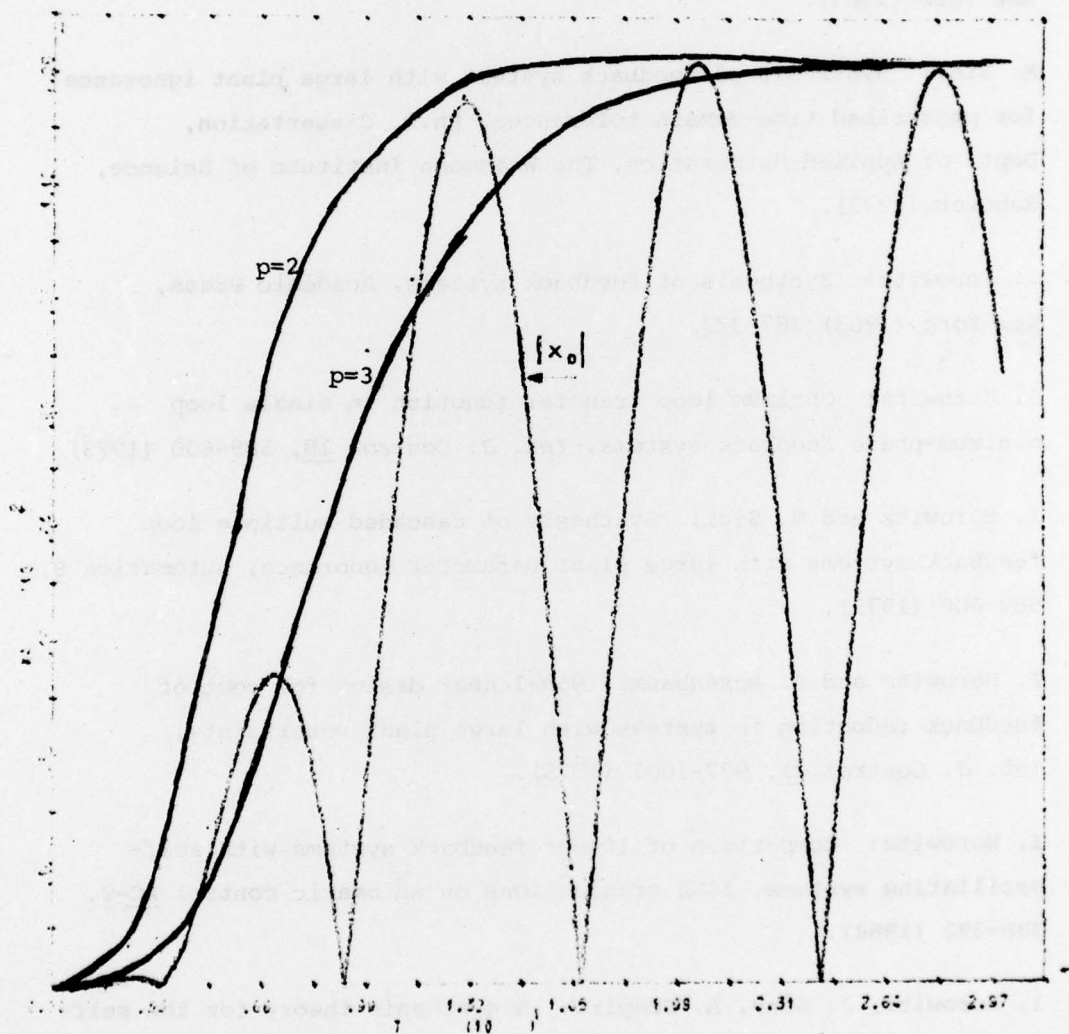


Figure IV-2 - Definition of Limit Cycle Build-up Dynamics

REFERENCES

1. M. Sidi and I. Horowitz: Synthesis of feedback systems with large plant ignorance for prescribed time-domain tolerances, Int. J. Control 16, 287-309 (1972).
2. I. Horowitz: Synthesis of feedback systems, Academic Press, New York (1963).
3. M. Sidi: Synthesis of feedback systems with large plant ignorance for prescribed time-domain tolerances, Ph.D. dissertation, Dept. of Applied Mathematics, The Weizmann Institute of Science, Rehovot (1973).
4. I. Horowitz: Synthesis of feedback systems, Academic Press, New York (1963) 287-373.
5. I. Horowitz: Optimum loop transfer function in single loop minimum-phase feedback systems, Int. J. Control 18, 589-600 (1973).
6. I. Horowitz and M. Sidi: Synthesis of cascaded multiple loop feedback systems with large plant parameter ignorance, Automatica 9, 589-600 (1975).
7. I. Horowitz and P. Rosenbaum: Non-linear design for cost of feedback reduction in systems with large plant uncertainty, Int. J. Control 21, 977-1001 (1975).
8. I. Horowitz: Comparison of linear feedback systems with self-oscillating systems, IEEE transactions on automatic control AC-9, 386-392 (1964).
9. I. Horowitz, J. Smay, A. Szapiro: A synthesis theory for the self-oscillating adaptive system (SOAS), Automatica (1974).
10. I. Horowitz, J. Smay, A. Szapiro: A synthesis theory for the externally excited adaptive system (EEAS), IEEE transactions on automatic control AC-19, No. 2, 101-107 (1974).

11. G. Zames and N.A. Shneyder: Dither in non-linear systems, IEEE transactions on automatic control AC-21, No. 5, 660-667 (1976).
12. A. Gelb and W.E. Vandervelde: Multiple-input describing functions and non-linear system design, Mc Graw-Hill (1968).
13. L.A. Mac Coll: Fundamentals of Servo mechanisms, Princeton, N.Z. Van Nostrand, 78-87 (1945).
14. A. Bersekerskii: Applying vibrators to eliminate non-linearities in automatic regulators, Automat. i telemekh., No. 8, 411-417 (1947).
15. H.S. Tsien: Engineering Cybernetics, Mc Graw-Hill, N.Y., 77-82 (1954).
16. J.C. Lozier: Carrier controlled relay servo, Electrical engineering 69, No. 12, 1052-1056 (1950).
17. A.R. Bergen and R.L. Franks: Justification of the describing function method, Siam J. Control 9, No. 4, 568-589 (1971).
18. Proc. symp. on self-adaptive control processes, Wright Air Dev. Centre, WPAFB, Dayton, Ohio, Tech. Rept. 59-49, ASTIA Doc., No. AD-209389, March (1959).
19. O.H. Shuck: Honeywell's history and philosophy in the adaptive control field, Wright Air Dev. Centre, WPAFB, Ohio, Tech. Rept., Jan. (1959).
20. L.W. Taylor Jr. and E.J. Adkins: Adaptive control and the X-15, NASA Flt. Res. Centre, Edwards, Calif., June 1 (1965) (Presented at Princeton University Conference on Aircraft Flying Qualities, June 17-18 (1965)).
21. A study to determine an automatic flight control configuration to provide a stability augmentation capability for a high-performance supersonic aircraft, Minn.-Honeywell Regulation Co., Aeronautical Dev., WADC TR-51-349 (Final), May (1958).

22. A. Gelb and W.E. Vandervelde: On limit cycling control systems, IEEE Trans. on Automatic Control AC-8, 142-157 (1963).
23. A. Gelb: The analysis and design of limit cycling adaptive automatic control systems, Sc.D. Dissertation, Dept. of Aeronautics and Astronautics, M.I.T., Cambridge, Sept. (1961).
24. P. Beckmann: Probability in communication engineering, Harcourt, Brace & World, Inc. (1967).
25. A. Szapiro and I. Horowitz: A two-loop self-oscillating system, presented at 13th IEEE Symposium on Adaptive Processes, Nov. 1974, Phoenix, Arizona, and published in Proceedings.
26. H.W. Bode: Network analysis and feedback amplifier design, Van Nostrand, New York (1945).
27. A. Papoulis: The Fourier integral and its application, Mac Graw-Hill (1968).